

Development of Dendrigrraft Polymers as Catalysts in Organic Synthesis

Thesis submitted to

Cochin University of Science and Technology

in partial fulfilment of the requirements for the degree of

Doctor of Philosophy

in

Chemistry

under the Faculty of Science

by

Mrs. Smitha George, M. Sc



**DEPARTMENT OF APPLIED CHEMISTRY
COCHIN UNIVERSITY OF SCIENCE AND TECHNOLOGY
COCHIN-682 022, KERALA, INDIA**

August 2015

Development of Dendrigraft Polymers as Catalysts in Organic Synthesis

Ph.D. Thesis under the Faculty of Science

By

Smitha George

Research Fellow

Department of Applied Chemistry

Cochin University of Science and Technology

Kochi, India 682022

Email: smithaprince80@gmail.com

Supervising Guide

Dr. K. Sreekumar

Professor

Department of Applied Chemistry

Cochin University of Science and Technology

Kochi, India 682022

Email: ksk@cusat.ac.in

Department of Applied Chemistry

Cochin University of Science and Technology

Kochi, India 682022

August 2015



DEPARTMENT OF APPLIED CHEMISTRY

COCHIN UNIVERSITY OF SCIENCE AND TECHNOLOGY

KOCHI - 682 022, INDIA

Phone : 0484-2575804, Telex : 885-5019 CU IN, Grams : CUSAT
Fax : 91-484-2575804, E-mail : chem@cusat.ac.in Web: www.cusat.ac.in/dac

Dr. K. Sreekumar

Professor

Ph: 0484-2575804

Email: ksk@cusat.ac.in

CERTIFICATE

This is to certify that the thesis entitled **“Development of Dendrigrraft Polymers as Catalysts in Organic Synthesis”** is a genuine record of original research work carried out by **Mrs. Smitha George**, under my supervision, in partial fulfilment of the requirements for the degree of Doctor of Philosophy in Chemistry of Cochin University of Science and Technology, and further that no part thereof has been presented before for the award of any other degree. All the relevant corrections and modifications suggested by the audience and recommended by the doctoral committee of the candidate during the presynopsis seminar have been incorporated in the thesis.

Cochin-22
24-08-2015

Dr. K. Sreekumar
(Supervising Guide)

Declaration

I hereby declare that the work embodied in the thesis entitled **“Development of Dendrigrraft Polymers as Catalysts in Organic Synthesis”** is based on original research work done by me under the supervision of **Dr. K. Sreekumar**, Professor, Department of Applied Chemistry, Cochin University of Science and Technology, Cochin-22, and the same has not been submitted elsewhere for the award of any other degree.

Cochin-22
24-08-2015

Mrs. Smitha George.

*“It is difficult to say what is impossible, for the dream of yesterday is the hope
of today and the reality of tomorrow.”*

Robert H. Goddard

Acknowledgement

Words often fall short to reveal one's deep regards. I take this opportunity to acknowledge and extend my sincere thanks to those who helped me to make this Ph.D. thesis possible.

First and foremost, I express my utmost gratitude and reverence to my guide Dr. K. Sreekumar, Professor, Department of Applied Chemistry, Cochin University of Science and Technology, without whom this thesis would have been a far-fetched dream. I am very thankful to him for giving me the opportunity to be in his research group. He offered me a topic which enabled me to push my boundaries and gave me full freedom to 'experiment' in my research work. He has always patiently mentored me at every stage without losing his temper. I thank him earnestly for painstakingly correcting the draft thesis well on time. I feel blessed to be one among his student community.

Dr. K. Girish Kumar, former HOD deserves special mention at this point. His motivation has helped me to venture confidently in competitive platforms and his constructive criticism has always boosted my morale.

My honest thanks go to Dr. N. Manoj, Head, Department of Applied Chemistry, CUSAT for providing me the opportunity to accomplish my research work in this department. I express my heartfelt gratitude to Dr. P. V. Mohanan, doctoral committee member. Dr. S. Prathapan, has been an encouraging presence during my time in the department. I would like to extend my sincere thanks to Dr. S. Sugunan, Dr. Muhammed Yusuff, Dr. Prathapachandra Kurup and Dr. P. A Unnikrishnan of the department who inspired me in one way or the other. I specially thank Dr. Sabura Begum for her kind friendship.

I have fond memories of my seniors who were ready to help me at the time of need and for the environment they provided me to experiment well in the lab. I thank them individually, Dr. Rajesh, Dr. Mangala, Dr. Kannan, Dr. Anoop and Dr. Elizabeth at this juncture. I thank Dr. Mahesh specially for his presence till time.

Life in a research lab is tedious, but my time in the lab was made enjoyable due to the togetherness with Ms. Jiby. I enjoyed the moments with Jiby, from the beginning of my research to this time and I enjoyed as senior together with her with equal sound of suggestions.

Ms Sinija P.S. was always with me offering help and I thank her wholeheartedly. Words are not enough to thank Ms. Anjaly Jacob, Ms. Jisha K. A. and Ms Sowmya Xavier who were always ready with help, be it in proof reading, structure documentation, or any other matter. I thank Ms. Jisha K.A for helping me in spectral analysis also. Dr. Jaimy K. B., the post doctoral fellow in our lab facilitated the MS end-note referencing along with Ms. Anjaly Jacob. I thank them wholeheartedly for their selfless aid. I also thank Ms. Anjali C.P and Ms. Jesny Jagan for the help I received. The help rendered by my juniors during the documentation of the research work, has been instrumental in the successful outcome of this thesis. Ms. Sherlymol P.B, her presence has always given me special homely affection. I am lucky to have her presence in the lab.

I remember here the presence of new juniors Ms. Letcy and Ms. Shaibuna.

I thank Dr. K.A. Maniram for the interest he took to deliver me an idea about how a good thesis should look like.

My thanks are also due to the Friends in the Department of Applied Chemistry, especially, Analytical and Biochemistry labs and other departments of CUSAT for their cooperation. I have fond memories of Jabia, Jithin, Dr. Mothi, Dr. Eason, Dr. Navya Antony, Dr Sandhya Unnithan, Dr. Reny, Dr. Reshma G., Dr Renjini Joseph, Dr Laina A.L., Divya Thomas, Anuja E.V and Rakesh. The special relationship I shared with Dr. Priya Briet and Dr. Jomon Jacob, will always stay with me.

I have fond memories of the project students Megha, Nihara and especially Shafna from IISER, Bhopal.

I can never forget the applauses bestowed on me by the Department of Applied chemistry as well as the University for my achievements.

I recollect the memories of the support offered by the friends during my participation in various cultural events especially Onam and Christmas Celebrations which always boosted me.

I would like to place on record my sincere thanks to the CSIR, Govt. of India for financial assistance in the form of fellowship.

The non-teaching staff of the Department of Applied Chemistry has always been ready with their help and support and I thank them.

The various instrumental analysis of my work was completed with the help of friends in other institutions. I sincerely thank Sona Narayanan, PSRT, CUSAT for GPC analysis; Krishnan Kartha, NIIST, Thiruvananthapuram for MALDI-MS analysis; Sunil Sekhar and Shabeeb, NCL, Pune for Solid state ^{13}C NMR analysis and Tittu Thomas, Dept of Physics, CUSAT for AFM analysis. Mr. Saji, STIC, CUSAT deserves special mention for his help in NMR analysis.

I would like to put in a word of appreciation for the services rendered by RGCB, TVM (MALDI-MS); AIIMS, Kochi (XPS), IIT, Chennai (Magnetic susceptibility); IIT, Mumbai (EPR) and STIC, CUSAT, specially, Dr. Shibu, Dr. Adarsh and Miss Anitha.

Mr. Vishnu, P., Alpha Chemicals and Diagnostics deserves special mention for the prompt supply of chemicals.

This thesis would not have been a reality, but for the sacrifices made by my family. I thank my appachan, who is no more now, used to stay with me during the initial stages of my research for the easy going of the work. Words are not enough to thank my ammachi who helped me face the hardships of my research with her taking up my role as mother and housewife. I remember the encouragement offered by my brother, papa and mummy during this period. My husband had been a pillar of strength with his love and support. I thank my kids, especially, Suzanne, my elder one for bearing my absence during their formative years.

Above all, I bow my head in reverence before the **God Almighty** for His blessings.

Smitha George

PREFACE

Introduction

Dendrigraft polymers or Dendronized polymers are currently under intense investigation with respect to various applications, including the synthesis of hierarchically structured materials, catalysis, applications in biosciences, as well as optoelectronic applications. In Dendronized polymers, the focal points of the dendrons are attached to the pendant functional groups at the repeat units along the polymer backbone. Multiple branching levels characterize the architecture of these molecules, in analogy to dendrimers and hyperbranched polymers. Their core is not a single unit, but a polymeric chain. Main distinguishing feature of these polymers is their synthesis, based on grafting reactions with polymeric side chains serving as backbone. In the case of branched polymeric core, the term Dendrigraft polymer was more appropriate than Dendronized polymer, because, dendritic units are grafted on the polymeric chain. In the synthesis of dendritic molecules, multistep solution chemistry presents a synthetic challenge, because of the need to purify products at every stage. In solid phase synthesis, no purification is required during intermediate stages. Reactions are driven to completion by the addition of excess reagents. In this technique, the product is anchored onto the support and after the reaction, the excess reagents are removed by filtration. Also, one can study the solution chemistry of the product by cleaving the same from the resin loaded polymer. The concept of dendritic polymer together with solid phase strategy has been applied. We have tried to establish Merrifield resin supported dendrigraft polymer as heterogeneous catalyst for organic transformations. The present thesis envisages the synthesis and characterization of dendrigraft polymers on Merrifield resin and the application of metal complexed dendrigraft polymers in the field of heterogeneous catalysis.

The motivation behind the work

- Peripheral functionality of PAMAM and PPI dendrimers developed previously from this laboratory were in the order of 1 to 2 mmols/g for G0 to G2 generations. So the present focus was to increase the amount of functionality at the low generation level itself.
- Dendronized polymers reported so far were based on linear polymeric core, the same synthesized from branched polymeric core are only few. So the present focus was to develop dendrigraft polymers having branched polymeric core.
- Reported dendronized polymers having linear polymeric core were synthesized using solution phase strategy, the same synthesized using solid phase strategy was not reported yet. So the present focus was to develop dendronized or dendrigraft polymers using solid phase strategy.

Objectives of the Work

- To design and develop Dendrigraft polymers having linear ethylene glycol initiated polyepichlorohydrin as core on a resin support.
- To design and develop Dendrigraft polymers having branched glycerol and pentaerythritol initiated polyepichlorohydrin as core on a resin support.
- To study the nature of Dendrigraft polymers after cleaving from the support.
- To synthesize and characterize Copper and Palladium Complexes of Dendrigraft polymers having Ethylene Glycol, Glycerol and Pentaerythritol initiated Polyepichlorohydrin as core.

- To evaluate the catalytic properties of polymer supported copper and palladium complexes of dendrigraft polymers in organic chemical transformations.

The thesis is presented in seven chapters, a brief summary of which is given here.

Chapter 1 is a general introduction to Dendritic Polymers, especially Dendrimers, Dendrigraft polymers and Dendronized polymers; the concept of solid phase organic synthesis and polymer based catalysis. A detailed review of the scientific literature relevant to the development of dendrigraft polymers, solid phase organic synthesis and dendritic polymer based catalysis are also included.

Chapter 2 describes the synthesis and characterization of dendrigraft polymers having ethylene glycol, glycerol and pentaerythritol initiated polyepichlorohydrin as core, anchored on Merrifield resin. Methods like IR and solid state ^{13}C NMR spectroscopy and TG-DTG are used to characterize the products of the reaction. Photolytic cleavage of dendrigraft polymer from the resin was achieved and solution chemistry of the dendritic polymer was studied.

Chapter 3 demonstrates the synthesis and characterization of copper complex of dendrigraft polymer having glycerol initiated polyepichlorohydrin as core. The catalyst was employed for the study of synthesis of Benzimidazole derivatives via the reaction between o-phenylenediamine and aldehydes or ketones. The experimental parameters were optimized, scope of substrates and reusability of the catalyst were studied. The mechanism of the reaction was also proposed. The use of the catalyst resulted in good yield of the products.

Chapter 4 demonstrates the synthesis and characterization of copper complex of dendrigraft polymer having ethylene glycol initiated

polyepichlorohydrin as core. The catalyst was employed for the synthesis of tetra-substituted imidazoles by a reaction between 1,2 diketone, aldehyde, amine and ammonium acetate. The experimental parameters were optimized, scope of substrates and reusability of the catalyst were studied. The mechanism of the reaction was also proposed. The catalyst was found to be an excellent one for the synthesis of tetra-substituted imidazoles.

Chapter 5 demonstrates the synthesis and characterization of palladium complex of dendrigraft polymer having ethylene glycol initiated polyepichlorohydrin as core. The catalyst was employed for the synthesis of Benzoxazole derivatives by a reaction between o-aminophenol and aldehyde. The experimental parameters were optimized, scope of substrates and reusability of the catalyst were studied and the mechanism of the reaction was proposed. The Pd complex of dendrigraft EG-G2 polymer was found to be a good catalyst for the synthesis of benzoxazole derivatives.

Chapter 6 demonstrates the synthesis and characterization of chiral dendrigraft polymer having pentaerythritol initiated polyepichlorohydrin as core and its copper complex. The synthesized catalyst was employed for the study of Aza Diels Alder reaction between aldimines and cyclohexenone. The experimental parameters were optimized, scope of substrates and reusability of the catalyst were studied and the mechanism of the reaction was proposed. The chiral catalyst derived from dendrigraft PEN-G2 was found to be an excellent catalyst for the synthesis of isoquinuclidines with high enantiomeric excess.

Chapter 7 presents the summary, major achievements and future outlook of the present study.

CONTENTS

Chapter-1 Introduction	1
1.1 Introduction to Dendritic Polymers	1
1.1.1 Dendrimers	2
1.1.2 Dendrigrraft Polymers	5
1.1.3 Dendronized Polymers	9
1.2 Solid Phase Organic Synthesis	20
1.3 Polymer Supported Catalysis	26
1.3.1 Dendrimers Supported on a Solid Phase	36
1.4 Origin, Objectives and Approach to the Thesis	44
1.5 Characterization Methods	44
1.6 References	47
Chapter-2 Development of Dendrigrraft Polymers having Ethylene Glycol, Glycerol and Pentaerythritol Initiated Polyepichlorohydrin as core	71
2.1 Introduction	71
2.1.1 Objective of the Present Work	74
2.2 Results & Discussion	74
2.2.1 Synthesis of Merrifield Resin Supported Dendrigrraft Polymer having Pentaerythritol Initiated PECH as Core- PEN-G2	74
2.2.2 Synthesis of Merrifield Resin Supported Dendrigrraft Polymer having Glycerol Initiated PECH as core - GLR-G2	96

2.2.3	Synthesis of Merrifield Resin Supported Dendrigraft Polymer having Ethylene Glycol Initiated PECH as core - EG-G2	103
2.3	Conclusions	109
2.4	Experimental Section	110
2.5	Characterization of Products	115
2.6	References	120
Chapter-3 Complexation of Dendrigraft Polymer GLR-G2 with Copper and Synthesis of Benzimidazole Derivatives 129		
3.1	Introduction	129
3.1.1	Benzimidazole Synthesis	129
3.2	Results & Discussion	138
3.2.1	Synthesis of Copper Complex of Dendrigraft Polymer having Glycerol Initiated PECH as Core	138
3.2.2	Catalyst Characterization	140
3.2.3	Catalytic Activity of Resin Supported Dendrigraft GLR-Gn-Cu Complex	142
3.3	Conclusions	157
3.4	Experimental Section	158
3.5	Characterization of Products	161
3.6	References	168

Chapter-4 Complexation of Dendrigrraft Polymer EG-G2 with Copper and Synthesis of Tetra-substituted Imidazoles	181
4.1 Introduction	181
4.1.1 Tetra-substituted Imidazole Synthesis	181
4.2 Results & Discussion	188
4.2.1 Synthesis of Copper Complex of Dendrigrraft Polymer having Ethylene Glycol Initiated PECH as Core	188
4.2.2 Catalyst Characterization	189
4.2.3 Catalytic Activity of Resin Supported Dendrigrraft EG-Gn-Cu Complex	196
4.3 Conclusions	206
4.4 Experimental Section	208
4.5 Characterization of Products	210
4.6 References	218
Chapter-5 Complexation of Dendrigrraft Polymer EG-G2 with Palladium and Synthesis of Benzoxazole Derivatives	227
5.1 Introduction	227
5.1.1 Benzoxazole Synthesis	227
5.2 Results & Discussion	234
5.2.1 Synthesis of Palladium Complex of Dendrigrraft Polymer having Ethylene Glycol Initiated PECH as Core	234

5.2.2 Catalyst Characterization	236
5.2.3 Catalytic Activity of Resin Supported Dendrigrraft EG-Gn-Pd Complex	241
5.3 Conclusions	247
5.4 Experimental Section	248
5.5 Characterization of Products	251
5.6 References	254
Chapter-6 Copper Complex of Chiral Modified Dendrigrraft PEN-G2 and Aza Diels-Alder Reaction	263
6.1 Introduction	263
6.1.1 Aza Diels-Alder Reaction	263
6.2 Results & Discussion	271
6.2.1 Synthesis of Copper Complex of Chiral Modified PEN-Gn Dendrigrraft Polymer	271
6.2.2 Catalyst Characterization	274
6.2.3 Catalytic Activity of Resin Supported Dendrigrraft PEN-Gn-Cu Complex	281
6.3 Conclusions	291
6.4 Experimental Section	292
6.5 Characterization of Products	296
6.6 References	299
Chapter-7 Summary and Outlook	307

Abstract

The chapter includes the classification of dendritic polymers with special emphasis on Dendrimers, Dendrigraft and Dendronized Polymers. A brief discussion on Dendronized and Dendrigraft Polymers with emphasis on synthesis strategies is presented. The concept of solid phase organic synthesis using polymer supported dendritic species is delineated. Recent reports on organic and inorganic polymer supported dendritic catalysts for organic chemical transformations are discussed. The chapter concludes with a statement on the origin and scope of the thesis.

1.1 Introduction to Dendritic Polymers

P. J. Flory had predicted the possibility of having dendritic macromolecular architecture way back in 1941.¹⁻³ Since then, much interest has been put on the synthesis of dendritic macromolecules. The dendritic topology has been recognized as the fourth major class of macromolecular architecture.⁴⁻⁷ The major artifact for such a classification has been the unique group of new properties exhibited by this class of polymers.⁸⁻¹³ Several synthetic approaches were reported for the preparation of dendrimers, which have led to a broad range of macromolecular structures. At present, dendrimers consist of three sub classes, namely, random hyperbranched polymers, dendrigraft polymers and dendrimers.

1.1.1 Dendrimers

Out of the three dendritic sub classes, dendrimers constitute the most important class. Tomalia was the first researcher to use the term ‘dendrimer’. He used this term when he published his results on PAMAM.^{14,15} The term dendrimer is derived from the Greek words dendri (branch tree-like) and meros (part of). Dendrimers are composed of monodisperse, low molecular weight, multifunctional core unit to which a defined number of dendrons are attached.

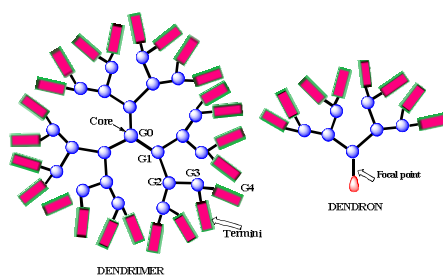


Fig 1.1. Structure of Dendrimer and Dendron¹⁶

They contain monodisperse, branched, oligomeric segments consisting of repeating units with an AB_m type functional group pattern. The degree of branching is almost 100%. The number of repeating units between the core and a terminal unit is referred to as the dendron generation (G_x).¹⁶⁻²⁰ Dendrimer synthesis involves hierarchical assembly that requires the construction of dendrons. Dendrimers have unique core-shell structures possessing three basic components. They are: a core, an interior of shells (generation) consisting of repetitive branch cell units and terminal functional groups in the periphery, as illustrated in Fig 1.1.

The synthesis of dendrimers has been performed by adopting either ‘divergent’ or ‘convergent’ strategies. Initially, the synthetic approaches

were mainly based on divergent methods. Vogtle *et al.* first reported the synthesis of several low molecular weight cascade structures using the divergent, *in situ* branch cell method.²¹ Dendritic branching rule was used to construct branch cells ‘in situ’ from monomers.

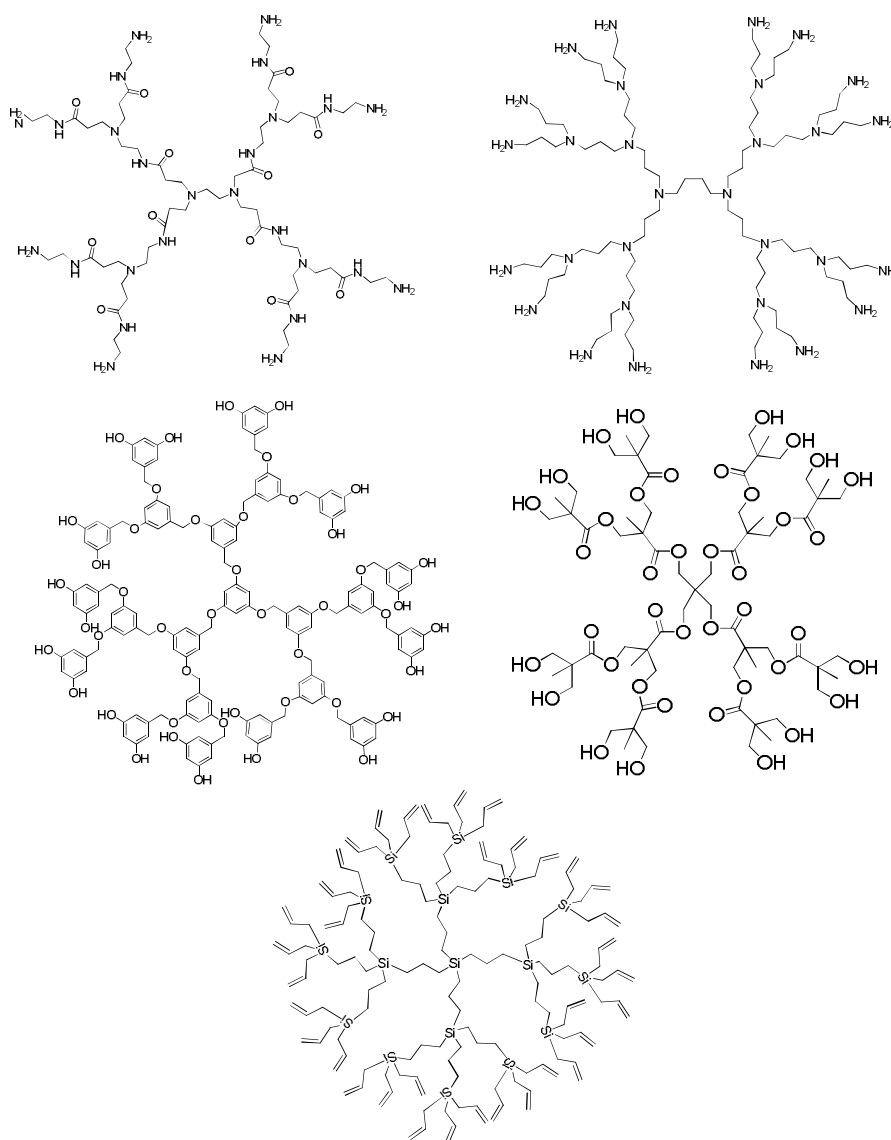


Fig 1.2 Structures of Dendrimers Commonly Used in Catalysis^{29,33-36}

In this case, the reaction involved a combination of addition of acrylonitrile followed by reduction chemistry. This method had serious limitations. Higher generation cascade structures, or dendrimers, could not be obtained by this method due to synthetic and analytical difficulties.²² At the same time, Tomalia reported a completely characterized series of high molecular weight, poly (amido amine) dendrimers.^{14,15} Tomalia used the combination of Michael addition and amidation chemistry. Tomalia's method succeeded in showing the first commercial route to dendrimers. This provided the first opportunity to observe the development of the unique dendrimer properties. It was recognized that the unique properties occurred only at higher generations (i.e. G=4 or higher). Newkome *et al* reported the first use of 'preformed branch cell' methodology.²³ Newkome's strategy involved the geometric coupling of 'preformed branch cell' reagents around a core. This helped to produce low molecular weight structures. Several dendrimer families including dendri-poly(ethers),²⁴ dendri-poly(thioethers) were prepared adopting Newkome's method.^{25,26} In all these reported methods, the systematic divergent growth of 'branch cells' was experimented. This defined shells within the 'dendrons' were initiated from the core. The ultimate shape of the dendrimer and the number of dendrons were determined by the multiplicity and directionality of the initiator sites on the core. The divergent method created dendrimers which constituted of groups of molecular trees that propagated outwardly from their roots (cores). The convergent construction of molecular trees was established by Hawker and Frechet²⁷⁻³⁰ followed by Miller and Neenan,³¹ by starting with the surface branch cell reagents. Researchers have succeeded in producing dendrons possessing a single reactive group at the root or focal point of the structure by amplifying with the generations. The corresponding dendrimers

can be generated by subsequent coupling of these reactive dendrons through their focal point to a common ‘anchoring core’. In this case, several functional groups are available at the focal point and periphery of the dendrons. Hence, the convergent synthesis is useful for the preparation of more complex macromolecular architectures including linear dendritic hybrids, block dendrimers or dendronized polymers.³²

Several families of dendrimers were used as catalysts during the past two decades (Fig 1.2). Commonly used dendrimers include polyamidoamines (PAMAM),³³ polypropylene imines (PPI),³⁴ polybenzyl ethers (Frechet-type),²⁹ polyaliphatic esters,³⁵ polycarbosilanes,³⁶ poly(ester amide)s (Newkome-type),³⁷ and allyl-ended arene cored dendrimer.³⁸ Several reviews have uncovered the mysteries behind dendrimer catalysis.³⁹⁻⁷⁸ Some significant results were reported from this laboratory on polymer supported PAMAM dendrimers as heterogeneous catalysts for various organic chemical transformations.⁷⁹⁻⁸⁶ The catalysts reported were as efficient as homogeneous dendritic catalysts. The characteristic properties of dendrimers make them interesting targets for various other applications also. They are used as molecular containers, drug delivery systems, as sensors, light harvesting devices etc.^{59,64,87-96}

1.1.2 Dendrigraft Polymers

Dendrigraft polymers may be considered as the third class under dendritic polymers. Independently, Tomalia *et al.*⁹⁷ and Gauthier *et al.*⁹⁸ had reported the first examples of dendrigraft polymers in 1991. A comparison of dendrimer and dendrigraft architectures is made in Fig 1.3. Reactive oligomers or polymers are used to produce dendrigrafts, instead of using monomers, as if in constructing dendrimers. The earlier approaches for the

synthesis involved the iterative grafting of ‘oligomeric reagents’. Similar to dendrimers, each iterative grafting step is referred to as a generation. This method gives the possibility of varying branch densities, as well as the size of the grafted branches. In these cases, ultra-high molecular weight dendrigrafts can be obtained at very low generation levels. This depends on the graft densities and molecular weights of the grafted branches. This approach involves convergent-type grafting principles. Reactive oligomers are grafted onto successive branched precursors to produce semi-controlled structures. In dendrigraft structures, grafting may occur along the entire length of each generational branch.

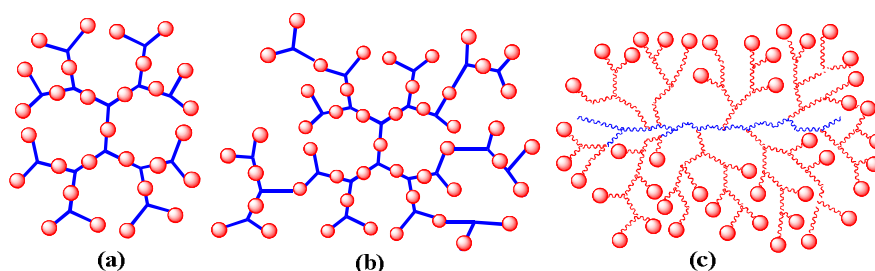


Fig 1.3 Comparison of Structures: a) Dendrimers b) Hyperbranched Polymers c) Dendrigraft Polymers.⁹⁷⁻⁹⁸

Dendrigraft polymers have less controlled structures. The branching densities cannot be determined exactly, they are somewhat arbitrary and difficult to control. Structures produced by so-called ‘graft from’ techniques, developed by Gnanou^{99,100} and Hendricks^{101,102} resemble the dendrimer architecture. Since the branch cell arms are derived from oligomeric segments, they are referred to as ‘polymeric dendrimers’.¹⁰³ Dendrigraft polymers are having more flexible and extended structures. They exhibit unique and different properties compared to the more compact traditional dendrimers.

Dendrigraft polymers can be generated through ionic polymerization. They combine the features common to dendrimers and random hyperbranched polymers. Dendrigrafts are generally synthesized from polymeric chains. They are assembled according to a dendrimer-like generational scheme. These consist of functionalization and grafting cycles (Fig 1.4).¹⁰⁴ Polymer chains can be grafted onto a linear (core) polymer which is randomly functionalized with reactive sites.

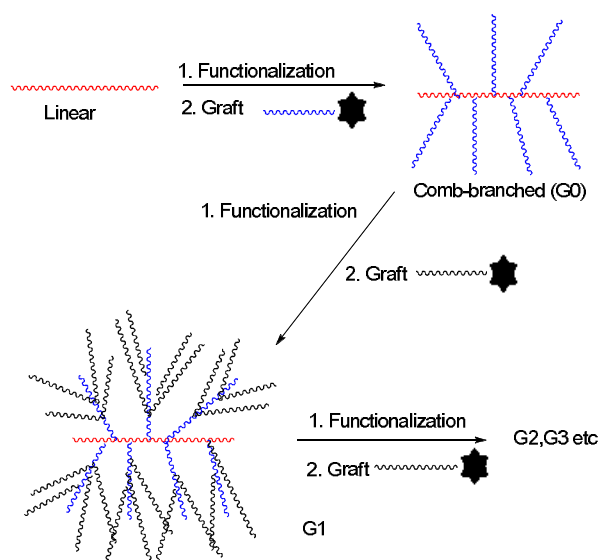


Fig 1.4 Synthetic Route to Dendrigraft Polymers¹⁰⁴

This process yields a comb-branched (or generation G0) architecture. To get higher generation dendrigraft macromolecules (i.e. G1, G2, etc.), the functionalization and grafting reactions have to repeat. They are prepared by linking macromolecular building blocks. High molecular weights are attained in few cycles. Several names were assigned to these dendritic graft polymers. Tomalia *et al.* had used the term Comb-burst polymers⁹⁷ by analogy to Starburst polymers. Later,

Tomalia himself changed the name to ‘dendrigraft polymers’.⁴ Gauthier and Moeller used the designation ‘arborescent graft polymers’,⁹⁸ but few others have used the term ‘polymeric dendrimers’.¹⁰⁵

Dendrigraft polymers are prepared by three methods. They are: (a) ‘grafting onto’, (b) ‘grafting from’, and (c) ‘grafting through’ methods. Dendrigraft polymers with tailored structure and topology are prepared by “grafting - onto” method. This method depends upon the introduction of grafting sites on a polymeric substrate, after which coupling with reactive ‘living’ polymer chains occurs. Characterization of the branches is easily achieved in this method. This can be achieved by removing a sample of the side chain from the reactor before the grafting reaction occurs. The number of grafts introduced and the average spacing between grafts can be calculated. This is done by measuring the molecular weight of the substrate, the side chains and the graft polymer.^{97,98}

In the ‘grafting from’ scheme, a polymeric substrate is first functionalized to bear a number of accessible reactive groups. These groups are activated to provide initiating sites. This is followed by addition of a monomer. Subsequently, the side chains from the backbone polymer grow. Here, the number of grafts and the molecular weight of the side chains cannot be determined exactly. When the polymeric substrates are having multiple charges, solubility problems are also encountered. This can lead to heterogeneous reaction conditions and usually a broader molecular weight distribution.⁹⁹⁻¹⁰²

The method used to produce comb-branched copolymers by the copolymerization of vinyl monomers with macromonomers is referred to as grafting through approach. The ‘grafting through’ technique is based

on the reaction of living polymeric chains with a capping agent. This will contain a polymerizable moiety (e.g. vinyl benzyl chloride). This leads to spontaneous coupling reactions, which are usually encountered in random hyperbranched polymer synthesis.¹⁰⁶⁻¹⁰⁸

The general synthetic route to dendrigraft polymers is described in Fig 1.4. Reactive sites are randomly introduced along a linear functionalized polymer core. Living polymeric chains are then grafted to the reactive sites, to give a comb-branched (G0) graft polymer. The introduction of functional groups onto the 'teeth' of the comb-branched structure followed by grafting, yields the G1 structure. Repeating the cycle of functional group introduction and grafting leads to G2 and higher generations.¹⁰⁴

In order to obtain well-defined dendrigraft polymers, the synthetic method based on grafting reactions must satisfy certain criteria. The ionic propagating centers derived from the monomer must possess good reactivity and living characteristics. It must be possible to incorporate reactive functional (grafting) sites along the polymer chains grafted during the previous reaction cycle. The grafting reaction should ideally proceed without side reactions and in high yield. If living polymerization techniques are employed, good control over the molecular weight and the molecular weight distribution is possible. This results in well-defined structures. A number of articles have appeared dealing with the synthesis of dendrigraft polymers during the past years.¹⁰⁹⁻¹¹⁵

1.1.3 Dendronized Polymers

The concept of dendrimer together with polymer constitutes various extensions of the dendrimer concept. In the case of dendrigraft polymers,

polymers are grafted on another polymer. The various conceptual extensions of the dendrimer concept are shown in the Figure (Fig 1.5).¹¹⁶

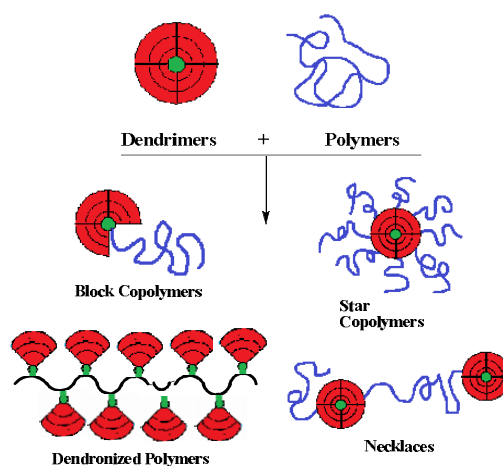


Fig 1.5 Polymer Architectures Derived from the Concept of Dendrimer and Linear Polymer¹²⁰

In the case of dendronized polymer, the focal points of the dendrons are connected to the pending functional groups. This occurs at every repeating unit along the polymer backbone. The result is a special case of a graft copolymer, a comb polymer.^{117, 118} This has the peculiar feature that all of the side chains are dendrons. Polymers with this architecture are now referred to as ‘dendronized polymers, or ‘denpols’.¹¹⁹ These terms are assigned to polymers having linear type core. In the present context, it is expected that the term dendrigraft polymer is more appropriate here. This is because; dendrons are grafted on the polymeric chain whether linear or branched. This differs from the situation of grafting of polymeric chain as in the case of Tomalia’s or Gauthier’s dendrigraft polymer. So it would be better to call dendronized polymer as dendrigraft or it can be grouped under the dendrigraft family.

Dendronized polymers were originally termed as ‘rod-shaped dendrimers’. This was reported in a patent filed by Tomalia *et al.*^{10,33,121} followed by two other articles. Frechet and Hawker, were the first to recognize similar ‘hybrid architectures’ of dendrimers and linear polymers (Fig. 1.5). They attached Frechet type dendrons to a styrene derivative and copolymerized it with styrene.¹²² Later, Percec *et al.*, recognized the predominant role of geometry in the self-assembly of polymers equipped with what they called ‘taper-shaped’ side chains.^{24,123-127} Schluter *et al.* had synthesized rod-like polymers with a conjugated backbone. He had recognized the relationship of dendron decoration with backbone conformation and the overall shape of the macromolecules.¹²⁸

Extensive research on dendronized polymers has put the field at the interface of organic chemistry, polymer synthesis, and materials science.^{62,129-141} The usual dendritic structures found in dendronized polymers are referred to as Frechet type dendrons,¹⁴² poly(amido amine) dendrons,¹²¹ Percec type dendrons,¹⁴³ and Mullen type dendrons.¹⁴⁴⁻¹⁴⁵ The most common types of polymer backbones used in dendronized polymers are poly(styrene) (PS), poly(methyl methacrylate) (PMMA), and poly(p-phenylene) (PPP). The general synthetic strategies may be conceptually distinguished into three categories (Fig 1.6). In *Graft-To Strategy*, preformed dendrons of the desired generation are coupled to the preformed polymer. This strategy is also referred to as the ‘convergent route’. In *Graft-From Strategy*, G1 dendrons are attached to the preformed polymer. Higher generations are grown by successive attachment of G1 dendrons. This approach is also termed the ‘divergent route’. In *Macromonomer Strategy*, dendrons of the desired generation

are equipped with a polymerizable group at their focal point and polymerized.¹²⁰

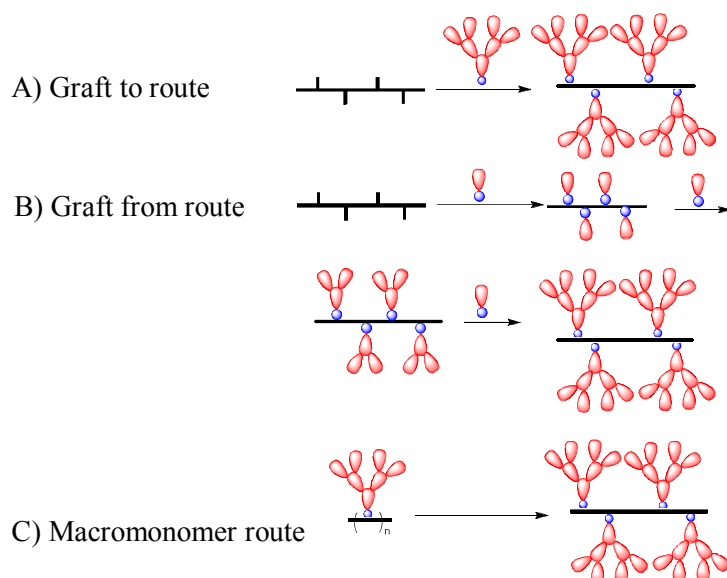
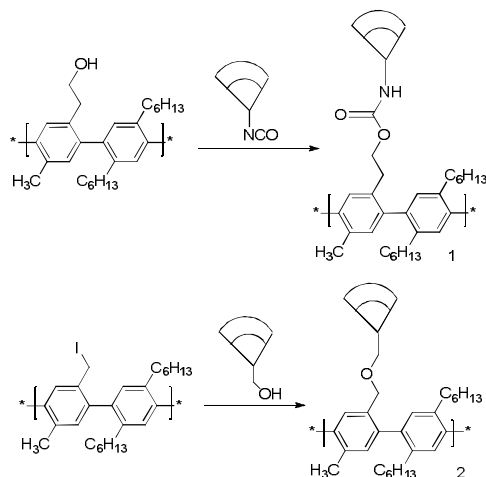


Fig 1.6 Schematic representation of synthetic strategies¹²⁰

1.1.3.1 The graft-to strategy

In the graft-to strategy, the synthesis starts from a preformed polymer chain with addition of preformed dendrons of the desired generation. The result is actually a graft copolymer rather than a structure perfect comb copolymer.^{117, 118} Here, the preformed dendritic side chains are grafted to the polymer backbone. This resembles a convergent strategy, because the preformed dendrons are attached in a convergent manner to the polymeric core molecule. Schluter *et al.* obtained dendronized poly (p-phenylene)s 1 and 2 (Scheme 1.1).¹⁴⁶⁻¹⁴⁸ Here, the degree of coverage was found to be decreasing with increasing generation of the dendron.



Scheme 1.1 Synthesis of poly(para-phenylene)s¹⁴⁷⁻¹⁴⁹

Bilibin *et al.* prepared G2 and G3 dendronized polymers carrying dendrons of L-aspartic acid and L-glutamic acid.¹⁴⁹⁻¹⁵⁰ In this case, the focal amino groups of the preformed dendrons were attached to an active ester derivative of poly(acrylic acid). Conversion to the dendronized polymer **3** (Fig 1.7) was followed by UV-Vis spectroscopy. Complete coverage was only achieved in the case of the G1 dendron.

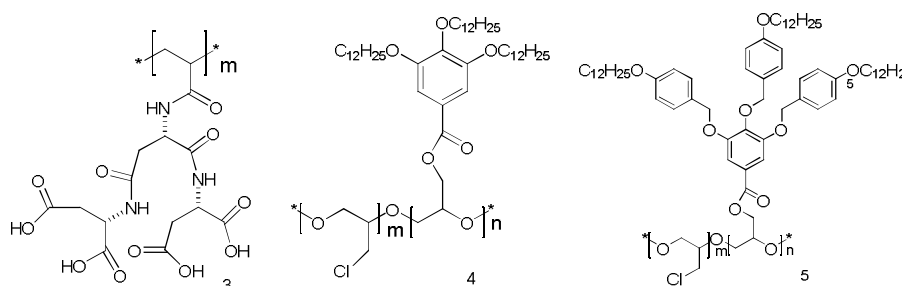


Fig 1.7 Dendronized Polymers Synthesized via Graft-to Route¹⁴⁹⁻¹⁵²

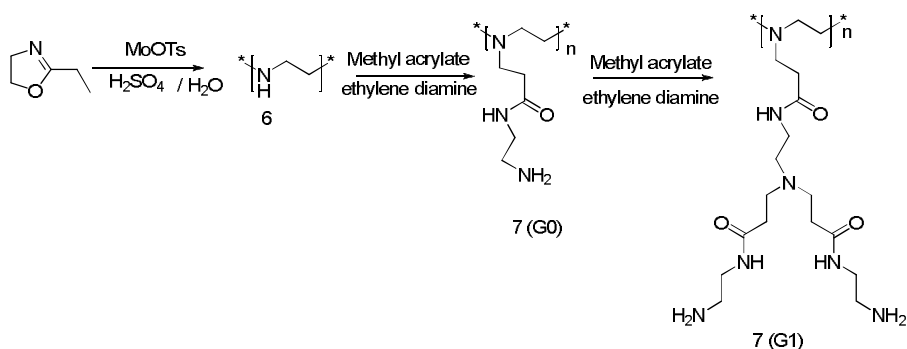
Ronda *et al.* grafted G1 Percec type dendrons to poly (epichlorohydrin) (PECH).¹⁵² The dendronized polyethers **4** obtained (Fig 1.7) exhibited a varying degree of coverage of 48–70%, as revealed from

NMR spectra. From GPC analysis using multiple angle laser light scattering (MALLS) detection, molecular weights of $M_n=700,000$ – $1,310,000$ and polydispersities of 1.89–2.18 were obtained. Similarly, the use of more bulky G1 dendrons led to polymers **5** with a degree of coverage of 39–57%. Molecular weight obtained was of the order of $M_n=1,610,000$ – $2,240,000$ and polydispersities of 1.70–2.24.¹⁵¹

1.1.3.2 The graft-from strategy

In the graft-from strategy, a two-step deprotection-coupling protocol is used whereby the dendron generation is increased successively by attaching G1 dendrons starting from the polymer core.³³ The resulting dendronized polymer is, again, a graft copolymer rather than a structure perfect comb copolymer.^{117, 118} Here, the dendritic side chains are grown off (or grafted from) the polymer backbone. This approach is comparable to a divergent synthetic strategy. The problems associated with the graft-from strategy are similar to that observed in a divergent synthesis of dendrimers. At higher generations, the required high number of simultaneous coupling is prone to create defect structures. The resulting defect species are difficult to remove from the desired product because they are too similar, both structurally and size-wise. This situation is even worse in the case of dendronized polymers as compared to classical dendrimers. Here, one starts with hundreds or thousands of functional groups and not with a few functional groups.¹⁰ In their first report on the synthesis of a dendronized polymer, Tomalia *et al.*^{10,33,121} used the linear poly (ethylene imine) **6** having a degree of polymerization of $P_n=100$ – 500 as the core (Scheme 1.2). In a two-step strategy, they built up successive generations by a Michael addition of the amine to methyl acrylate and

subsequent amide coupling with ethylene diamine and obtained **7**. The reaction conditions required 1260–10,000 fold excess of ethylene diamine per ester group and reaction times of 5–8 days. This highlights the difficulty of the strategy. Transmission electron microscopy (TEM) images revealed interesting rod-shaped features.¹²¹



Scheme 1.2 Synthesis of PAMAM Based Dendronized Polymer^{10,33,121}

A number of examples for the graft-from route deal with flexible siloxane polymers. Mery *et al.* attached silane dendrons on a poly (hydromethylsiloxane) polymer via platinum catalyzed hydrosilylation chemistry (Fig 1.8). Here, an excess of allyl trichlorosilane was used followed by reaction of the resulting chlorosilane functions with an allyl Grignard compound.¹⁵³ The resulted G1 dendronized polymer **8** (Fig 1.8) was obtained in 60% yield. The synthesis of the corresponding G2 dendronized polymer via reaction with HSiCl_3 and an allyl Grignard compound resulted in 50% yield and with a degree of coverage of up to 84%. The subsequent synthesis of a G3 dendronized polymer failed completely.

Kim *et al.* tried the synthesis of similar silane dendron functionalized poly (siloxane)s via a two-step procedure of hydrosilylation and subsequent

alkenylation. The polymers **9** obtained (Fig 1.8) differ from the Mery polymers in that they have only twofold instead of threefold branching units.¹⁵⁴ However, attempts to synthesize a G3 dendron functionalized polymer was a failure. The related polymers **10** were also prepared using a similar approach. The same authors also reported the synthesis of G1 and G2 siloxane dendron functionalized polymers **11** (Fig 1.8) via a two-step protocol involving hydrosilylation and alcoholysis with an alkenol.¹⁵⁵

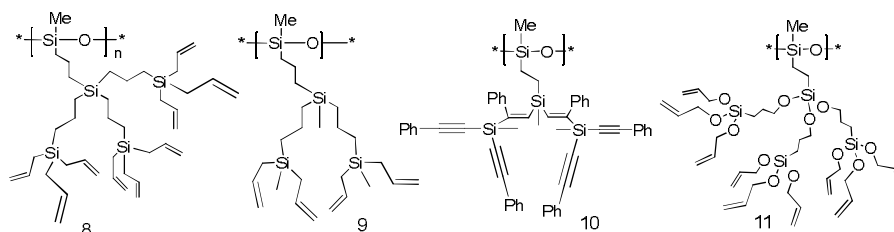


Fig 1.8 Dendronized Polymer Obtained via Graft- from Approach¹⁵⁴⁻¹⁵⁶

1.1.3.3 The macromonomer strategy

In the macromonomer strategy, the dendronized polymers are obtained via the attachment of a polymerizable group to the focal points of a preformed dendron and subsequent polymerization of the ‘macromonomers’.¹⁵⁶ This has one obvious advantage over the other two strategies. It does not involve a post-polymerization reaction. As a result, if a polymerization is feasible, the resulting polymers must exhibit a quantitative degree of dendron attachment. Hence, they are ‘structurally perfect’ comb polymers.^{117, 118} They are still not monodisperse. This is because of the inherent polydispersity in molecular weight inevitably associated with any type of polymerization reaction. Kallitsis *et al.* synthesized dendronized aromatic- aliphatic (rigid-flexible) polyethers **12** using Williamson etherification between G1 and G2 dendronized α,ω -

dihydroxyterphenyls with α,ω -dibromoalkanes (Fig. 1.9).¹⁵⁶ The polymerization reactions were carried out in a two-phase system (water/1,2-dichlorobenzene) in the presence of a phase transfer catalyst. They also synthesized polyethers **13** comprising quinquephenyl units decorated with two G2 Frechet type dendrons (Fig 1.9). Polymerization resulted in only moderate molecular weights of up to $M_n=17,900$ (PDI=2.1).¹⁵⁷

Kallitsis, *et al.* extended the investigations to similar polymers **14** (Fig 1.9) using G1 and G2 dendrons decorated with alkyl chains which helped to improve the overall solubility.¹⁵⁷ Typical molecular weights ranged from $M_n = 27,500$ (PDI=3.1, Pn = 21) to $M_n = 61,400$ (PDI = 2.5, Pn = 45) for G1, and from $M_n = 12,000$ (PDI = 2.2, Pn = 5) to $M_n = 32,200$ (PDI = 2.8, Pn = 13) for G2. The materials exhibited two separate melting points for the dendritic side chains and the main chain, respectively.

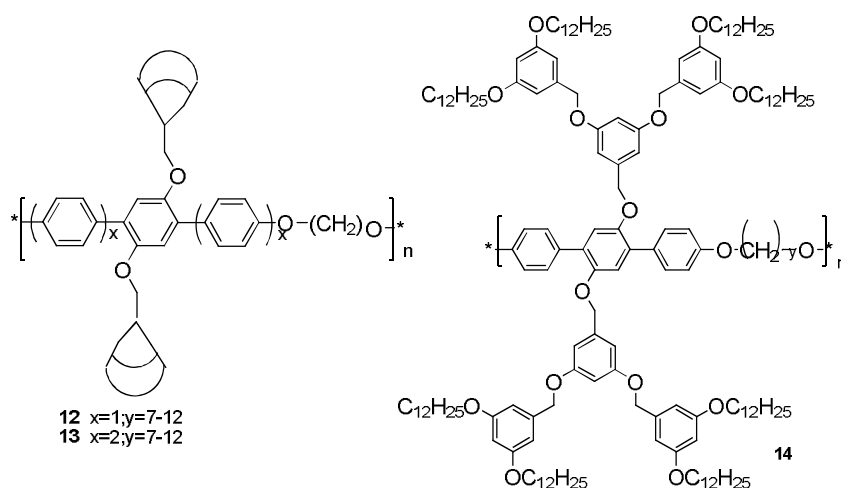


Fig 1.9 Dendronized Polymer Synthesized Using Macromonomer Strategy^{156,157}

Schluter *et al.* recognized the synthetic potential of a combined strategy for the synthesis of high molecular weight, high generation dendronized polymers. They synthesized G4 dendronized poly(styrene)s with a combination of macromonomer and graft-from strategy.^{158,159}

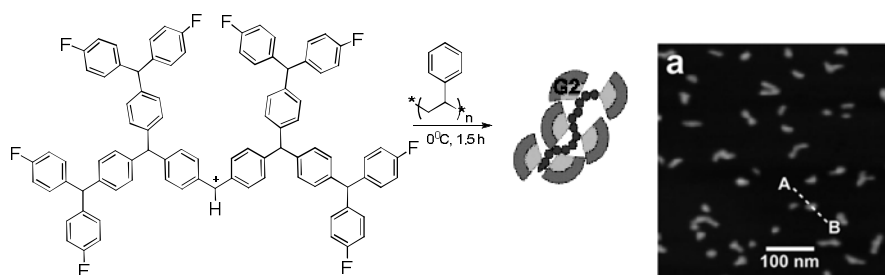


Fig 1.10 Synthesis of polystyrene dendronized polymer via combination of macromonomer and graft-from strategy and AFM image of the polystyrene DP.¹³⁰

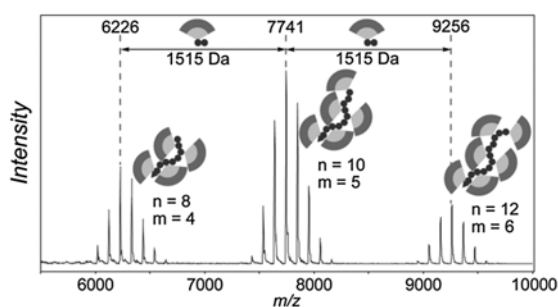


Fig 1.11 MALDI MS spectrum of polystyrene DP¹³⁰

Recently, a dendronized polymer was synthesized by the reaction of dendritic diarylcarbenium ions with unfunctionalized polystyrene.¹³⁰ The polymers obtained by the reaction of the first and the second generation dendritic diarylcarbenium ions with polystyrenes were well characterized by MALDI-TOF MS (Fig 1.11) and SEC-MALLS analysis and observed by AFM (Fig 1.10). The length and height of the string like structures of dendronized polymers were found out.

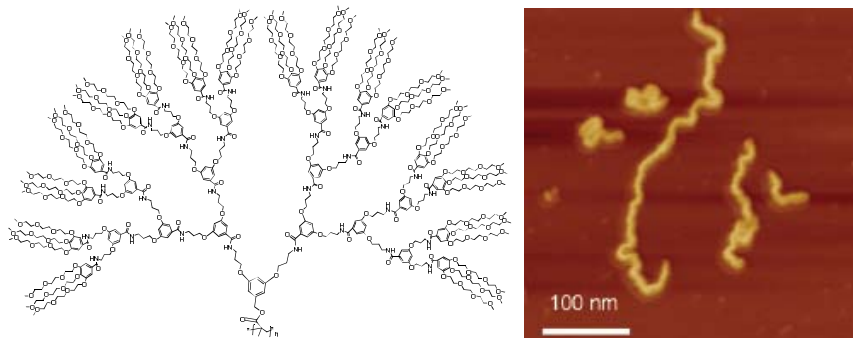


Fig 1.12 Polystyrene grafted diarylcarbenium ion and its AFM¹³⁷

Core/shell amphiphilic dendronized polymers were synthesized. They contained peripherally decorated OEG- (oligoethylene glycol) units (Fig 1.12). They were non-charged, water soluble cylindrical objects of varying cross-sectional diameter (thickness).¹³⁷ Shell and core consisted of a branching unit with three methyl-terminated triethylene glycol arms. They also contained 1, 2, 3, or 4 generations of known amide-based dendrons. They were all held together by a PMMA-type main chain backbone.

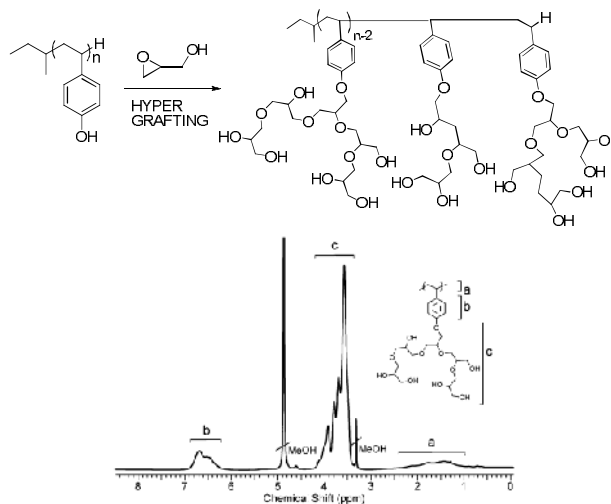


Fig 1.13 Synthesis of dendronized polymer having oligoethylene glycol at the periphery and its proton NMR spectrum¹³⁵

Frey *et al.* studied the hypergrafting of hyperbranched polyglycerol on to poly 4-hydroxystyrene.¹³⁵ Successful grafting with control over molecular weight ($10\text{-}31\text{ kg mol}^{-1}$) and low PDI was achieved (Fig1.13).

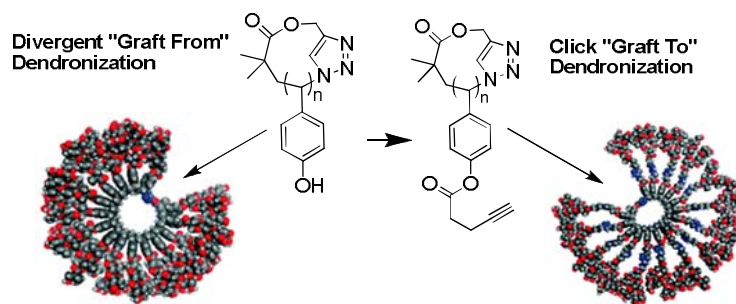


Fig 1.14 Cyclic dendronized polymer¹³¹

Grayson *et al.* reported click dendronized polymer via click cyclisation followed by graft to or graft from route¹³¹ (Fig 1.14). The divergent “graft from” approach appears to lead to materials with broad PDI at high DP, whereas the “graft to” approach yields more well-defined dendronized cyclic polymers at larger DP.

Various strategies and synthetic methods for the preparation of dendronized polymers are now well established. Nevertheless, it is still not an easy task to synthesize high molecular weight, high generation dendronized polymers. Synthetic chemists will have to continue to improve the synthetic methods, in particular with respect to the control of molecular weight, and the inclusion of higher generation dendrons.

1.2 Solid Phase Organic Synthesis

Ever since the preparation of the first tetrapeptide, Leu-Ala- Gly-Val, produced on a solid-phase, the SPPS method started to gain general acceptance.¹⁶⁰ The solid-phase organic synthesis (SPOS) (Fig 1.15) has

emerged as a powerful tool in the synthesis of organic molecules exploiting combinatorial approach.¹⁶¹⁻¹⁶³ In SPOS, the solid support-bound substrates are elaborated synthetically using excess of reagents to drive reactions to completion.¹⁶⁴ Desired products can be isolated easily by simple filtration and removed from the support material. In SPOS, the substrate is coupled to a chemically inert insoluble polymer by a covalent bond. This bond must remain stable during the whole chemical process, allowing the cleavage of the product from the resin at the end of the synthetic pathway.

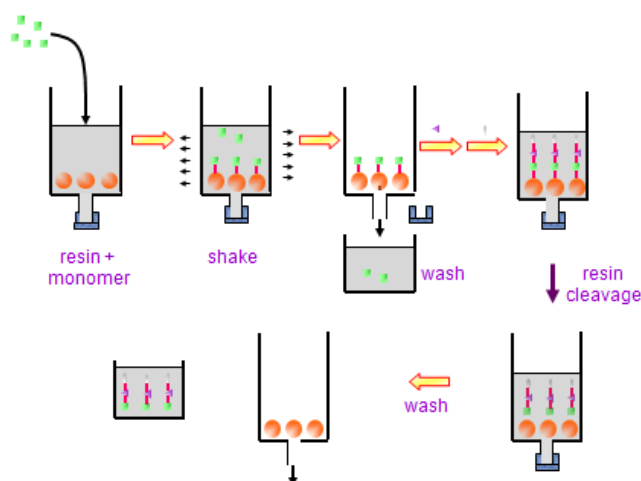


Fig 1.15 Schematic representation of SPOS¹⁶⁰

The solid-phase method has a principal advantage upon the synthesis carried out in solution, the facility in the purification process which can allow the automation of the whole synthesis. Moreover, the SPOS presents additional advantages: the possibility of using excess of reagents to ensure the completion of reactions and the "pseudo-dilution" effect.¹⁶⁵ It is possible to study the solution chemistry of the product by cleaving the same from the resin loaded polymer.

In spite of these advantages, SPOS also presents some important drawbacks: it can be difficult to adapt some conventional solution phase chemistry to a solid-phase format; the progress of solid-phase reactions is difficult to monitor. The SPOS has expanded its action field towards the synthesis of polyfunctionalized molecules and medicinal chemistry. The SPOS saves time, one of the most important features at the initial stage of a new drug discovery program. SPOS has made combinatorial chemistry successful and feasible.¹⁶⁶ Both inorganic and organic polymers have been used as supports or to mediate or promote organic reactions.^{167,168} The use of inorganic oxides, silica and modified silica, alumina, zeolites, clays, etc. have found wide applications in promoting various organic reactions.^{85,86,169-173}

On the other hand, organic polymers such as polystyrene (PS) or Merrifield resin have remained the major choice, besides the use of some other polymers.¹⁷⁴⁻¹⁷⁷ The choice of solid phase, polymers with suitable linkers, the nature of binding with the substrate/reagent (covalent or noncovalent), stability, and recyclability have remained some of the salient points for successful and efficient solid-phase synthetic protocol.

SPOS is particularly suitable for synthesis of oligomeric and polymeric compounds. Here, automation of repetitive synthesis steps is possible, which results in reproducibility and higher yields compared to manual laboratory work. A further advantage is that toxic or obnoxious low molecular weight compounds can be made odourless and less toxic when they are attached to solid polymer supports. This makes handling of these materials easier. The solid-supported chemistry can also be adapted to flow systems for both industrial and laboratory scale applications.¹⁷⁸

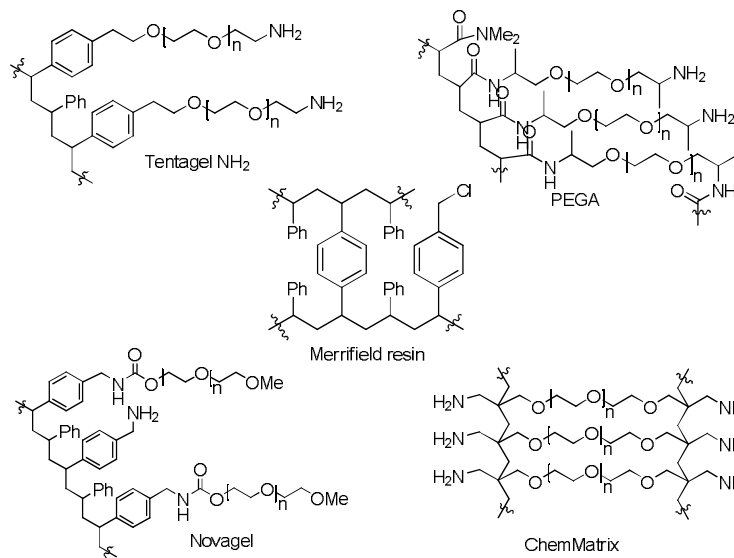
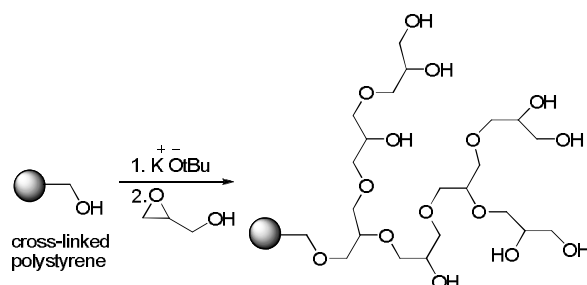


Fig 1.16 Structures of some common resins^{137,181,184,185,189,194}

There are two types of organic polymer supports: gel type microporous resins and macroporous resins. In addition to these, there are soluble polymer supports.^{179,180} There have been large number of polymer supports developed for SPOS. The most commonly used resins (Fig 1.16) are polystyrene cross-linked with divinylbenzene (DVB-PS) or 1,4-bis (vinyl phenoxy) butane¹⁸¹ (Janda Jel), polystyrene- poly(ethylene glycol) graft copolymers^{182,183} (PEG-PS, Tentagel or TG, Argogel, Novagel), polyacrylamides^{184,185}(Pepsyn), polyacrylamides cross-linked with PEG¹⁸⁶ (PEGA), PEG cross-linked ethoxylate acrylate resin¹⁸⁷(CLEAR), cross-linked PEG¹⁸⁸(ChemMatrix), and Silica^{189,190}(controlled pore glass, *i.e.* CPG). The support material is mostly in bead form in either 100–200 mesh (75–152 μm) or 200–400 mesh (37– 75 μm) range. Degree of cross-linking determines how much a polymer can swell. Low level of cross-linker yields exceedingly swellable, mechanically weak resin networks. Highly cross-

linked polymers, though mechanically stronger, do not swell much even in good solvents.¹⁹¹⁻¹⁹³

One of the major drawbacks of PEG as a support in organic synthesis is that, it can be functionalized only at the terminal ends. Thus, its loading level is inversely proportional to its molecular weight. To overcome this limitation, while maintaining the general polyether structure of PEG, polyglycerol has been studied (Scheme 1.4).¹⁹⁵



Scheme 1.4 Grafting of polyglycerol on to Merrifield resin¹⁹⁶

In order to simplify and speed up polymer separation, polyglycerol has been grafted onto polystyrene resin to get a heterogeneous support using a heterogeneous alcohol core. Polystyrene - *graft*- polyglycerol has similar properties to Tentagel in terms of swelling. This has the key advantage of having a much higher loading capacity, up to 4.3 mmol g⁻¹ compared to less than 1.0 mmol g⁻¹ for Tentagel. However, one potential drawback is that, it is functionalized with nonequivalent alcohol groups.

When demand for resins with high loading was increased, research was focussed on bead-loading enhancement via a dendrimerisation process. Resins with loading up to 96 nmol/ bead were prepared by solid-phase dendrimerisation using a symmetrical 1-3 C-branched isocyanate

monomer.¹⁹⁶ Dendrimer resin beads have shown compatibility for many chemical conditions, however high functional group density could produce undesirable site–site interactions.¹⁹⁷

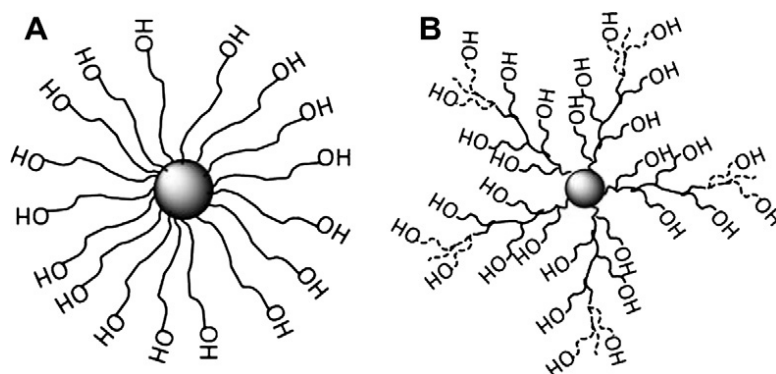


Fig 1.17 The Polystyrene–PEG resins by different methods (A–unbranched PSt–PEG; B–branched PSt–PEG).¹⁹⁸

Polystyrene resin with high loading capacity was prepared by grafting poly (ethylene glycol) acrylate monomer to Merrifield resin (Fig 1.17). This was achieved through activators generated by electron transfer atom transfer radical polymerization.¹⁹⁹ The grafted resins demonstrate good swelling ability in both polar and nonpolar solvents. The swelling ability of the grafted resin was increased two-fold of Merrifield resin in the polar solvents. It enabled high functional group loading up to 0.5–1.2 mmol g⁻¹ compared with the conventional polystyrene-*graft*-poly (ethylene glycol) (0.15–0.25 mmol g⁻¹).^{83,199} Recently, a facile solid-phase synthesis of inverse poly(amidoamine) dendrons was developed.²⁰⁰ Upon introduction of AB₂-type monomers, each dendron generation was constructed via one reaction. G2 to G5 dendrons were constructed in a peptide synthesizer in 93, 89, 82, and 78% yields, respectively, within 5 days.

A wide range of organic polymers have been used as supports in organic synthesis, in order to facilitate separation of the products from reagents or catalysts used to prepare it. Some of the important milestones in this field include the development of materials for the encapsulation of heterogeneous metal catalysts. This has led to situations in which leaching of less than a part per million of the entrapped species was observed.⁸⁸ Future developments in this field undoubtedly will take advantage of some of the recent advances in polymer synthesis technology.

1.3 Polymer Supported Catalysis

The development of well-defined catalysts that enable rapid and selective chemical transformations which can be separated from the product is still an important challenge.²⁰¹ Catalyst separation can be made easy by attaching the homogeneous catalyst to insoluble supports.²⁰²⁻²⁰⁴ Materials such as modified silica and cross-linked polystyrene are particularly suited as heterogeneous catalyst supports because of their high physical strength and chemical inertness. The catalytic species become more stable and show more selectivity when they are attached to the solid support. The most important advantage in using a functionalized polymer as support of a catalyst is the simplification of product work-up, *i.e.*, separation, and isolation. For separation and isolation of products, simple filtration is sufficient. Complex chromatographic techniques are not usually required. Expensive materials can be efficiently retained when attached to a polymer support. If appropriate chemistry is available, they can be recycled many times. Malodorous and harmful substances can be handled easily by attaching them to polymers and they can be easily separated from the final product. In addition, polymer

supported catalysts can be manipulated easily. Large amount of diversity can be introduced by techniques of combinatorial chemistry like mix and split method.²⁰⁵ But the problems related to this approach are the non-uniform and partly unknown structures of the heterogenized catalysts, mass transport limitations due to slow diffusion, the generally lower activity compared to the homogeneous analogue, and metal leaching. Metal leaching can be suppressed by using properly chosen ligands that coordinate strongly to the metal. Organic polymers show solvent-dependent swelling properties that can strongly influence the catalytic performance. The use of soluble supports leads to recyclable catalyst systems that do not suffer from mass transfer limitations. They can lead to systems with activities similar to their monomeric analogues.²⁰⁶

Dendrimers as soluble supports have recently attracted a lot of attention, since these well-defined macromolecular structures enable the construction of precisely controlled catalyst structures.²⁰⁷ The number of catalytic species attached to the support as well as their location can be regulated. This particular aspect is of crucial importance for the catalytic performance of the system. Moreover, the globular shape of the higher generations of dendrimers is particularly suited for membrane filtration.²⁰⁸ Dendritic catalysts can be recycled using similar techniques as applied for their monomeric analogues such as precipitation, two-phase catalysis, and immobilization on insoluble supports. In addition, the large size and the globular structure of the dendrimer, compared to the substrates and the products, can be utilized to facilitate catalyst-product separation by means of nanofiltration.²⁰⁹ Nanofiltration can be performed batch-wise and in a continuous-flow membrane reactor

(CFMR). Dendritic catalysts can show the kinetic behaviour and thus the activity and selectivity of a conventional homogeneous catalyst. They can be recovered from the reaction medium easily. Other advantages of dendritic catalysis include the ability to fine-tune the catalytic centres by ligand design and the ability to perform mechanistic studies on these uniformly distributed catalytic sites attached to the support.⁶⁵

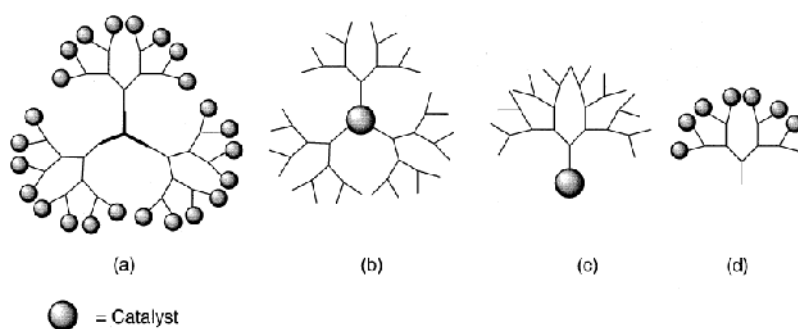
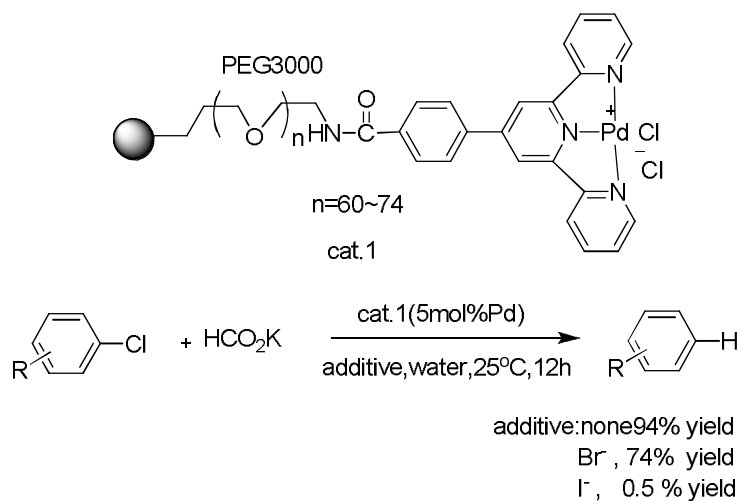


Fig 1.18 Dendritic catalyst architectures²¹⁰

The catalytic performance of the system depends on the dendritic architecture. One should therefore distinguish the polymer as either periphery functionalized, core-functionalized or focal point-functionalized systems (Fig 1.18). Periphery-functionalized dendrimers have their catalysts located at the surface of the dendrimer support. The active sites are therefore directly available to the substrate. This is in contrast to core-functionalized systems in which the substrate enters the dendrimer prior to reaction. The high accessibility allows reaction rates that are comparable with homogeneous systems. The periphery-functionalized systems contain multiple reaction sites. This results in extremely high local catalyst concentrations. There exist proximal interactions between catalytic groups and steric crowding at the periphery of dendritic catalysts. This may lead to cooperative effects and a certain selectivity profile, which could further

increase the catalytic effect.²¹¹ In core (and focal point)-functionalized dendrimers, the catalyst could especially benefit from the site isolation created by the environment of the dendritic structure. Site isolation effects in dendrimers can be beneficial for other functionalities. Core-functionalized dendritic catalysts may benefit from the local environment created by the dendrimer which differs from the bulk solution.⁹ The combination of the advantages of solid supported system along with dendritic system together constitutes the third approach, *i.e.* solid supported dendritic systems. Recent interest in the development of environmentally benign synthesis has evoked a renewed interest in developing polymer-bound dendritic catalysts for organic synthesis that maintain high activity and selectivity.^{212,213} The polymer support may be linear, cross-linked, dendritic or a polymer supported dendritic entity. A brief discussion on dendritic and polymer supported dendritic catalysts is provided starting from the non-dendritic one.



Scheme 1.5 Hydrodechlorination of aryl chlorides by polymer supported terpyridine Pd complex²¹⁵

Polymer-supported terpyridine palladium complex was found to promote hydrodechlorination of aryl chlorides with potassium formate in seawater (Scheme 1.5).²¹⁴ Generally, reductive cleavage of aryl chlorides using transition metal catalysts is more difficult than that of aryl bromides and iodides (reactivity: I > Br > Cl). In the reported instance, the results did not follow the general trend. The authors have investigated the reaction inhibition agents and found a method to remove these inhibitors. The polymeric catalysts showed high catalytic activity and high reusability for transfer reduction in seawater.

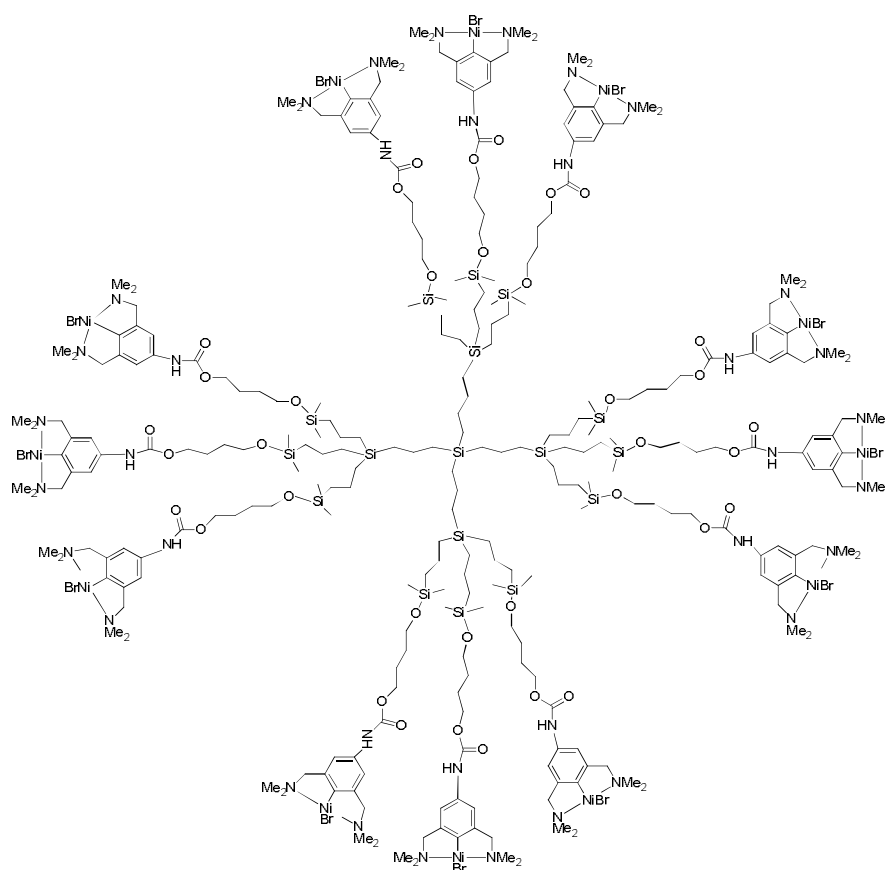


Fig 1.19 Polysilane dendrimer catalyst²¹⁶

The polysilane dendrimers (Fig 1.19) which are functionalized at their periphery with metal-containing catalytically active sites show regiospecific catalytic activity for the Kharasch addition of polyhalogenoalkanes to carbon-carbon double bonds. It was shown to be possible to remove the nanoscale catalytic macromolecules from the solution of products using filtration methods.²¹⁵

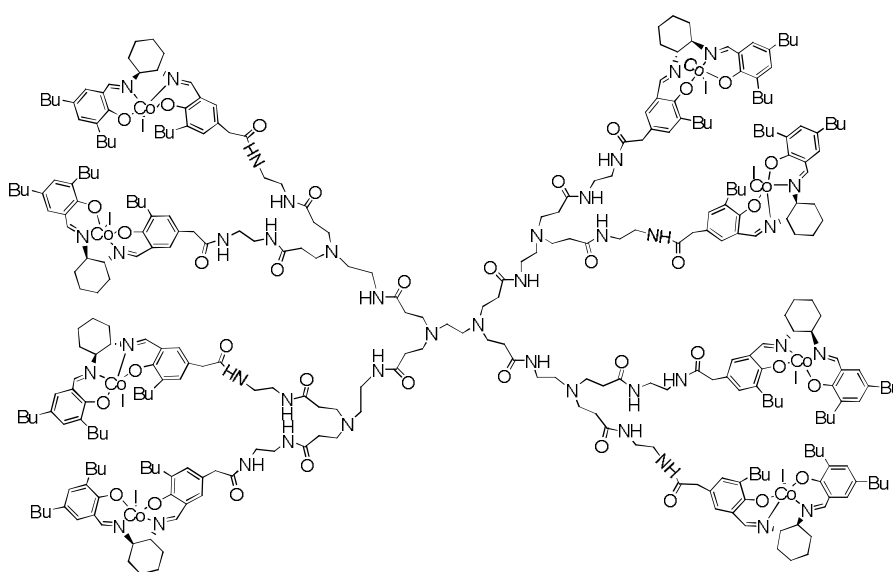


Fig 1.20 Jacobsen's dendritic [Co(salen) complex]²¹⁷

The hydrolytic kinetic resolution (HKR) of terminal epoxides is supposed to proceed using cobalt (salen) complexes as catalysts (Fig 1.20).²¹⁶ The catalytic activities of G1 to G3 PAMAM dendrimers containing 4, 8 and 16 catalytic residues at the periphery were superior to those of the monomeric and dimeric catalysts, indicating a positive dendrimer effect. This effect was assigned to the dendritic confinement of the Co-salen complexes at the surface of the macromolecule that was claimed to reinforce cooperative catalytic activity.

On increasing the dendrimer generation, the periphery became bulky, restricting access of the substrate to the catalytic metal centre. Therefore, a better spatial separation of catalytic sites in the dendrimer should be arranged.

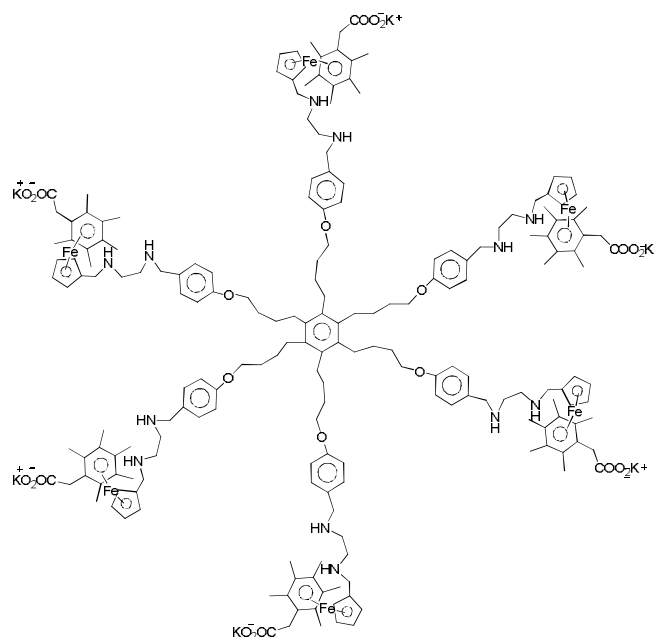


Fig 1.21 Astruc's water-soluble star-shaped catalyst for cathodic reduction of nitrates and nitrites to ammonia²¹⁹

This problem was recognized in several such systems. It was suggested that star-shaped structures containing catalysts at the branch termini should not suffer from such steric constraints.²¹⁷ Star-shaped hexanuclear catalysts containing six CpFeI (arene) complexes (Fig 1.21) are efficient redox catalysts for nitrate and nitrite reduction to ammonia in water. This could occur without kinetic loss compared with monometallic catalysts.²¹⁸ This shows that, there was no steric inhibition at the periphery. This was often encountered in dendritic frameworks loaded with catalysts at the branch termini (negative dendritic effect).²¹⁹

Catalysis of ring-closing metathesis (RCM), cross metathesis (CM) and enyne metathesis (EYM) of hydrophobic substrates was reported in water and air under ambient or mild conditions using low catalytic amounts (0.08 mol%) of a suitably designed “click” dendrimer (Fig 1.22).⁷⁴ The catalyst could be reused many times. This was similar to Grubbs’ second generation olefin-metathesis catalyst.^{75,220,221} Dendrimer plays the protecting role of a nanoreactor towards the catalytically active species, in particular, the sensitive ruthenium-methylene intermediate, involved in the metathesis catalytic cycle, preventing catalyst decomposition in the presence of an olefin substrate.

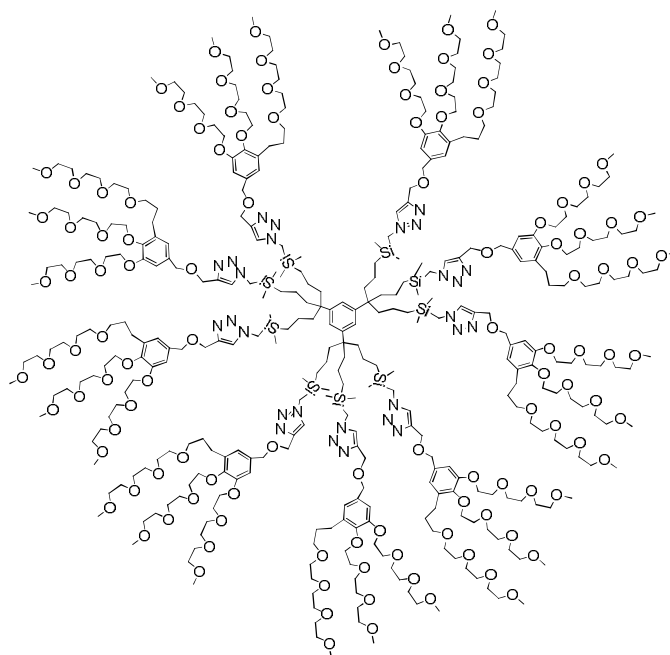


Fig 1.22 PEG-ended water-soluble dendrimer for Grubbs-catalyzed olefin metathesis of hydrophobic substrates in water⁷⁴

The development of core-functionalized chiral dendritic phosphorus ligands including diphosphines, monodentate phosphoramidites, and P,N-ligands was achieved by incorporating the ligand functions to the core or the

focal point of Frechet-type dendrons⁶² (Fig 1.23). Their transition metal (Ru, Rh, or Ir) complexes have been applied in the asymmetric hydrogenation of prochiral olefins and ketones, as well as some challenging imine-type substrates. All reactions were carried out in a homogeneous manner, and the structure–property relationships in some cases were established. The sterically demanding dendritic wedges were found to play important roles in catalytic properties. They exhibited better catalytic activities or enantioselectivities or both when compared with those obtained from the corresponding monomeric catalysts. In addition, the dendritic catalysts could be readily recycled by means of solvent precipitation, water- or temperature-induced two phase separation. Study has thus demonstrated that dendrimer catalysis could combine the advantages of both classical heterogeneous and homogeneous catalysis.

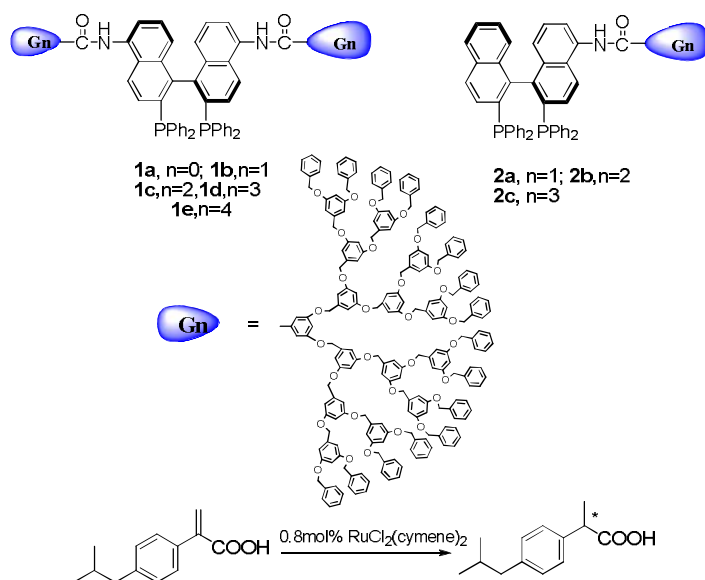


Fig 1.23 Structure of dendritic BINAP ligands and asymmetric hydrogenation of 2-(4-isobutylphenyl) acrylic acid using dendritic BINAP ligands⁶²

The 27-ferrocenyl-terminated and the 27-cobalticenium-terminated metallodendrimers were reported using hydrosilylation reactions and click synthesis methodology.⁶⁰ Both the dendrimers are isostructural in their neutral forms. They show the same intensities for the redox exchange between their neutral and cationic forms. This corresponds approximately to the transfer of 27 electrons, as deduced from the Bard–Anson equation (Fig. 1. 24).²²²

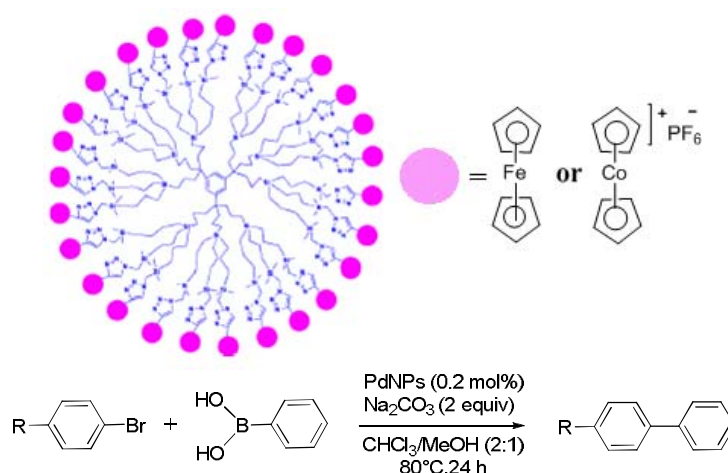


Fig. 1.24 Schematic diagram of 27-ferrocenyl-terminated and 27-Cobalticenium terminated dendrimer and Suzuki Miyaura coupling reaction⁶⁰

The ferrocenyl terminated metallodendrimer was used to generate dendrimer-encapsulated palladium nanoparticles (PdDENS). Their catalytic activity was evaluated for the Suzuki–Miyaura C–C coupling with various substituted aryl bromides (0.2 mol% of Pd per mole of substrate used). This activity is lower than that of previously studied dendrimers containing longer tethers.⁶³ It was better than using ferrocenyl terminated metallodendrimer, emphasizing the crucial role of the peripheral thickness of dendrimers that encapsulate PdNPs.

1.3.1 Dendrimers Supported on a Solid Phase

The synthesis of libraries on solid supports has many advantages over the solution phase approach. The one-bead-one-compound concept makes the solid phase chemistry especially attractive for the split-and-mix methodology. Each bead can be separately screened for active compounds. Soluble supports do not have this feature. However, the small quantity of compound that is obtained from a single bead hampers routine screening. Furthermore, identification of active compounds on beads requires tagging or deconvolution techniques. These limitations to single-bead screening can be overcome by increasing the loading capacity one order of magnitude by attaching dendrimers to the solid support.²²³ All the major resin supported dendrimers reported during the last two decades are cited,^{196,224-274} a few important ones among them are discussed.

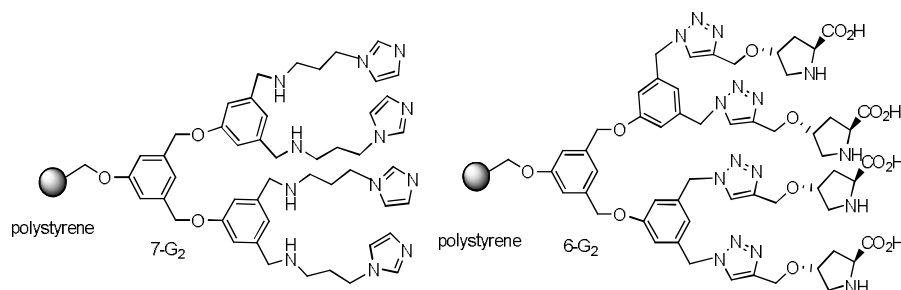


Fig 1.25 Polystyrene supported benzylether dendron modified with proline and aminopropylimidazole.^{271,273}

Portnoy *et al.* reported the synthesis of polystyrene supported benzylether dendron modified with proline at the periphery (6-G₂, Fig 1.25). Positive dendrimeric effects on yields and enantioselectivities were observed in the reaction of acetone with functionalized benzaldehydes.²⁷³

A related reaction, the Baylis–Hillman reaction of methyl vinyl ketone with 4-nitrobenzaldehyde, was carried out with aminopropylimidazole-functionalized benzylether dendrons immobilized on polystyrene (7-G2).²⁷¹ In this case also, a positive dendrimeric effect on the catalytic efficiency was observed, compared to imidazole directly immobilized on the resin.

Later, Portnoy reported the synthesis of polymer-supported dendrimers, decorated at the periphery with N-alkylated imidazoles (Fig 1.26). The author has presented the details of the exploration of their activity, recyclability, and dendritic effects, in the catalysis of the Baylis–Hillman reaction.²⁷⁵ The present catalyst was more effective than proline alone modified catalyst. The polystyrene-supported N-alkylimidazole-based dendritic catalysts exhibited one important feature of multivalent architecture for an organocatalyst. The yields in the model reaction of methyl vinyl ketone with p-nitrobenzaldehyde were more than tripled when a non-dendritic catalyst was replaced by a second- or third-generation analogue.²⁷⁶ Moreover, the reaction of less active substrates did not occur with the non-dendritic catalyst and proceeded to a significant extent only with the analogous catalysts of higher generations. The expected reason of the dendritic effect is the assistance of the second, nearby imidazole moiety in the presumably rate-determining proton transfer in the intermediate adduct, after the first imidazole unit induced the formation of the new carbon-carbon bond.

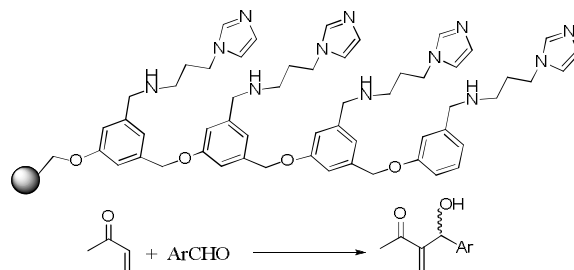
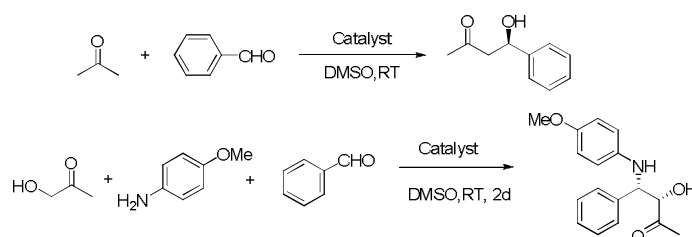


Fig 1.26 The polystyrene-supported N-alkylimidazole-based dendritic catalysts²⁷⁵

Importance of dendritic architecture towards proline based catalyst was demonstrated using enantioselective aldol and Mannich reactions (Scheme 1.6).²⁶⁸ L-proline was immobilized as an ester or amide on polyether dendritic spacers attached to polystyrene.



Scheme 1.6 Aldol and Mannich reactions with polymer bound dendritic L-proline²⁶⁸

The ester functionalized catalysts showed a remarkable positive dendritic effect on the yield and enantioselectivity, in the aldol reaction of acetone with aromatic aldehydes. The positive dendritic effect of the L-proline appended catalytic systems on the yield, diastereo- and enantioselectivity of a three-component Mannich reaction was more significant (Scheme 1.6). The enantiomeric excess was increased corresponding to an increase in the yield in the case of supported dendritic L-proline compared to the detached proline. This is a clear case of the influence of dendritic architecture.

A recent report on sterically congested polyether dendrimer using solid phase assembly up to third generation has demonstrated the unexpected cleavage into monomeric units under acidic conditions (Fig 1.27).²⁷⁷ The predicted reason is the increased electron density of the aromatic rings of the monomeric units destabilizing the bonds, connecting them in the dendritic framework. The authors have suggested a solution to this problem. They have suggested to increase the acidity of the medium in order to undergo complete degradation.

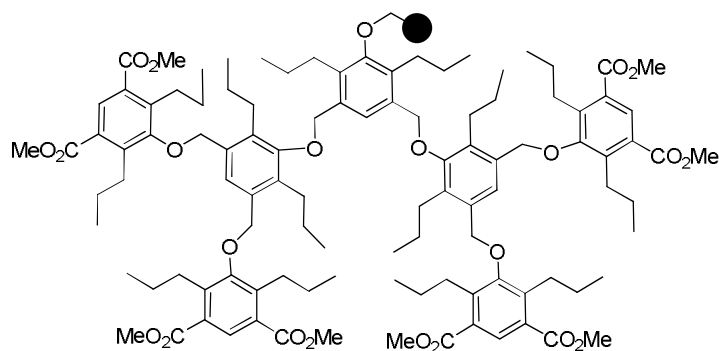
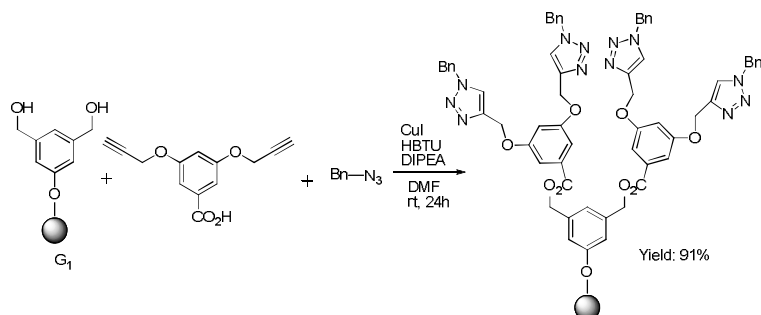


Fig 1.27 Polyether dendrons on solid support²⁷⁷

Functionalization of Wang polystyrene resin was done by combined approach of esterification and CuAAC (Copper-Catalyzed Alkyne-Azide Cycloaddition) in a one-pot reaction (Scheme 1.7). It was also demonstrated for the first time that it was possible to combine esterification with either Glaser or Eglinton acetylene-couplings in a one-pot reaction.²⁷²⁻²⁷⁷ Finally, it was demonstrated that the esterification, CuAAC, and Glaser-coupling reactions were all compatible with each other, and it was possible to run in parallel esterification/ CuAAC and esterification/ Glaser coupling in a single vessel.²⁷⁸



Scheme 1.7 Functionalization of Wang polystyrene resin²⁷⁸

A novel strategy for the production of gold nanoparticles on PAMAM-grafted polystyrene–divinylbenzene beads by immobilizing a reductant onto polymer microspheres was reported.²⁷⁹ The resulting catalyst was highly efficient and stable for the aerobic oxidation of primary and secondary benzyl alcohols and for the homocoupling of phenylboronic acids under mild conditions. Moreover, the catalyst was easily recoverable and could be reused fourteen times without significant loss of activity.

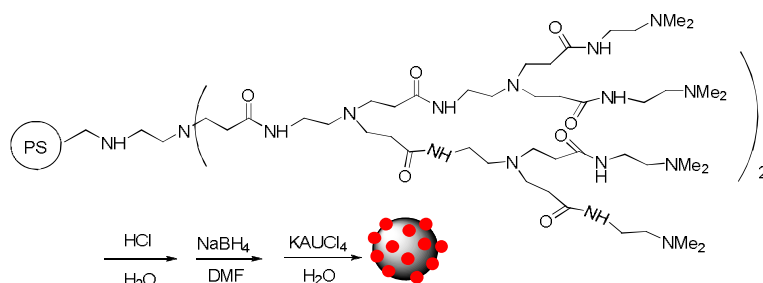


Fig 1.28 Synthesis of gold nanoparticles on PAMAM-grafted polystyrene²⁷⁹

In contrast, the AuNP catalyst prepared using the conventional approach exhibited a dramatic loss of catalytic activity in the repetition experiments. So PAMAM functionalization followed by reductant complexation and transition metal salt reduction is an effective method for the synthesis of immobilized transition metal nanoparticle catalysts (Fig 1.28).

The first use of polystyrene-supported poly(amidoamine) (PAMAM) dendrimers as heterogeneous basic organocatalysts for carbon–carbon bond formation was reported by Sreekumar *et.al.*⁸⁰ First, second and third generations have been used as reusable base catalysts in Knoevenagel condensations of carbonyl compounds with active methylene compounds. The reactions proceeded in short periods of time and with 100% selectivity. A similar catalyst was reported for three component Mannich reaction between aldehydes, ketones and amines in water with good to excellent yields and high selectivity in the presence of zero and first generation poly (amidoamine) (PAMAM) dendrimers.²⁸⁰ The products and the catalyst were separated by simple biphasic extraction. The catalyst was found to be reusable. The PAMAM catalyst was also reported for nucleophilic ring opening of epoxides by anilines under mild conditions.⁸¹ Higher generation dendrimer showed increased catalytic activity. The catalytic activity of supported dendrimer was compared with the unsupported one and found that the supported dendrimer was a much more active catalyst. The higher activity of the supported dendrimer is assumed to be due to the better hydrophobic or hydrophilic interaction existing between the polystyrene matrix and the polar dendritic chains.

Manganese complexes of polystyrene-supported poly (amidoamine) dendrimer were reported for oxidation of secondary alcohols.⁸² The catalysts showed high stability and efficiency under various reaction conditions and with different substrates. The catalysts could be recycled. The supported PAMAM palladium nanoparticles were used as heterogeneous catalysts for the Suzuki coupling between aryl

boronic acids and aryl halides.⁸⁴ Various factors affecting the catalyst's performance were studied. Higher generation dendrimer gave well-defined nanoparticles without agglomeration and these particles showed good catalytic performance.

Sreekumar *et al.* also reported PPI dendrimers for Knoevenagel condensation reaction (Fig 1.29). An iterative synthesis including double Michael addition of acrylonitrile to the primary amino groups on cross-linked polystyrene support followed by reduction of nitrile groups to amino groups gave poly (propylene imine) dendrimers up to third generation attached to the polystyrene support.⁷⁹ The supported dendrimer was used as an organocatalyst for Knoevenagel condensations. The supported catalyst showed good selectivity and the product was obtained in excellent yield under green reaction conditions.

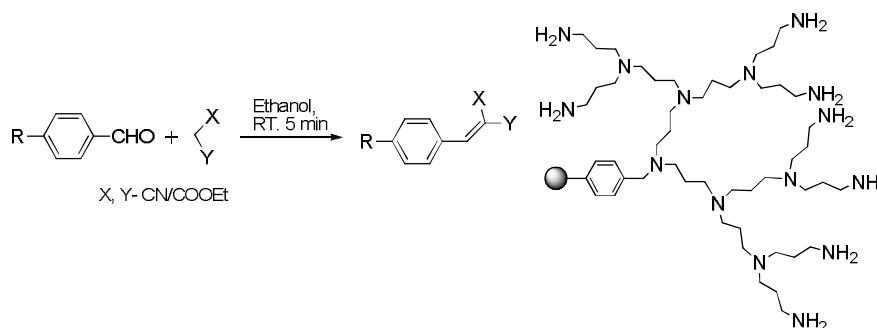


Fig 1.29 PPI catalyst for Knoevenagel condensation⁷⁹

Polysilane supported polyamine dendrimer system for Knoevenagel condensation reaction was reported recently by Sreekumar *et al.*⁸⁶ Polysilane support was synthesized by the polymerization of trichloromethylsilane. The poly (propyleneimine) (PPI) dendrimer was generated on the polymer support by divergent method. The dendrimer was synthesized up to three

generations (G3). The dendrimer functionalized polysilane (PS-PPIG3) was found to contain high concentration of terminal amino groups. The catalytic activity of the PS-PPIG3 dendrimer was generalized by conducting the Knoevenagel condensation reaction with diverse sets of substrates, and was found to be an efficient organocatalyst. The condensation product could be easily separated from the reaction medium because of the heterogeneous nature of the polymer support. The reaction conditions were optimized, and the catalyst was found to be reusable.

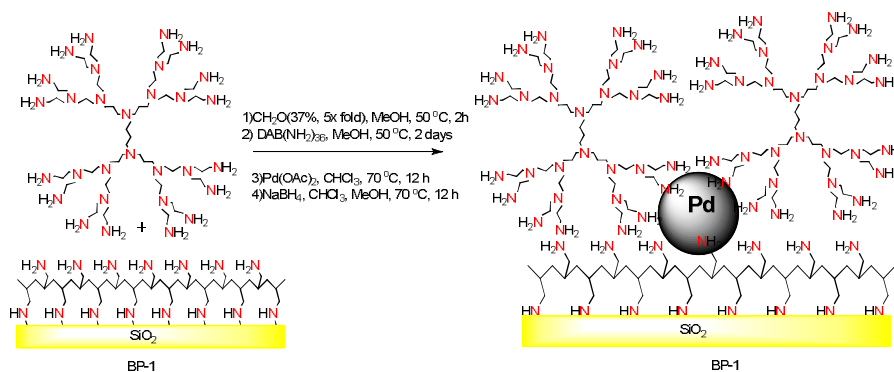


Fig 1.30 Grafting to silica and incorporation of Pd nanoparticle into PPI dendrimer⁷⁸

New heterogeneous hydrogenation catalysts, based on Pd nanoparticles and poly (propyleneimine) (PPI) dendrimers of the third generation that have been covalently grafted to a silica surface modified with poly (allyl amine) (PAA) have been reported (Fig 1.30).⁷⁸ The synthesized materials are effective catalysts for the selective hydrogenation of dienes to monoenes and phenyl acetylene to styrene at very high substrate: Pd ratios with turnover rates higher than those for related Pd nanoparticle catalysts. The synthesized catalyst was found to be reused without any loss of activity in the case of styrene and isoprene.

1.4 Origin, Objectives and Approach to the Thesis

Most of the works discussed in the field of catalysis were using dendrimers or hyperbranched polymers. Our focus is on the new trend in dendritic architecture, *i.e.*, dendronized or dendrigraft polymer. During the last few years, dendronized as well as dendrigraft polymers are well notified for their application in the field of material science due to their structural perfection. Nobody, within our knowledge, have tried these systems for catalytic applications, particularly, the synthesis of these systems on a polymer support. We have taken the challenge to synthesize this architecture on polystyrene support. Our intention was to create the dendrigraft architecture having large amount of peripheral functionality even at the low generation level. The present approach was centred on the synthesis of dendrigraft systems on the polystyrene support and functionalization of the periphery of the low generation polymer.

The objectives of the research described in this thesis are: to prepare and characterize polymer-supported dendrigraft polymers, to investigate the amount of peripheral functionality, to prepare their transition metal complexes, and to utilize the metal complexes in certain organic chemical transformations. The dendrigraft polymer - metal complexes were fully characterized and their efficiency as heterogeneous catalyst for the synthesis of some heterocyclic compounds was studied.

1.5 Characterisation Methods

The IR spectra were recorded with samples as KBr pellets using JASCO 4100 FTIR spectrometer. The spectra were recorded at ambient temperature by making pressed pellets of the compounds. Solid state CP-

MAS ^{13}C -NMR spectra were recorded with a Bruker 400 MHz instrument with a spinning rate of 7 KHz (NCL, Pune). The ^1H and ^{13}C NMR spectra of compounds were recorded using a JEOL JNM-ECS400 spectrometer using CDCl_3 or $\text{DMSO-}d_6$ as solvent and TMS as an internal standard (STIC, CUSAT). Melting points were determined in open capillary tubes on a Büchi Melting Point B-540 apparatus and are uncorrected. GC analysis was carried out on a 1200 L Single Quadruple, Varian Gas Chromatograph model. The SEM characterization was carried out using the JEOL Model Scanning Electron Micrograph with an attached energy-dispersive X-ray detector. Scanning was done at the 1–20 μm range and images were taken at a magnification of 15–20 kV. Data were obtained using INCA software. The standardization of the data analysis is an integral part of the SEM-EDX instrument employed (STIC, CUSAT). TEM analysis was carried out with JEM 2100 HRTEM (STIC, CUSAT). AFM analysis was carried out with Nanosurf easyscan 2 by spin coating the sample on a glass plate. MALDI-TOF/MS analysis was performed on Bruker Daltonics UltrafleXtreme model equipped with smart beam solid state laser (337nm) in reflectron positive ion mode using 19KV acceleration voltage. The samples were co-crystallized with α -cyano-4-hydroxycinnamic acid matrix on the target plate (384-well ground steel plate; Bruker Daltonics, Bremen, Germany) and external peptide mass calibration was applied (Peptide mixture 1) as per the manufacturer's instructions (RGCB and NIIST, Thiruvananthapuram, Kerala, India). Thermogravimetric analysis was performed using a Perkin Elmer, Diamond TG/DTA system at a heating rate of $10^\circ\text{C min}^{-1}$ under an atmosphere of nitrogen using an aluminium pan. Magnetic susceptibilities of the complexes were measured by the Gouy method, using $\text{Hg}[\text{Co}(\text{NCS})]$ as the calibrant

(IIT, Chennai). The copper and palladium content was estimated with the help of atomic emission spectroscopy, ICP-AES Thermo Electron IRIS INTREPID IIXSP DUO model (STIC, CUSAT). The samples were prepared by first igniting them in a Bunsen flame. Subsequently, the residue was acid digested followed by evaporation to dryness. To the dry mass, 20 mL of distilled water was added and the metal content was estimated in AES. The metal contents were also obtained from EDX analysis (STIC, CUSAT). The diffuse reflectance UV-Vis spectra of the solid samples were recorded using UV-Vis-NIR Ocean Optics Spectrophotometer SD 2000 model equipped with a diffuse reflectance accessory. The powder X-ray diffraction (XRD) patterns were recorded on a Bruker AXS. D8 Advance X-ray diffractometer (STIC, CUSAT). XPS measurements were carried out using a multi-probe system (Omicron Nanotechnology, Germany) equipped with a dual Mg/Al X-ray source and a hemispherical analyzer operating at constant analyzer energy (CAE) mode. The Mg K α X-ray source was operated at 300 W and 15 kV. The base pressure in the analyzing chamber was maintained at 1×10^{-10} mbar. Charging of the samples was corrected by setting the binding energy of the adventitious carbon (C 1s) at 284.6 eV (AIMS, Cochin). EPR analysis was performed using JES –FA200 ESR Spectrometer (IIT, Mumbai). The enantiomeric purity of the endo- and exo products were determined by HPLC on a Chiralpak IB-3 column eluted with a mixture of hexane/iPrOH (90:10) at a flow rate of 0.5 mL min⁻¹ and detected at 254 nm.

1.6 References

- [1] Flory P. J., *Journal of the American Chemical Society*, **1941**, 63, 3083-3090.
- [2] Flory P. J., *Journal of the American Chemical Society*, **1941**, 63, 3091-3096.
- [3] Flory P. J., *Journal of the American Chemical Society*, **1941**, 63, 3096-3100.
- [4] Tomalia D. A., Brothers II H. M., Piehler L. T., Hsu Y., *Polymeric Materials Science and Engineering*, **1995**, 73, 75-79
- [5] Tomalia D. A., *Macromolecular Symposium*, **1996**, 101, 243-255.
- [6] Dvornic P. R., Tomalia D. A., *Science Spectra*, **1996**, 5, 36-41.
- [7] Naj A. K., *Persistent Inventor Markets a Molecule in The Wall Street Journal: New York*, **1996**, p.B1.
- [8] Tomalia D. A., Esfand R., *Chemistry & Industry*, **1997**, 11, 416-420.
- [9] Hecht S., Frechet J. M. J., *Angewandte Chemie-International Edition*, **2001**, 40, 74-91.
- [10] Tomalia D. A., Naylor A. M., Goddard W. A., *Angewandte Chemie-International Edition in English*, **1990**, 29, 138-175.
- [11] Frechet J. M. J., Hawker C. J., Gitsov I., Leon J. W., *Journal of Macromolecular Science-Pure and Applied Chemistry*, **1996**, A33, 1399-1425.
- [12] Vogtle F., Fischer M., *Angewandte Chemie-International Edition*, **1999**, 38, 884-905.
- [13] Voit B. I., *Acta Polymerica*, **1995**, 46, 87-99.

- [14] Tomalia D. A., Dewald J. R., Hall M. J., Martin S. J., Smith P. B., *1st SPSJ International Polymer Conference, Kyoto, Japan, 1984*, 65.
- [15] Tomalia D. A., Baker H., Dewald J., Hall M., Kallos G., Martin S., Roeck J., Ryder J. Smith P., *Polymer Journal*, **1985**, 17, 117-132.
- [16] Frechet J. M. J., Tomalia D. A., *Dendrimers and Other Dendritic Polymers. J Wiley & Sons, West Sussex, 2001*.
- [17] Grayson S. M., Frechet J. M. J., *Chemical Reviews*, **2001**, 101, 3819-3867.
- [18] Tomalia D. A., Frechet J. M. J., *Journal of Polymer Science Part A-Polymer Chemistry*, **2002**, 40, 2719-2728.
- [19] Newkome G. R., Moorefield C. N., Vogtle F., *Dendrimers and Dendrons-Concepts, Syntheses, Applications. Weinheim: Wiley-VCH, 2001*.
- [20] Bosman A. W., Janssen H. M., Meijer E. W., *Chemical Reviews*, **1999**, 99, 1665-1688.
- [21] Buhleier E., Wehner W., Vogtle F., *Synthesis*, **1978**, 2, 155-158.
- [22] Moors R., Vogtle F., *Chemische Berichte-Recueil*, **1993**, 126, 2133-2135.
- [23] Newkome G. R., Yao Z.-Q., Baker G. R., Gupta V. K., *Journal of Organic Chemistry*, **1985**, 50, 2003-2004.
- [24] Padias A. B., Hall Jr. H. K., Tomalia D. A., *Journal of Organic Chemistry*, **1987**, 52, 5305-5312.
- [25] Lothian-Tomalia M. K., Hedstrand D. M., Tomalia D. A., Padias A. B., Hall H. K., *Tetrahedron*, **1997**, 53, 15495-15513.

-
- [26] Newkome G. R., Moorfield C. N., Vogtle F., *Dendritic Molecules*, VCH Weinheim, **1996**.
- [27] Frechet J. M. J., Jiang Y., Hawker C. J., Philippides A. E., *Proceedings of IUPAC International Symposium on Macromolecules at Seoul*, **1989**, 19-21.
- [28] Hawker C. J., Frechet J. M. J., *Journal of the American Chemical Society*, **1990**, 112, 7638-7647.
- [29] Hawker C. J., Frechet J. M. J., *Journal of the Chemical Society-Chemical Communications*, **1990**, 1010-1013.
- [30] Hawker C. J., Frechet J. M. J., *Macromolecules*, **1990**, 23, 4726-4729.
- [31] Miller T. M., Neenan T. X., *Chemistry of Materials*, **1990**, 2, 346-349.
- [32] Frechet J. M. J., *Science*, **1994**, 263, 1710-1715.
- [33] Tomalia D. A., Dewald J. R., *Dow Chemical Co. US Patent, US 4558120*, **1985**.
- [34] de Brabander-Van E. M. M., den Berg E. W. M., *Angewandte Chemie International Edition in English*, **1993**, 32, 1306-1308.
- [35] Ihre H., de Jesus O. L. P., Frechet J. M. J., *Journal of the American Chemical Society*, **2001**, 123, 5908-5917.
- [36] Krska S. W., Seyferth D., *Journal of the American Chemical Society*, **1998**, 120, 3604-3612.
- [37] Newkome G. R., Behera R. K., Moorefield C. N., Baker G. R., *Journal of Organic Chemistry*, **1991**, 56, 7162-7167.

- [38] Ruiz J., Lafuente G., Marcen S., Ornelas C., Lazare S., Cloutet E., Blais J. C., Astruc D., *Journal of the American Chemical Society*, **2003**, 125, 7250-7257.
- [39] Svenson S., Tomalia D. A., *Advanced Drug Delivery Reviews*, **2005**, 57, 2106-2129.
- [40] Lee C. C., MacKay J. A., Frechet J. M. J., Szoka F. C., *Nature Biotechnology*, **2005**, 23, 1517-1526.
- [41] Svenson S., Chauhan A. S., *Nanomedicine*, **2008**, 3, 679-702.
- [42] Choi Y., Thomas T., Kotlyar A., Islam M. T., Baker J. R., *Chemistry & Biology*, **2005**, 12, 35-43.
- [43] Grinstaff M. W., *Journal of Polymer Science Part A-Polymer Chemistry*, **2008**, 46, 383-400.
- [44] Tekade R. K., Kumar P. V., Jain N. K., *Chemical Reviews*, **2009**, 109, 49-87.
- [45] Ahn T. S., Thompson A. L., Bharathi P., Muller A., Bardeen C. J., *Journal of Physical Chemistry B*, **2006**, 110, 19810-19819.
- [46] Astruc D., Boisselier E., Ornelas C., *Chemical Reviews*, **2010**, 110, 1857-1959.
- [47] El Brahmī N., El Kazzouli S., Mignani S., Bousmina M., Majoral J. P., *Tetrahedron*, **2013**, 69, 3103-3133.
- [48] El Kazzouli S., El Brahmī N., Mignani S., Bousmina M., Zablocka M., Majoral J. P., *Current Medicinal Chemistry*, **2012**, 19, 4995-5010.
- [49] Astruc D., Heuze K., Gatard S., Mery D., Nlate S., Plault L., *Advanced Synthesis & Catalysis*, **2005**, 347, 329-338.

- [50] Helms B., Frechet J. M. J., *Advanced Synthesis & Catalysis*, **2006**, 348, 1125-1148.
- [51] Mery D., Astruc D., *Coordination Chemistry Reviews*, **2006**, 250, 1965-1979.
- [52] Reek J. N. H., Arevalo S., Van Heerbeek R., Kamer P. C. J., Van Leeuwen P., *Advances in Catalysis*, **2006**, 49, 71-151.
- [53] Hwang S.-H., Shreiner C. D., Moorefield C. N., Newkome G. R., *New Journal of Chemistry*, **2007**, 31, 1192-1217.
- [54] de Jesus E., Flores J. C., *Industrial & Engineering Chemistry Research*, **2008**, 47, 7968-7981.
- [55] Martinez-Olid F., Benito J. M., Flores J. C., de Jesus E., *Israel Journal of Chemistry*, **2009**, 49, 99-108.
- [56] Astruc D., *Tetrahedron-Asymmetry*, **2010**, 21, 1041-1054.
- [57] Astruc D., *Nature Chemistry*, **2012**, 4, 255-267.
- [58] John A., Nachtigall F. M., Santos L. S., *Current Organic Chemistry*, **2012**, 16, 1776-1787.
- [59] Caminade A. M., Ouali A., Keller M., Majoral J.-P., *Chemical Society Reviews*, **2012**, 41, 4113-4125.
- [60] Gatard S., Deraedt C., Rapakousiou A., Sonet D., Salmon L., Ruiz J., Astruc D., *Organometallics*, **2015**, 34, 1643-1650.
- [61] Rapakousiou A., Djeda R., Grillaud M., Li N., Ruiz J., Astruc D., *Organometallics*, **2014**, 33, 6953-6962.
- [62] He Y.-M., Feng Y., Fan Q.-H., *Accounts of Chemical Research*, **2014**, 47, 2894-2906.

- [63] Newkome G. R., Shreiner C., *Chemical Reviews*, **2010**, 110, 6338-6442.
- [64] Lu Y., Sun B., Li C., Schoenfish M. H., *Chemistry of Materials*, **2011**, 23, 4227-4233.
- [65] Wang D., Astruc D., *Coordination Chemistry Reviews*, **2013**, 257, 2317-2334.
- [66] Wang D., Denux D., Ruiz J., Astruc D., *Advanced Synthesis & Catalysis*, **2013**, 355, 129-142.
- [67] Keller M., Hameau A., Spataro G., Ladeira S., Caminade A.-M., Majoral J.-P., Ouali A., *Green Chemistry*, **2012**, 14, 2807-2815.
- [68] Pagliaro M., Pandarus V., Ciriminna R., Beland F., Cara P. D., *Chemcatchem*, **2012**, 4, 432-445.
- [69] Keller M., Colliere V., Reiser O., Caminade A.-M., Majoral J.-P., Ouali A., *Angewandte Chemie-International Edition*, **2013**, 52, 3626-3629.
- [70] Wittmann S., Schaetz A., Grass R. N., Stark W. J., Reiser O., *Angewandte Chemie-International Edition*, **2010**, 49, 1867-1870.
- [71] Maity P., Yamazoe S., Tsukuda T., *ACS Catalysis*, **2013**, 3, 182-185.
- [72] Servin P., Laurent R., Gonsalvi L., Tristany M., Peruzzini M., Majoral J.-P., Caminade A.-M., *Dalton Transactions*, **2009**, 42, 4432-4434.
- [73] Servin P., Laurent R., Dib H., Gonsalvi L., Peruzzini M., Majoral J.-P., Caminade A.-M., *Tetrahedron Letters*, **2012**, 53, 3876-3879.

- [74] Diallo A. K., Boisselier E., Liang L., Ruiz J., Astruc D., *Chemistry-A European Journal*, **2010**, 16, 11832-11835.
- [75] Vougioukalakis G. C., Grubbs R. H., *Chemical Reviews*, **2010**, 110, 1746-1787.
- [76] Candelon N., Lastecoueres D., Diallo A. K., Aranzaes J. R., Astruc D., Vincent J.-M., *Chemical Communications*, **2008**, 6, 741-743.
- [77] Liang L., Ruiz J., Astruc D., *Advanced Synthesis & Catalysis*, **2011**, 353, 3434-3450.
- [78] Karakhanov E., Maximov A., Kardasheva Y., Semernina V., Zolotukhina A., Ivanov A., Abbott G., Rosenberg E., Vinokurov V., *ACS Applied Materials & Interfaces*, **2014**, 6, 8807-8816.
- [79] Krishnan G. R., Sreekumar K., *Tetrahedron Letters*, **2014**, 55, 2352-2354.
- [80] Krishnan G. R., Sreekumar K., *European Journal of Organic Chemistry*, **2008**, 2008, 4763-4768.
- [81] Krishnan G. R., Sreekumar K., *Polymer*, **2008**, 49, 5233-5240.
- [82] Krishnan G. R., Sreekurnar K., *Applied Catalysis A-General*, **2009**, 353, 80-86.
- [83] Warshawsky A., Kalir R., Deshe A., Berkovitz H., Patchornik A., *Journal of the American Chemical Society*, **1979**, 101, 4249-4258.
- [84] Krishnan G. R., Sreekumar K., *Soft Materials*, **2010**, 8, 114-129.
- [85] Mangala K., Sreekumar K., *Applied Organometallic Chemistry*, **2013**, 27, 73-78.

- [86] Mangala K., Sreekumar K., *Journal of Applied Polymer Science*, **2015**, 132, 41593 (1-7).
- [87] Nishide H., Tsuchida E., Shimidazu N., Yamada A., Keneko M., *Macromolecular Chemistry, Rapid Communications*, **1982**, 5, 544-546.
- [88] Traficante C. I., Delpiccolo C. M. L., Mata E. G., *ACS Combinatorial Science*, **2014**, 16, 211-214.
- [89] Franiak-Pietryga I., Ziolkowska E., Ziemba B., Appelhans D., Voit B., Szewczyk M., Gora-Tybor J., Robak T., Klajnert B., Bryszewska M., *Molecular Pharmaceutics*, **2013**, 10, 2490-2501.
- [90] Dobrovolskaia M. A., Patri A. K., Simak J., Hall J. B., Semberova J., Lacerda S. H. D. P., McNeil S. E., *Molecular Pharmaceutics*, **2012**, 9, 382-393.
- [91] El Brahmī N., El Kazzouli S., Mignani S. M., Essassi E. M., Aubert G., Laurent R., Caminade A.-M., Bousmina M. M., Cresteil T., Majoral J.-P., *Molecular Pharmaceutics*, **2013**, 10, 1459-1464.
- [92] Setaro F., Brasch M., Hahn U., Koay M. S. T., Cornelissen J. J. L. M., de la Escosura A., Torres T., *Nano Letters*, **2015**, 15, 1245-1251.
- [93] Wu W., Ye C., Qin J., Li Z., *ACS Applied Materials & Interfaces*, **2013**, 5, 7033-7041.
- [94] Yang L., da Rocha S. R. P., *Molecular Pharmaceutics*, **2014**, 11, 1459-1470.
- [95] Avaritt B. R., Swaan P. W., *Molecular Pharmaceutics*, **2015**, 12, 1961-1969.

-
- [96] Matai I., Sachdev A., Gopinath P., *ACS Applied Materials & Interfaces*, **2015**, 7, 11423-11435.
- [97] Tomalia D. A., Hedstrand D. M., Ferritto M. S., *Macromolecules*, **1991**, 24, 1435-1438.
- [98] Gauthier M., Moller M., *Macromolecules*, **1991**, 24, 4548-4553.
- [99] Six J. L., Gnanou Y., *Macromolecular Symposia*, **1995**, 95, 137-150.
- [100] Taton D., Cloutet E., Gnanou Y., *Macromolecular Chemistry and Physics*, **1998**, 199, 2501-2510.
- [101] Trollsas M., Hedrick J. L., *Journal of the American Chemical Society*, **1998**, 120, 4644-4651.
- [102] Trollsas M., Hedrick J. L., *Macromolecules*, **1998**, 31, 4390-4395.
- [103] Roovers J., Comanita B., *Branched Polymers I*, **1999**, 142, 179-228.
- [104] Tomalia D. A., Christensen J. B., Boas U., *Dendrimers, Dendrons and Dendritic Polymers: Discovery, Applications, and the Future*, Cambridge University Press, **2012**.
- [105] Roovers J., *Advances in Polymer Science*, **1999**, 142, 180-228.
- [106] Knauss D. M., Huang T. Z., *Macromolecules*, **2002**, 35, 2055-2062.
- [107] Knauss D. M., Huang T. Z., *Macromolecules*, **2003**, 36, 6036-6042.
- [108] Chalari I., Hadjichristidis N., *Journal of Polymer Science Part A-Polymer Chemistry*, **2002**, 40, 1519-1526.
- [109] Gauthier M., Munam A., *Macromolecules*, **2010**, 43, 3672-3681.
- [110] Sanchez Cadena L.-E., Gauthier M., *Polymers*, **2010**, 2, 596-622.

- [111] Konkolewicz D., Monteiro M. J., Perrier S., *Macromolecules*, **2011**, 44, 7067-7087.
- [112] Zhang H., He J., Zhang C., Ju Z., Li J., Yang Y., *Macromolecules*, **2012**, 45, 828-841.
- [113] van Dongen M. A., Vaidyanathan S., Holl-Mark M. B., *Soft Matter*, **2013**, 9, 11188-11196.
- [114] Ibrahim A., Koval D., Kasicka V., Faye C., Cottet H., *Macromolecules*, **2013**, 46, 533-540.
- [115] Hirao A., Goseki R., Ishizone T., *Macromolecules*, **2014**, 47, 1883-1905.
- [116] Hedrick J. L., Magbitang T., Connor E. F., Glauser T., Volksen W., Hawker C. J., Lee V. Y., Miller R. D., *Chemistry-A European Journal*, **2002**, 8, 3308-3319.
- [117] Elias H.-G., *Makromolekule, Weinheim M., Wiley-VCH*, **2002**.
- [118] Jenkins A. D., Kratochvil P., Stepto R. F. T., Suter U. W., *Pure and Applied Chemistry*, **1996**, 68, 2287-2311.
- [119] Schluter A. D., Bothe H., *Chemische Berichte*, **1991**, 124, 584-590.
- [120] Frauenrath H., *Progress in Polymer Science*, **2005**, 30, 325-384.
- [121] Yin R., Zhu Y., Tomalia D. A., Ibuki H., *Journal of the American Chemical Society*, **1998**, 120, 2678-2679.
- [122] Hawker C. J., Frechet J. M. J., *Polymer*, **1992**, 33, 1507-1511.
- [123] Percec V., Heck J., *Journal of Polymer Science Part A-Polymer Chemistry*, **1991**, 29, 591-597.

-
- [124] Percec V., Heck J., Lee M., Ungar G., Alvarezcastillo A., *Journal of Materials Chemistry*, **1992**, 2, 1033-1039.
- [125] Percec V., Heck J., Tomazos D., Falkenberg F., Blackwell H. , Ungar G., *Journal of the Chemical Society-Perkin Transactions I*, **1993**, 2799-2811.
- [126] Percec V., Heck J., Ungar G., *Macromolecules*, **1991**, 24, 4957-4962.
- [127] Percec V., Lee M., Heck J., Blackwell H. E., Ungar G., Alvarezcastillo A., *Journal of Materials Chemistry*, **1992**, 2, 931-938.
- [128] Freudenberger R., Claussen W., Schluter A. D., Wallmeier H., *Polymer*, **1994**, 35, 4496-4501.
- [129] Chen Y. , Xiong X., *Chemical Communications*, **2010**, 46, 5049-5060.
- [130] Nokami T., Watanabe T., Musya N., Morofuji T., Tahara K., Tobe Y., Yoshida J. I., *Chemical Communications*, **2011**, 47, 5575-5577.
- [131] Laurent B. A., Grayson S. M., *Journal of the American Chemical Society*, **2011**, 133, 13421-13429.
- [132] Kang E.-H., Lee I. S., Choi T.-L., *Journal of the American Chemical Society*, **2011**, 133, 11904-11907.
- [133] Terashima T., Mes T., De Greef T. F. A., Gillissen M. A. J., Besenius P., Palmans A. R. A. , Meijer E. W., *Journal of the American Chemical Society*, **2011**, 133, 4742-4745.
- [134] Park C., Lee J., Kim C., *Chemical Communications*, **2011**, 47, 12042-12056.
- [135] Schuell C., Frey H., *ACS Macro Letters*, **2012**, 1, 461-464.

- [136] Yu H., Schlueter A. D., Zhang B., *Macromolecules*, **2012**, 45, 8555-8560.
- [137] Zhang B., Schlueter A. D., *New Journal of Chemistry*, **2012**, 36, 414-418.
- [138] Carlmark A., Malmstrom E., Malkoch M., *Chemical Society Reviews*, **2013**, 42, 5858-5879.
- [139] Yan J., Li W., Zhang A., *Chemical Communications*, **2014**, 50, 12221-12233.
- [140] Borisov O. V., Polotsky A. A., Rud O. V., Zhulina E. B., Leermakerse F. A. M., Birshtein T. M., *Soft Matter*, **2014**, 10, 2093-2101.
- [141] Sun H.-J., Zhang S., Percec V., *Chemical Society Reviews*, **2015**, 44, 3900-3923.
- [142] Wooley K. L., Hawker C. J., Frechet J. M. J., *Journal of the American Chemical Society*, **1991**, 113, 4252-4261.
- [143] Hudson S. D., Jung H. T., Percec V., Cho W. D., Johansson G., Ungar G., Balagurusamy V. S. K., *Science*, **1997**, 278, 449-452.
- [144] Morgenroth F., Kubel C., Mullen K., *Journal of Materials Chemistry*, **1997**, 7, 1207-1211.
- [145] Setayesh S., Grimsdale A. C., Weil T., Enkelmann V., Mullen K., Meghdadi F., List E. J. W., Leising G., *Journal of the American Chemical Society*, **2001**, 123, 946-953.
- [146] Rehahn M., Schluter A. D., Wegner G., Feast W. J., *Polymer*, **1989**, 30, 1060-1062.

-
- [147] Karakaya B., Claussen W., Schafer A., Lehmann A., Schluter A. D., *Acta Polymerica*, **1996**, 47, 79-84.
- [148] Karakaya B., Claussen W., Gessler K., Saenger W., Schluter A. D., *Journal of the American Chemical Society*, **1997**, 119, 3296-3301.
- [149] Bilibin A., Zorin I., Saratovsky S., Moukhina I., Egorova G., Girbasova N., *Macromolecular Symposia*, **2003**, 199, 197-208.
- [150] Girbasova N., Aseyev V., Saratovsky S., Moukhina I., Tenhu H., Bilibin A., *Macromolecular Chemistry and Physics*, **2003**, 204, 2258-2264.
- [151] Ronda J. C., Reina A., Giamerini M., *Journal of Polymer Science Part A-Polymer Chemistry*, **2004**, 42, 326-340.
- [152] Ronda J. C., Reina J. A., Cadiz V., Giamberini M., Nicolais L., *Journal of Polymer Science Part A-Polymer Chemistry*, **2003**, 41, 2918-2929.
- [153] Ouali N., Mery S., Skoulios A., Noirez L., *Macromolecules*, **2000**, 33, 6185-6193.
- [154] Kim C., Kang S., *Journal of Polymer Science Part A-Polymer Chemistry*, **2000**, 38, 724-729.
- [155] Kim C., Kwark K., *Journal of Polymer Science Part A-Polymer Chemistry*, **2002**, 40, 976-982.
- [156] Andreopoulou A. K., Kallitsis J. K., *Macromolecules*, **2002**, 35, 5808-5815.
- [157] Andreopoulou A. K., Carbonnier B., Kallitsis J. K., Pakula T., *Macromolecules*, **2004**, 37, 3576-3587.

- [158] Shu L. J., Gossl I., Rabe J. P., Schluter A. D., *Macromolecular Chemistry and Physics*, **2002**, 203, 2540-2550.
- [159] Shu L. J., Schafer T., Schluter A. D., *Macromolecules*, **2000**, 33, 4321-4328.
- [160] Merrifield R. B., *Journal of the American Chemical Society*, **1963**, 85, 2149-2154.
- [161] Booth S., Hermkens P. H. H., Ottenheijm H. C. J., Rees D. C., *Tetrahedron*, **1998**, 54, 15385-15443.
- [162] Fruchtel J. S., Jung G., *Angewandte Chemie-International Edition in English*, **1996**, 35, 17-42.
- [163] Thompson L. A., Ellman J. A., *Chemical Reviews*, **1996**, 96, 555-600.
- [164] Marquardt M., Eifler-Lima V. L., *Quimica Nova*, **2001**, 24, 846-855.
- [165] Delgado M., Janda K. D., *Current Organic Chemistry*, **2002**, 6, 1031-1043.
- [166] Brase S., *Combinatorial Chemistry on Solid Phase, Topics in Current Chemistry, Springer-Verlag: Berlin*, **2007**, 278.
- [167] Gravert D. J., Janda K. D., *Chemical Reviews*, **1997**, 97, 489-509.
- [168] Clark J. H., Kybett A. P., Macquarrie D. J., *Polymer-Supported Synthesis, VCH, New York*, **1992**.
- [169] Singh M. S., Chowdhury S., *RSC Advances*, **2012**, 2, 4547-4592.
- [170] Tanaka K., *Solvent-Free Organic Synthesis, Wiley-VCH GmbH & Co. KGaA, Weinheim, Germany*, **2003**, 121-133.
- [171] Kannan V., Sreekumar K., *Journal of Molecular Catalysis A-Chemical*, **2013**, 376, 34-39.

- [172] Varma R. S., *Pure and Applied Chemistry*, **2001**, 73, 193-198.
- [173] Kannan V., Sreekumar K., Gil A., Vicente M. A., *Catalysis Letters*, **2011**, 141, 1118-1122.
- [174] Svec F., Frechet J. M. J., *Science*, **1996**, 273, 205-211.
- [175] Hori M., Gravert D. J., Wentworth P., Janda K. D., *Bioorganic & Medicinal Chemistry Letters*, **1998**, 8, 2363-2368.
- [176] Chen S. Q., Janda K. D., *Journal of the American Chemical Society*, **1997**, 119, 8724-8725.
- [177] Malenfant P. R. L., Frechet J. M. J., *Chemical Communications*, **1998**, 23, 2657-2658.
- [178] Hodge P., *Industrial & Engineering Chemistry Research*, **2005**, 44, 8542-8553.
- [179] Lu J., Toy P. H., *Chemical Reviews*, **2009**, 109, 815-838.
- [180] Bergbreiter D. E., Tian J., Hongfa C., *Chemical Reviews*, **2009**, 109, 530-582.
- [181] Toy P. H., Janda K. D., *Tetrahedron Letters*, **1999**, 40, 6329-6332.
- [182] Zalipsky S., Chang J. L., Albericio F., Barany G., *Reactive Polymers*, **1994**, 22, 243-258.
- [183] Bayer E., Dengler M., Hemmasi B., *International Journal of Peptide and Protein Research*, **1985**, 25, 178-186.
- [184] Atherton E., Clive D. L. J., Sheppard R. C., *Journal of the American Chemical Society*, **1975**, 97, 6584-6585.
- [185] Arshady R., Atherton E., Clive D. L. J., Sheppard R. C., *Journal of Chemical Society- Perkin Transactions*, **1981**, 1, 529-537.

- [186] Meldal M., *Journal of Combinatorial Chemistry*, **2000**, 02, 108–119.
- [187] Kempe M., Barany G., *Journal of the American Chemical Society*, **1996**, 118, 7083–7093.
- [188] Renil M., Meldal M., *Tetrahedron Letters*, **1996**, 37, 6185–6188.
- [189] Bayer E., Jung G., Halász I., Sebastian I., *Tetrahedron Letters*, **1970**, 11, 4503–4505.
- [190] Adams S. P., Kavka K. S., Wykes E. J., Holder S. B., Galluppi G. R., *Journal of the American Chemical Society*, **1983**, 105, 661–663.
- [191] Cilli E. M., Oliveira E., Marchetto R., Nakaie C. R., *Journal of Organic Chemistry*, **1996**, 61, 8992–9000.
- [192] Santini R., Griffith M. C., Qi M., *Tetrahedron Letters*, **1998**, 39, 8951–8954.
- [193] Malavolta L., Nakaie C. R., *Tetrahedron*, **2004**, 60, 9417–9424.
- [194] Meldal M., *Tetrahedron Letters*, **1992**, 33, 3077–3080.
- [195] Roller S., Turk H., Stumbe J. F., Rapp W., Haag R., *Journal of Combinatorial Chemistry*, **2006**, 8, 350–354.
- [196] Lebreton S., Newcombe N., Bradley M., *Tetrahedron Letters*, **2002**, 43, 2475–2478.
- [197] Basso A., Bradley M., *Tetrahedron Letters*, **2003**, 44, 2699–2702.
- [198] Zhang R., Li Q., Zhang J., Li J., Ma G., Su Z., *Reactive & Functional Polymers*, **2012**, 72, 773–780.
- [199] Tsuchida E., Nishide H., Shimidazu N., Yamada N., Keneko M., *Die Makromolekulare Chemie, Rapid Communications*, **1981**, 2, 621–626.

- [200] Huang A. Y.-T., Tsai C.-H., Chen H.-Y., Chen H.-T., Lu C.-Y., Lin Y.-T., Kao C.-L., *Chemical Communications*, **2013**, 49, 5784-5786.
- [201] Baker R. T., Tumas W., *Science*, **1999**, 284, 1477-1479.
- [202] Richmond M. K., Scott S. L., Alper H., *Journal of the American Chemical Society*, **2001**, 123, 10521-10525.
- [203] Sandee A. J., Petra D. G. I., Reek J. N. H., Kamer P. C. J., van Leeuwen P., *Chemistry-A European Journal*, **2001**, 7, 1202-1208.
- [204] Sandee A. J., Reek J. N. H., Kamer P. C. J., van Leeuwen P., *Journal of the American Chemical Society*, **2001**, 123, 8468-8476.
- [205] Toy P. H., Lam Y., *Solid-Phase Organic Synthesis*, Wiley, New York, **2012**.
- [206] Chechik V., Crooks R. M., *Journal of the American Chemical Society*, **2000**, 122, 1243-1244.
- [207] Gong A., Fan Q., Chen Y., Liu H., Chen C., Xi F., *Journal of Molecular Catalysis A: Chemistry*, **2000**, 159, 225-232.
- [208] Sirkar K. K., Shanbhag P. V., Kovvali A. S., *Industrial & Engineering Chemistry Research*, **1999**, 38, 3715-3737.
- [209] Marquardt T., Luning U., *Chemical Communications*, **1997**, 17, 1681-1682.
- [210] van Heerbeek R., Kamer P. C. J., van Leeuwen P., Reek J. N. H., *Chemical Reviews*, **2002**, 102, 3717-3756.
- [211] Adams R. D., Cotton F. A., *Catalysis by Di- and Polynuclear Metal Cluster Complexes*; Wiley-VCH: New York, **1998**, 1153-11180.

- [212] Pomogailo A. D., *Catalysis by Polymer-Immobilized Metal Complexes*, Springer-Verlag: Berlin, **1998**.
- [213] Seneci P., *Solid-Phase Synthesis*, Wiley, New York, **2001**.
- [214] Suzuka T., Sueyoshi H., Maehara S., Ogasawara H., *Molecules*, **2015**, 20, 9906-9914.
- [215] Knapen J. W. J., Vandermade A. W., Dewilde J. C., Vanleeuwen P., Wijkens P., Grove D. M., Vankoten G., *Nature*, **1994**, 372, 659-663.
- [216] Breinbauer R., Jacobsen E. N., *Angewandte Chemie-International Edition*, **2000**, 39, 3604-3607.
- [217] Rigaut S., Delville M. H., Astruc D., *Journal of the American Chemical Society*, **1997**, 119, 11132-11133.
- [218] Valerio C., Rigaut S., Ruiz J., Fillaut J. L., Delville M. H., Astruc D., *Bulletin of the Polish Academy of Sciences-Chemistry*, **1998**, 46, 309-318.
- [219] Myers V. S., Weir M. G., Carino E. V., Yancey D. F., Pande S., Crooks R. M., *Chemical Science*, **2011**, 2, 1632-1646.
- [220] Grubbs R. H., *Handbook of Metathesis*, Wiley-VCH, Weinheim, **2002**, 132-145.
- [221] Trnka T. M., Grubbs R. H., *Accounts of Chemical Research*, **2001**, 34, 18-29.
- [222] Flanagan J. B., Margel S., Bard A. J., Anson F. C., *Journal of the American Chemical Society*, **1978**, 100, 4248-4253.
- [223] Lebreton S., Monaghan S., Bradley M., *Aldrichimica Acta*, **2001**, 34, 75-83.

- [224] Swali V., Wells N. J., Langley G. J., Bradley M., *Journal of Organic Chemistry*, **1997**, 62, 4902-4903.
- [225] Wells N. J., Davies M., Bradley M., *Journal of Organic Chemistry*, **1998**, 63, 6430-6431.
- [226] Wells N. J., Basso A., Bradley M., *Biopolymers*, **1998**, 47, 381-396.
- [227] Basso A., Evans B., Pegg N., Bradley M., *Tetrahedron Letters*, **2000**, 41, 3763-3767.
- [228] Basso A., Pegg N., Evans B., Bradley M., *European Journal of Organic Chemistry*, **2000**, 23, 3887-3891.
- [229] Basso A., Evans B., Pegg N., Bradley M., *Chemical Communications*, **2001**, 8, 697-698.
- [230] Cho J. K., Kim D. W., Namgung J., Lee Y. S., *Tetrahedron Letters*, **2001**, 42, 7443-7445.
- [231] Fromont C., Bradley M., *Chemical Communications*, **2000**, 4, 283-284.
- [232] Chhabra S. R., Mahajan A., Chan W. C., *Journal of Organic Chemistry*, **2002**, 67, 4017-4029.
- [233] Tam J. P., Lu Y. A., Yang J. L., *European Journal of Biochemistry*, **2002**, 269, 923-932.
- [234] Taniguchi Y., Shirai K., Saitoh H., Yamauchi T., Tsubokawa N., *Polymer*, **2005**, 46, 2541-2547.
- [235] Tsubokawa N., Kotama K., Saitoh H., Nishikubo T., *Composite Interfaces*, **2003**, 10, 609-619.
- [236] Reynhardt J. P. K., Alper H., *Journal of Organic Chemistry*, **2003**, 68, 8353-8360.

- [237] Zweni P. P., Alper H., *Advanced Synthesis & Catalysis*, **2004**, 346, 849-854.
- [238] Chung Y. M., Rhee H. K., *Chemical Communications*, **2002**, 238-239.
- [239] Chung Y. M., Rhee H. K., *Comptes Rendus Chimie*, **2003**, 6, 695-705.
- [240] Sakai K., Teng T. C., Katada A., Harada T., Uemura S., Asami Y., Sakata M., Kunitake M., Hirayama C., *Chemistry Letters*, **2001**, 6, 510-511.
- [241] Sakai K., Teng T. C., Katada A., Harada T., Yoshida K., Yamanaka K., Asami Y., Sakata M., Hirayama C., Kunitake M., *Chemistry of Materials*, **2003**, 15, 4091-4097.
- [242] Bu J., Judeh Z. M. A., Ching C. B., Kawi S., *Catalysis Letters*, **2003**, 85, 183-187.
- [243] Bu J., Li R. J., Quah C. W., Carpenter K. J., *Macromolecules*, **2004**, 37, 6687-6694.
- [244] Dahan A., Portnoy M., *Journal of Polymer Science Part A-Polymer Chemistry*, **2005**, 43, 235-262.
- [245] Wang C. L., Zhu G. S., Li J., Cai X. H., Wei Y. H., Zhang D. L., Qiu S. L., *Chemistry-A European Journal*, **2005**, 11, 4975-4982.
- [246] Lebreton S., How S. E., Buchholz M., Yingyongnarongkul B. E., Bradley M., *Tetrahedron*, **2003**, 59, 3945-3953.
- [247] Pan B. F., Cui D. X., Gao F., He R., *Nanotechnology*, **2006**, 17, 2483-2489.

- [248] Ling F. H., Lu V., Svec F., Frechet J. M. J., *Journal of Organic Chemistry*, **2002**, 67, 1993-2002.
- [249] Dahan A., Portnoy M., *Macromolecules*, **2003**, 36, 1034-1038.
- [250] Dahan A., Portnoy M., *Journal of the American Chemical Society*, **2007**, 129, 5860-5869.
- [251] Dahan A., Weissberg A., Portnoy M., *Chemical Communications*, **2003**, 1206-1207.
- [252] Tuchman-Shukron L., Portnoy M., *Advanced Synthesis & Catalysis*, **2009**, 351, 541-546.
- [253] Dilly S. J., Carlisle S. J., Clark A. J., Shepherd A. R., Smith S. C., Taylor P. C., Marsh A., *Journal of Polymer Science Part A-Polymer Chemistry*, **2006**, 44, 2248-2259.
- [254] Marsh A., Carlisle S. J., Smith S. C., *Tetrahedron Letters*, **2001**, 42, 493-496.
- [255] Acosta E. J., Carr C. S., Simanek E. E., Shantz D. F., *Advanced Materials*, **2004**, 16, 985-989.
- [256] Acosta E. J., Gonzalez S. O., Simanek E. E., *Journal of Polymer Science Part A-Polymer Chemistry*, **2005**, 43, 168-177.
- [257] Chi C. Y., Wu J. S., Wang X. H., Zhao X. J., Li J., Wang F. S., *Tetrahedron Letters*, **2001**, 42, 2181-2184.
- [258] Chen H. T., Huh S., Wiench J. W., Pruski M., Lin V. S. Y., *Journal of the American Chemical Society*, **2005**, 127, 13305-13311.
- [259] Corma A., Garcia H., Leyva A., *Chemical Communications*, **2003**, 2806-2807.

- [260] Huang J. W., Shi M., *Advanced Synthesis & Catalysis*, **2003**, 345, 953-958.
- [261] Zhao B., Jiang X., Li D., Jiang X., O'Lenick T. G., Li B., Li C. Y., *Journal of Polymer Science Part A-Polymer Chemistry*, **2008**, 46, 3438-3446.
- [262] Kwong C. K.-W., Huang R., Zhang M., Shi M., Toy P. H., *Chemistry-A European Journal*, **2007**, 13, 2369-2376.
- [263] Luo S., Zheng X., Xu H., Mi X., Zhang L., Cheng J.-P., *Advanced Synthesis & Catalysis*, **2007**, 349, 2431-2434.
- [264] Akagawa K., Sakamoto S., Kudo K., *Synlett*, **2011**, 817-820.
- [265] Giacalone F., Gruttadauria M., Marculescu A. M., D'Anna F., Noto R., *Catalysis Communications*, **2008**, 9, 1477-1481.
- [266] Dahan A., Portnoy M., *Chemical Communications*, **2002**, 22, 2700-2701.
- [267] Dahan A., Portnoy M., *Organic Letters*, **2003**, 5, 1197-1200.
- [268] Kehat T., Goren K., Portnoy M., *New Journal of Chemistry*, **2012**, 36, 394-401.
- [269] Spasser L., Portnoy M., *Journal of Polymer Science Part A-Polymer Chemistry*, **2010**, 48, 6009-6013.
- [270] Tuchman-Shukron L., Miller S. J., Portnoy M., *Chemistry-A European Journal*, **2012**, 18, 2290-2296.
- [271] Goren K., Portnoy M., *Chemical Communications*, **2010**, 46, 1965-1967.
- [272] Mansour A., Kehat T., Portnoy M., *Organic & Biomolecular Chemistry*, **2008**, 6, 3382-3387.

- [273] Kehat T., Portnoy M., *Chemical Communications*, **2007**, 26, 2823-2825.
- [274] Weissberg A., Halak B., Portnoy M., *Journal of Organic Chemistry*, **2005**, 70, 4556-4559.
- [275] Goren K., Karabline-Kuks J., Shiloni Y., Barak-Kulbak E., Portnoy M., *Chemistry-A European Journal*, **2015**, 21, 1191-1197.
- [276] Asano K., Matsubara S., *Synlett*, **2009**, 35-38.
- [277] Karabline J., Portnoy M., *Organic & Biomolecular Chemistry*, **2012**, 10, 4788-4794.
- [278] Eppel S., Portnoy M., *Tetrahedron Letters*, **2013**, 54, 5056-5060.
- [279] Zheng J., Lin S., Zhu X., Jiang B., Yang Z., Pan Z., *Chemical Communications*, **2012**, 48, 6235-6237
- [280] Krishnan G. R., Thomas J., Sreekumar K., *ARKIVOK*, **2009**, 10, 106-120.

Chapter-2

DEVELOPMENT OF DENDRIGRAFT POLYMERS HAVING ETHYLENE GLYCOL, GLYCEROL AND PENTAERYTHRITOL INITIATED POLYEPICHLOROHYDRIN AS CORE

Abstract

Synthesis of Multi-arm Star Dendrigraft amidoamine polymer with polyepichlorohydrin core has been demonstrated on a solid resin support to achieve the heterogeneous nature for catalytic applications. In earlier studies of supported dendritic systems, no effort was initiated to synthesize a dendritic polymer having high functionality in the low generation. In this study, we have functionalized Merrifield resin support with polyepichlorohydrin initiated by ethylene glycol, glycerol and pentaerythritol. The synthesized polymers, EG-Gn, GLR-Gn and PEN-Gn were characterized.

2.1 Introduction

Recently, great attention has been directed towards the synthesis of Dendrigraft or Dendronized polymers.¹⁻⁸ Most of the reported Dendronized polymers were synthesized from linear polymeric core.^{1,9-13} Dendronized polymers synthesized from cyclic or branched polymeric core are only few.^{14,15} This has emerged as a new concept in macromolecular design and materials science due to their unique structures which are seldom achieved by dendrimers and linear polymers.¹⁶⁻³⁰ Modification of linear polymers with dendritic reagents is one of the most popular approaches for the

synthesis of dendronized linear polymers. The design and synthesis of linear polymers bearing appropriate functional groups to introduce dendritic substituents is important.³¹⁻³⁸ However, synthesis of these polymers is practically difficult due to the lengthy purification procedure after every stage. So we have tried to synthesize Dendrigrift or Dendronized polymer having branches and also linear polymeric core on a solid resin support using Merrifield's solid phase synthesis concept.³⁹⁻⁴⁵

Solid phase synthesis of dendritic polymers is really a challenge, because of the large number of reactions that take place simultaneously during the building up of each generation and the number increases exponentially with increase in generation. Conversely, solid phase synthesis provides some inherent advantages over orthodox solution synthesis.⁴⁶ Synthesis of dendrimers need large excess of reagents for obtaining high purity and defect free products and solid phase synthesis usually use large excess of reagents. Purification of intermediates is easy in solid phase synthesis, which is the most difficult and time-consuming process in solution phase synthesis of dendrimers. In addition, the polymeric resins on which the dendrimer is synthesized can be used as highly loaded resin for combinatorial library synthesis, with particular emphasis on one bead one compound approach.^{47,48}

The most widely studied dendrimer attached to insoluble support is poly (amidoamine) dendrimer. In 1997, Bradley and co-workers introduced the solid phase synthesis of PAMAM dendrimers on organic polymer support.⁴¹ Initially, the dendrons were prepared on Tentagel^R up

to the fourth generation. The assembly of the dendrons followed the divergent synthetic strategy developed by Tomalia *et al.* for PAMAM dendrimers in solution.⁴⁹ It was based on alternating steps of double Michael addition of terminal primary amines to methyl acrylate and aminolysis of the terminal esters formed with 1,2-alkanediamines. Later, the approach was extended to PAMAM dendrons on polystyrene beads equipped with a short PEG spacer.⁵⁰ First to fourth generation poly (amidoamine) dendrimers were synthesized on the polymer. The reaction proceeded smoothly for the synthesis of first and second generation dendrimers. Third and fourth generation dendrimers showed defect structures as observed from ESI MS data. These defects may be due to the steric hindrance and increased number of reactions that had to take place for this synthesis. These dendronised resins were used as high load resins for the synthesis of various molecules.⁵¹

The present approach to synthesize dendrigraft or dendronized polymers includes similar strategy of Michael addition and amination, but follows fewer steps and more number of branches compared to conventional PAMAM dendrimer. To the best of our knowledge, this is the first attempt to synthesize Dendrigraft polymers having branched polymeric core on a resin support. Most of the reports were about single core high generation dendritic systems.^{39,42,43,52-65} So far, no report has appeared on the synthesis of amidoamine polymer on a polymeric core. Our aim was to synthesize dendritic systems having large amount of functionality even in the low generation level and we have adopted a

‘graft from strategy’ to synthesize these systems using polymeric core on Merrifield resin.

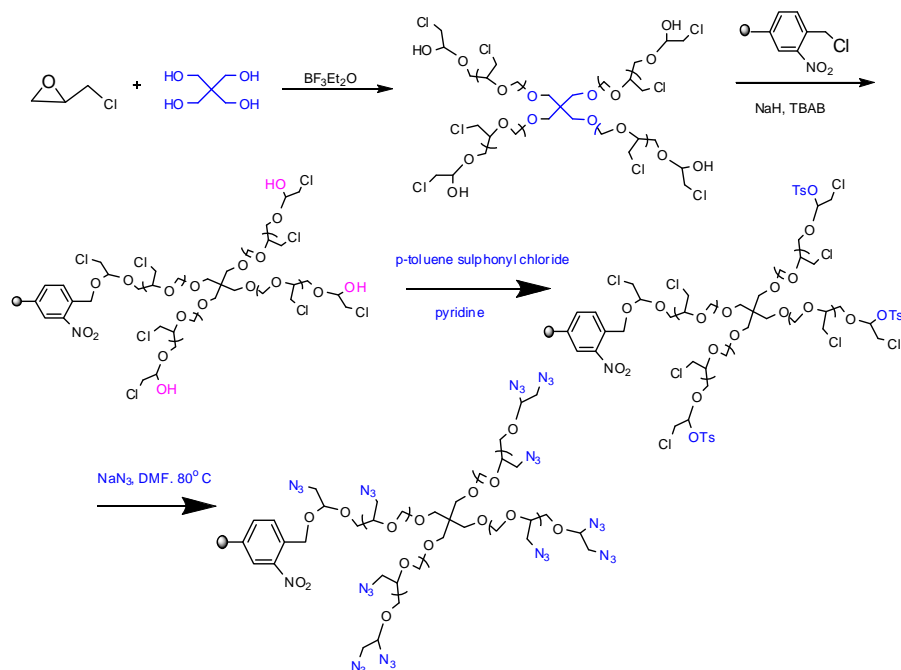
2.1.1 Objective of the Present Work

Synthesis of Merrifield resin supported PAMAM dendrimers for catalytic applications was reported from this laboratory previously.⁶² Its amine capacity was found to be between 1 and 2 mmols gm^{-1} for G0 to G3 generations. Here, we have tried to increase the amine capacity even at the low generation level. For this purpose, we have selected pentaerythritol, glycerol and ethylene glycol initiated polyepichlorohydrin (PECH) as core, coupled to the Merrifield resin and amidoamine dendrons were made to grow on it. The highlight of the present synthesis is that, in contrast to other dendritic polymers, large number of amidoamine groups can be incorporated in a single step as well as in low generation. In this chapter, the solid phase synthesis of low generation amidoamine dendronized polymer having pentaerythritol, glycerol and ethylene glycol initiated polyepichlorohydrin (PECH) as core is reported.

2.2 Results & Discussion

2.2.1 Synthesis of Merrifield Resin Supported Dendrigrft Polymer having pentaerythritol initiated PECH as Core

The resin supported dendrigrft azide polymer was synthesized using the schematic procedure (Scheme 2.1).



Scheme 2.1 Synthesis of resin supported azide polymer

The branched hydroxyl terminated PECH (polyepichlorohydrin) was prepared by the ring opening polymerization of the oxirane group in ECH (epichlorohydrin) in the presence of pentaerythritol by activated monomer mechanism (AMM).⁶⁶ It was a light yellow viscous liquid.

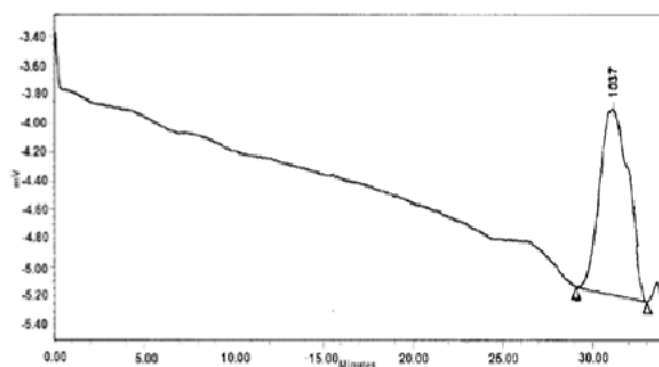


Fig 2.1 GPC profile of PECH

From GPC (Fig 2.1), the molecular weight of PECH was found to be 1037 with polydispersity index of 1.27. The ^1H NMR spectrum indicated that the hydroxyl groups at the terminal ends were secondary in nature (Fig 2.2).

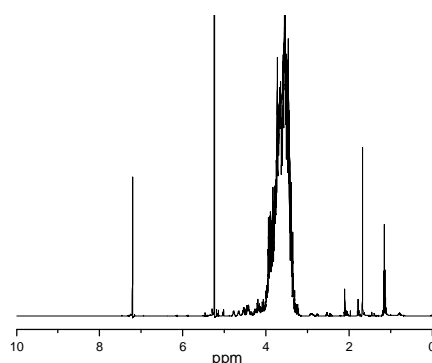


Fig 2.2 ^1H NMR spectrum of PECH

Merrifield resin (1% cross-linked with DVB) was gifted from Thermax India Ltd. Its chlorine capacity was found to be 5.2 mmols g^{-1} . It was made photoactive by the introduction of a nitro group at the ortho position of chloromethyl group.⁶⁷ The PECH was coupled to the resin using sodium hydride and tetrabutyl ammonium bromide.^{68,69}

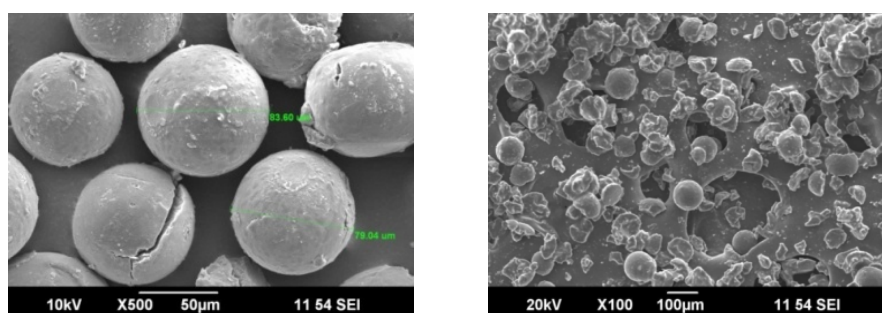


Fig 2.3 Scanning electron micrograph of (a) nitrated Merrifield Resin (MR) (b) PECH attached Merrifield Resin

After coupling, chlorine capacity was found to be 7.2 mmols g^{-1} by Volhards method. SEM micrographs of nitrated Merrifield Resin and PECH attached MR is shown in the figure (Fig 2.3). From the scanning electron micrographs, it was found that, after modification with PECH, beads with low extent of grafting were spherical with an appearance similar to the precursor resin particles. SEM EDAX showed that 18 atom% of chlorine was present in the sample (Fig 2.4).

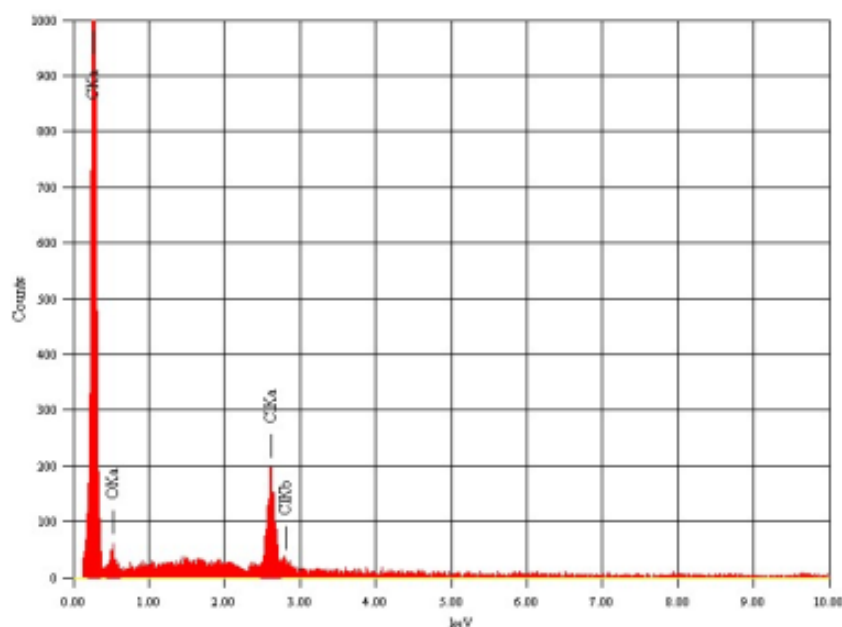


Fig 2.4 EDX spectrum of PECH attached Merrifield Resin

In the IR spectrum of nitrated Merrifield resin, the peak at 1596 cm^{-1} and 1360 cm^{-1} corresponds to the stretching vibrations due to NO_2 group (Fig 2.5a). The IR spectrum of PECH coupled Merrifield resin showed a band at 1107 cm^{-1} and a broad band at 3430 cm^{-1} which corresponded to C-O-C stretching of ether linkage and due to the hydroxyl group of polyepichlorohydrin (Fig 2.5b).

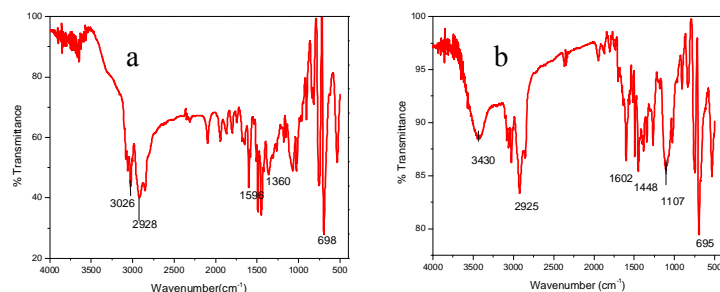


Fig 2.5 IR Spectra of (a) nitrated and (b) PECH attached Merrifield Resin

In solid state CP MAS ^{13}C NMR spectrum, broad signal around 50-85 ppm includes $\text{CH}_2\text{-OH}$, CH-O-CH_2 carbons of polyepichlorohydrin, the signal around 125 to 150 ppm is due to carbons of polystyrene support and 0-50 ppm includes carbons due to alkyl part of both support and PECH (Fig 2.6).

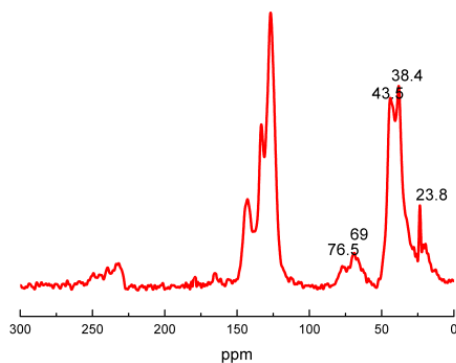


Fig 2.6 Solid State CP MAS ^{13}C NMR Spectrum of PECH attached Merrifield Resin

In the TG curve of PECH attached resin, two mass loss steps were observed. The first decomposition corresponded to nearly 54 % mass loss in the temperature around 323 °C. The second stage was completed around 413 °C. The first step of mass loss in TG could be attributed to elimination of chlorinated compounds. The mass loss above 400 °C was due to the

breakdown of the polymer backbone (Fig 2.7).⁷⁰ These observations give clear evidence for the attachment of PECH to the Merrifield resin.

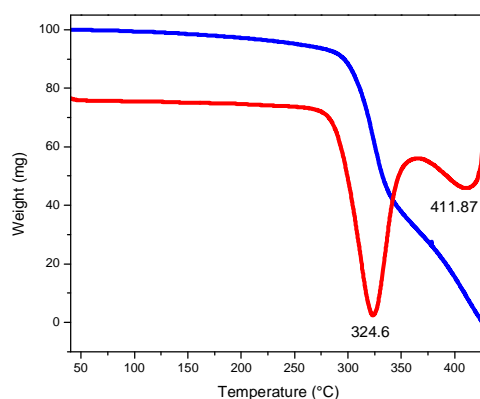


Fig 2.7 TG-DTG plot of PECH loaded Merrifield Resin

The hydroxyl groups of PECH loaded resin was estimated quantitatively. The amount of hydroxyl groups was found to be 1.86 mmol g^{-1} of the polymer. The hydroxyl group of the polymer was reacted with p-toluene sulphonyl chloride (TsCl) in pyridine.⁷¹ After tosylation, percentage of sulphur was found to be 2.44 % from CHNS data (C-68.39%, H-5.66%, S-2.44% and N-1.55%).

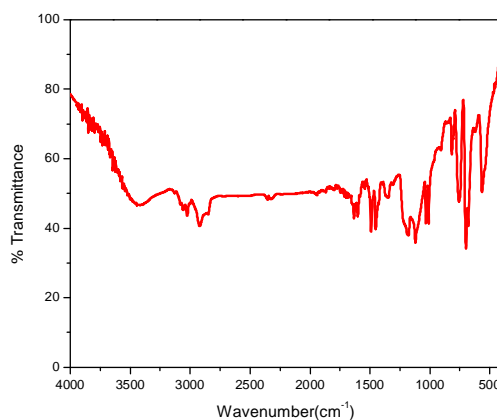


Fig 2.8 IR spectra of tosylated PECH loaded Merrifield Resin

The disappearance of broad peak around 3500 cm^{-1} in the IR spectrum of tosylated PECH indicated the alteration of hydroxyl group to tosyl group (Fig 2.8). During tosylation, it was observed that the yield was decreased to half by keeping the reaction for more time. This was due to the cleavage of the ether linkages in the polymer by the reaction with TsCl.⁷² The situation was same when 4% cross-linked Merrifield resin was used. The reaction was also monitored with p-toluene sulphonyl chloride in triethylamine. But there was no great noticeable change with respect to the yield of the product. The azidation of tosylated PECH was carried out using sodium azide in dimethylformamide at 85-90 °C.^{73,74} An intense peak at 2100 cm^{-1} in IR spectrum indicated the presence of azide functionality (Fig. 2.9).

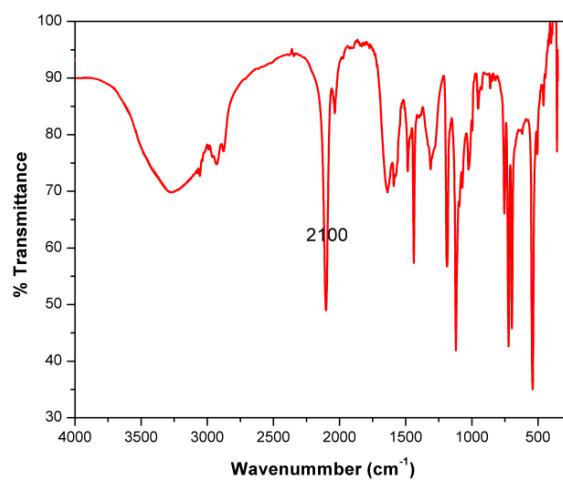


Fig 2.9 IR spectra of polyazide resin

In the solid state CP MAS ^{13}C NMR spectrum, due to the conversion of $\text{CH}_2\text{-Cl}$ of PECH to $\text{CH}_2\text{-N}_3$, the signal at 43.5 ppm was shifted to 38.5 ppm (Fig 2.10). The colour of the resin was changed to brown.

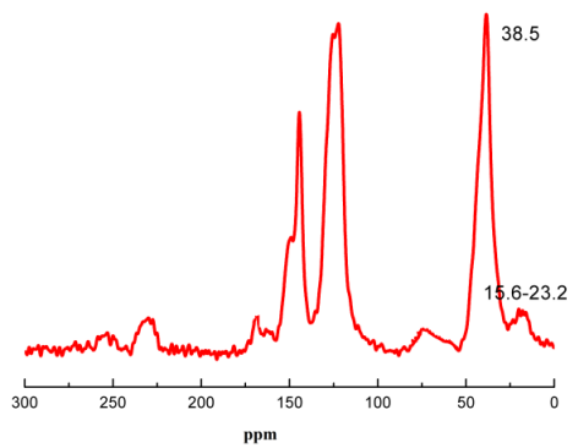
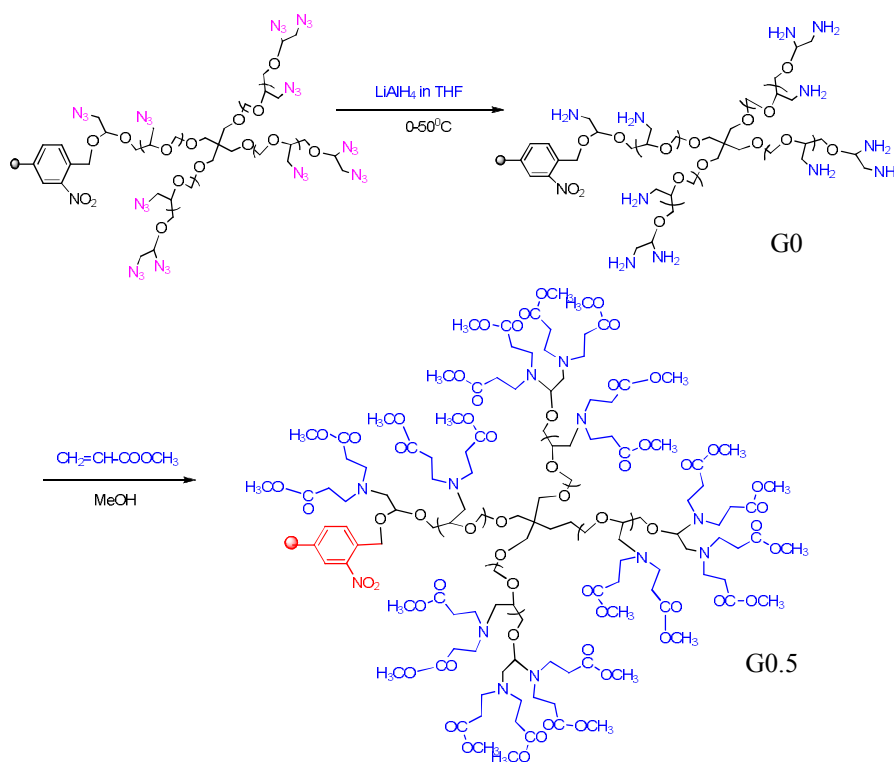


Fig 2.10 Solid State CP MAS ^{13}C NMR Spectrum of polyazide on Merrifield Resin



Scheme 2.2 Synthesis of G 0.5 dendrigraft polymer

The polyazide on reduction with lithium aluminium hydride in THF got converted to $-\text{CH}_2\text{NH}_2$ (Scheme 2.2).⁷⁵ In the IR spectrum of G0 polymer, the peak at 2100 cm^{-1} had completely disappeared and a peak at 3451 cm^{-1} showed the presence of amine functionality (Fig 2.11). The quantitative estimation showed the presence of 9.125 mmols of amine per gram of the resin. This high amine capacity compared with previously reported polyamines could happen only if the resin was loaded with PECH.

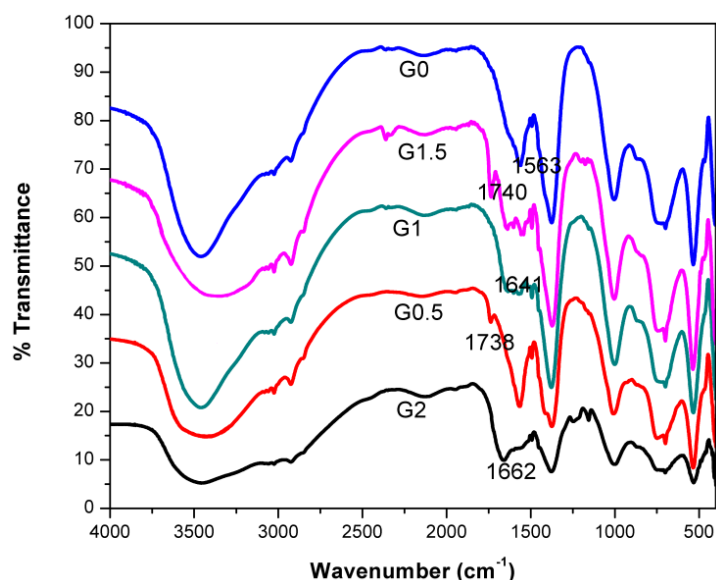


Fig 2.11 IR Spectra of PEN-G0, PEN-G0.5, PEN-G1, PEN-G1.5, PEN-G2

Quantification of the number of amino groups from DTG result was very close to the value obtained by analytical methods (Fig 2.12).⁷⁶ In the TG trace of G0 polymer, the first mass loss of about 20 % at $186\text{ }^\circ\text{C}$ was due to the elimination of amine as molecular nitrogen. The second mass loss of about 40 % at $404\text{ }^\circ\text{C}$ was due to the degradation of polyether chains.

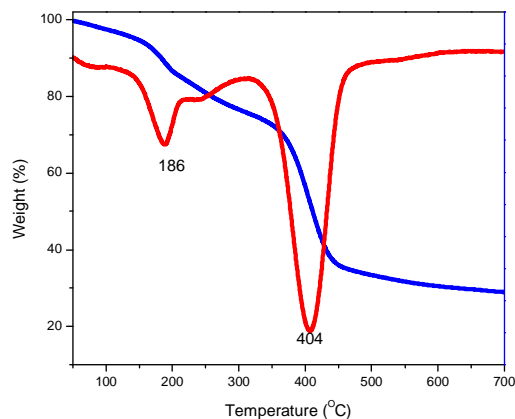


Fig 2.12 TG-DTG Plot of PEN-G0

The Michael addition of the G0 polyamine with methyl acrylate in methanol showed a peak at 1738 cm^{-1} in the IR spectrum of G0.5 (Fig 2.11).⁴⁹ Even though IR spectrum showed vibration bands in the region around 3400 cm^{-1} , negative Kaiser ninhydrin test result confirmed the absence of free amino groups.

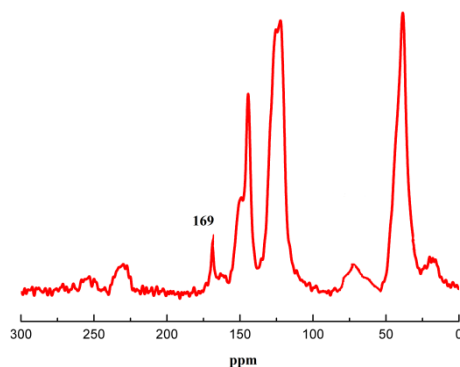
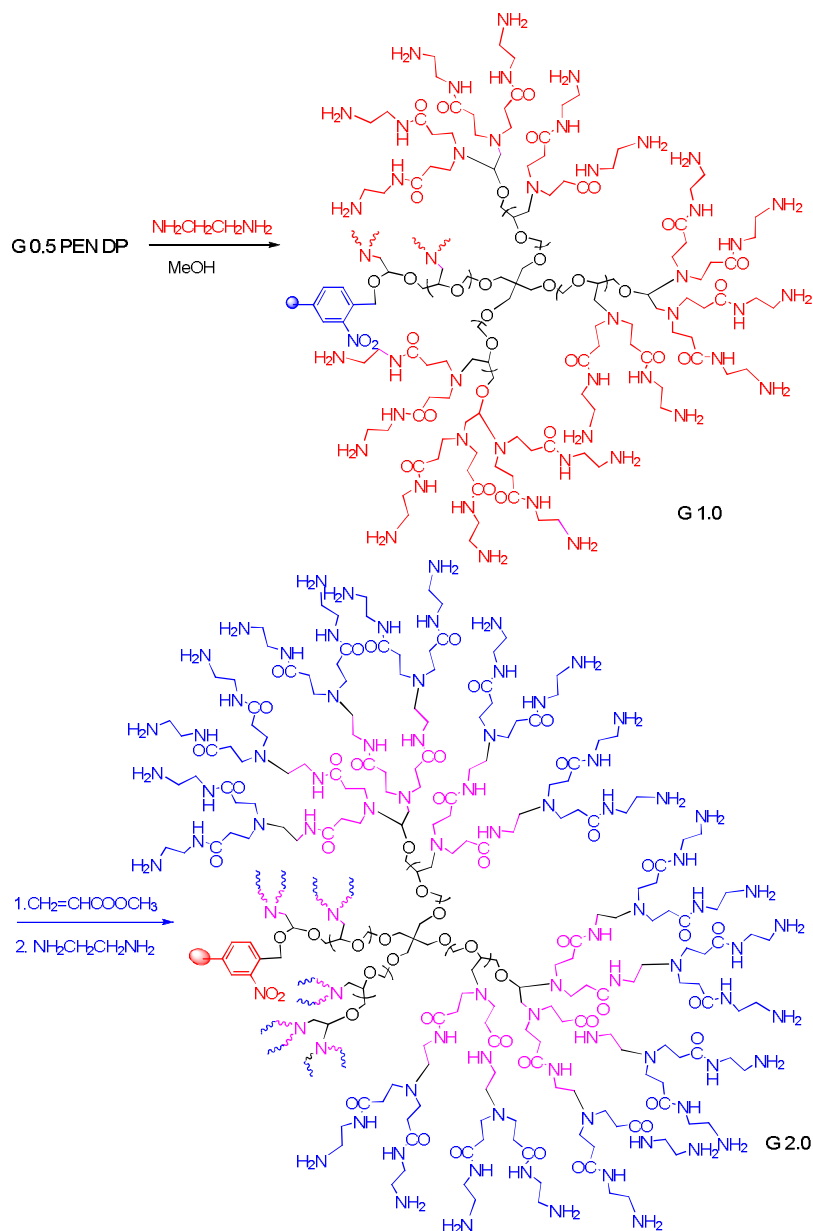


Fig 2.13 Solid State CP MAS ^{13}C NMR Spectrum of PEN-G0.5 Polymer

In the solid state CP MAS ^{13}C NMR spectrum of G0.5, appearance of a peak at 169 ppm (Figure. 2.13) confirmed the incorporation of ester functionality.



Scheme 2.3 Synthesis of G2.0 dendrigraft polymer

The G 0.5 polymer on amination with ethylene diamine got converted to amidoamine G1 polymer (Scheme 2.3).⁷⁷ In the IR spectrum

of G1 polymer, bands at 1641 and 3466 cm^{-1} are due to the amide carbonyl and amine moiety of the polymer (Fig 2.11). Both Michael addition and amination reaction took prolonged time for completion because of the poor swelling of resin loaded polymer in methanol. The amine capacity of G1 polymer was found to be 18.75 mmols g^{-1} .

In the TG curve of G1 resin; two mass loss steps were observed. The first decomposition corresponded to nearly 26 % mass loss in the temperature around 200 °C. The second stage mass loss of 30 % was observed around 383 °C (Fig. 2.14). The first step of mass loss in TG can be attributed to elimination of molecular nitrogen form the amino groups. The mass loss near 400 °C was due to the thermal degradation of the polymer backbone leading to the formation of hydrogen, carbon monoxide, carbon dioxide, methane, ammonia, hydrogen cyanide gas and other higher hydrocarbons.⁷⁰

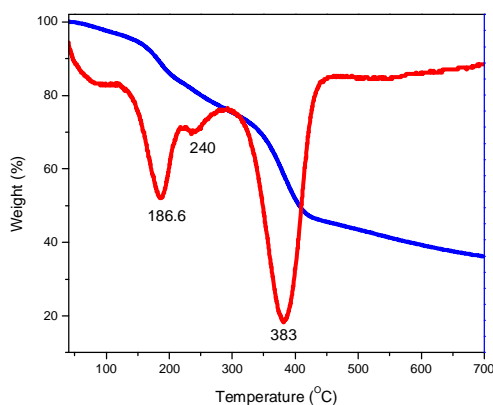


Fig 2.14 TG-DTG Plot of PEN-G1

The synthesis procedure was repeated to get G2 DP (Dendrigrraft polymer). Michael addition of G1 polymer resulted in the conversion of G1 to G1.5 Dendrigrraft Polymer. The peak at 1641 cm^{-1} in the IR spectrum due to carbonyl stretching of amide -C=O of PEN-G1 got

converted to 1740 cm^{-1} after Michael addition with methyl acrylate (Fig 2.11). In the solid state CP MAS ^{13}C NMR spectrum of PEN-G1.5, the signal at 169.4 ppm corresponds to ester carbon (Fig 2.15).

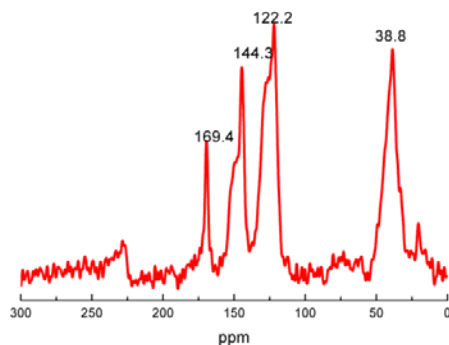


Fig 2.15 Solid State CP MAS ^{13}C NMR Spectrum of PEN G1.5 Polymer

The above G1.5 polymer on amination with ethylene diamine was converted to G2 polymer. The IR spectrum of PEN-G2 polymer showed vibration band at 1662 cm^{-1} due to carbonyl stretching of amide carbonyl and the band at 1740 cm^{-1} in the G1.5 due to ester functionality was disappeared (Fig 2.11). TG plot of PEN-G2 polymer showed similar decomposition pathway as that of G1 polymer, but a total mass loss of 36 % at 194.7 and $272.4\text{ }^{\circ}\text{C}$, and a 25 % mass loss at $407\text{ }^{\circ}\text{C}$ had occurred (Fig 2.16).

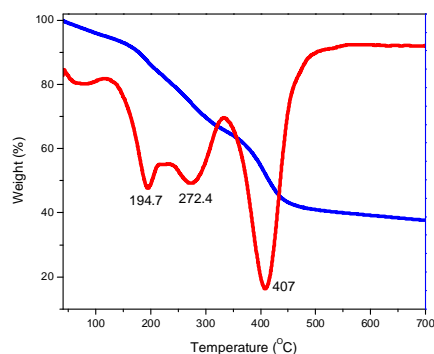


Fig 2.16 TG-DTG Plot of PEN-G2

Scanning electron micrograph of G2 DP shows irregular agglomerates of different shapes (Fig 2.17). The loss of spherical nature was due to the crushing of the supported Dendronized polymer due to prolonged stirring or may be due to the umbrella effect (to stretch to maximum extent) of the resin supported dendritic polymer.

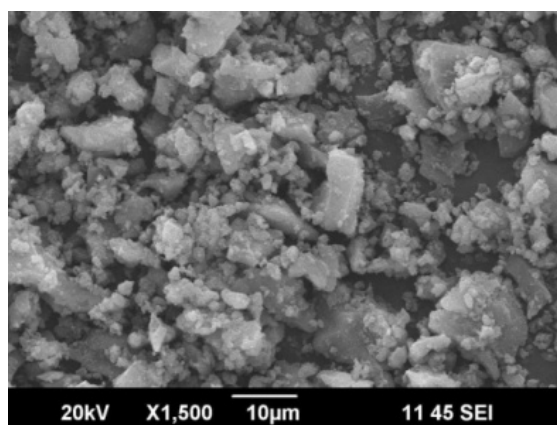


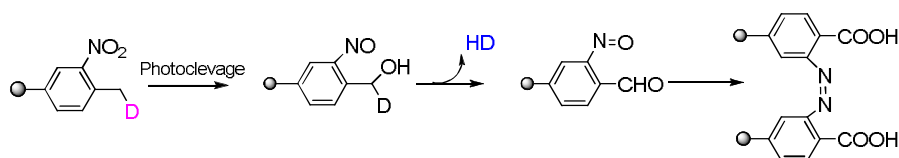
Fig 2.17 SEM image of PEN-G2

The amine capacity of G2 polymer was found to be 25 mmols g^{-1} which was not in good agreement with the theoretical value. This discrepancy is probably due to defective growth of the dendrons as a result of steric crowding and also due to hydrogen bonding which results in the lack of availability of free amine functionality for carrying out the Michael addition and subsequent reactions and also to a small extent of interpenetration of branches to one another.

2.2.1.1 Characterization of Photolytically Cleaved PEN-G2 Dendrigraft Polymer

Under photolytic conditions, the G0, G1 and G2 dendrigraft polymer undergo cleavage from the support. On photolytic cleavage, the

nitro group on polystyrene resin was converted to nitroso group with the elimination of dendritic polymer (Scheme 2.4).⁷⁸



Scheme 2.4 Mechanism of Photolytic Cleavage

The resultant G0 polymer was a brown viscous liquid, soluble in DMSO and methanol. The Chem Bio 3D image of G0 polymer cleaved from the support is shown in the Fig 2.18.

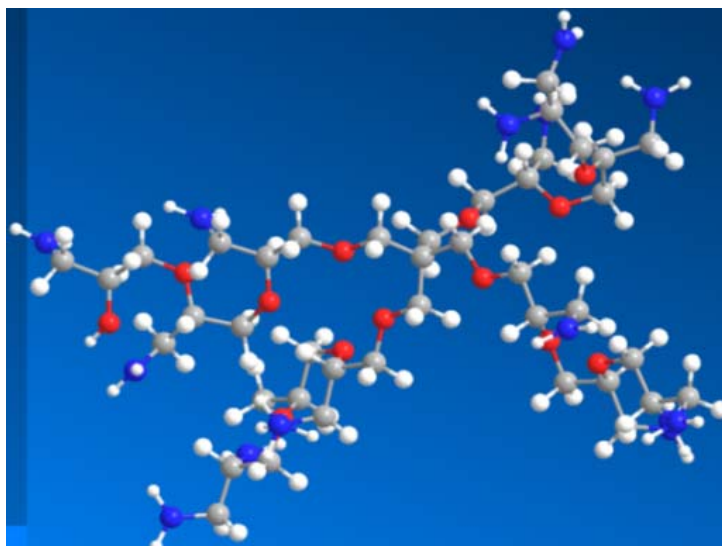


Fig 2.18 Chem Bio 3D image of G0 Dendrigraft Polymer

The ¹H NMR spectrum shows that the polymeric arms are somewhat similar (Fig 2.19). The appearance of peaks in the range 3.2-3.9 ppm in the ¹H NMR spectrum is due to the CH₂-O, CH-O and NH₂ protons of the polymer. The observed behaviour suggests that growth is regulated by a feedback mechanism due to confinement imposed by the support.⁷⁹

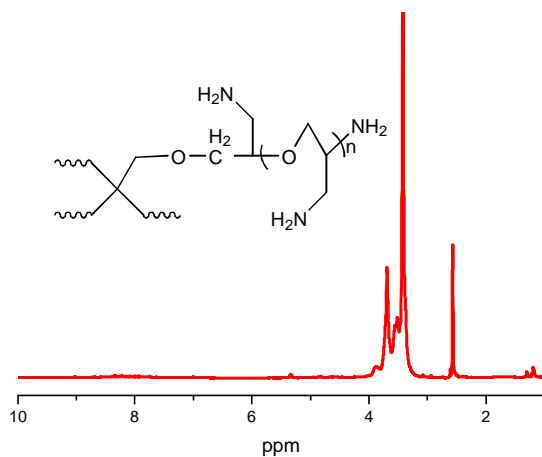


Fig 2.19 ¹H NMR Spectrum of PEN-G0 Polymer

From MALDI TOF MS analysis, the molecular weight of the polymer was found to be 884, which was agreeable with the theoretical value (Fig 2.20).

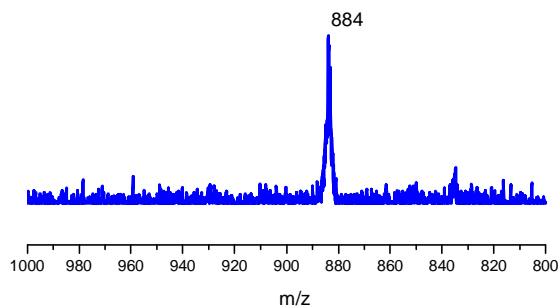


Fig 2.20 MALDI MS Spectrum of PEN-G0 Polymer

Resin loaded G1 polymer on photolytic cleavage gives a brown viscous liquid. One issue that needs to be addressed is the solubility of Dendronized polymers (DP). It has been known that, in general, DPs containing large number of free peripheral amine groups have low solubility in most commonly used solvents.⁸⁰ The lower solubility of the branched chains was attributed to their high propensity to

crystallization.²⁸ Inspection of the ^1H NMR spectrum of the G1 DP cleaved from the resin clearly indicates the appearance of amide proton at 7.9 ppm which was absent in G0 DP (Figure 2.21).

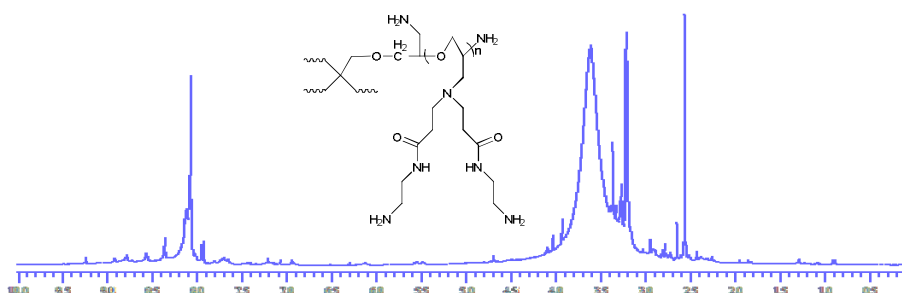


Fig 2.21 ^1H NMR Spectrum of PEN-G1 Polymer

To determine the exact number of dendritic substituents introduced, MALDI-TOF MS analysis was performed (matrix: dihydroxybenzoic acid) with the dendronized PEN-G1 polymer (Fig 2.22). But polymers with polydispersity index greater than 1.2 are difficult to be characterized with MALDI MS due to the signal intensity discrimination against higher mass oligomers.⁸¹⁻⁸³ The MALDI-TOF MS of PEN-G1 exhibited several peaks. Focus may be given to two major peaks. The peak at 2857.55 Da is derived from nine dendritic substituents on a pentaerythritol initiated polyether chain. The base peak at 1664.39 Da is derived from four dendritic substituents on a pentaerythritol initiated polyether chain. These results indicate that the G0 polymer was modified to ~70 % with dendron substituents on the polyether backbone. Generally, in order to minimize defects or cyclisation and to ensure complete reaction, as we go from lower to higher generation, large molar excess of the reagents have to be taken.⁸⁴

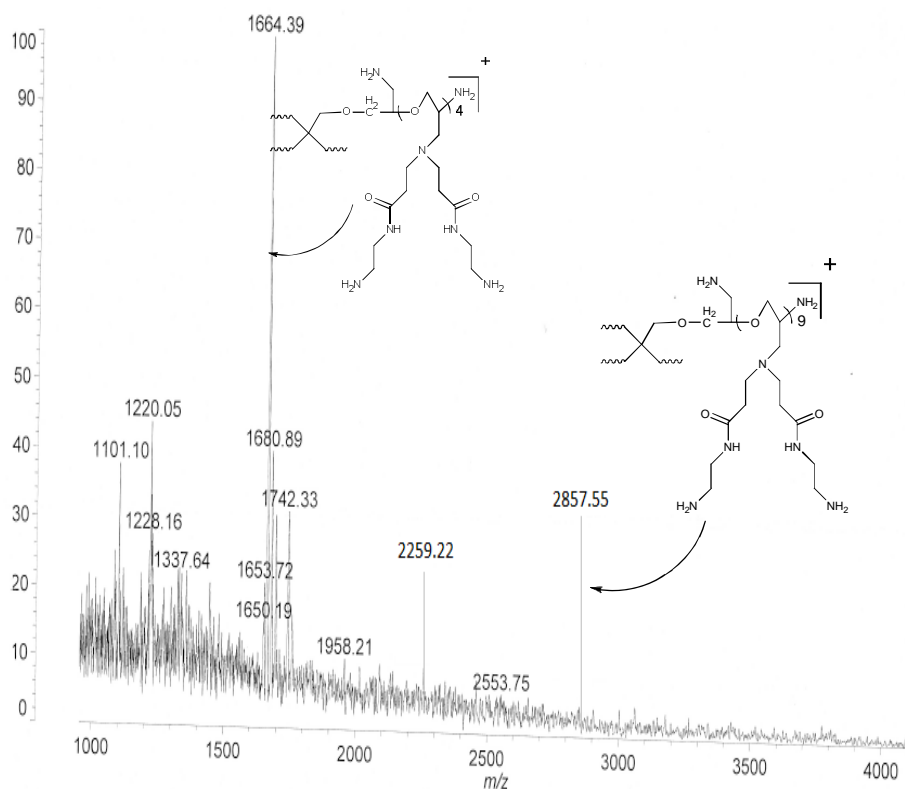


Fig 2.22 MALDI MS Spectrum of PEN-G1 Polymer

To confirm the introduction of dendritic substituents onto polyether, dendronized G1 polymer was analyzed by atomic force microscopy (AFM) (Fig. 2.23).⁸⁵ Samples for AFM analysis were prepared by spin coating methanolic solution of the dendronized polymer on a glass plate and AFM analysis was performed in the tapping mode. The AFM image of the film of G1 polymer deposited from higher concentration (0.1 % w/w) at a scan width of 75 μm shows spherical aggregates of different sizes.

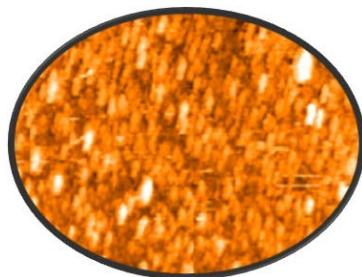


Fig 2.23 AFM image of PEN-G1 Polymer

The ^1H NMR spectrum can provide general information, such as repeating unit or uniformity of branches but cannot confirm the absolute purity of the macromolecules, particularly the identity and number of end groups. This is in large part because, any signal that originates from the small proportion of end groups is overwhelmed by that of the numerous repeating units. As a result ^1H NMR spectrum provides little utility in elucidating polymer end groups, either qualitatively or quantitatively.^{50,86-87} The ^1H NMR spectrum of PEN-G2 Dendronized polymer shows broadening of peaks (Fig 2.24) in comparison with PEN-G1 DP.

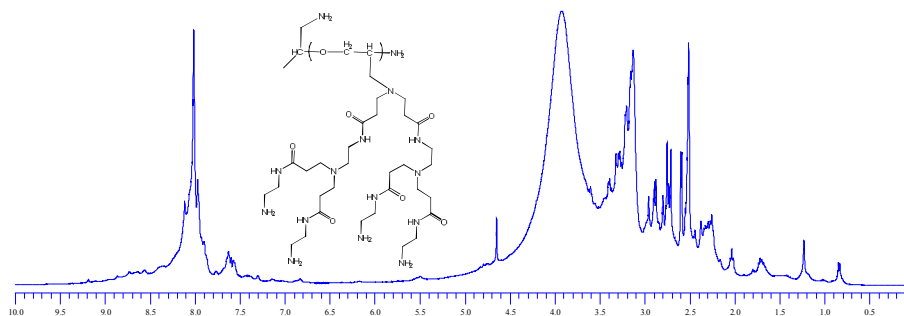


Fig 2.24 ^1H NMR spectrum of PEN-G2 Polymer

Two problems are commonly encountered during the synthesis of high generation dendritic polymers, the occurrence of structural defects and dendritic aggregation due to the interdigitation of dendritic arms.⁸⁸ In this regard, defects in the dendritic structure can arise through incomplete

reactions brought about by steric congestion at the periphery or backfolding of flexible dendritic branches, which hides their functional groups. The highest molecular weight of the PEN-G2 polymer from MALDI MS analysis was found to be 3966.02 with a base peak at 1225.41 and another major peak at 1662.72 (Fig 2.25). The molecular weight at 3966.02 shows that out of the 9 G1 dendritic substituents, only 5 of them got converted to G2.

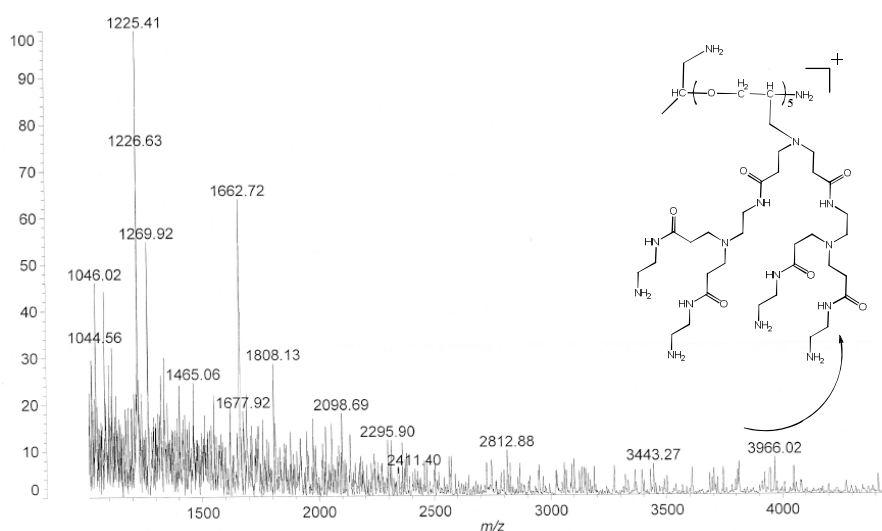


Fig 2.25 MALDI MS Spectrum of PEN-G2 Polymer

The peak at 1662.72 corresponds to the formation of one G2 dendron unit. The peak at 1225.41 is due to cleavage of G2 dendritic unit from the polymeric backbone. The highest mass of 3966 shows that only 30% of dendron substituents are incorporated. The lower experimental mass compared to theoretical mass can be due to missing branches. The difference in experimental and theoretical masses can partially be attributed to structural defects, because, errors can also be due to the polydisperse nature of the polymer. Also, the lower mass may be due to the thermal

decomposition of the high generation polymer in comparison with lower generation dendrigraft polymers.⁸⁹

Like conventional PAMAM starburst dendrimers, the salient structural peculiarity is their fractal symmetry in constitution⁹⁰ i.e., a geometric pattern that is repeated (iterated) at every smaller (or larger) scales to produce (self similar) irregular shapes and surfaces that cannot be represented by classical (Euclidian) geometry. Fractals are used especially in computer modelling of irregular patterns and structures found in nature. The fractal nature of the star burst dendrimer structures precludes long-range order.⁹¹⁻⁹³ Therefore, their morphologies and shapes have not yet been defined by X-ray spectroscopic techniques.



Fig 2.26 AFM image of PEN-G2 Polymer

Molecular simulations of the PAMAM dendrimers have indicated that the early full generations ($G = 1-2$) are characterized by asymmetric disk like shapes. These correspond to open structures that can be readily penetrated by solvent. Higher generations possess a nearly spherical shape, which corresponds to closed, densely packed surface structures.⁹⁴ In contrast to dendrimers, dendrigraft polymers show more closed or

spherical nature at low generation, but at higher generations, polymeric arms are more stretched and have rod like appearance.⁷

The shape of dendronized polymer in the case of PEN-G2 was analyzed by atomic force microscopy (AFM) as in the case of PEN-G1. In AFM, the film uniformity is mostly determined by the concentration of the dendritic solution regardless of generation.⁹⁵ The AFM image of the G2 polymer from lower concentration (0.01 wt%) at a scan width of 15 μm around 10 nm shows a small elongated worm or string like appearance (Fig 2.26). Since polyether backbone is only having approximately 10-13 units, the length of the worm that we observed is agreeable with the length of the polyether oligomer. Despite the approximate nature owing to uncertainties associated with the AFM technique (tip convolution), it was clear that the average worm length corresponds to the length of the parent polyether, whereas the height of the polymer chain depends upon the dendron generation.⁹⁶

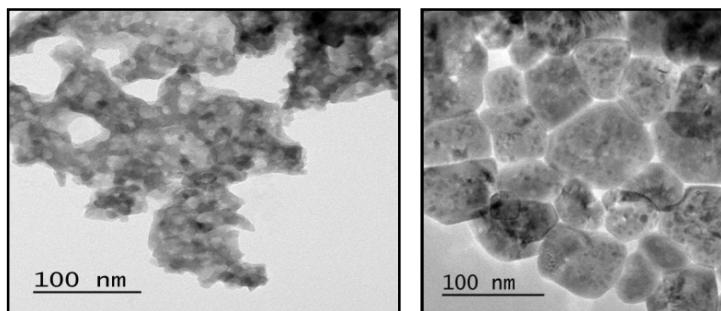


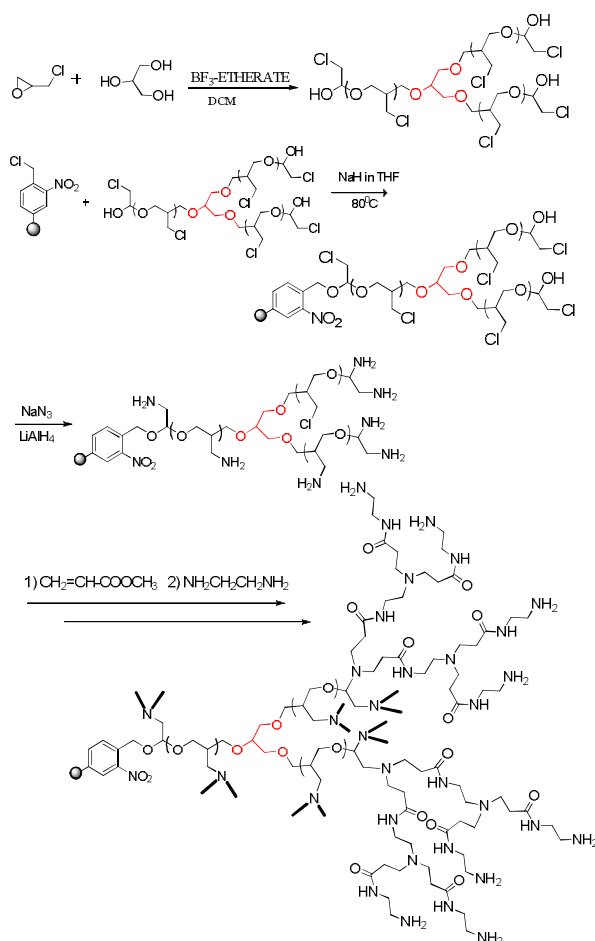
Fig 2.27 TEM image of PEN-G2 polymer

The TEM micrograph of the PEN-G2 polymer in methanolic solution shows polygon shape with low molecular weight polymers aggregate inside the polygon. The polygon shape with longest-extension diameter of up to 13.7 nm may be due to the clustering of polymeric arms in

solution (Fig 2.27). Reports regarding dendrigraft polymers say that they are elongated due to linear polymeric core with dendritic arms. But in solution they remain as spherical.⁹⁷

2.2.2 Synthesis of Merrifield Resin Supported Dendrigraft Polymer having Glycerol Initiated PECH as Core - GLR-G2

The resin supported dendrigraft amidoamine polymer was synthesized using the schematic procedure (Scheme 2.5).



Scheme 2.5 Synthesis of GLR-G2 Dendrigraft Polymer

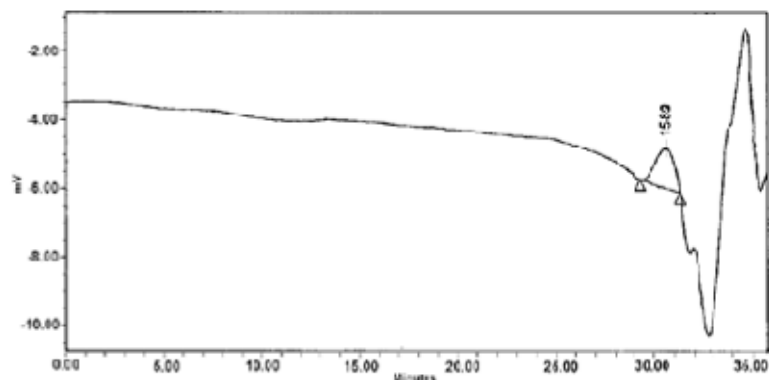


Fig 2.28 GPC Profile of glycerol initiated PECH

The branched hydroxyl terminated PECH (polyepichlorohydrin) was prepared by the ring opening polymerization of the oxirane group in ECH (epichlorohydrin) in the presence of glycerol by activated monomer mechanism (AMM).⁶⁶ It was a colorless viscous liquid. From GPC (Fig 2.28), the molecular weight of PECH was found to be 1589 with a polydispersity of 1.06.

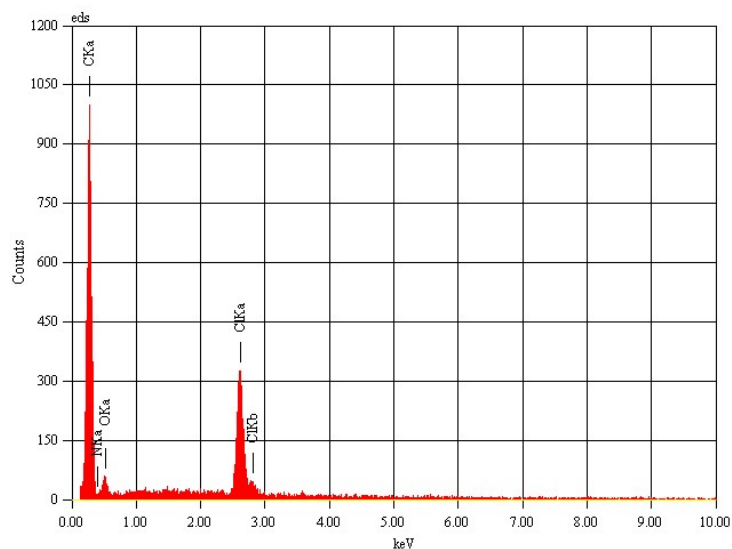


Fig 2.29 EDX Spectrum of glycerol initiated PECH coupled Merrifield Resin

Merrifield Resin was made photoactive by the introduction of a nitro group at the ortho position of chloromethyl group.⁶⁷ The PECH was coupled to the resin using sodium hydride and tetrabutyl ammonium bromide.^{68,69}

After coupling, chlorine capacity was found to be 12.863 mmols g⁻¹. The EDX spectrum shows carbon, oxygen and chlorine as the main constituents of the polymer (Fig 2.29).

In the CP MAS ¹³C NMR spectrum of the PECH coupled Merrifield Resin, the peak at 69.9 ppm shows the incorporation of polyether chain (Fig. 2.30). The hydroxyl groups of PECH loaded resin was estimated quantitatively and was found to be 1.43 mmol g⁻¹ of the polymer. The hydroxyl group of the polymer was reacted with p-toluene sulphonyl chloride (TsCl) in pyridine.⁷¹ After tosylation, percentage of sulphur was found to be 1.63 % from CHNS data.

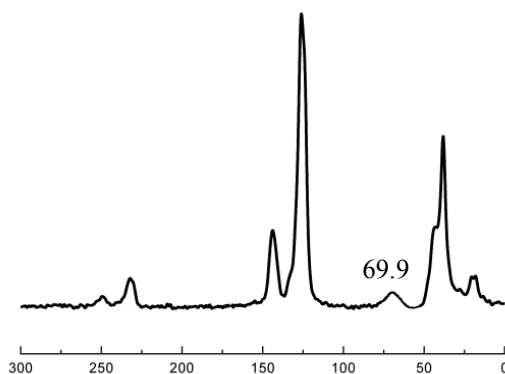


Fig 2.30 Solid State CP MAS ¹³C NMR spectra of GLR-PECH coupled Merrifield Resin

The azidation of tosylated PECH was carried out using sodium azide in dimethyl formamide at 85-90°C.^{73,74} An intense band at 2100 cm⁻¹

¹ in IR spectrum indicated the presence of azide functionality (Fig. 2.31). The colour of the resin was changed to brown. The polyazide on reduction with lithium aluminium hydride in THF got converted to the polyamine.⁷⁵ In the IR spectrum, the band at 2100 cm^{-1} had completely disappeared and a band at 3477 cm^{-1} showed the presence of amine functionality (Fig 2.31). The quantitative estimation showed the presence of 13.45 mmols of amine per gram of the resin.

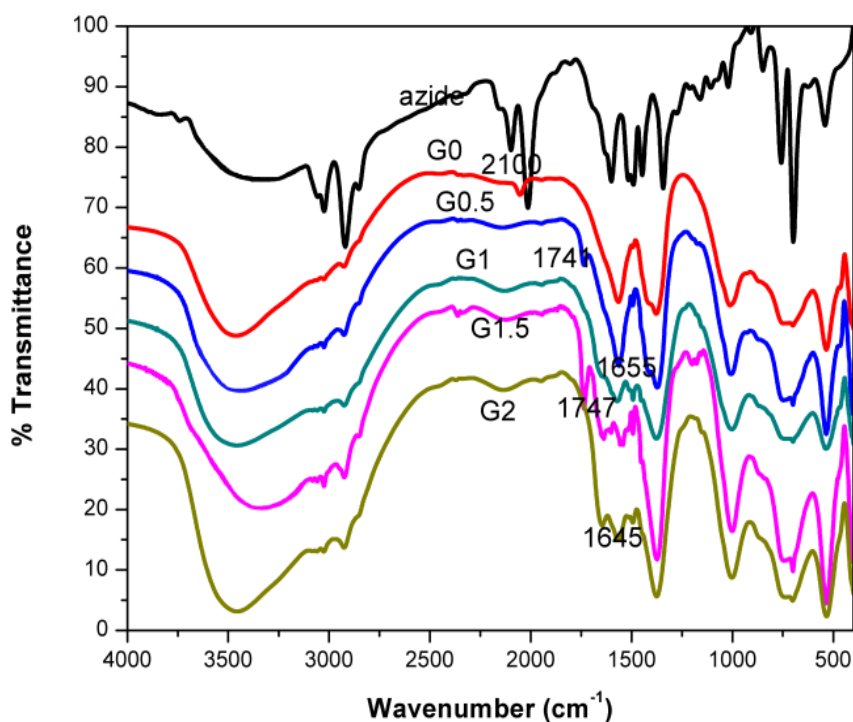


Fig 2.31 IR Spectra of GLR-Gn Polymer

In the TG curve of G0 polymer, the first mass loss of about 25 % around 200 °C was due to the elimination of amine as molecular nitrogen. The second mass loss of about 36 % at 382 °C was due to the polyether degradation (Fig 2.32).

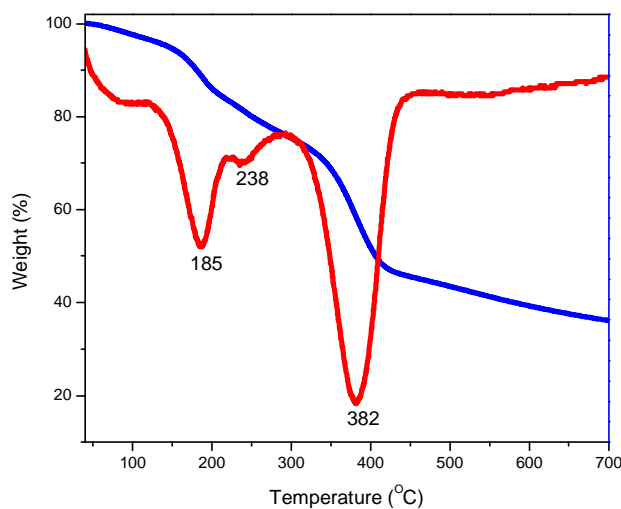


Fig 2.32 TG-DTG Profile of GLR-G0 Polymer

The Michael addition of the G₀ polyamine with methyl acrylate in methanol showed a peak at 1741 cm⁻¹ in the IR spectrum (Fig 2.31).⁴⁹ In the solid state ¹³C NMR spectrum of G 0.5, the signal corresponding to 169.8 ppm is due to carbonyl carbon of ester functionality (Fig 2.33).

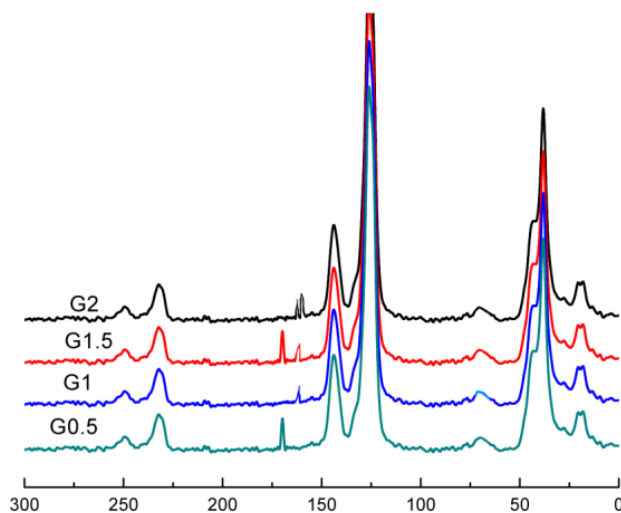


Fig 2.33 Solid State CP MAS ¹³C NMR spectra of GLR-Gn Resin

The above polymer on amination with ethylene diamine was converted to amidoamine G1 polymer.⁷⁷ In the IR spectrum of G1 polymer, bands at 1655 cm^{-1} and 3482 cm^{-1} are due to the carbonyl and amine moiety of the polymer (Fig 2.31). The amine capacity of G₁ polymer was found to be 22.13 mmol g^{-1} . In the solid state ^{13}C NMR spectrum, the peak corresponding to 167.4 ppm corresponds to carbonyl carbon of amide functionality (Fig 2.33). In the TG curve of G1 resin; two mass loss steps were observed. The first decomposition corresponded to nearly 30 % mass loss in the temperature around $213\text{ }^{\circ}\text{C}$. The second stage mass loss of 40 % was observed around $410\text{ }^{\circ}\text{C}$ (Fig 2.34).

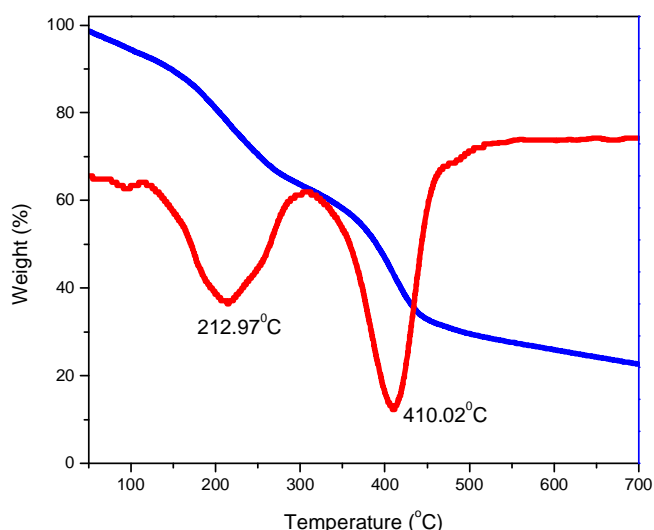


Fig 2.34 TG-DTG Profile of GLR-G1 Polymer

The synthesis procedure was repeated to get G2 Dendronized polymer. The Michael addition of the G₁ polyamine with methyl acrylate in methanol showed a peak at 1747 cm^{-1} in the IR spectrum (Fig 2.31).⁴⁹ In the solid state ^{13}C NMR spectrum, the signal corresponding to 169.8 ppm and 167.2 ppm are due to carbonyl carbon of ester and amide

functionality respectively (Fig 2.33). The above polymer on amination with ethylene diamine was converted to amidoamine G2 polymer.⁷⁷ In the IR spectrum of G2 polymer, peaks at 1645 cm^{-1} and 3482 cm^{-1} are due to the carbonyl and amine moiety of the polymer (Fig 2.31). In the solid state ^{13}C NMR spectrum, the signals corresponding to 167.2 ppm and 167.8 ppm correspond to carbonyl carbon of different amide functionality (Fig 2.33). The amine capacity of G2 polymer was found to be 30.24 mmol g^{-1} which was higher than that of PEN-G2 polymer. TG curve of G2 polymer shows similar decomposition pathway as that of G1 polymer, but exhibited a mass loss of 42 % between $120\text{--}250\text{ }^{\circ}\text{C}$ and 45 % at $416\text{ }^{\circ}\text{C}$ (Fig 2.35).

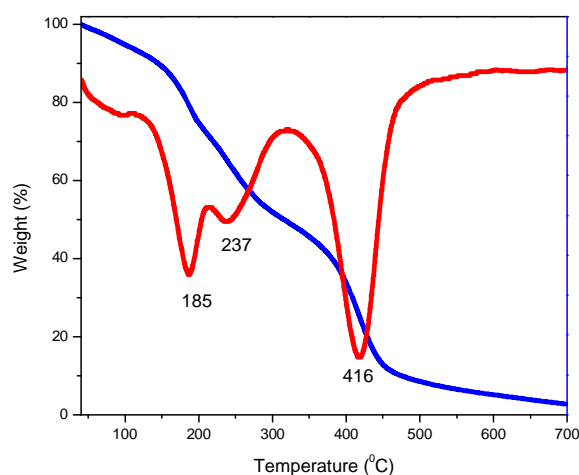


Fig 2.35 TG-DTG Profile of GLR-G2 Polymer

In order to find the mass of the GLR-G2 polymer attached to the Merrifield resin, the resin carrying the GLR-G2 polymer was cleaved photolytically. The molecular weight obtained from MALDI analysis was 2927, which corresponded to 9 dendritic units on the polyether backbone (Fig 2.36).

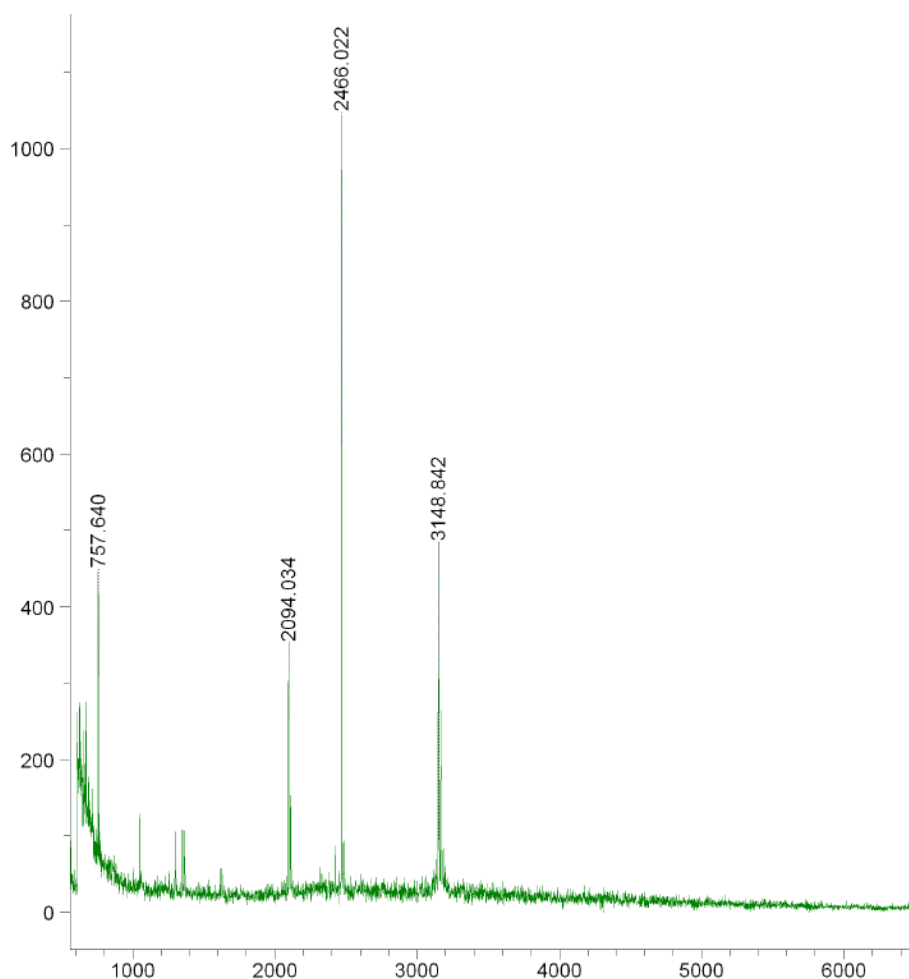
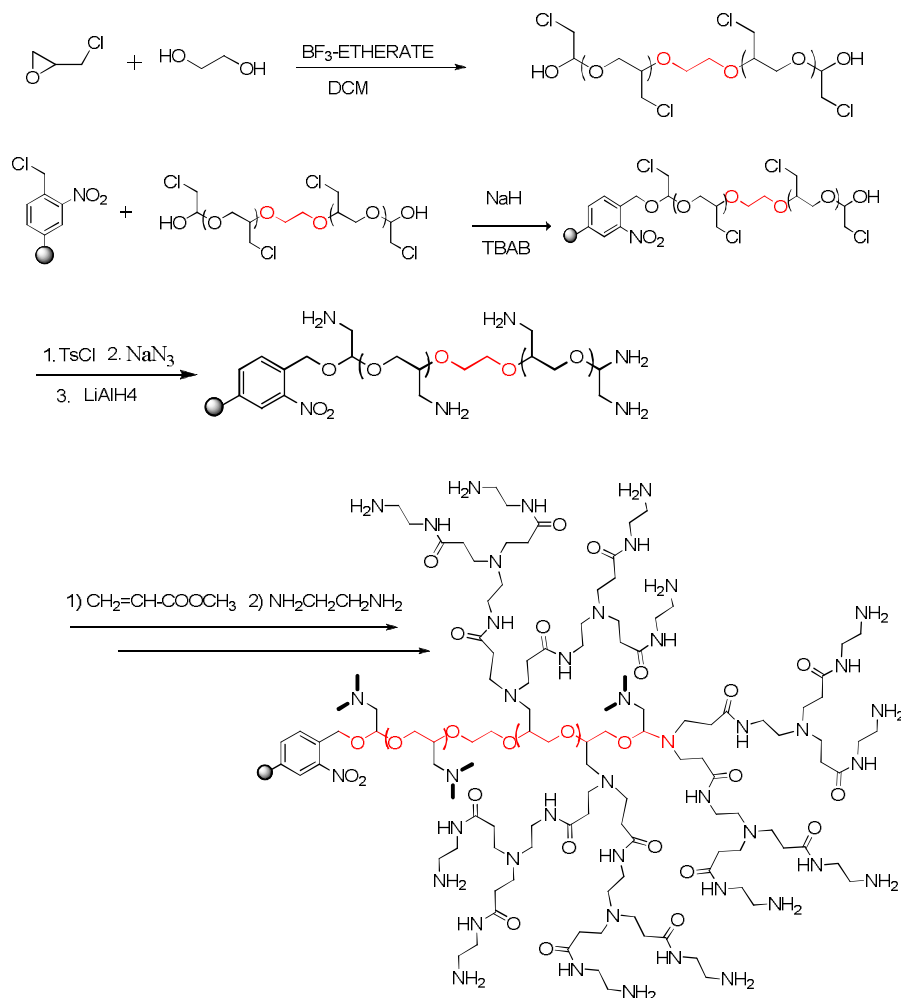


Fig 2.36 MALDI-TOF MS spectrum of GLR-G2

2.2.3 Synthesis of Merrifield Resin supported Dendrgraft Polymer having Ethylene Glycol Initiated PECH as Core - EG-G2

The resin supported dendrgraft amidoamine polymer was synthesized using the schematic procedure (Scheme 2.6).



Scheme 2.6 Synthesis of EG-G2 dendrigraft polymer

The linear hydroxyl terminated PECH (polyepichlorohydrin) was prepared by the ring opening polymerization of the oxirane group in ECH (epichlorohydrin) in the presence of ethylene glycol by activated monomer mechanism (AMM).⁶⁶ It was a colorless viscous liquid. From GPC (Fig 2.37), the molecular weight of PECH was found to be 1200 with a polydispersity of 1.28.

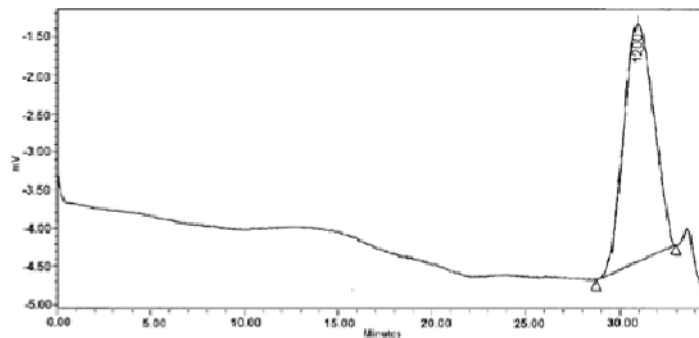


Fig 2.37 GPC Profile of ethylene glycol initiated PECH

Merrifield resin was made photoactive by the introduction of a nitro group at the ortho position of chloromethyl group.⁶⁷ The PECH was coupled to the resin using sodium hydride and tetrabutyl ammonium bromide.⁶⁸ After coupling, chlorine capacity was found to be 10.23 mmols g⁻¹.

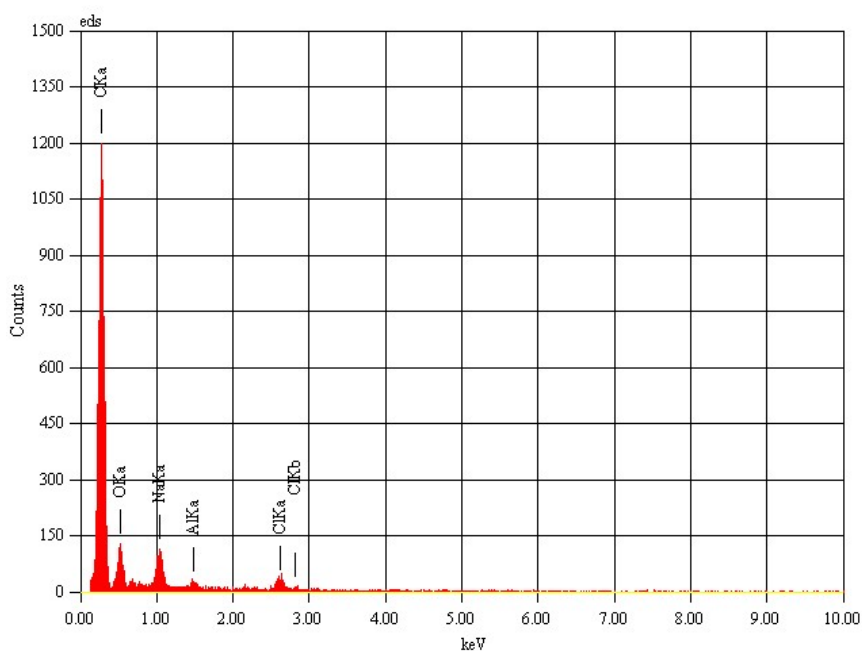


Fig 2.38 EDX Spectrum of ethylene glycol initiated PECH coupled Merrifield Resin

EDX spectrum showed carbon, oxygen and chlorine as the main constituents of the polymer (Fig 2.38). The hydroxyl groups of PECH loaded resin was estimated quantitatively and was found to be 1.03 mmol g^{-1} of the polymer. The hydroxyl group of the polymer was reacted with *p*-toluene sulphonyl chloride (TsCl) in pyridine.⁷¹ After tosylation, percentage of sulphur was found to be 0.84 % from CHNS data. The azidation of tosylated PECH was carried out using sodium azide in dimethyl formamide at 85-90 °C.^{73,74} An intense peak at 2100 cm^{-1} in the IR spectrum indicated the presence of azide functionality (Fig. 2.39). The colour of the resin was changed to brown. The polyazide on reduction with lithium aluminium hydride in THF got converted to polyamine.⁷⁵ In the IR spectrum, the peak at 2100 cm^{-1} had completely disappeared and a peak at 3470 cm^{-1} showed the presence of amine functionality (Fig 2.39). The quantitative estimation showed the presence of 10.49 mmols of amine per gram of the resin.

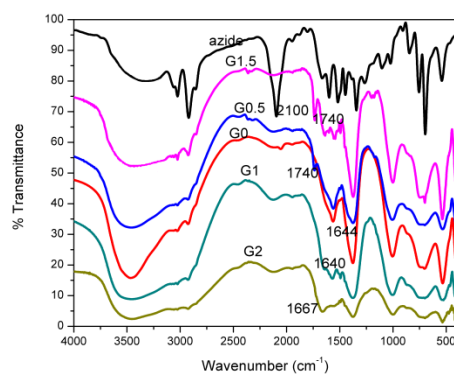


Fig 2.39 IR Spectra of EG-Gn Polymer

In the TG curve of G0 polymer, the mass loss of about 21.1 % around 150-250 °C is due to the elimination of amine as molecular nitrogen. The second mass loss of about 65 % at 407 °C is due to the degradation of the polymer chain (Fig 2.40).

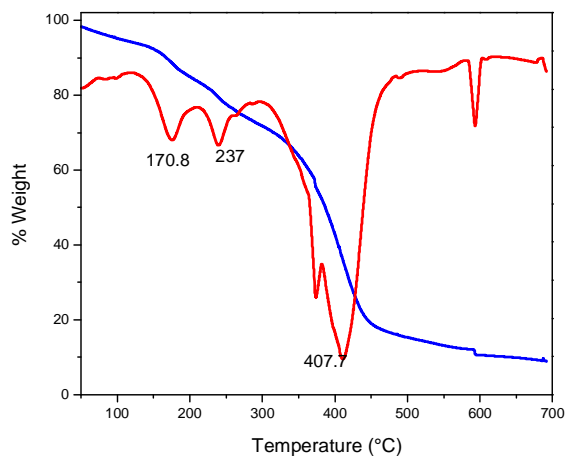


Fig 2.40 TG-DTG Profile of EG-G0 Polymer

The Michael addition of the G₀ polyamine with methyl acrylate in methanol showed a peak at 1740 cm⁻¹ in the IR spectrum (Fig 2.39).⁴⁹ In the solid state ¹³C NMR spectrum, the signal corresponding to 169.8 ppm is due to carbonyl carbon of ester functionality (Fig 2.41).

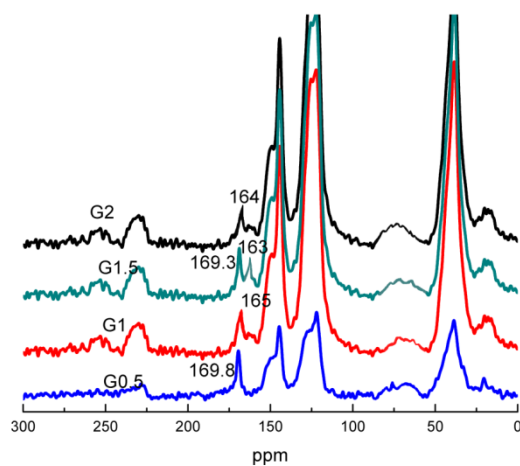


Fig 2.41 Solid State CP MAS ¹³C NMR Spectra of EG-G_n Polymers

The G 0.5 polymer on amination with ethylene diamine, was converted to amidoamine G1 polymer (Scheme 2.6).⁷⁷ In the IR spectrum

of G1 polymer, peaks at 1640 and 3478 cm^{-1} are due to the amide carbonyl and amine moiety of the polymer (Fig 2.39). The amine capacity of G1 polymer was found to be 18.06 mmols g^{-1} . In the solid state ^{13}C NMR, the peak corresponding to 165 ppm corresponds to amide functionality in G1 polymer (Fig 2.41).

In the TG curve of G1 attached resin; three mass loss steps were observed. The first two decompositions corresponded to nearly 22.5 % mass loss in the temperature region 150-320 $^{\circ}\text{C}$. The second stage mass loss was observed around 408 $^{\circ}\text{C}$ due to polyether chain degradation (Fig 2.42).

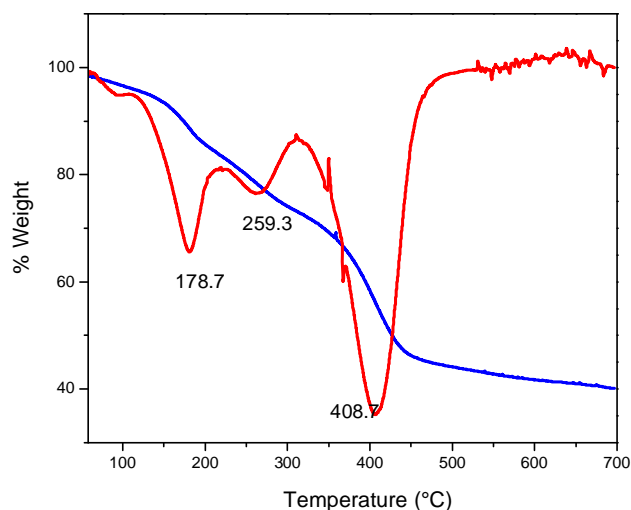


Fig 2.42 TG-DTG Profile of EG-G1 Polymer

The synthesis procedure was repeated to get G2 Dendronized polymer. The Michael addition of the G₁ polyamine with methyl acrylate in methanol resulted in G1.5 polymer which showed a peak at 1740 cm^{-1} in the IR spectrum (Fig 2.39).⁴⁹ In the solid state ^{13}C NMR spectrum, the signals corresponding to 169.3 ppm and 163 ppm are due to carbonyl

carbon of ester and amide functionality respectively (Fig 2.41). The above polymer on amination with ethylene diamine was converted to amidoamine G2 polymer.⁷⁷ In the IR spectrum of G2 polymer, peaks at 1667 cm^{-1} and 3455 cm^{-1} are due to the carbonyl and amine moiety of the polymer (Fig 2.39). The amine capacity of G2 polymer was found to be 24.96 mmol g^{-1} . In the solid state ^{13}C NMR, the signal corresponding to 164 ppm corresponds to carbonyl carbon of amide functionality (Fig 2.41).

TG curve of G2 polymer shows similar decomposition pathway as that of G1 polymer, mass loss of 28.9 % between $190\text{--}300\text{ }^{\circ}\text{C}$ and 25 % at $412\text{ }^{\circ}\text{C}$ were observed (Fig 2.43).

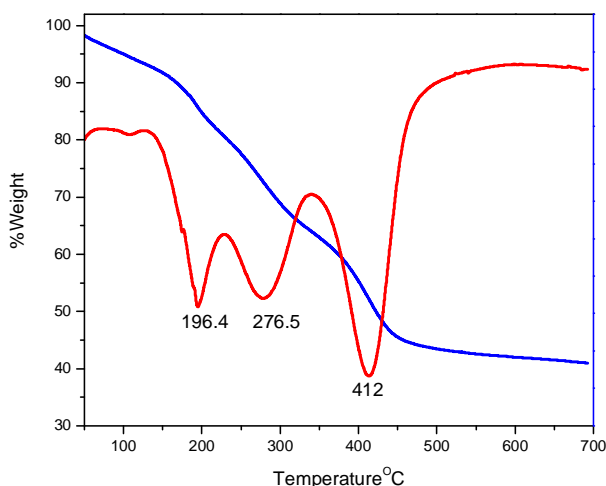


Fig 2.43 TG-DTG Profile of EG-G2 Polymer

2.3 Conclusions

Polyepichlorohydrin was coupled to Merrifield resin in order to increase the loading capacity. Novel families of dendrigraft G0, G1 and G2 amine polymer having pentaerythritol, glycerol and ethylene glycol initiated polyepichlorohydrin as core have been synthesized and characterized.

Characterization of dendrigraft amidoamine polymer having pentaerythritol initiated polyepichlorohydrin as core has been done after photolytic cleavage of the same from the support. Amount of amino group in the G0, G1 and G2 series was found to be comparable for dendrigraft polymer having ethylene glycol and pentaerythritol initiated polyepichlorohydrin as core while the same was found to be higher for dendrigraft polymer having glycerol initiated polyepichlorohydrin as core. This may be due to the monodispersity and high molecular weight of glycerol initiated polyepichlorohydrin compared to other polycore polyepichlorohydrins.

2.4 Experimental Section

2.4.1 Materials

Chloromethyl polystyrene (1% DVB crosslinked, 100–200 mesh) was obtained from Thermax India Ltd. as a gift sample. It was washed with methanol, dioxane and acetone and dried under vacuum. Sodium hydride, Tetrabutyl ammonium bromide, p-toluene sulphonyl chloride, Sodium azide, LiAlH_4 , methyl acrylate and ethylene diamine all were purchased from local vendors and were used as received. All solvents were distilled by standard procedures prior to use.

2.4.2 Preparation of 3-nitro-4-chloromethylpolystyrene

Chloromethyl polystyrene (5 g) was added slowly in small lots with stirring to fuming nitric acid (50mL) taken in a 250 mL RB flask and cooled to 0 °C. The addition was very slow that the temperature was not allowed to rise above 5 °C. After the completion of addition, the temperature was maintained at 0-5 °C for 1 h with constant stirring. The temperature was slowly brought to 30 °C with in a period of 3 h. The

reaction mixture was heated slowly to 50 °C for 1 day. It was poured over crushed ice. The polymer beads were recovered by filtration, washed with water, dioxane and methanol.

2.4.3 Preparation of polyepichlorohydrin- PECH

Epichlorohydrin (15.65 mL, 0.2 mol) was added through a dropping funnel to a cooled reaction mixture containing dichloromethane (15 mL), Pentaerythritol (1.36 g, 0.01 mol) and BF₃-etherate (1.256 mL, 0.01 mol) with constant stirring. The reaction mixture was stirred for 24 h at 30 °C. After completion of the reaction, the reaction mixture was taken in a separating funnel and washed with saturated sodium carbonate solution followed by distilled water. The solvent was removed under vacuum. In the case of glycerol initiated PECH, the amount of various reactants were 11.742 mL (0.15 mol) epichlorohydrin and 0.73 mL (0.01 mol) glycerol. In the case of ethylene glycol initiated PECH, 7.828 mL (0.1 mol) epichlorohydrin and 0.557 mL (0.01 mol) ethylene glycol with the same amount of BF₃ etherate were added.

2.4.4 Coupling of PECH to the Resin

Sodium hydride (1 g) was added to a stirred solution of PECH (5.0-6.0 g) in dry DMF (50 mL) at 0 °C. After 2 h, Merrifield resin (1.0 g), and tetrabutyl ammonium bromide (216 mg, 0.62 mmol) were added and the mixture was shaken at room temperature for 20 h. The reaction was quenched by addition of water (20 mL) and the resin was filtered followed by washing with DMF/Water (1:1, 3 times), DMF (3 times), THF (3 times) and dichloromethane (3 times) and dried to constant weight under vacuum to yield the PECH loaded resin. The unreacted

PECH was removed by soxhlet extraction with dichloromethane and dried under vacuum for 24 h.

2.4.5 Estimation of hydroxyl group

0.5 g of the hydroxyl compound was taken in a RB flask fitted with a condenser. 10 mL of the acetylating mixture (1 volume acetic anhydride + 4 volume anhydrous pyridine) was added. It was heated on a boiling water bath for 60 min. The reaction mixture was removed from water bath, 20 ml distilled water was added, shaken well to ensure complete hydrolysis of the unchanged acetic anhydride, cooled and allowed to stand for 10 min. The solution was titrated with 1 N NaOH using phenolphthalein as indicator.

2.4.6 Tosylation of hydroxyl group

The resin supported PECH (1.0 g) was dispersed in pyridine and cooled to -5 °C. A cold solution of p-toluene sulphonyl chloride (0.7g, 0.004 mol) in 5 mL pyridine was added slowly. Upon complete addition, the temperature was held at -5 °C for 30 min, and allowed to come to 30 °C overnight. The contents of the flask were quenched by pouring ice water. It was filtered and washed with ice water, methanol, ether and acetone.

2.4.7 Synthesis of Polyazide

The resin supported tosylated PECH (1.0 g) was allowed to swell in DMF, sodium azide (0.455 g, 0.007 mol) in 10ml DMF was added and heated at 85-90 °C for one day. It was filtered and washed with water, methanol, dichloromethane and acetone. The resin obtained was dried under vacuum for 24 h.

2.4.8 Synthesis of Polyamine (Synthesis of G0 polymer)

The azide substituted resin (1 g) was suspended in dry THF taken in a RB flask and kept at 0 °C in an ice bath. Slurry of LiAlH₄ (0.304 g, 0.008 mol) in dry THF was added drop wise to the reaction mixture with stirring. The reaction mixture was kept at 0 °C for 1h. The temperature was slowly brought to 50 °C. It was stirred at 50 °C for two days to ensure complete reduction. Excess LiAlH₄ was removed by adding ethyl acetate. It was filtered under vacuum, washed with ethyl acetate, THF, ether, water, methanol and acetone. The resin was dried under vacuum for 24 h.

2.4.9 Estimation of amine capacity

The polystyrene resin bearing the amino groups (100 mg) was suspended in HCl (0.1M, 40 ml) for 24 h with occasional stirring. The resin was filtered and washed with distilled water. The filtrate and washings were collected. The unreacted HCl was determined by titration against standard NaOH solution with the use of phenolphthalein indicator. A blank titration was also carried out. From the titre values, the amount of amino groups per gram of the resin was calculated.

2.4.10 Michael addition reaction (Synthesis of G 0.5 polymer)

The resin (0.5 g) was added in portions to a RB flask containing excess methyl acrylate (0.68 mol, 8 mL) and methanol (5 mL) at room temperature with stirring. The reaction mixture was stirred at room temperature for 7 days under an atmosphere of nitrogen. The reaction was monitored using Ninhydrin test. After the reaction, excess methyl acrylate was decanted; methanol (10 mL) was added. The solution was

filtered, and washed with methanol, ethanol, ether, and acetone. It was dried under vacuum for 24 h.

2.4.11 Procedure for transamination (Synthesis of G1 polymer)

The resin (1.0 g) was added in small portions with stirring to a mixture of excess ethylene diamine (0.135 mol, 10 mL) and methanol (50 mL) taken in a RB flask and cooled to 0 °C in an ice salt bath. The reaction mixture was stirred at 0 °C for 1h and the temperature was allowed to rise to the room temperature and stirred at room temperature for 7 days to ensure complete reaction. After the completion of the reaction, the resin was filtered under vacuum and washed well with DMF, dichloromethane, methanol and ether. It was dried under vacuum for 24 h.

2.4.12 Michael addition reaction (Synthesis of G1.5 polymer)

The resin (1.0 g) was added in portions to a RB flask containing excess methyl acrylate (0.27 mol, 25 mL) and methanol (30 mL) at room temperature with stirring. The reaction mixture was stirred at room temperature for 10 days under an atmosphere of nitrogen. The reaction was monitored using Ninhydrin test. After the reaction, excess methyl acrylate was decanted; methanol was added. The solution was filtered and washed with methanol, ethanol, ether, and acetone. It was dried under vacuum for 24 h.

2.4.13 Procedure for transamination (Synthesis of G2 polymer)

The resin (1.0 g) was added in small portions with stirring to a mixture of excess ethylene diamine (0.27 mol, 20 mL) and methanol (20 mL) taken in a RB flask and cooled to 0°C in an ice salt bath. The reaction mixture was stirred at 0 °C for 1h and the temperature was allowed to rise to

the room temperature and stirred at room temperature for 7 days to ensure complete reaction. After the completion of the reaction, the resin beads were filtered under vacuum and washed with DMF, dichloromethane, methanol and ether. It was dried under vacuum for 24 h.

2.4.14 Photolytic cleavage

Resin (500 mg) was suspended in methanol (50 mL) in the reaction chamber of an immersion type photo reactor. The suspension was degassed for 1h with dry nitrogen and irradiated with Philips HP 125W medium pressure Hg lamp at 340-350 nm for 24 h with constant stirring. A solution of CuSO₄ was circulated through the outer jacket of the reactor to filter off light waves below 320 nm. After photolysis, resin beads were filtered and washed with methanol. Combined filtrate and washings were evaporated under vacuum.

2.5 Characterization of Products

1. 3-nitro-4-chloromethylpolystyrene

Yellow beads; Yield: 5.2 g; IR (cm⁻¹): 3026 cm⁻¹, 2928 cm⁻¹, 1596 cm⁻¹, 1360 cm⁻¹.

2. Pentaerythritol initiated Polyepichlorohydrin (PEN-PECH)

Pale yellow viscous liquid; Mp (GPC): 1037. Polydispersity: 1.27; Yield: 13 g; IR (cm⁻¹): 3430, 2925, 1107, 695; ¹H NMR (400 MHz, CDCl₃) δ: 3.2-4.0 (m, CH₂, CH & OH), 1.1 (CH), 1.8 (CH₂) ppm;

3. Merrifield Resin supported PEN-PECH

Yield: 2.81 g; Chlorine Capacity: 7.17 mmols/g; IR (cm⁻¹): 3430, 3026, 2925, 1602, 1528, 1448, 1360, 1107, 695; Solid State ¹³C NMR (100M

Hz.): 19, 23.8, 38.4, 43.5, 69, 76.5, 125.76, 132.96, 142.22 ppm;
Hydroxyl group capacity: 1.86 mmolsg⁻¹.

4. Merrifield Resin supported tosylated PEN-PECH

Yield: 1.08 g; % S-2.44; IR (cm⁻¹); 3456, 3025, 2935, 1627, 1596, 1482, 1360, 1117, 1010, 700.

5. Merrifield Resin supported PEN-polyazide

Yield: 1.21 g; IR (cm⁻¹); 3026, 2900, 2100, 1596, 1458, 1360, 1075. Solid State ¹³C NMR (100 MHz): 15.6, 19, 23.2, 38.5, 75.0, 125.76, 148.8 ppm;

6. Merrifield Resin supported PEN-polyamine-G0

Yield: 0.82 g; Amine Capacity: 9.13 mmols/g; IR (cm⁻¹); 3462, 3451, 3026, 2928, 1375, 1006;

After photolytic cleavage: ¹H NMR (400 MHz, DMSO-d₆) δ: 3.9(26 NH proton), 3.2-3.8(48 CH₂ & 10 CH) ppm. ¹³C NMR (100 MHz, DMSO-d₆): 78, 77.7, 70.2, 68.8, 68.6, 53.4, 51.6, 51 ppm; MALDI MS: 884.

7. Merrifield Resin supported PEN-polyester-G 0.5

Yield: 1.4 g; IR (cm⁻¹); 2900, 1738, 1350, 1245: Solid State ¹³C NMR (100 MHz); 169, 148.7, 123.8, 65, 38.5, 18 ppm.

8. Merrifield Resin supported PEN-Polyamidoamine-G1.0

Yield: 1.5 g; Amine Capacity: 16.02 mmolsg⁻¹; IR (cm⁻¹); 3500, 2915, 1641, 1375, 1041;

After photolytic cleavage: ¹H NMR (400 MHz, DMSO-d₆) δ: 8.2 (18 amide proton), 3.5-4 (44 NH proton), 3.1-3.4(192 CH₂ & 10 CH) ppm; ¹³C NMR (100 MHz, DMSO-d₆): 164.6, 56.3, 48.5, 41.2, 39.7, 39.1, 38.9, 38.6, 38.3, 37.2, 36.9, 14.1 ppm; MALDI MS: 2857.55.

9. Merrifield Resin supported PEN-polyamidoester-G 1.5

Yield: 2.95 g; IR (cm^{-1}); 2980, 1740, 1356, 1086; Solid State ^{13}C NMR (100M Hz); 169.4, 144.3, 122.2, 38.8, 22 ppm.

10. Merrifield Resin supported PEN-Polyamidoamine-G 2.0

Yield: 1.6 g; Amine Capacity: 25.12 mmols/g; IR (cm^{-1}); 3500, 2915, 1662, 1385, 1038;

After photolytic cleavage: ^1H NMR (400 MHz, DMSO-d_6): 8.1 (26 amide proton), 3.5-4.5 (50 NH proton), 2.8-3.5 (258 CH_2 & 10 CH) ppm; ^{13}C NMR (100 MHz, DMSO-d_6): 168.8, 167.7, 164.6, 55, 43.4, 41.1, 40.6, 39, 38.6, 38.3, 37.2, 35.5, 28.3, 21.8, 17.5 ppm; MALDI MS: 3966.02.

11. Glycerol initiated Polyepichlorohydrin (GLR-PECH)

Colourless viscous liquid; Mp (GPC): 1589; Polydispersity: 1.06; Yield: 15 g; IR (cm^{-1}); 3620, 1380, 1097, 710; ^1H NMR (400 MHz, CDCl_3): 3.2-4.3 (m, CH_2 , CH & OH) ppm.

12. Merrifield Resin supported GLR-PECH

Yield: 4.3 g; Chlorine Capacity: 12.863 mmols/g; Hydroxyl group Capacity: 1.43 mmols/g.

IR (cm^{-1}); 3431, 3026, 2912, 1620, 1535, 1426, 1360, 1129, 700; Solid State ^{13}C NMR (100 MHz): 19, 38.6, 42.2, 69.9, 130.2, 148.6 ppm.

13. Merrifield Resin supported tosylated GLR-PECH

Yield: 1.06 g; % S; 1.63; IR (cm^{-1}); 3054, 2935, 1678, 1528, 1421, 1457, 1360, 1045, 1034, 700.

14. Merrifield Resin supported GLR-polyazide

Yield: 1.34 g; IR (cm⁻¹): 2900, 2100, 1474, 1135; Solid State ¹³C NMR (100 MHz): 19, 23.8, 43.3, 65.0, 125.76, 132.96, 148.2 ppm.

15. Merrifield Resin supported GLR-polyamine-G0

Yield: 1.0 g; Amine Capacity: 13.45 mmol/g. IR (cm⁻¹): 3477, 1655, 1586, 1340, 1047; Solid State ¹³C NMR (100 MHz): 18.2, 22.8, 36.3, 41.2, 65.0, 125.76, 132.96, 147.3 ppm.

16. Merrifield Resin supported GLR-polyester-G0.5

Yield: 3.2 g; IR (cm⁻¹): 3026, 2912, 1741, 1310, 1265, 1056; Solid State ¹³C NMR (100 MHz); 169.8, 144, 125, 65, 45, 20 ppm.

17. Merrifield Resin supported GLR-Polyamidoamine-G1.0

Yield: 1.7 g; Amine Capacity: 22.13 mmol/g; IR (cm⁻¹): 3477, 2935, 1655, 1375, 1041; Solid State ¹³C NMR (100 MHz); 167.4, 144, 125, 65, 45, 20 ppm.

18. Merrifield Resin supported GLR-polyamidoester-G1.5

Yield: 3.34 g; IR (cm⁻¹): 2984, 1747, 1376, 1043; Solid State ¹³C NMR (100 MHz); 169.8, 167.2, 144, 125, 65, 45, 20 ppm.

19. Merrifield Resin supported GLR-Polyamidoamine-G 2.0

Yield: 1.8 g; Amine Capacity: 30.24 mmol/g; IR (cm⁻¹): 3473, 2958, 1645, 1375, 1041; Solid State ¹³C NMR (100 MHz); 167.8, 167.2, 168, 144, 125, 65, 48, 20 ppm.

After Photolytic cleavage: MW (MALDI): 3148.8.

20. Ethylene Glycol initiated Polyepichlorohydrin (EG-PECH)

Yield: 13 g; Colorless viscous liquid; Mp (GPC): 1200; Polydispersity: 1.28; IR (cm^{-1}): 3640, 1320, 1047, 700; ^1H NMR (400 MHz, CDCl_3): 3.4-4.5 (m, CH_2 , CH & OH) ppm;

21. Merrifield Resin supported EG-PECH

Yield: 3.2 g; Chlorine Capacity: 10.23 mmols/g; Hydroxyl group Capacity: 1.03 mmols/g;

IR (cm^{-1}): 3433, 3024, 2982, 1638, 1559, 1362, 1456, 1143, 700; Solid State ^{13}C NMR (100 MHz,): 18.7, 23.9, 38.6, 42.3, 50, 60, 65.0, 75, 125.76, 132.96, 142.22 ppm.

22. Merrifield Resin supported tosylated EG-PECH

Yield: 1.0 g; % S; 0.84 mmols/g; IR (cm^{-1}): 3050, 2905, 1625, 1512, 1489, 1476, 1093, 1046, 700.

23. Merrifield Resin supported EG-polyazide

Yield: 1.14 g; IR (cm^{-1}) 2900, 2100, 1454, 1348, 1035; Solid State ^{13}C NMR (100 MHz,): 19.3, 23.6, 43.6, 65.0, 125.76, 132.96, 142.22 ppm.

24. Merrifield Resin supported EG-polyamine-G 0

Yield: 1.04 g; Amine Capacity: 10.49 mmols/g; IR (cm^{-1}): 3470, 3026, 2928, 1644, 1388, 1046; Solid State ^{13}C NMR (100 MHz,): 18.2, 23.8, 33.3, 41.8, 65.0, 125.76, 132.96, 143.2 ppm.

25. Merrifield Resin supported EG-polyester-G 0.5

Yield: 2.3 g; IR (cm^{-1}): 3028, 2951, 1740, 1348, 1054; Solid State ^{13}C NMR (100 MHz,); 169.8, 148, 125, 75, 45 ppm.

26. Merrifield Resin supported EG-Polyamidoamine-G 1.0

Yield: 1.15 g; Amine Capacity: 18.06 mmols/g; IR (cm⁻¹): 3478, 1640, 1348, 1035; Solid State¹³C NMR (100M Hz,); 165, 148, 125, 75, 45, 19 ppm.

27. Merrifield Resin supported EG-polyamidoester-G 1.5

Yield: 2.4 g; IR (cm⁻¹): 2956, 1740, 1348, 1035; Solid State¹³C NMR (100M Hz,); 169.3, 163, 148, 130, 125, 65, 45, 18.3 ppm.

28. Merrifield Resin supported EG-Polyamidoamine-G2.0

Yield: 13 g; Amine Capacity: 24.96 mmols/g; IR (cm⁻¹): 3455, 1667, 1348, 1035; Solid State¹³C NMR (100M Hz,); 164, 163.5, 148, 133, 125, 63, 45, 18.2 ppm.

2.6 References

- [1] Yan J., Li W., Zhang A., *Chemical Communications*, **2014**, 50, 12221-12233.
- [2] Sun H. J., Zhang S., Percec V., *Chemical Society Reviews*, **2015**, 44, 3900-3923.
- [3] Park C., Lee J., Kim C., *Chemical Communications*, **2011**, 47, 12042-12056.
- [4] Nokami T., Watanabe T., Musya N., Morofuji T., Tahara K., Tobe Y., Yoshida J.I., *Chemical Communications*, **2011**, 47, 5575-5577.
- [5] Borisov O. V., Polotsky A. A., Rud O. V., Zhulina E. B., Leermakerse F. A. M., Birshtein T. M., *Soft Matter*, **2014**, 10, 2093-2101.

-
- [6] Zhang B., Schlueter A. D., *New Journal of Chemistry*, **2012**, 36, 414-418.
- [7] Carlmark A., Malmstrom E., Malkoch M., *Chemical Society Reviews*, **2013**, 42, 5858-5879.
- [8] Chen Y., Xiong X., *Chemical Communications*, **2010**, 46, 5049-5060.
- [9] Schuell C., Frey H., *ACS Macro Letters*, **2012**, 1, 461-464.
- [10] Yu H., Schlueter A. D., Zhang B., *Macromolecules*, **2014**, 47, 4127-4135.
- [11] Yu H., Schlueter A. D., Zhang B., *Macromolecules*, **2012**, 45, 8555-8560.
- [12] Kang E. H., Lee I. S., Choi T. L., *Journal of the American Chemical Society*, **2011**, 133, 11904-11907.
- [13] Terashima T., Mes T., De Greef T. F. A., Gillissen M. A. J., Besenius P., Palmans A. R. A., Meijer E. W., *Journal of the American Chemical Society*, **2011**, 133, 4742-4745.
- [14] Laurent B. A., Grayson S. M., *Journal of the American Chemical Society*, **2011**, 133, 13421-13429.
- [15] Feng X., Taton D., Ibarboure E., Chaikof E. L., Gnanou Y., *Journal of the American Chemical Society*, **2008**, 130, 11662-11676.
- [16] Schluter A. D., Rabe J. P., *Angewandte Chemie-International Edition*, **2000**, 39, 864-883.
- [17] Schluter A. D., *Journal of Polymer Science Part A-Polymer Chemistry*, **2001**, 39, 1533-1556.

- [18] Zhang A. F., Shu L. J., Bo Z. S., Schluter A. D., *Macromolecular Chemistry and Physics*, **2003**, 204, 328-339.
- [19] Frauenrath H., *Progress in Polymer Science*, **2005**, 30, 325-384.
- [20] Lee C. C., MacKay J. A., Frechet J. M. J., Szoka F. C., *Nature Biotechnology*, **2005**, 23, 1517-1526.
- [21] Rudick J. G., Percec V., *Accounts of Chemical Research*, **2008**, 41, 1641-1652.
- [22] Rosen B. M., Wilson C. J., Wilson D. A., Peterca M., Imam M. R., Percec V., *Chemical Reviews*, **2009**, 109, 6275-6540.
- [23] Rajaram S., Choi T. L., Rolandi M., Frechet J. M. J., *Journal of the American Chemical Society*, **2007**, 129, 9619-9621.
- [24] Li W., Zhang A., Schlueter A. D., *Macromolecules*, **2008**, 41, 43-49.
- [25] Li W., Zhang A., Feldman K., Walde P., Schlueter A. D., *Macromolecules*, **2008**, 41, 3659-3667.
- [26] Zhuang W., Kasemi E., Ding Y., Kroeger M., Schlueter A. D., Rabe J. P., *Advanced Materials*, **2008**, 20, 3204-3210.
- [27] Boydston A. J., Holcombe T. W., Unruh D. A., Frechet J. M. J., Grubbs R. H., *Journal of the American Chemical Society*, **2009**, 131, 5388-5389.
- [28] Guo Y., van Beek J. D., Zhang B., Colussi M., Walde P., Zhang A., Kroeger M., Halperin A., Schlueter A. D., *Journal of the American Chemical Society*, **2009**, 131, 11841-11854.
- [29] Popa I., Zhang B., Maroni P., Schlueter A. D., Borkovec M., *Angewandte Chemie-International Edition*, **2010**, 49, 4250-4253.

- [30] Zhang B., Wepf R., Fischer K., Schmidt M., Besse S., Lindner P., King B. T., Sigel R., Schurtenberger P., Talmon Y., Ding Y., Kroeger M., Halperin A., Schlueter A. D., *Angewandte Chemie-International Edition*, **2011**, 50, 737-740.
- [31] Grayson S. M., Frechet J. M. J., *Macromolecules*, **2001**, 34, 6542-6544.
- [32] Zhuravel M. A., Davis N. E., Nguyen S. T., Koltover I., *Journal of the American Chemical Society*, **2004**, 126, 9882-9883.
- [33] Helms B., Mynar J. L., Hawker C. J., Frechet J. M. J., *Journal of the American Chemical Society*, **2004**, 126, 15020-15021.
- [34] Khan F. Z., Shiotsuki M., Nishio Y., Masuda T., *Macromolecules*, **2007**, 40, 9293-9303.
- [35] Gao M., Jia X., Kuang G., Li Y., Liang D., Wei Y., *Macromolecules*, **2009**, 42, 4273-4281.
- [36] Percec V., Aqad E., Peterca M., Rudick J. G., Lemon L., Ronda J. C., De B. B., Heiney P. A., Meijer E. W., *Journal of the American Chemical Society*, **2006**, 128, 16365-16372.
- [37] Rudick J. G., Percec V., *New Journal of Chemistry*, **2007**, 31, 1083-1096.
- [38] Boisselier E., Shun A. C. K., Ruiz J., Cloutet E., Belin C., Astruc D., *New Journal of Chemistry*, **2009**, 33, 246-253.
- [39] Dahan A., Portnoy M., *Journal of the American Chemical Society*, **2007**, 129, 5860-5869.
- [40] Brown R. C. D., *Journal of the Chemical Society-Perkin Transactions 1*, **1998**, 3293-3320.

- [41] Swali V., Wells N. J., Langley G. J., Bradley M., *Journal of Organic Chemistry*, **1997**, 62, 4902-4903.
- [42] Kehat T., Goren K., Portnoy M., *New Journal of Chemistry*, **2007**, 31, 1218-1242.
- [43] Huang A. Y.-T., Tsai C.-H., Chen H.-Y., Chen H.-T., Lu C.-Y., Lin Y.-T., Kao C.-L., *Chemical Communications*, **2013**, 49, 5784-5786.
- [44] Bharathi P., Moore J. S., *Journal of the American Chemical Society*, **1997**, 119, 3391-3392.
- [45] Lu S. M., Alper H., *Journal of the American Chemical Society*, **2003**, 125, 13126-13131.
- [46] Fruchtel J. S., Jung G., *Angewandte Chemie-International Edition in English*, **1996**, 35, 17-42.
- [47] Haag R., *Chemistry-A European Journal*, **2001**, 7, 327-335.
- [48] Lebreton S., Monaghan S., Bradley M., *Aldrichimica Acta*, **2001**, 34, 75-83.
- [49] Tomalia D. A., Baker H., Dewald J., Hall M., Kallos G., Martin S., Roeck J., Ryder J., Smith P., *Polymer Journal*, **1985**, 17, 117-120.
- [50] Wells N. J., Basso A., Bradley M., *Biopolymers*, **1998**, 47, 381-396.
- [51] Wells N. J., Davies M., Bradley M., *Journal of Organic Chemistry*, **1998**, 63, 6430-6431.
- [52] Krishnan G. R., Sreekumar K., *Tetrahedron Letters*, **2014**, 55, 2352-2354.

- [53] Arya P., Rao N. V., Singkhonrat J., Alper H., Bourque S. C., Manzer L. E., *Journal of Organic Chemistry*, **2000**, 65, 1881-1885.
- [54] Lebreton S., Newcombe N., Bradley M., *Tetrahedron Letters*, **2002**, 43, 2475-2478.
- [55] Lu J., Toy P. H., *Chemical Reviews*, **2009**, 109, 815-838.
- [56] Delort E., Nguyen-Trung N.-Q., Darbre T., Reymond J.-L., *Journal of Organic Chemistry*, **2006**, 71, 4468-4480.
- [57] Diaz-Mochon J. J., Fara M. A., Sanchez-Martin R. M., Bradley M., *Tetrahedron Letters*, **2008**, 49, 923-926.
- [58] Goren K., Portnoy M., *Chemical Communications*, **2010**, 46, 1965-1967.
- [59] Kehat T., Portnoy M., *Chemical Communications*, **2007**, 2823-2825.
- [60] Tuchman-Shukron L., Portnoy M., *Advanced Synthesis & Catalysis*, **2009**, 351, 541-546.
- [61] Kapoor M. P., Kasama Y., Yokoyama T., Yanagi M., Inagaki S., Hironobu N., Juneja L. R., *Journal of Materials Chemistry*, **2006**, 16, 4714-4722.
- [62] Krishnan G. R., Sreekumar K., *European Journal of Organic Chemistry*, **2008**, 4763-4768.
- [63] Lindner J.-P., Roeben C., Studer A., Stasiak M., Ronge R., Greiner A., Wendorff H. J., *Angewandte Chemie-International Edition*, **2009**, 48, 8874-8877.
- [64] Krishnan G. R., Sreekumar K., *Polymer*, **2008**, 49, 5233-5240.

- [65] Caminade A.-M., Ouali A., Keller M., Majoral J.-P., *Chemical Society Reviews*, **2012**, 41, 4113-4125.
- [66] Ito K. U., Usami N., Yamashita, Y. *Polymer Journal* ,1979 ,11, 171-174.
- [67] Merrifield R. B., *Journal of the American Chemical Society*, **1963**, 85, 2149-2151.
- [68] Barbara A., Stoochnoff N., Benoiton L., *Tetrahedron letters*, **1973**, 14, 21-25.
- [69] Karabline J., Portnoy M., *Organic & Biomolecular Chemistry*, **2012**, 10, 4788-4794.
- [70] Sahu S. K., Panda S. P., Sadafule D. S., Kumbhar C. G., Kulkarni S. G., Thakur J. V., *Polymer Degradation and Stability*, **1998**, 62, 495-500.
- [71] Gaur B., Lochab B., Choudhary V., Varma I. K., *Journal of Macromolecular Science-Polymer Reviews*, **2003**, C43, 505-545.
- [72] Milton H. J., Struck E. C., Case M. G., Steven P. M., *Journal of Polymer Science*, **1984**, 22, 341-345.
- [73] Biedron T., Kubisa P., Penczek S., *Journal of Polymer Science Part A-Polymer Chemistry*, **1991**, 29, 619-628.
- [74] Ampleman G., *US Patent*, **1992**, 5,124,463.
- [75] Liu P., Wu X., Pu Z., Su P. Z., *Analytica Chimica Acta*, **2005**, 95, 695-698.
- [76] Arisawa H., Brill T. B., *Combustion and Flame*, **1998**, 112, 533-544.
- [77] Tomalia D. A., Baker J R H., Dewald M. H., Kallos G., Martin S., Roeck J., Ryder J., Smith P., *Macromolecules* **1986**, 19, 2466-2472.

- [78] Guillier F., Orain D., Bradley M., *Chemical Reviews*, **2000**, 100, 2091-2157.
- [79] Luiz F. P., Ricardo R., Eduardo F. M., *Journal of the American Chemical Society*, **2013**, 135, 11513-11156.
- [80] Shu L., *Dendronized Polystyrene: Synthesis, Characterization and SFM Investigations of Cylindrical Nanoobjects*, **2001**, Ph.D. Dissertation, University of Berlin, Germany.
- [81] Schriemer D. C., Li L., *Analytical Chemistry*, **1997**, 69, 4176-4183.
- [82] Schaiberger A. M., Moss J. A., *Journal of the American Society for Mass Spectrometry*, **2008**, 19, 614-619.
- [83] Bahr U., Deppe A., Karas M., Hillenkamp F., Giessmann U., *Analytical Chemistry*, **1992**, 64, 2866-2869.
- [84] Tomalia D. A., Frechet M.J., *Dendrimers and Dendritic Polymers*, **2001**, Wiley series in Polymer Science, 587-604.
- [85] Sheiko S. S., Moller M., *Chemical Reviews*, **2001**, 101, 4099-4123.
- [86] Ji H. N., Nonidez W. K., Advincula R. C., Smith G. D., Kilbey S. M., Dadmun M. D., Mays J. W., *Macromolecules*, **2005**, 38, 9950-9956.
- [87] Myers B. K., Zhang B., Lapucha J. E., Grayson S. M., *Analytica Chimica Acta*, **2014**, 808, 175-189.
- [88] Thi-Thanh-Tam N., Martin B., Ali R., Hans J. R., Lieberwirth I., Müllen K., *Journal of the American Chemical Society*, **2013**, 135, 4183-8186.
- [89] Ottaviani M. F., Bossmann S., Turro N. J., Tomalia D. A., *Journal of the American Chemical Society*, **1994**, 116, 661-671.

- [90] Tomalia D. A., Naylor A. M., Goddard W. A., *Angewandte Chemie-International Edition in English*, **1990**, 29, 138-175.
- [91] Tomalia D. A., Dewald J. R., *US Patent*, **1985**, 4,507,466, 4,558,120.
- [92] Tomalia D. A., Dewald J. R., *US Patent*, **1986**, 4,568,737, 4,587,329, 4 631 337, 4,694,064.
- [93] Tomalia D. A., Dewald J. R., *US Patent*, **1989**, 4,857,599.
- [94] Naylor A. M., Goddard W. A., Kiefer G. E., Tomalia D. A., *Journal of the American Chemical Society*, **1989**, 111, 2339-2341.
- [95] Li J., Pihler L. T., Qin D., Baker J., J.R. , Tomalia D. A., *Langmuir* **2000**, 16, 5613-5616.
- [96] Shu L. J., Schafer T., Schluter A. D., *Macromolecules*, **2000**, 33, 4321-4328.
- [97] Xie D., Jiang M., Zhang G., Chen D., *Chemistry A European Journal*, **2007**, 13, 3346-3353.

Chapter-3

COMPLEXATION OF DENDRIGRAFT POLYMER GLR-G2 WITH COPPER AND SYNTHESIS OF BENZIMIDAZOLE DERIVATIVES

Abstract

The copper complexes of G0, G1 and G2 dendrigraft polymer having glycerol initiated polyepichlorohydrin as core have been synthesized and characterized. Copper complexes of G0, G1 and G2 were found to be excellent catalysts for the synthesis of benzimidazole derivatives via the reaction between o-phenylenediamine with aldehydes. Aliphatic and cyclic ketones also showed good conjugation towards o-phenylenediamine. A detailed study of the synthesis of benzimidazole derivatives was done with GLR-G2 copper catalyst. Final oxidation step was conducted using air and ethanol was used as the solvent for this reaction.

3.1 Introduction

3.1.1 Benzimidazole Synthesis

Benzimidazoles are bicyclic compounds, consisting of fusion of benzene and imidazole, which are the structural elements of numerous dyes and monomers for solar cell applications and have interesting biological properties.¹ Benzimidazole derivatives have been found to possess enormous therapeutic applications including antiviral, antihypertensive, antiulcer, antifungal, antihistaminic, and anticancer activities.²⁻¹⁴ For example, the glycinamide-containing benzimidazoles have valuable pharmacological

properties such as anti-CCR2 and antithrombotic activities.^{15,16} Several 3-benzimidazol-2-yl-1H-quinoxalin-2-ones coordinate with Ru or Os to give the complexes with antiproliferative activity.¹⁷ Many 4-amino-3-benzimidazol-2-yl-hydroquinolin-2-one derivatives exhibit attractive antitumor activity.¹⁸ The benzimidazole derivatives exhibit significant activity against several viruses such as HIV, herpes (HSV-1), and influenza,¹⁹ certain coumarin-hinged benzimidazoles inhibit hepatitis C virus and can be utilized for the treatment of related liver diseases.²⁰ Benzimidazole moiety was present in a number of pharmacologically important molecules such as albendazole/ mebendazole/ thiabendazole (antihelmentic), omeprazole (antiulcer), etc (Fig 3.1).²¹

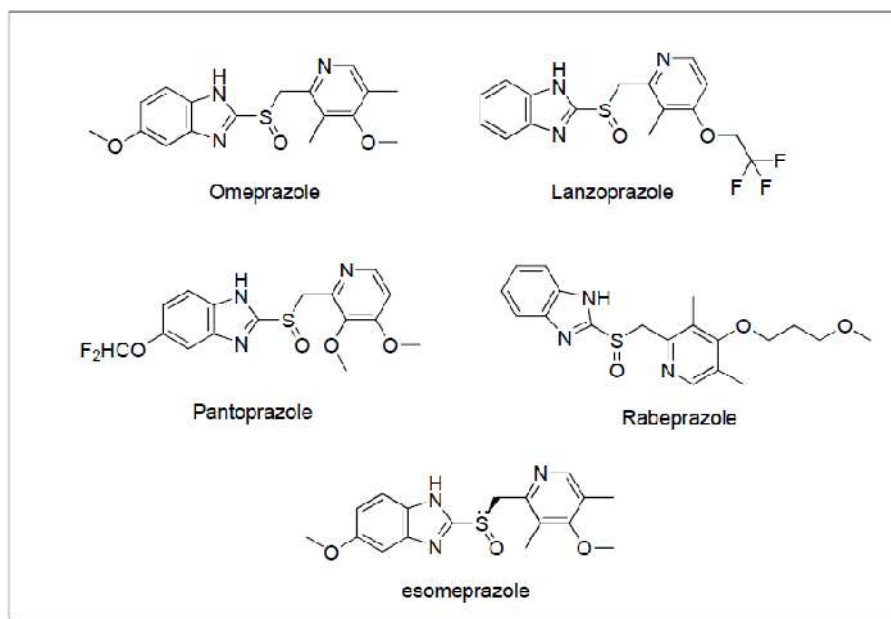


Fig 3.1 Established antiulcer agents in clinical practice

The discovery of this class of drugs provides an outstanding case history of modern drug development and also points out the unpredictability

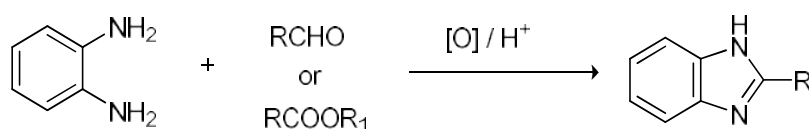
of pharmacological activity from structural modification of a prototype drug molecule.²² Their derivatives were also found to exhibit cytotoxic activity.²³ Substituted benzimidazole derivatives are evaluated by their ability to inhibit gastric H^+ /K^+ ATPase and by blocking the gastric acid secretion. Benzimidazole derivatives such as 2-[[2-(2-pyridyl) methyl] thio]-1-H benzimidazole has shown selective activities against gastric pathogen *Helicobacter pylori*, the probable mechanism being as inhibitor of *H. Pylori*.^{24, 25} Various therapeutic strategies have been utilized for the acid induced ulcer, such as acid neutralizing agents, acid inhibitory agents, antagastin agents, ulcer insulators and promoters of ulcer healing agents.²⁶

The imidazole moieties also serve as important intermediates in numerous organic reactions²⁷⁻³² and were used as important ligands for transition metals in various organic transformations.³³⁻³⁶ The interest in benzimidazole chemistry has been revived by the discovery that the 5, 6-dimethyl benzimidazole moiety is part of the chemical structure of vitamin B-12.³⁷ In the light of the affinity they display towards a variety of enzymes and protein receptors, medicinal chemists would certainly classify them as 'privileged sub-structures' for drug design.³⁸ 2,2-Disubstituted 2H-benzo [d]imidazole derivatives have been used in material chemistry also.³⁹⁻⁵⁰ Due to their wide applications, the preparation of benzimidazole has gained considerable attention in recent years.

3.1.1.1 Methods of Synthesis

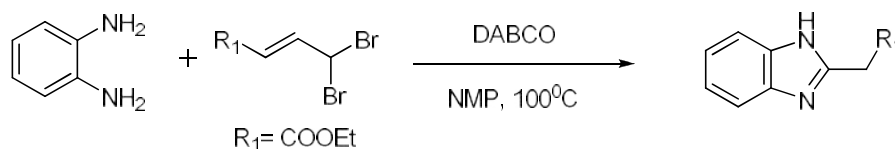
The wide-spread interest in benzimidazole containing structures has prompted extensive studies for their synthesis. There are two general methods for the synthesis of 2-substituted benzimidazoles. One is the coupling of 1,2-phenylenediamines and carboxylic acids⁵¹⁻⁵⁵ or their

derivatives which often require strong acidic conditions,⁵⁶⁻⁵⁸ and sometimes combines with very high temperatures or the use of microwave irradiation.⁵⁹⁻⁶¹ The other way involves a two-step procedure that includes the oxidative cyclo-dehydrogenation of aniline Schiff's bases, which are often generated in situ from the condensation of 1,2-phenylenediamines and aldehydes (Scheme 3.1). In the latter reactions, various oxidants have been used.^{39-50, 62}



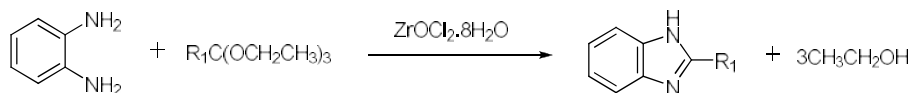
Scheme 3.1

Different catalysts and different methods were also reported for the synthesis of these heterocycles. Wang Shen et al., described an efficient method for the synthesis of substituted benzimidazoles from 1,1-dibromoethenes and *o*-diaminobenzenes. The reaction employs DABCO as the base and NMP as the solvent (Scheme 3.2).⁶³



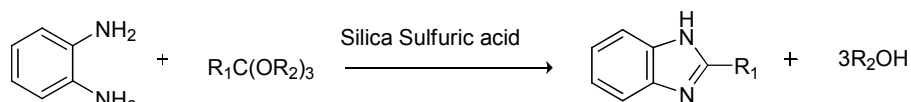
Scheme 3.2

Mohammadpoor-Baltork et al., developed a new and efficient method for the preparation of benzimidazoles from reactions of orthoesters with *o*-substituted aminoaromatics and 2-amino-3-hydroxypyridine in the presence of catalytic amounts of the moisture stable, inexpensive ZrOCl₂·8H₂O under solvent-free conditions (Scheme 3.3).⁶⁴



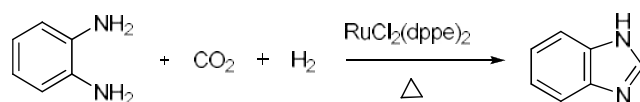
Scheme 3.3

The same group of authors have described an efficient method for the preparation of benzimidazoles and oxazolo[4,5-*b*]pyridines from reactions of orthoesters with *o*-substituted aminoaromatics and 2-amino-3-hydroxypyridine in the presence of silica-sulfuric acid under heterogeneous and solvent-free conditions (Scheme 3.4).⁶⁵



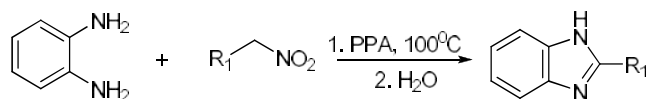
Scheme 3.4

Z. Liu et al., reported that cyclization of *o*-phenylenediamines by CO₂ in the presence of H₂ has resulted in benzimidazoles in excellent yields using RuCl₂(dppe)₂ as the catalyst (Scheme 3.5).⁶⁶



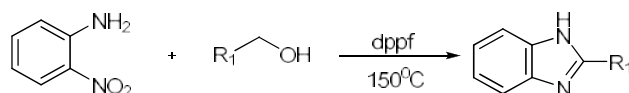
Scheme 3.5

A.V. Aksenov et al., demonstrated that PPA-induced umpolung triggered efficient nucleophilic addition of inactivated anilines to nitroalkanes to produce N-hydroxyimidamides.⁶⁷ The latter undergo sequential acid-promoted cyclocondensation with ortho-NH moieties to afford benzimidazole (Scheme 3.6).



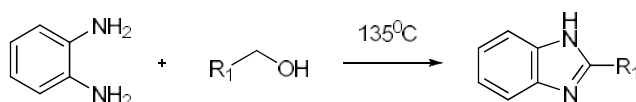
Scheme 3.6

G. Li et al., have described a simple and efficient method for an iron-catalyzed reaction to prepare benzimidazoles from 2-nitroanilines and benzylic alcohols by hydrogen transfer reaction (Scheme 3.7).⁶⁸



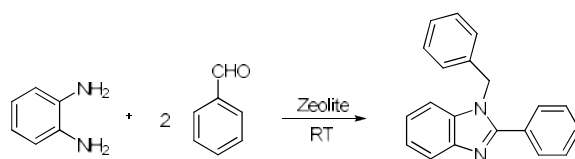
Scheme 3.7

M.R. Marri et al., have described a protocol for the one-pot synthesis of benzimidazoles from a variety of aryl alcohols and 1,2-diaminoarenes under solvent- and catalyst-free conditions (Scheme 3.8).⁶⁹



Scheme 3.8

M. Kumarraja et al., demonstrated the use of a highly ordered nanoporous aluminosilicate (MMZY) as a catalyst for the synthesis of benzimidazoles from 1,2-diaminobenzene and aromatic aldehydes. The reactions are highly chemoselective and afford 1,2-disubstituted benzimidazoles in excellent yield (Scheme 3.9).⁷⁰



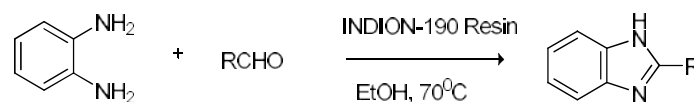
Scheme 3.9

3.1.1.2 Comparison of Performance

In the last decades, use of various catalytic systems has been established for the synthesis of benzimidazole derivatives from 1,2-

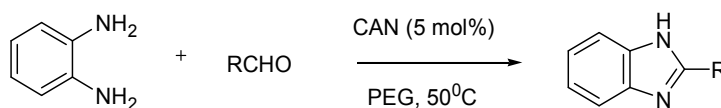
phenylenediamine and aldehydes.^{69, 71-101} A few examples are discussed here to compare the performance of the present catalyst with the reported ones using the conventional method of benzimidazole synthesis. It was clear that even though the results were satisfactory or excellent for the below mentioned catalysts, the methods discussed used high temperature or homogeneous conditions.

N. Sekar et al., developed a protocol for the preparation of benzimidazoles from reactions of aldehydes with *o*-substituted aminoaromatics in the presence of catalytic amount of INDION-190 resin in ethanol as solvent at 70°C and obtained high yields of the products (Scheme 3.10).¹⁰²



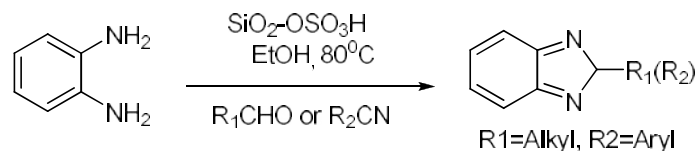
Scheme 3.10

M. Kidwai et al., reported that ceric ammonium nitrate (CAN) was an efficient catalyst for the synthesis of benzimidazole derivatives from *o*-phenylenediamine and aldehydes in polyethylene glycol (PEG) solvent at 50°C (Scheme 3.11).¹⁰³



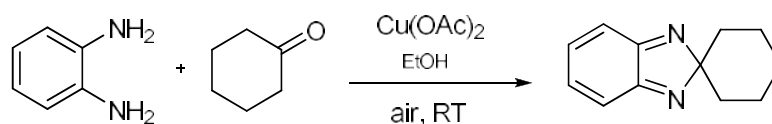
Scheme 3.11

B. Sadeghi et al., reported silica sulfuric acid (SiO₂-OSO₃H) as an eco-friendly and reusable catalyst for the synthesis of benzimidazole derivatives from *o*-phenylenediamine and aldehydes or benzonitriles under **reflux** in ethanol (Scheme 3.12).¹⁰⁴



Scheme 3.12

H. Fu et al., developed a highly efficient **homogeneous** copper catalyzed method for the conjugation of aromatic-1,2-diamines with ketones leading to 2,2-disubstituted 2H-benzo[d]imidazole derivatives (Scheme 3.13).¹⁰⁵



Scheme 3.13

3.1.2 Dendritic Complexes

During the last decade, those working with dendrimers have switched their focus from the initial synthetic directions explored mainly by organic chemists to a more applied emphasis. Thus, metallodendrimers are gaining interest from a materials science perspective because of their unique physical properties, substantial structural diversity, leading to potential photophysical and catalytic applications.¹⁰⁶⁻¹⁰⁹ A large number of metallodendrimers and their catalytic investigations have been reported including those based on polyamidoamine,¹¹⁰ polycarbosilane,¹¹¹ polyamide,¹¹² polyarylether¹¹³⁻¹¹⁵ and polypropyleneimine¹¹⁶⁻¹²² supports, to name a few. Several first- and second generation PPI metallodendrimers bearing four and eight metal centres have been previously reported.¹¹⁶

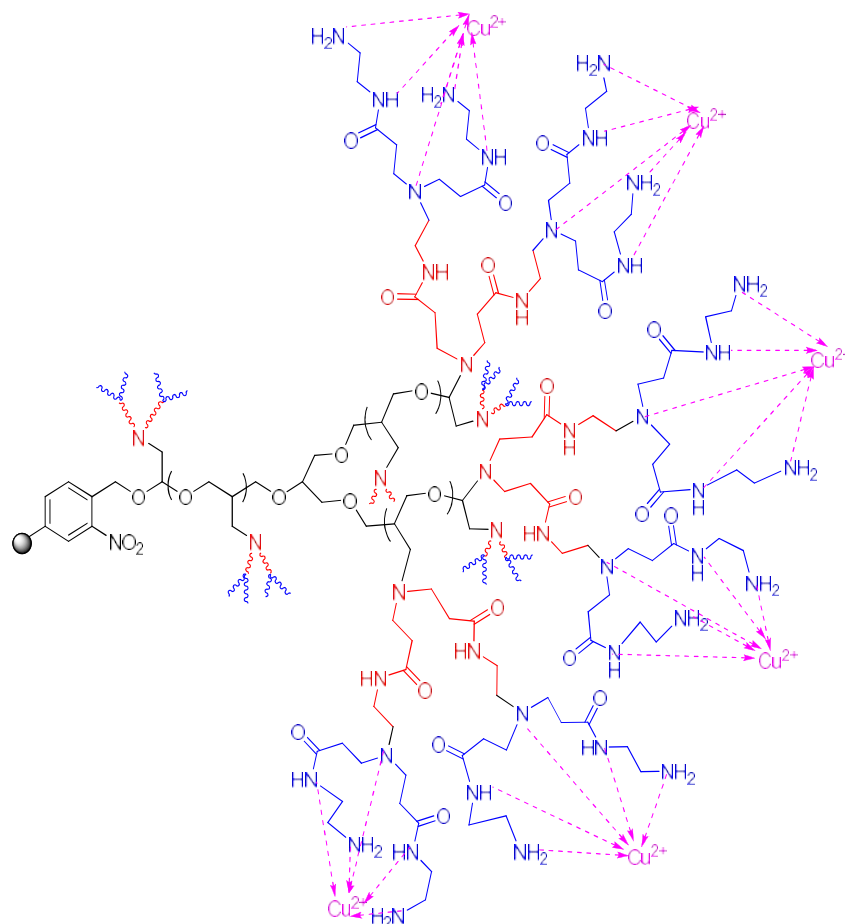


Fig 3.2 Merrifield resin supported dendrigraft GLR-G2-Cu polymer having glycerol initiated PECH as core

Copper complexes are well known for their catalytic activity. Recently, copper and other metal complexes of dendritic and nondendritic polymer as catalyst for organic reactions have been developed from this laboratory.^{110, 123-127} In the present work, we have tried to develop copper complexes of dendrigraft polymer having glycerol initiated polyepichlorohydrin as core, GLR-Gn-Cu in order to increase the efficiency of the reaction (Fig 3.2).

3.1.3 Objective of the Present Work

Recently, copper catalysed reactions with inexpensive and less toxic copper-catalysts^{105,128-132} and molecular oxygen have shown wide application with high tolerance of functional groups in benzimidazole synthesis.¹³³⁻¹³⁸ Most of the reported catalysts were homogeneous, even though, they applied green chemistry principles or the reported heterogeneous catalysts used high temperature or oxidants other than molecular oxygen. So we have tried to combine the benefits of both heterogeneous and dendritic behaviour to address the above mentioned issues.

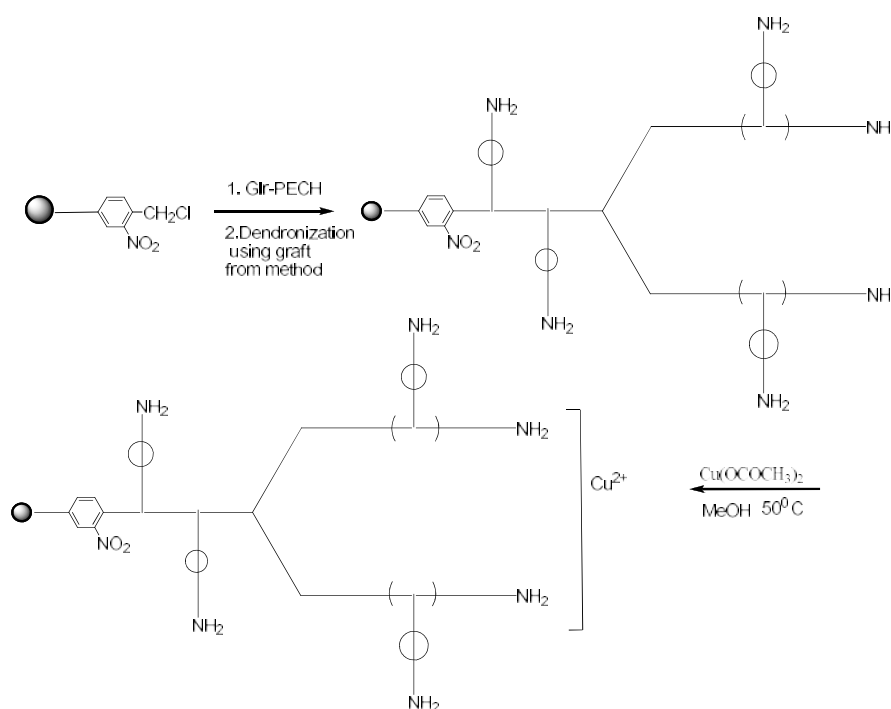
The present chapter deals with the synthesis and characterization of copper complex of dendrigraft polymer having glycerol initiated polyepichlorohydrin as core. The catalyst was employed for the synthesis of benzimidazole derivatives via the reaction between *o*-phenylenediamine and aldehydes or ketones. The experimental parameters were optimized, scope of substrates and reusability of the catalyst were investigated. The mechanism of the reaction is also proposed in this chapter.

3.2 Results & Discussion

3.2.1 Synthesis of Copper Complex of Dendrigraft Polymer with Glycerol Initiated PECH as Core

Chloromethylated polystyrene crosslinked with 1% DVB was used as the support mainly owing to its superior flexibility, which was known to facilitate the grafting of metal ions via dendritic ligands.¹³⁹ The synthesis of G_n dendrigraft polymer having glycerol initiated polyepichlorohydrin as core (GLR-G_n) was reported in chapter 2. The

amino group loading of G₀, G₁ and G₂ dendrigraft polymer was found to be 13.45, 22.13 and 30.24 mmolg⁻¹ respectively (Table 3.1). The copper complex of each of the GLR-G_n polymer was synthesized by adopting the schematic procedure (Scheme 3.14).



Scheme 3.14. Merrifield resin supported dendrigraft GLR-G₂-Cu polymer having glycerol initiated PECH as core.

For the complexation of dendrigraft polymer with copper, the copper salt and solvent was optimized. It was found that copper acetate in methanol at a temperature of 50°C was found to be the best condition for the complexation of copper with GLR-G_n dendritic polymer. Factors such as the maintenance of the required contact time and temperature were also found to be important for the desired synthesis. The effort to

increase the loading by increasing the contact time to 2 days and temperature of about 50°C was successful. It is noteworthy that the catalysts are non-hygroscopic, stable and can be stored for a prolonged period of time without any change in its catalytic efficiency. The copper coordinated dendritic polymer appeared as dark green powder.

3.2.2 Catalyst Characterization

The synthesized catalyst was characterized with different techniques which are discussed.

3.2.2.1 ICP-AES Analysis

The copper loading for GLR-G0-Cu, GLR-G1-Cu and GLR-G2-Cu, based on ICP-AES analysis and confirmed by EDX analysis, were found to be 16.20, 28.40 and 44.39 % of the polymer, respectively and the results are given in Table 3.1. It is therefore assumed that average of 2.16 ligands was bound to Cu moieties in GLR-G2 complex.

Table 3.1 Analytical data for GLR-Gn and GLR-Gn-Cu

Polymer	Amine capacity (mmols/g)	Copper loading (%) (ICP-AES)	Copper loading (mmols/g)	Copper loading (%) (EDX)
GLR-G0-(Cu)	13.45	16.20	2.55	15.94
GLR-G1-(Cu)	22.13	28.40	4.47	28.23
GLR-G2-(Cu)	30.24	44.39	6.99	43.27

The peak for ester was not present in the IR spectrum indicating that acetate ion was not included in the co-ordination sphere. The room temperature magnetic moments of the copper (II) complexes fall in the

range 1.9 - 2.2 B.M, which are very close to the spin only value for d^9 . The Cu complexes were paramagnetic in nature, as was evident from the magnetic susceptibility measurements, which was consistent with the presence of Cu centers in their +2 oxidation states.

3.2.2.2 SEM & Energy Dispersive X-ray (EDX) Analysis

The morphological changes occurring on the surface of the Merrifield resin, as a consequence of the grafting of the polyamidoamine with glycerol initiated polyepichlorohydrin as core and the subsequent loading of copper ions, was examined by employing scanning electron microscopy.

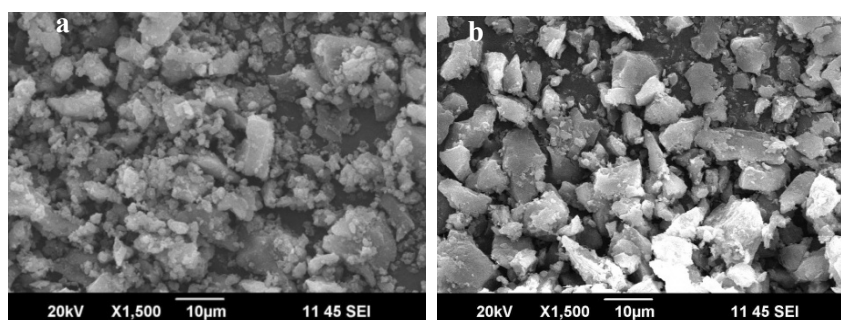


Fig 3.3 Scanning electron micrographs of (a) GLR-G2 and (b) GLR-G2-Cu

The micrographs revealed that the smooth and flat surface of the starting Merrifield resin got disrupted and became crushed into powder, which, then aggregated into small units. But after complexation with copper, the polymer showed metallic lustre (Fig 3.3 a & b). Even though, the SEM micrographs show randomly oriented aggregates, after complexation with copper, each aggregate became more compact.

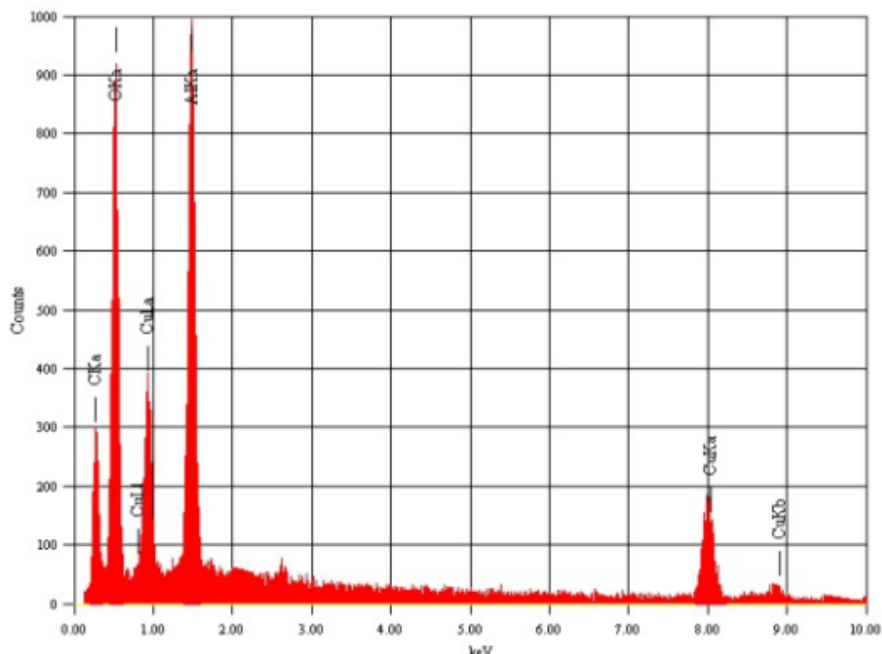


Fig 3.4 EDX spectrum of GLR-G2-Cu

Energy dispersive X-ray spectroscopic analysis, which provides in situ chemical analysis of the bulk, was carried out focusing multiple regions over the surface of the polymer. EDX spectra clearly showed Cu, C, N and O as the constituents of the catalyst (Fig 3.4). The results presented in Table 1 are the average of the data from the different regions. The data obtained on the composition of the compounds from the energy dispersive X-ray spectroscopy, were consistent with the elemental analysis values (Table 3.1).

3.2.2.3 IR Spectral Studies

The IR spectra showed characteristic differences between the spectral pattern originating from the dendrigraft–copper complexes and the spectra of the dendrigraft polymer. The IR spectra are presented in

Fig 3.5 and the significant features are summarized in Table 2. The broadness of the band due to stretching of amine was observed to be reduced to a small extent in the spectrum of the copper complex suggesting coordination of Cu by the dendritic amine ligands. Apart from the typical absorptions at ~ 3441 ($\nu_{\text{sym}}(\text{NH})$), 2923 ($\nu_{\text{aliphatic}}(\text{CH})$), 1633 ($\nu_{\text{secondary amide}}(\text{CO})$), 1565 ($\nu_{\text{bend}}(\text{NH})$) or ($\nu_{\text{stretch asymm}}(\text{N-O})$), 1410 ($\nu_{\text{bend}}(\text{C-O-H})$) or ($\nu_{\text{stretch symm}}(\text{N-O})$), 1015 ($\nu_{\text{CN stretch}}(\text{C-NH})$) and 700 cm^{-1} ($\nu_{\text{NH wag}}(\text{CH-NH})$), the spectra of G2-Cu showed new band at $\sim 950\text{ cm}^{-1}$ which is attributable to $\nu(\text{Cu-N})$, giving clear indication of complexation of copper moiety to dendritic polymeric matrix.

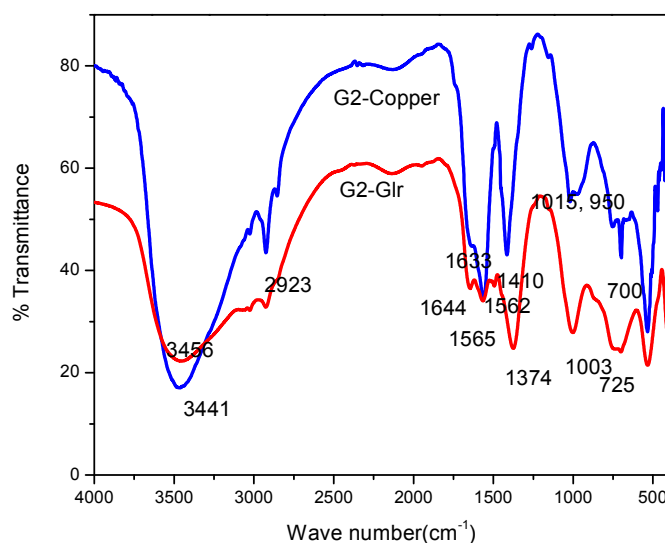


Fig 3.5 IR spectra of G2-G2 and G2-G2-Cu

Upon complexation of Cu ions in the dendritic G2 resins, the spectra of G2 exhibited a distinct shift of $\nu_{\text{stretch}}(\text{NH})$ to a lower frequency and that of $\nu_{\text{bend}}(\text{NH})$ to a higher frequency (Table 3.2), compared to the uncomplexed polymer, along with some sharpening of bands. The position of the $\nu_{\text{stretch}}(\text{NH})$ absorption in the polymeric complexes was

altered only to a small extent compared to uncomplexed dendritic matrix. It is therefore inferred that all the amino groups have not participated in coordination.

Table 2 Infrared (IR) spectral data for GLR-G2 and GLR-G2-Cu

Polymer	$\nu_{\text{stretch}}(\text{NH})$	$\nu_{\text{bend}}(\text{NH})$	$\nu_{\text{stretch}}(\text{NHCO})$	$\nu_{\text{bend}}(\text{C-OH})$	$\nu_{\text{stretch}}(\text{C-N})$	$\nu_{\text{stretch}}(\text{Cu-N})$	$\nu_{\text{wag}}(\text{NH})$
GLR-G2	3456	1562	1644	1374	1003	-	725
GLR-G2-Cu	3441	1565	1633	1410	1015	950	700

The presence of polymer bound copper in GLR-G2-Cu, has been confirmed from the occurrence of typical well-resolved $\nu(\text{Cu-N})$ vibration modes at $\sim 950\text{ cm}^{-1}$. The prominent absorption at $\sim 725\text{ cm}^{-1}$ has been narrowed and shifted towards lower frequency region at ca 700 cm^{-1} assigned to $\nu_{\text{wag}}(\text{N-H})$ of primary or secondary amines.

3.2.2.4 Electronic Spectral Studies (UV-Vis DRS)

Organic ligands upon complexation with transition metal ions, due to interaction with the metal ion, show interesting changes in the electronic properties of the system. New features or bands in the visible region due to d-d absorption and charge transfer spectra from metal to ligand (M \rightarrow L) or ligand to metal (L \rightarrow M) can be observed and this data can be processed to obtain information regarding the structure and geometry of the compounds. R. M. Crooks et al., examined complexation between PAMAM dendrimers and Cu^{2+} in aqueous solution using UV-Vis spectroscopy.¹⁰⁸ In the absence of $\text{G}_4\text{-OH}$, Cu^{2+} exists primarily as $[\text{Cu}(\text{H}_2\text{O})_6]^{2+}$. This complex gives rise to a broad, weak absorption band centered at 810 nm, which arises from the d-d transition of Cu^{2+} in a tetragonally distorted octahedral or square-planar H_2O -ligand field. In the presence of 0.05 mM hydroxyl terminated

PAMAM dendrimers (Gn-OH, n = 2, 3, and 4), λ_{\max} for the d-d transition was shifted to 605 nm.

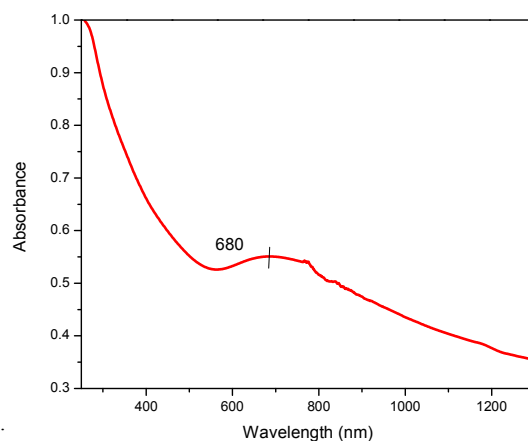


Fig 3.6 UV-Vis-DRS spectrum of GLR-G2-Cu

The diffuse reflectance UV-Vis spectra of GLR-G2-Cu (Fig 3.6) displayed a broad peak in the region of 580–780 nm with maximum intensity at 680 nm which is characteristic of five coordinated copper complexes having square pyramidal geometry. The peak may be ascribed to the absorption due to overlapping of allowed d-d transitions in copper after coordination with dendritic ligands.

3.2.2.5 EPR Spectral Studies

EPR Spectral studies of GLR-G2-Cu show typical axial spectra with four hyperfine lines, which are characteristics of monomeric copper (II) complexes. The g and A values are obtained from the simulated spectrum (Fig 3.7) given in Table 3.3. In the present case, g_{\parallel} is found to be greater than g_{\perp} . This predicts a square pyramidal geometry to five coordinated complex rather than a trigonal bipyramidal structure which would be expected to have g_{\perp} greater than g_{\parallel} . Thus GLR-G2-Cu comprises

of coordination of copper to two amine nitrogens, two amide nitrogens and one tertiary nitrogen of amidoamine unit.

Table 3.3 Splitting parameters g and A

Polymer	g_{\parallel}	g_{\perp}	g_{av}	A_{\parallel}	A_{\perp}	A_{av}
GLR-G2-Cu	2.25	2.05	2.11	175.2	13.81	64.73

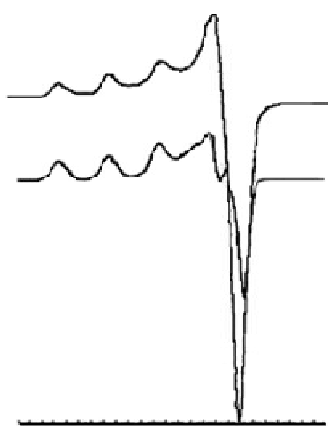


Fig 3.7 Experimental and simulated EPR spectra of GLR-G2-Cu

I.A. Gentle et al., studied the EXAFS data for copper(II)-PAMAM solutions and the data were fitted with acceptable parameters using a model in which primary amine, amide and tertiary amine nitrogen atoms were involved in bonding with the copper (II) ion to form five- and six membered rings.^{106,140}

3.2.2.6 X-ray Diffraction Studies

The room-temperature X-ray diffraction patterns of the dendrigraft polymer, GLR-G2 and the Copper complexed dendrigraft polymer GLR-G2-Cu on Merrifield resin are overlaid in the figure (Fig 3.8). The GLR-G2 sample displayed diffraction peaks at 2θ values of 15.0, 23.0, 31.3, 35.0, 40.0, 54.0 and 62.8°. These values are close to the

ones observed for the GLR-G2-Cu, which were ascribed to the (200), (100), (110), (440), (111), (311) and (303) planes, respectively.

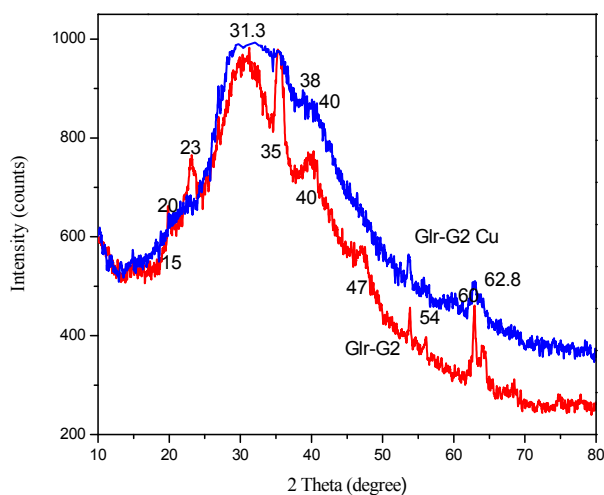


Fig 3.8 X-ray diffraction (XRD) pattern of GLR-G2 and GLR-G2-Cu

After complexation with copper, the diffraction peaks at 2θ value of 47.0° and 20° corresponding to (220) and (311) got disappeared or decreased in intensity while a weak and broad peak at 60° corresponding to (222) plane appeared indicating a mixed behaviour of crystalline and amorphous nature. This observation confirms that the copper ion has been anchored to the polymer matrix to yield the polymer supported dendritic copper catalyst GLR-G2-Cu.

3.2.2.7 X-ray Photoelectron Spectroscopy

XPS is an effective technique for studying the electronic properties of the species formed on the surface. Fig 3.9 presents the Cu (2p) XPS spectra of the polymer anchored Cu complexes. The catalyst displayed characteristic Cu $2p_{3/2}$ singlet with peak located at 934.3 eV. Strong satellite peaks were observed at 942, 943.2, 954.3 and 962.4 eV.

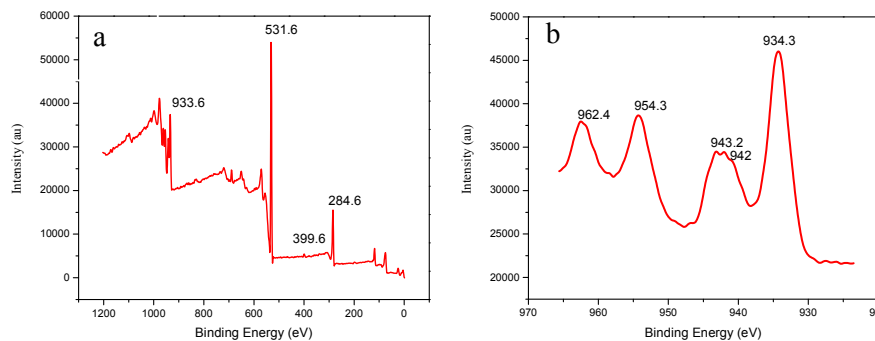


Fig 3.9 XPS spectra of Cu (2p_{3/2}) peak for GLR-G2-Cu (a) wide (b) deconvoluted

The binding energy values observed are in good agreement with the available literature data for Cu ions in the 2+ oxidation state.¹⁴¹ The presence of Cu (II) in supported dendritic compound has thus been confirmed from the results of XPS analysis. The XPS results are also consistent with the paramagnetic nature of the catalysts, as evidenced by the magnetic susceptibility measurements.

3.2.2.8 TG-DTG Analysis

Evaluation of the thermogravimetric data of the GLR-G2 functionalized resins and the corresponding Cu loaded dendrigraft polymer was performed. Considerable extent of decomposition was observed in the thermogram of both GLR-G2 and GLRG2-Cu at the temperature 406 and 409°C owing to the degradation of the polymeric backbone. This occurs as a common feature of the polystyrene species (Fig 3.10).¹⁴² In GLR-G2-Cu polymer, the first step of the decomposition is attributable to the loss of non-coordinated water, occurring in the temperature range of 65-105°C. Apart from this, in the case of GLRG2-Cu, a decomposition step with a weight loss of 32.6 % occurs in the temperature range of 180–220°C. By analogy with the thermal decomposition characteristics of GLR-G2 undergoing

decomposition with a weight loss of 18.2% and 16.9% occurring in the temperature range of 185-190°C and 220-250°C respectively, it is revealed that, copper ions are bound quantitatively to the polymer matrix.

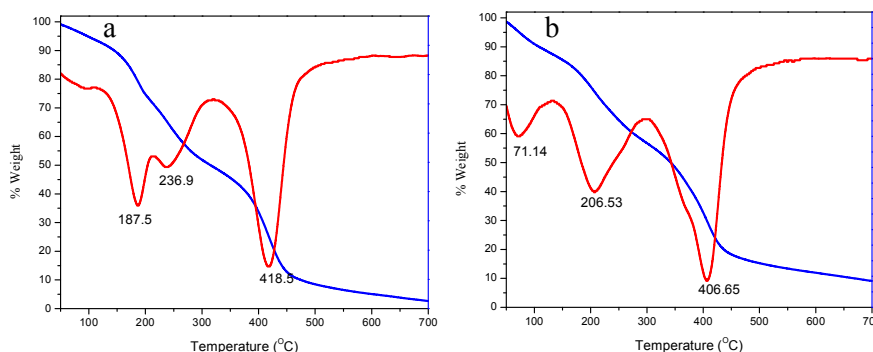


Fig 3.10 TG-DTG plot of (a) GLR-G2 and (b) GLR-G2-Cu

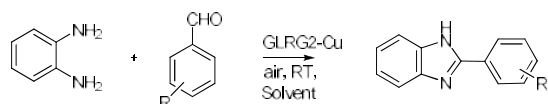
From the reports regarding polyazides and polyamines,¹⁴³ the decompositions may be ascribed to the release of amines as nitrogen, carbonyls as CO or CO₂ and the degradation of the polymeric backbone to be left with a residue containing copper oxide. The TG-DTG analysis data for the compounds are thus in agreement with their incorporation and percentage composition.

3.2.3 Catalytic Activity of Resin Supported Dendrigraft GLR-Gn-Cu Complex

3.2.3.1 Synthesis of Benzimidazole Derivatives

In a survey of catalytic activity, dendrigraft GLR-Gn copper complexes were employed in the synthesis of benzimidazole derivatives. A variety of benzimidazole derivatives have been synthesized in excellent yields from aromatic aldehyde and aliphatic or cyclic ketones (Scheme 3.15). The effect of various reaction parameters, such as type of solvent,

reaction temperature, substrate ratio, catalyst concentration, etc., were evaluated by using benzaldehyde and 1,2-phenylenediamine as model substrates and GLR-G2-Cu as the catalyst, in order to optimize the reaction conditions. The emphasis in the present work has been to conduct the reactions using environmentally safe solvents including water and to avoid the use of chlorinated solvents. Nevertheless, apart from water, methanol, ethanol, acetonitrile, we have screened the reaction in DMF as well.



Scheme 3.15 Synthesis of benzimidazoles.

The nature of solvent was observed to have a profound effect on the activity of the catalyst and the product selectivity of the reaction. The reactions were performed at ambient temperature under magnetic stirring. From the results presented in Tables 3.4 & 3.5 it is evident that the reaction conducted in the molar ratio of *o*-phenylenediamine : benzaldehyde of 1:1.2 in ethanol at room temperature proceeded smoothly to selectively yield 2-phenyl-1H-benzo[d]imidazole as the exclusive product.

Table 3.4 Optimization of solvent^a

Solvent	Yield (%)
DMF	20
CH ₃ CN	23
Ethanol	100
Methanol	94
Water	72

^a Reaction conditions: 1,2-phenylenediamine (1 mmol), benzaldehyde (1.2 mmol), catalyst-20 mg, RT, Yield from GC.

Increasing the catalyst amount reduces the reaction time from 80 min (with 3.5 mol % catalyst) to 60 min (with 7.0 mol% catalyst). Even though, water as solvent gave 72 % yield, ethanol was found to be the solvent of choice. Thus, in order to attain high conversion, the substrate molar ratio of benzaldehyde and *o*-phenylenediamine was selected as 1.2 : 1.0 and 10 mg catalyst (7 mol%) in ethanol at room temperature in the presence of air have been found to be the optimum.

Table 3.5 Optimization of amount of catalyst

Amount of catalyst (mg)	Amount of catalyst (mol %)	Time (min)	Yield (%) ^a
5	3.5	80	100
10	7.0	60	100
15	10.5	40	100
20	14.0	40	100

^aReaction conditions: 1,2-phenylenediamine (1 mmol), benzaldehyde (1.2 mmol), Ethanol-5ml, RT, Yield from GC.

Further, we have studied the generation effect on benzimidazole synthesis (Table 3.6). Ketones are more reactive such that even the GLR-G0-Cu catalyst showed 100% conversion.

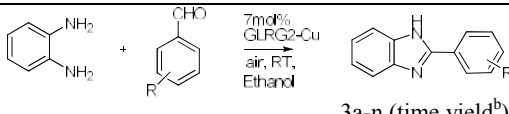
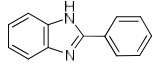
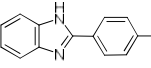
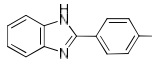
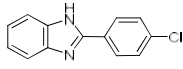
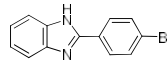
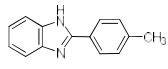
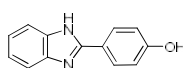
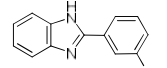
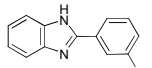
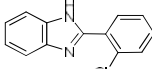
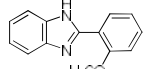
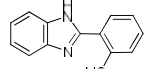
Table 3.6 Generation effect on the synthesis of benzimidazole derivatives^a

Benzimidazole derivative from	%Yield		
	GLR-G0-Cu	GLR-G1-Cu	GLR-G2-Cu
Benzaldehyde	96	96	100
Cyclohexanone	100	100	100

^aReaction conditions: 1,2-phenylenediamine (1 mmol), benzaldehyde / cyclohexanone (1.2 mmol), Ethanol-5ml, RT, Catalyst- 7 mol%. Yield from GC.

In the case of aldehydes, G0, G1 and G2 dendrigraft copper catalyst showed 96, 100 and 100 % product yield respectively. Therefore, all generations of GLR-Gn-Cu are active catalysts towards the synthesis of benzimidazole derivatives. The negative dendritic effect was not pronounced here and the usual concept of slow reaction of supported catalysts was also not observed.

Table 3.7 Synthesis of benzimidazole derivatives^a

 3a-n (time,yield ^b)		
 3a (1h, 94%)	 3b (1h, 89%)	 3c (3h, 89%)
 3d (2h, 94%)	 3e (1h, 92%)	 3f (3h, 82%)
 3g (2h, 84%)	 3h (3h, 86%)	 3i (3h, 92)
 3j (3h, 86%)	 3k (3h, 82%)	 3l (3h, 84%)
^a Reaction conditions: o-phenylenediamine (1 mmol), aldehyde (1.2 mmol), Ethanol-5 ml, RT, Catalyst- 7 mol %. ^b Isolated Yield.		

After optimizing the reaction conditions, scope of different substrates was examined (Table 3.7). All the substrates showed

completion of reaction within few hours. Most of the reactions of 1,2-phenylenediamine and aromatic aldehydes resulted in good-to-excellent yields, irrespective of whether an electron-withdrawing or an electron-donating group was present, *ie.*, both electron withdrawing and electron releasing substituent showed good rate of conversion. But the position of substitution on the phenyl ring of benzaldehyde affects the reaction yield.

Interestingly, chloro (Table 3.7, 3d), bromo (Table 3.7, 3e), nitro (Table 3.7, 3b), and methoxy (Table 3.7, 3c) groups at para position furnished higher yields compared to those at ortho position. However, the chloro group at ortho position provided lesser yield than at meta position (Table 3.7, 3j).

With the optimum reaction conditions in hand, we have investigated the scope of dendritic copper-catalyzed conjugations of aromatic 1,2-diamines towards aliphatic and cyclic ketones also. As shown in Table 3.8, the examined substrates provided good to excellent yields. For ketones, the reactivity depended on their electronic effect, aromatic ketones were reluctant to undergo this conjugation. The substrates with higher charge density on the carbon of the carbonyl and larger steric hindrance provided lower yields.

The vital role of the catalyst, leading to the formation of the desired product, was confirmed by conducting a blank experiment without the catalyst. In the absence of the catalyst, the reaction was sluggish and gave only trace amount of the product. We have further compared the heterogeneous reaction with the reported homogeneous copper acetate catalyst also (Table 3.8, Ref.105). Results show that dendritic effect enhances the catalytic behaviour to a large extent.

Table 3.8 Synthesis of benzimidazole derivatives using ketones^a

 7mol\% GLRG2-Cu $\xrightarrow[\text{Ethanol}]{\text{air, RT,}}$ $\text{3a}_1\text{-3l}_1$ (time, yield) ^b (time, yield) ¹⁰⁵		
 3a_1 (30 min, 96%) (3h, 91%)	 3b_1 (60 min, 84%) (5h, 95%)	 3c_1 (120 min, 81%) (6h, 78%)
 3d_1 (120 min, 85%) (6h, 93%)	 3e_1 (120 min, 87%) (6h, 87%)	 3f_1 (120 min, 84%) (6h, 85%)
 3g_1 (120 min, 68%) (6h, 61%)	 3h_1 (120 min, 84%)	 3i_1 (30 min, 94%) (3h, 89%)
 3j_1 (30 min, 94%) (1h, 93%)	 3k_1 (240 min, 86%) (6h, 88%)	 3l_1 (240 min, 73%) (8h, 73%)
^a Reaction conditions: 1,2-phenylenediamine (1 mmol), ketone (1.2 mmol), Ethanol-5 ml, RT, Catalyst- 7 mol % . ^b Isolated yield.		

3.2.3.2 Recyclability of the Catalyst

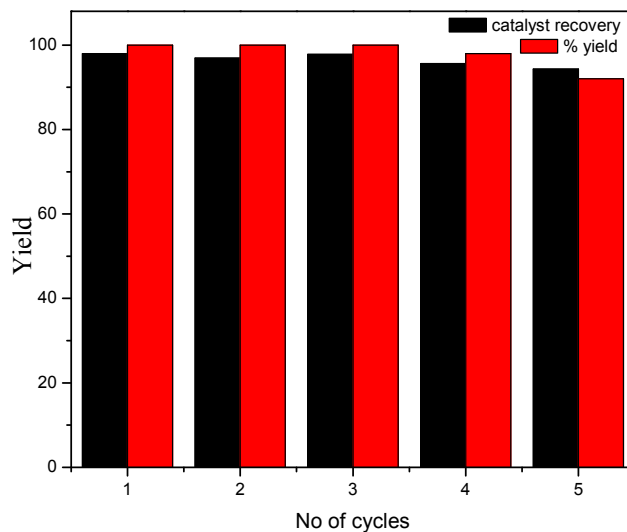
After completion of the reaction, the solution was filtered, washed with ethyl acetate (3 -10 mL), acetone and dried under vacuum at 50°C for about 5 h. The catalyst recovered was weighed and reused without loss of a significant catalytic activity.

Table 3.9 Recycling of GLR-G2-Cu catalyst^a

No. of Cycles	Catalyst weight (mg)	Catalyst recovered (mg)	Recovery (%)	Product yield ^a (%)
1	10	9.8	98.0	100
2	9.8	9.5	96.9	100
3	9.5	9.3	97.8	100
4	9.3	8.9	95.6	98
5	8.9	8.4	94.3	92

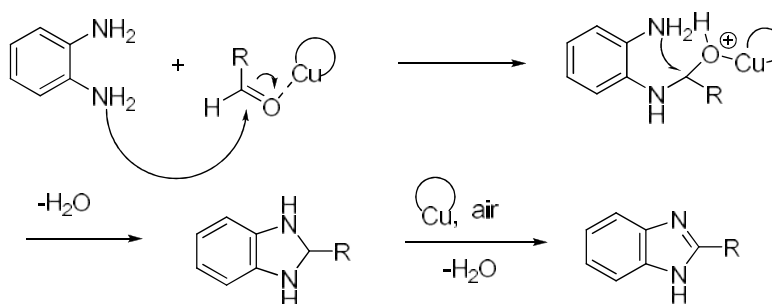
^aReaction conditions: 1,2-phenylenediamine (1 mmol), cyclohexanone (1.2 mmol), Ethanol-5 ml, RT, Yield from GC.

Details regarding catalyst recovery with percentage yield and the corresponding bar diagram are depicted in Table 3.9 and Fig 3.11. Successive runs were carried out in order to see the recyclability of the catalyst. After fifth cycle, 94.3% of catalyst was recovered and reused with 92 % conversion.

**Fig 3.11.** Bar diagram of recycling of GLR-G2-Cu catalyst^a

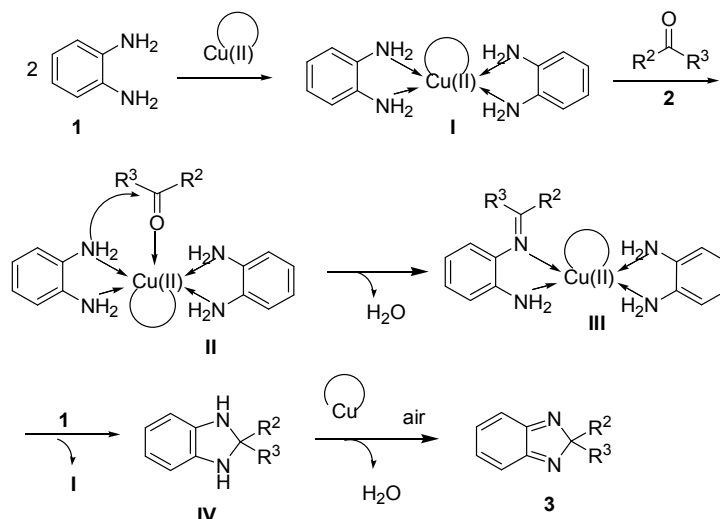
3.2.3.3 The Proposed Mechanism

In order to explore the mechanism of the dendritic copper-catalyzed conjugation of aromatic 1,2-diamines with aldehydes or ketones, a control experiment was performed without catalyst and oxygen. Treatment of 1,2-phenylenediamine with benzaldehyde in the absence of air (nitrogen atmosphere) produced only trace amount of the product. But the reaction can happen in an aerated condition at a higher temperature even in the absence of catalyst.¹⁴⁴



Scheme 3.16. Possible mechanism for copper-catalyzed conjugation of *o*-phenylenediamine with aldehydes.

The result showed that the participation of copper catalyst can increase the rate of the reaction by increasing the rate of formation of the intermediate. Therefore, a possible mechanism for the copper-catalyzed conjugation is proposed in Scheme 3.16. As far as the chemistry of copper (II) is concerned, the reaction presumably proceeds *via* activation of aldehyde by Cu catalyst followed by imine formation and the resulting imine further reacts with the other -NH₂ group of 1,2-phenylenediamine resulting in the formation of dihydrobenzimidazole. Subsequently, dihydrobenzimidazole undergoes aromatization under aerial oxidation to give benzimidazole as shown in Scheme 3.16.



Scheme 3.17 Possible mechanism for copper-catalyzed conjugation of aromatic 1,2-diamines with ketones

In the case of ketones, a different mechanism was proposed for the formation of the product (Scheme 3.17). First, two molecules of *o*-phenylenediamine coordinate together in the presence of Cu catalyst providing complex **I**, and treatment of **I** with ketone leads to **II**. Nucleophilic attack of the amino group to the carbonyl in **II** and dehydration gives the imine-copper complex **III**. Intramolecular addition of the *ortho*-amino group to the imine in **III** in the presence of the catalyst affords **IV** leaving **I**. Subsequently, dihydrobenzimidazole undergoes aromatization under aerial oxidation to give benzimidazole as shown in Scheme 3.17. Further, the cooperative behaviour of dendritic ligands enhances the catalytic activity.

3.3 Conclusions

In conclusion, we have developed a highly efficient dendritic copper catalyzed method for the conjugation of aromatic 1,2-diamine with aldehydes and ketones. The developed copper complexes of G0, G1 and

G2 dendrigraft polymer having glycerol initiated polyepichlorohydrin as core were characterized and all were found to be excellent catalysts for the synthesis of benzimidazole derivatives *via* the reaction between 1,2-phenylenediamine with carbonyl compounds. The reaction occurred even with low generation *ie.*, GLR-G0-Cu polymer. After optimizing the reaction conditions, a detailed study of the synthesis of benzimidazole derivatives was done with GLR-G2 copper catalyst. Comparison of GLR-G2-Cu catalyst with nondendritic copper acetate was also done. The main features of the synthesis include: (1) air was used as the terminal oxidant, (2) ethanol was used as the solvent, (3) only small amount of catalyst was needed to drive the reaction and (4) water was the only by-product in this reaction. All the reactions were performed at room temperature and it showed outstanding tolerance of both aldehydes and ketones. The synthetic protocols are straightforward, safe, environmentally clean, and free from halogenated solvents or any other additives such as a co-catalyst or acid. Procedural simplicity, simple recovery and reusability of catalysts meet the requirements of benign chemistry. So the present catalyst will be of wide practical application in various fields. Further investigation on application of this catalyst for other organic reactions is in progress.

3.4 Experimental Section

3.4.1 Materials

Anhydrous copper acetate, 1,2-phenylenediamine, aldehydes, aliphatic and cyclic ketones were purchased from local vendors and were used as received. All solvents were purified by standard procedures prior to use.

3.4.2 Synthesis of copper complex of dendrigraft GLR-G2 polymer having glycerol initiated polyepichlorohydrin as core

Merrifield resin supported GLR-Gn polymer was allowed to swell in DMF for 2 h. A 50 mL round bottom flask was charged with 250 mg of Merrifield resin supported GLR-Gn polymer having “x” mmols of amine capacity. Quantitative amount corresponding to “x” mmols of anhydrous copper acetate in 10 mL methanol was added to the reaction flask. The reaction mixture was stirred at 50°C for about two days (48h). The polymer was filtered and washed with water. The filtrate and washings were collected together and concentrated. This concentrated solution was used for the estimation of metal ions by standard methods. The polymer-supported metal complex was washed with methanol (20 mL x 3), dioxane (20 mL x 3) and acetone (20 mL x 3) followed by drying at 50°C for 3 h.

3.4.3 General procedure for the synthesis of benzimidazole derivatives from aldehydes /ketones

A 25 mL RB flask having side inlet was charged with a magnetic stirrer and ethanol (5.0 mL). o-Phenylenediamine (1.0 mmol), aldehyde/ketone (1.2 mmol) and catalyst GLR-G2-Cu (7 mol %, 10mg) were added to the flask. The mixture was stirred at room temperature (~25°C) under air. After the reaction was completed (TLC and GC determination), the resulting solution was filtered, washed with ethyl acetate, methanol and acetone, concentrated by a rotary evaporator, and the residue was purified by column chromatography on silica gel using the eluent hexane : ethyl acetate (9:1,v/v) to provide the desired target product.

3.4.4 Test for Heterogeneity of the Reaction

With an aim to confirm that the cyclization reactions occurred *via* a heterogeneous catalytic process, and to examine whether there was any leaching of the metal complex from the polymer-bound dendrigraft catalyst, viz. GLR-G2-Cu, into the reaction medium during the synthesis of benzimidazole, separate experiments were conducted under standard conditions. The filtrate obtained by separating the solid catalyst after completion of the reaction was extracted with ethyl acetate. The aqueous layer was subsequently treated with a fresh batch of reactants in a reaction vessel and the reactions were allowed to continue. There was no formation of the product. This suggests that the reaction does not proceed after removal of the catalyst. Moreover, the presence of copper could not be detected when the filtrate, obtained after isolating the solid catalysts by filtration, was subjected to AAS analysis. The possibility of the copper species leaching out of the catalyst can thus be ruled out on the basis of the evidence gathered, which also proves the heterogeneous nature of the catalytic process.

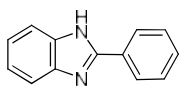
3.4.5 Regeneration and Recycling of the Catalyst

The reusability of the catalyst for subsequent catalytic cycles was examined using cyclohexanone and 1,2-phenylenediamine as the substrate. In the oxidative cyclisation reaction, after the completion of the reaction, the solid catalyst was separated from the reaction mixture by filtration, washed with ethyl acetate, methanol and acetone. It was dried in vacuum at 50°C for about 5h. The dried solid catalyst was weighed and added to a fresh reaction mixture of cyclohexanone (1.2 mmol), and 1,2-phenylenediamine (1 mmol) and ethanol (5 mL). The progress of the reaction was monitored by thin layer

chromatography (TLC) and GCMS. The procedure for the above mentioned system was repeated for five reaction cycles.

3.5 Characterization of Products

2-Phenyl-1H-benzo[d]imidazole (3a)



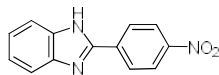
Off white solid, mp 293°C.

^1H NMR (400 MHz, DMSO- d_6) δ : 12.91 (br. s, 1H), 8.19 (d, J = 7.35 Hz, 2H), 7.67–7.47 (m, 5H), 7.21 (d, J = 4.3 Hz, 2H) ppm.

^{13}C NMR (100 MHz, DMSO- d_6) δ : 151.2, 130.2, 130.2, 128.9, 126.4 ppm.

MS, m/z : 194.

2-(4-Nitrophenyl)-1H-benzo[d]imidazole (3b)



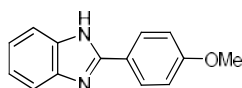
Pink red solid, mp 317°C.

^1H NMR (400 MHz, DMSO- d_6) δ : 7.19–7.22 (m, 2 H), 7.54–7.56 (m, 1 H), 7.65–7.67 (m, 1 H), 8.32 (d, J = 8.0 Hz, 2 H), 8.37 (d, J = 8.8 Hz, 2 H), 13.20 (b s, 1 H) ppm.

^{13}C NMR (100 MHz, DMSO- d_6) δ : 120.0, 123.1, 124.4, 127.5, 129.6, 136.1, 147.9, 149.1 ppm.

MS, m/z : 239.

2-(4-Methoxyphenyl)-1H-benzo[d]imidazole (3c)

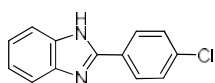


Colourless solid, mp 219°C.

^1H NMR (400 MHz, DMSO- d_6) δ : 12.75 (b s, 1 H), 8.12 (dd, J = 8.0, 4.0 Hz, 2 H), 7.62 (d, J = 8.0 Hz, 1 H), 7.49 (d, J = 8.0 Hz, 1 H), 7.20–7.13 (m, 2 H), 7.11 (d, J = 8.0 Hz, 2 H), 3.84 (s, 3 H) ppm.

^{13}C NMR (100 MHz, DMSO- d_6) δ : 151.37, 143.89, 134.98, 128.02, 122.69, 122.09, 121.48, 118.50, 114.38, 111.06, 55.34 ppm.

MS, m/z : 224.

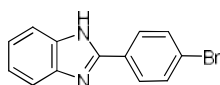
2-(4-Chlorophenyl)-1H-benzo[d]imidazole (3d)

Colourless solid, mp 290°C.

^1H NMR (400 MHz, DMSO- d_6) δ : 6.95–7.0 (d, 1H), 7.16–7.24 (m, 3H), 7.29–7.54 (m, 3H), 7.58–8.13 (dd, 1H). 12.21 (b s, 1 H) ppm.

^{13}C NMR (100 MHz, DMSO- d_6) δ : 115.1, 122.8, 128.7, 128.9, 132.6, 134.2, 141.5, 153.1 ppm.

MS, m/z: 228.

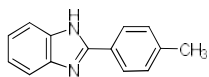
2-(4-Bromophenyl)-1H-benzo[d]imidazole (3e)

Off white solid, mp 282°C.

^1H NMR (400 MHz, DMSO- d_6) δ : 13.05 (b s, 1 H), 8.11 (d, J = 8.6 Hz, 2 H), 7.76 (d, J = 8.6 Hz, 2 H), 7.76–7.55 (m, 2 H), 7.26–7.17 (m, 2 H) ppm.

^{13}C NMR (100 MHz, DMSO- d_6) δ : 150.24, 131.99, 129.40, 128.38, 123.27, 122.35 ppm.

MS, m/z: 271.99.

2-(4-Methylphenyl)-1H-benzo[d]imidazole (3f)

Colourless solid, mp 270°C.

^1H NMR (400 MHz, DMSO- d_6) δ : 2.32 (s, 3 H), 7.22 (d, 2 H), 7.34–7.37 (m, 2 H), 7.47–7.63 (m, 2 H), 8.11 (d, 2 H), 12.63 (b s, 1 H) ppm.

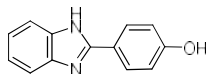
^{13}C NMR (100 MHz, DMSO- d_6) δ : 22.3, 112.5, 119.2, 122.4, 122.9, 127.1, 127.8, 129.9, 140.1, 143.9, 152.3 ppm.

MS, m/z: 208.

2-(4-Hydroxyphenyl)-1H-benzo[d]imidazole (3g)

Colourless solid, mp 255°C.

¹H NMR (400 MHz, DMSO-d₆) δ: 6.97 (d, 2 H), 7.14–7.17 (m, 2 H), 7.46–7.93 (m, 4 H), 12.52 (b s, 1 H) ppm.



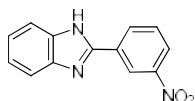
¹³C NMR (100 MHz, DMSO-d₆) δ: 114.5, 115.2, 120.7, 121.3, 127.9, 140.3, 144.9, 157.6 ppm.

MS, m/z: 210.

2-(3-Nitrophenyl)-1H-benzo[d]imidazole (3h)

Off white solid, mp 203°C.

¹H NMR (400 MHz, DMSO-d₆) δ: 12.21 (b s, 1H), 7.28-7.45 (m, 4H), 7.62 - 7.82 (m, 2H), and 8.45- 9.05 (m, 2H) ppm.



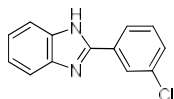
¹³C NMR (100 MHz, DMSO-d₆) δ: 121.0, 123.0, 124.4, 132.0, 131.7, 135.6, 148.5, 149.2 ppm.

MS, m/z: 239.

2-(3-Chlorophenyl)-1H-benzo[d]imidazole (3i)

Colourless solid, mp 235°C,

¹H NMR (400MHz, DMSO-d₆) δ: 7.45 - 7.60 (m, 4H), 7.62 - 7.72 (m, 2H), and 8.30 - 8.45 (m, 2H) ppm.



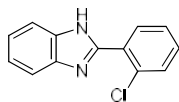
¹³C NMR (100 MHz, DMSO-d₆) δ: 121.0, 123.0, 124.4, 131.0, 131.7, 132.6, 148.5, 149.2 ppm.

MS, m/z: 228.

2-(2-Chlorophenyl)-1H-benzo[d]imidazole (3j)

Pink red solid, mp 232°C.

¹H NMR (400 MHz, DMSO-d₆) δ: 7.21 (q, J= 2.6 Hz, 2H), 7.50-7.54 (m, 3H), 7.66 (q, J= 3.8 Hz, 2H) 7.90 (t, 1 H, J= 9.4 Hz), 12.73 (b s, 1H, NH) ppm.



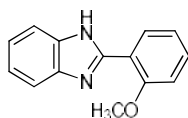
¹³C NMR (100 MHz, DMSO-d₆) δ: 158.6, 152.6, 141.0, 138.5, 129.3, 128.9, 127.3, 123.6, 123.3, 121.1, 118.5, 118.4, 115.1 ppm.

MS, m/z: 228.

2-(2-Methoxyphenyl)-1H-benzo[d]imidazole (3k)

Colourless solid, mp 174°C.

¹H NMR (400 MHz, DMSO-d₆) δ: 13.5 (b s, 1H), 8.29 (d, J = 7.2 Hz, 1H), 7.76 - 7.74 (m, 2H), 7.63 - 7.59 (m, 1H), 7.39 - 7.32 (m, 3H), 7.22 - 7.18 (m, 1H), 4.06 (s, 3H) ppm.



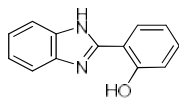
¹³C NMR (100 MHz, DMSO-d₆) δ: 157.3, 152.9, 141.7, 138.5, 131.5, 129.7, 123.6, 123.3, 121.5, 118.5, 118.4, 116.6, 115.2, 56.1 ppm.

MS, m/z: 224.

2-(2-Hydroxyphenyl)-1H-benzo[d]imidazole (3l)

Colourless solid, mp 252°C.

¹H NMR (400 MHz, DMSO-d₆) δ: 12.92 (s, 2H, NH, OH), 7.59–7.56 (m, 2H), 7.43 (d, 1H, J = 7.4 Hz), 7.27–7.24 (m, 2H), 7.19 (t, 1H, J = 7.5 Hz), 7.00 (t, 1H, J = 7.5 Hz), 6.92 (d, 1H, J = 7.5 Hz) ppm.



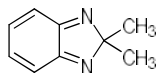
¹³C NMR (100 MHz, DMSO-d₆) δ: 158.6, 152.0, 137.7, 137.5, 131.0, 129.9, 123.6, 123.3, 121.1, 118.5, 118.4, 115.1, 111.4 ppm.

MS, m/z: 210.

2,2-Dimethyl-2H-benzo[d]imidazole (3a).

Brown oil.

¹H NMR (400 MHz, CDCl₃) δ: 7.19 (dd, 2H, J = 7.3, 2.7 Hz), 7.00 (dd, 2H, J = 7.3, 2.7 Hz), 1.54 (s, 6H) ppm.



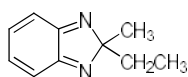
¹³C NMR (100 MHz, CDCl₃) δ: 159.5, 134.5, 126.0, 104.4, 21.6 ppm.

MS, m/z: 146.

2-Ethyl-2-methyl-2H-benzo[d]imidazole (3b).

Yellow oil.

¹H NMR (400 MHz, CDCl₃) δ: 7.20 (dd, 2H, *J* = 7.3, 3.2 Hz), 7.01 (dd, 2H, *J* = 7.3, 3.2 Hz), 2.07 (q, 2H, *J* = 7.3 Hz), 1.51 (s, 3H), 0.74 (t, 3H, *J* = 7.3 Hz) ppm.

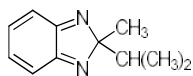


¹³C NMR (100 MHz, CDCl₃) δ: 159.8, 134.4, 125.8, 107.1, 29.3, 19.9, 8.9 ppm.

MS, *m/z*: 160.**2-isoPropyl-2-methyl-2H-benzo[d]imidazole (3c).**

Yellow oil.

¹H NMR (400 MHz, CDCl₃) δ: 7.20 (dd, 2H, *J* = 7.3, 2.7 Hz), 7.00 (dd, 2H, *J* = 7.3, 2.7 Hz), 2.30 (m, 1H, *J* = 6.8 Hz), 1.47 (s, 3H), 0.95 (d, 6H, *J* = 6.8 Hz) ppm.

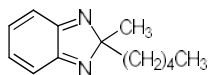


¹³C NMR (100 MHz, CDCl₃) δ : 159.8, 134.4, 125.7, 109.8, 35.0, 18.6, 18.3 ppm.

MS, *m/z*: 174.**2-Methyl-2-pentyl-2H-benzo[d]imidazole (3d).**

Yellow oil.

¹H NMR (400 MHz, CDCl₃) δ: 7.20 (dd, 2H, *J* = 7.2, 2.7 Hz), 7.00 (dd, 2H, *J* = 7.2, 2.7 Hz), 2.00-1.97 (m, 2H), 1.51 (s, 3H), 1.26-1.11 (m, 6H), 0.83 (t, 3H, *J* = 6.8 Hz) ppm .



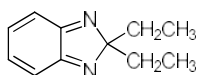
¹³C NMR (100 MHz, CDCl₃) δ: 159.7, 134.4, 125.8, 107.1, 36.2, 32.0, 24.1, 22.4, 20.4, 14.0 ppm.

MS, *m/z*: 202.

2,2-Diethyl-2*H*-benzo[*d*]imidazole (3e).

Brown oil.

¹H NMR (400 MHz, CDCl₃) δ: 7.20 (dd, 2H, *J* = 7.8, 2.7 Hz), 7.01 (dd, 2H, *J* = 7.8, 2.7 Hz), 2.12 (q, 4H, *J* = 7.3 Hz), 0.67 (t, 6H, *J* = 7.3 Hz) ppm.

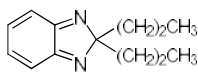


¹³C NMR (100 MHz, CDCl₃) δ: 160.3, 134.4, 125.6, 109.9, 27.8, 8.4 ppm.

MS, *m/z*: 174.**2,2-Dipropyl-2*H*-benzo[*d*]imidazole (3f).**

Brown oil.

¹H NMR (400 MHz, CDCl₃) δ: 7.19 (dd, 2H, *J* = 7.5, 3.1 Hz), 7.00 (dd, 2H, *J* = 7.5, 3.1 Hz), 2.06-2.01 (m, 4H), 1.07-0.99 (m, 4H), 0.82 (t, 6H, *J* = 7.2 Hz) ppm.

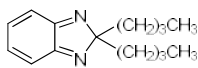


¹³C NMR (100 MHz, CDCl₃) δ: 160.1, 134.3, 125.6, 109.7, 37.3, 17.2, 14.3 ppm.

MS, *m/z*: 202.**2,2-Dibutyl-2*H*-benzo[*d*]imidazole (3g).**

Yellow oil.

¹H NMR (400 MHz, CDCl₃) δ: 7.20 (dd, 2H, *J* = 7.3, 2.7 Hz), 7.00 (dd, 2H, *J* = 7.3, 2.7 Hz), 2.07-2.02 (m, 4H), 1.26-1.20 (m, 4H), 1.02-0.98 (m, 4H), 0.82 (t, 6H, *J* = 7.3 Hz) ppm.



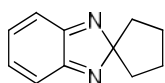
¹³C NMR (100 MHz, CDCl₃) δ: 160.0, 134.2, 125.5, 109.4, 34.7, 25.9, 22.8, 13.7 ppm.

MS, *m/z* 230.

Spiro[benzo[d]imidazole-2,1'-cyclopentane] (3h)

Brown oil.

¹H NMR (400 MHz, CDCl₃) δ: 7.22 (dd, 2H, *J* = 7.2, 3.1 Hz),
7.00 (dd, 2H, *J* = 7.2, 3.1 Hz), 2.32-1.98 (m, 4H), 1.75-1.68 (m,
4H) ppm.

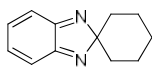


¹³C NMR (100 MHz, CDCl₃) δ: 159.4, 134.2, 126.0, 84.2,
38.6, 21.6 ppm.

MS, *m/z* 172.**Spiro[benzo[d]imidazole-2,1'-cyclohexane] (3i).**

Brown oil.

¹H NMR (400 MHz, CDCl₃) δ: 7.22 (dd, 2H, *J* = 7.2, 3.1 Hz),
7.00 (dd, 2H, *J* = 7.2, 3.1 Hz), 2.20-1.92 (m, 4H), 1.79-1.72 (m,
2H), 1.65-1.64 (m, 4H) ppm.

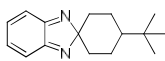


¹³C NMR (100 MHz, CDCl₃) δ: 159.4, 134.2, 126.0, 107.2,
32.6, 25.6, 24.7 ppm.

MS, *m/z*: 186.12.**4'-tert-Butylspiro[benzo[d]imidazole-2,1'-cyclohexane] (3j).**

White solid. mp 141-143 °C.

¹H NMR (400 MHz, CDCl₃) δ: 7.27-7.18 (m, 2H), 6.99 (dd, 2H, *J*
= 7.5, 3.1 Hz), 2.47 (td, 2H, *J* = 13.4, 3.1 Hz), 1.99-1.95 (m, 2H),
1.76 (qd, 2H, *J* = 12.7, 2.7 Hz), 1.39-1.26 (m, 2H), 0.97 (s, 9H),
0.92-0.87 (m, 1H) ppm.



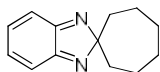
¹³C NMR (100 MHz, CDCl₃) δ: 159.8, 159.0, 134.1, 126.1, 125.9,
107.1, 47.9, 33.1, 32.5, 27.8, 25.8 ppm.

MS, *m/z*: 242.

Spiro[benzo[d]imidazole-2,1'-cycloheptane] (3k).

Yellow solid. mp 92-93 °C.

¹H NMR (400 MHz, CDCl₃) δ: 7.18 (dd, 2H, *J* = 7.5, 3.1 Hz), 6.97 (dd, 2H, *J* = 7.5, 3.1 Hz), 1.98-1.96 (m, 4H), 1.84-1.80 (m, 4H), 1.72-1.69 (m, 4H) ppm.



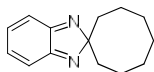
¹³C NMR (100 MHz, CDCl₃) δ: 158.9, 134.2, 126.0, 110.9, 34.0, 29.9, 25.1 ppm.

MS, *m/z*: 200.

Spiro[benzo[d]imidazole-2,1'-cyclooctane] (3l)

Yellow solid. mp 103-105 °C.

¹H NMR (400 MHz, CDCl₃) δ: 7.20 (dd, 2H, *J* = 7.5, 3.1 Hz), 6.98 (dd, 2H, *J* = 7.5, 3.1 Hz), 1.99-1.98 (m, 4H), 1.84-1.73 (m, 6H), 1.68-1.64 (m, 4H) ppm.



¹³C NMR (100 MHz, CDCl₃) δ: 159.2, 134.3, 126.2, 110.8, 30.0, 28.6, 25.1, 25.0 ppm.

MS, *m/z*: 214.

3.6 References

- [1] Zaifoglu B., Sendur M., Unlu N. A., Toppare L., *Electrochimica Acta*, **2012**, 85, 78-83.
- [2] Roth T., Morningstar M. L., Boyer P. L., Hughes S. H., Buckheit R. W., Michejda C. J., *Journal of Medicinal Chemistry*, **1997**, 40, 4199-4207.
- [3] Kim J. S., Gatto B., Yu C., Liu A., Liu L. F., LaVoie E. J., *Journal of Medicinal Chemistry*, **1996**, 39, 992-998.

-
- [4] Gravatt G. L., Baguley B. C., Wilson W. R., Denny W. A., *Journal of Medicinal Chemistry*, **1994**, 37, 4338-4345.
- [5] Horton D. A., Bourne G. T., Smythe M. L., *Chemical Reviews*, **2003**, 103, 893-930.
- [6] Boiani M., Boiani L., Merlino A., Hernandez P., Chidichimo A., Cazzulo J. J., Gonzalez M., *European Journal of Medicinal Chemistry*, **2009**, 44, 4426-4433.
- [7] Merlino A., Benitez D., Chavez S., Da Cunha J., Hernandez P., Tinoco L. W., Gonzalez M., *Medchemcomm*, **2010**, 1, 216-228.
- [8] Soderlind K. J., Gorodetsky B., Singh A. K., Bachur N. R., Miller G. G., Lown J. W., *Anti-Cancer Drug Design*, **1999**, 14, 19-36.
- [9] Dai D., Burgeson J. R., Gharaibeh D. N., Moore A. L., Larson R. A., Cerruti N. R., Hruby D. E., *Bioorganic & Medicinal Chemistry Letters*, **2013**, 23, 744-749.
- [10] Husain A., Rashid M., Shaharyar M., Siddiqui A. A., Mishra R., *European Journal of Medicinal Chemistry*, **2013**, 62, 785-798.
- [11] Payne J. E., Bonnefous C., Symons K. T., Nguyen P. M., Sablad M., Rozenkrants N., Smith N. D., *Journal of Medicinal Chemistry*, **2010**, 53, 7739-7755.
- [12] Palmer A. M., Chiesa V., Schmid A., Muench G., Grobbel B., Zimmermann P. J., Hes D., *Journal of Medicinal Chemistry*, **2010**, 53, 3645-3674.
- [13] Lin S. N., Yang L., *Tetrahedron Letters*, **2005**, 46, 4315-4319.
- [14] Boiani M., Boiani L., Denicola A., Torres de Ortiz S., Serna E., Vera de Bilbao N., Gonzalez M., *Journal of Medicinal Chemistry*, **2006**, 49, 3215-3224.

- [15] Cherney R. J., Mo R., Meyer D. T., Pechulis A. D., Guaciaro M. A., Lo Y. C., Carter P. H., *Bioorganic & Medicinal Chemistry Letters*, **2012**, 22, 6181-6184.
- [16] Gerlach K., *US Patent 20050272792*; *Chemical Abstract*, **2005**, 144, 22924-22929.
- [17] Ginzinger W., Muehlhassner G., Arion V. B., Jakupec M. A., Roller A., Galanski M., Keppler B. K., *Journal of Medicinal Chemistry*, **2012**, 55, 3398-3413.
- [18] Renhowe P. A., Pecchi S., Shafer C. M., Machajewski T. D., Jazan E. M., Taylor C., Harris A. L., *Journal of Medicinal Chemistry*, **2009**, 52, 278-292.
- [19] Morningstar M. L., Roth T., Farnsworth D. W., Smith M. K., Watson K., Buckheit R. W., Jr., Michejda C. J., *Journal of Medicinal Chemistry*, **2007**, 50, 4003-4015.
- [20] Zhu Z. J., Lippa B., Drach J. C., Townsend L. B., *Journal of Medicinal Chemistry*, **2000**, 43, 2430-2437.
- [21] Tamm I., *Science*, **1954**, 120, 847-848.
- [22] Tsay S. C., Hwu J. R., Singha R., Huang W.-C., Chang Y. H., Hsu M.-H., Neyts J., *European Journal of Medicinal Chemistry*, **2013**, 63, 290-298.
- [23] Sih J. C., Im W. B., Robert A., Graber D. R., Blakeman D. P., *Journal of Medicinal Chemistry*, **1991**, 34, 1049-1062.
- [24] Kuhler T. C., Fryklund J., Bergman N. A., Weilitz J., Lee A., Larsson H., *Journal of Medicinal Chemistry*, **1995**, 38, 4906-4916.

- [25] Carcanagu D., Shue Y.K., Wuonola M.A., Nickelsen M.U., Joubran C., Abedi J.K., Jones J., Kuhler T.C., *Journal of Medicinal Chemistry*, **2002**, 45, 4300-4309.
- [26] Seth S.D., *Text Book of Pharmacology*, 2nd ed, Elsevier, New Delhi, **1999**, 390-393.
- [27] Lee S. C., Shin D., Cho J. M., Ro S., Suh Y. G., *Bioorganic & Medicinal Chemistry Letters*, **2012**, 22, 1891-1894.
- [28] Travins J. M., Bernotas R. C., Kaufman D. H., Quinet E., Nambi P., Feingold I., Wrobel J., *Bioorganic & Medicinal Chemistry Letters*, **2010**, 20, 526-530.
- [29] Preston P. N., *Chemical. Reviews*, **1974**, 74, 279–314.
- [30] Tomilov Y. V., Platonov D. N., Frumkin A. E., Lipilin D. L., Salikov R. F., *Tetrahedron Letters*, **2010**, 51, 5120-5123.
- [31] Bai Y. J., Lu J., Shi Z., Yang B. Q., *Synlett*, **2001**, 4, 544-546.
- [32] Hasegawa E., Yoneoka A., Suzuki K., Kato T., Kitazume T., Yanagi K., *Tetrahedron*, **1999**, 55, 12957-12968.
- [33] Pujar, M. A., Bharamgoudar T. D., *Transition Metal Chemistry*, **1988**, 13, 423–425.
- [34] Rodionov V. O., Presolski S. I., Gardinier S., Lim Y.-H., Finn M. G., *Journal of the American Chemical Society*, **2007**, 129, 12696-12704.
- [35] Rodionov V. O., Presolski S. I., Gardinier S., Lim Y.-H., Finn M. G., *Journal of the American Chemical Society*, **2013**, 135, 1626-1629.
- [36] Kose M., Mckee V., *Polyhedron*, **2014**, 75, 30–39.
- [37] Barker H. A., Smyth R. D., Weissbach H., Toohey J. I., Ladd, J. N., Volcani B. E., *Journal of Biological Chemistry*, **1960**, 235, 480-488.

- [38] Mason J. S., Morize I., Menard P. R., Cheney D. L., Hulme C., Labaudiniere R. F., *Journal of Medicinal Chemistry*, **1999**, 42, 3251-3264.
- [39] Song S., Jin Y., Park S. H., Cho S., Kim I., Lee K., Suh H., *Journal of Materials Chemistry*, **2010**, 20, 6517-6523.
- [40] Kim J., Park S. H., Kim J., Cho S., Jin Y., Shim J. Y., Suh H., *Journal of Polymer Science Part A-Polymer Chemistry*, **2011**, 49, 369-380.
- [41] Ozelcaglayan A. C., Sendur M., Akbasoglu N., Apaydin D. H., Cirpan A., Toppare L., *Electrochimica Acta*, **2012**, 67, 224-229.
- [42] Song S., Han H., Kim Y., Lee B. H., Park S. H., Jin Y., Suh H., *Solar Energy Materials and Solar Cells*, **2011**, 95, 1838-1845.
- [43] Song S., Kang I., Kim G.-h., Jin Y., Kim I., Kim J. Y., Suh F., *Synthetic Metals*, **2012**, 162, 225-230.
- [44] Song S., Kim J., Shim J. Y., Kim G., Lee B. H., Jin Y., Suh H., *Synthetic Metals*, **2012**, 162, 988-994.
- [45] Li C., Zhang F., Yang Z., Qi C., *Tetrahedron Letters*, **2014**, 55, 5430-5433.
- [46] Ghosh P., Subba R., *Tetrahedron Letters*, **2015**, 56, 2691-2694.
- [47] Hao L., Zhao Y., Yu B., Zhang H., Xu H., Liu H., *Green Chemistry*, **2014**, 16, 3039-3044.
- [48] Yu B., Zhang H., Zhao Y., Chen S., Xu J., Huang C., Liu Z., *Green Chemistry*, **2013**, 15, 95-99.
- [49] Cano R., Ram D. S., Yus M., *Journal of Organic Chemistry*, **2011**, 76, 654-660.

- [50] Osowska K., Miljanic C-S., *Journal of the American Chemical Society*, **2011**, 133, 724–727.
- [51] Grimmet M. R., Katritzky A. R., Rees C. W., *Comprehensive Heterocyclic Chemistry*, **1984**, Pergamon Press, Oxford.
- [52] Wright J. B., *Chemical Reviews*, **1951**, 48, 396-541.
- [53] Middleton R. W., Wibberley D. G., *Journal of Heterocyclic Chemistry*, **1980**, 17, 1757-1760.
- [54] Hisano T., Ichikawa M., Tsumoto K., Tasaki M., *Chemical & Pharmaceutical Bulletin*, **1982**, 30, 2996-2998.
- [55] Geratz J. D., Stevens F. M., Polakoski K. L., Parrish R. F., *Archives of Biochemistry Biophysics*, **1979**, 197, 551–559.
- [56] Czarny A., Wilson W. D., Boykin D. W., *Journal of Heterocyclic Chemistry*, **1996**, 33, 1393-1397.
- [57] Tidwell R. R., Geratz J. D., Dann O., Volz G., Zeh D., Loewe H., *Journal of Medicinal Chemistry*, **1978**, 21, 613–623.
- [58] Fairley T. A., Tidwell R. R., Donkor I., Naiman N. A., Ohemeng K. A., Lombardy R. J., Cory M., *Journal of Medicinal Chemistry*, **1993**, 36, 1746-1753.
- [59] Bourgrin K., Loupy A., Soufiaoui M., *Tetrahedron*, **1998**, 54, 8055–8064.
- [60] Reddy G. V., Rao V., Narsaiah B., Rao P. S., *Synthetic Communications*, **2002**, 32, 2467-2476.
- [61] Ben-Alloum A., Bakkas S., Soufiaoui M., *Tetrahedron Letters*, **1998**, 39, 4481-4484.

- [62] Hati S., Patra G. K., Naskar J. P., Drew M. G. B., Datta D., *New Journal of Chemistry*, **2001**, 25, 218-220.
- [63] Shen W., Kohn T., Fu Z., Jiao X., Lai S., Schmitt M., *Tetrahedron Letters*, **2008**, 49, 7284-7286.
- [64] Baltork I. M., Khosropour A. R., Hojati S.F., *Catalysis Communications*, **2007**, 8, 1865-1870.
- [65] Baltork I. M., Moghadam M., Tangestaninejad S., Mirkhani V., Zolfigol M. A., Hojati S. F., *Journal of the Iranian Chemical Society*, **2008**, 5, 65-70.
- [66] Yu B., Zhang H., Zhao Y., Chen S., Xu J., Huang C., Liu Z., *Green Chemistry*, **2013**, 15, 95-99.
- [67] Aksenov A. V., Smirnov A. N., Aksenov N. A., Bijieva A. S., Aksenova I. V., Rubin M., *Organic & Biomolecular Chemistry*, **2015**, 13, 4289-4295.
- [68] Li G., Wang J., Yuan B., Zhang D., Lin Z., Li P., Huang H., *Tetrahedron Letters*, **2013**, 54, 6934-6936.
- [69] Marri M. R., Peraka S., Macharla A. K., Mamede N., Kodumuri S., Nama N., *Tetrahedron Letters*, **2014**, 55, 6520-6525.
- [70] Senthilkumar S., Kumarraja M., *Tetrahedron Letters*, **2014**, 55, 1971-1974.
- [71] Du L.-H., Wang Y.-G., *Synthesis-Stuttgart*, **2007**, 675-678.
- [72] Heravi M. M., Sadjadi S., Oskooie H. A., Shoar R. H., Bamoharram F. F., *Catalysis Communications*, **2008**, 9, 504-507.
- [73] Ravi V., Ramu E., Vuay K., Rao A. S., *Chemical & Pharmaceutical Bulletin*, **2007**, 55, 1254-1257.

- [74] Bahrami K., Khodaei M. M., Kavianinia I., *Synthesis-Stuttgart*, **2007**, 547-550.
- [75] Bahrami K., Khodaei M. M., Naali F., *Journal of Organic Chemistry*, **2008**, 73, 6835-6837.
- [76] Navarrete-Vazquez G., Moreno-Diaz H., Aguirre-Crespo F., Leon-Rivera I., Villalobos-Molina R., Munoz-Muniz O., Estrada-Soto S., *Bioorganic & Medicinal Chemistry Letters*, **2006**, 16, 4169-4173.
- [77] Chakrabarty M., Karmakar S., Mukherji A., Arima S., Harigaya Y., *Heterocycles*, **2006**, 68, 967-974.
- [78] Ma H., Wang Y., Wang J., *Heterocycles*, **2006**, 68, 1669-1673.
- [79] Zhang Z.-H., Yin L., Wang Y.-M., *Catalysis Communications*, **2007**, 8, 1126-1131.
- [80] Trivedi R., De S. K., Gibbs R. A., *Journal of Molecular Catalysis A-Chemical*, **2006**, 245, 8-11.
- [81] Chari M. A., Shobha D., Sasaki T., *Tetrahedron Letters*, **2011**, 52, 5575-5580.
- [82] Kumar A., Maurya R. A., Ahmad P., *Journal of Combinatorial Chemistry*, **2009**, 11, 198-201.
- [83] Khan A. T., Parvin T., Choudhury L. H., *Synthetic Communications*, **2009**, 39, 2339-2346.
- [84] Narsaiah A. V., Reddy A. R., Yadav J. S., *Synthetic Communications*, **2011**, 41, 262-267.
- [85] Lei M., Ma L., Hu L., *Synthetic Communications*, **2012**, 42, 2981-2993.

- [86] Abdollahi-Alibeik M., Moosavifard M., *Synthetic Communications*, **2010**, 40, 2686-2695.
- [87] Havaladar F. H., Mule G., Dabholkar B., *Synthetic Communications*, **2011**, 41, 2304-2308.
- [88] Riadi Y., Mamouni R., Azzalou R., El Haddad M., Routier S., Guillaumet G., Lazar S., *Tetrahedron Letters*, **2011**, 52, 3492-3495.
- [89] Shelkar R., Sarode S., Nagarkar J., *Tetrahedron Letters*, **2013**, 54, 6986-6990.
- [90] Leutbecher H., Constantin M.-A., Mika S., Conrad J., Beifuss U., *Tetrahedron Letters*, **2011**, 52, 605-608.
- [91] Chen Y.-X., Qian L.-F., Zhang W., Han B., *Angewandte Chemie-International Edition*, **2008**, 47, 9330-9333.
- [92] Inamdar S. M., More V. K., Mandal S. K., *Tetrahedron Letters*, **2013**, 54, 579-583.
- [93] Punniyamurthy T., Velusamy S., Iqbal J., *Chemical Reviews*, **2005**, 105, 2329-2363.
- [94] Yuan J., Zhao Z., Zhu W., Li H., Qian X., Xu Y., *Tetrahedron*, **2013**, 69, 7026-7030.
- [95] Osowska K., Miljanic O. S., *Journal of the American Chemical Society*, **2011**, 133, 724-727.
- [96] Kim J., Kim J., Lee H., Lee B. M., Kim B. H., *Tetrahedron*, **2011**, 67, 8027-8033.
- [97] Kathirvelan D., Reddy S. R. B., *Indian Journal of Chemistry*, **2013**, 52, 1152-1156.

- [98] Alonso F., Moglie Y., Radivoy G., Yus M., *Journal of Organic Chemistry*, **2011**, 76, 8394-8405.
- [99] Saha P., Ali M. A., Ghosh P., Punniyamurthy T., *Organic & Biomolecular Chemistry*, **2010**, 8, 5692-5699.
- [100] Nagasawa Y., Matsusaki Y., Hotta T., Nobuta T., Tada N., Miura T., Itoh A., *Tetrahedron Letters*, **2014**, 55, 6543-6546.
- [101] Bachhav H. M., Bhagat S. B., Telvekar V. N., *Tetrahedron Letters*, **2011**, 52, 5697-5701.
- [102] Padalkar V. S., Gupta V. D., Phatangare K. R., Patil V. S., Umape P. G., Sekar N., *Green Chemistry Letters and Reviews*, **2012**, 5, 139-145.
- [103] Kidwai M., Jahan A., Bhatnagar D., *Journal of Chemical Sciences*, **2010**, 122, 607-612.
- [104] Sadeghi B., Nejad M. G., *Journal of Chemistry*, **2013**, 2013, 1-5.
- [105] Lu J., Yang H., Jin Y., Jiang Y., Fu H., *Green Chemistry*, **2013**, 15, 3184-3187.
- [106] Ottaviani M. F., Bossmann S., Turro N. J., Tomalia D. A., *Journal of the American Chemical Society*, **1994**, 116, 661-671.
- [107] Gorman C., *Advanced Materials*, **1998**, 10, 295-309.
- [108] Zhou L., Russell D. H., Zhao M. Q., Crooks R. M., *Macromolecules*, **2001**, 34, 3567-3573.
- [109] Ottaviani M. F., Cangioti M., Fattori A., Coppola C., Posocco P., Laurini E., Pricl S., *Physical Chemistry Chemical Physics*, **2014**, 16, 685-694.
- [110] Krishnan G. R., Sreekumar K., *Soft Materials*, **2010**, 8, 114-129.

- [111] de Groot D., Emmerink P. G., Coucke C., Reek J. N. H., Kamer P. C. J., van Leeuwen P., *Inorganic Chemistry Communications*, **2000**, 3, 711-713.
- [112] Bourgu S. C., Alper H., Manzer L.E., Arya P., *Journal of the American Chemical Society*, **2000**, 122, 956-958.
- [113] Blom B., Overett M. J., Meijboom R., Moss J. R., *Inorganica Chimica Acta*, **2005**, 358, 3491-3496.
- [114] Hearshaw M. A, Moss J. R, *Chemical Communications*, **1999**,1-8
- [115] Fujihara T., Obora Y., Tokunaga M., Sato H., Tsuji Y., *Chemical Communications*, **2005**, 4526-4528.
- [116] Smith G., Chen R., Mapolie S., *Journal of Organometallic Chemistry*, **2003**, 673, 111-115.
- [117] Malgas R., Mapolie S. F., Ojwach S. O., Smith G. S., Darkwa J., *Catalysis Communications*, **2008**, 9, 1612-1617.
- [118] Smith G. S., Mapolie S. F., *Journal of Molecular Catalysis A-Chemical*, **2004**, 213, 187-192.
- [119] Ahamad T., Alshehri S. M., Mapolie S. F., *Catalysis Letters*, **2010**, 138, 171-179.
- [120] Govender P., Antonels N. C., Mattsson J., Renfrew A. K., Dyson P. J., Moss J. R., Smith G. S., *Journal of Organometallic Chemistry*, **2009**, 694, 3470-3476.
- [121] Bergbreiter D. E., Tian J., Hongfa C., *Chemical Reviews*, **2009**, 109, 530-582.
- [122] Antonels N. C., Moss J. R., Smith G. S., *Journal of Organometallic Chemistry*, **2011**, 696, 2003-2007.

- [123] Kannan V., Sreekumar K., *Journal of Molecular Catalysis A-Chemical*, **2013**, 376, 34-39.
- [124] Krishnan G. R., Sreekumar K., *Applied Catalysis A-General*, **2009**, 353, 80-86.
- [125] Krishnan G. R., Sreerekha R., Sreekumar K., *Letters in Organic Chemistry*, **2009**, 6, 17-21.
- [126] Mangala K., Sreekumar K., *Journal of Applied Polymer Science*, **2013**, 127, 717-723.
- [127] Mangala K., Sreekumar K., *Journal of Applied Polymer Science*, **2015**, 132, 41593-41599.
- [128] Wendlandt A. E., Suess A. M., Stahl S. S., *Angewandte Chemie-International Edition*, **2011**, 50, 11062-11087.
- [129] Chen C., Peng J., *Journal of Organic Chemistry*, **2011**, 76, 716-719.
- [130] Shi Z., Zhang C., Tang C., Jiao N., *Chemical Society Reviews*, **2012**, 41, 3381-3430.
- [131] Campbell A. N., Stahl S. S., *Accounts of Chemical Research*, **2012**, 45, 851-863.
- [132] Liu C., Zhang H., Shi W., Lei A., *Chemical Reviews*, **2011**, 111, 1780-1824.
- [133] Surry D. S., Buchwald S. L., *Chemical Science*, **2010**, 1, 13-31.
- [134] Monnier F., Taillefer M., *Angewandte Chemie-International Edition*, **2009**, 48, 6954-6971.
- [135] Evano G., Blanchard N., Toumi M., *Chemical Reviews*, **2008**, 108, 3054-3131.
- [136] Ma D., Cai Q., *Accounts of Chemical Research*, **2008**, 41, 1450-1460.

- [137] Rao H., Fu H., *Synlett*, **2011**, 745-769.
- [138] Liu T., Fu H., *Synthesis-Stuttgart*, **2012**, 44, 2805-2824.
- [139] Wang D., Astruc D., *Coordination Chemistry Reviews*, **2013**, 257, 2317-2334.
- [140] Tran M. L., Gahan L. R., Gentle I. R., *Journal of Physical Chemistry B*, **2004**, 108, 20130-20136.
- [141] Biesinger M. C., Lau L. W. M., Gerson A. R., Smart R. S. C., *Applied Surface Science*, **2010**, 257, 887-898.
- [142] Sahu S. K., Panda S. P., Sadafule D. S., Kumbhar C. G., Kulkarni S. G., Thakur J. V., *Polymer Degradation and Stability*, **1998**, 62, 495-500.
- [143] Francis A. U., Venkatachalam S., Kanakavel M., Ravindran P. V., Ninan K. N., *European Polymer Journal*, **2003**, 39, 831-841.
- [144] Lin S., Yang L., *Tetrahedron Letters*, **2005**, 46, 4315-4319.

Chapter-4

COMPLEXATION OF DENDRIGRAFT POLYMER EG-G2 WITH COPPER AND SYNTHESIS OF TETRA-SUBSTITUTED IMIDAZOLES

Abstract

The Copper complexes of G0, G1 and G2 dendrigraft polymer having ethylene glycol initiated polyepichlorohydrin as core have been synthesized and characterized. Copper complexes of G0, G1 and G2 were found to be excellent catalysts for tetra-substituted imidazole derivatives via the reaction between benzil, aldehyde, amine and ammonium acetate. In comparison, for the synthesis of tetra-substituted imidazoles, EG-G2-Cu catalyst was found to be better over EG-G2-Pd catalyst. Conducting the reactions at room temperature, use of heterogeneous dendritic catalyst and use of solvents like ethanol are important points of benefit in terms of green chemistry principles.

4.1 Introduction

4.1.1 Tetra-substituted Imidazole Synthesis

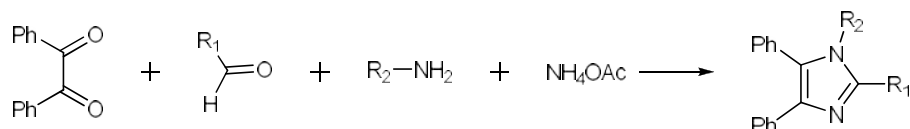
Multicomponent reaction (MCR) based organic synthesis contributes to sustainability by shortening the synthetic route. It combines at least three reactants at a time in the same pot to generate a product incorporating all the atoms of the reactants in a single step in contrast to a divergent multistep synthesis.¹⁻⁴ The efficiency, mild reaction conditions, atom economy, and high convergence of a one-pot reaction makes it an important tool for

implementing green chemistry. Multicomponent reactions are powerful tools in modern drug discovery processes, because they are important sources of molecular diversity, allowing rapid, automated and high throughput generation of organic compounds. This versatile applicability highlights the importance of access to efficient synthetic routes to highly substituted imidazole derivatives.^{5,6} Tetra-substituted imidazole is the most active constituent in many biological systems such as olmesartan and drug molecules as well as other natural products of pharmaceutical importance.⁷⁻⁹ The heterocyclic scaffolds comprising 2,4,5-tri-substituted and 1,2,4,5-tetra-substituted imidazoles are present in compounds possessing versatile pharmacological action, such as anti-inflammatory agents,¹⁰ CSBP kinase inhibitor,¹¹ anti-bacterial agents,¹² glucagon receptor antagonists,¹³ p38 MAP kinase inhibitors,¹⁴⁻¹⁶ modulators of Pgp-mediated multidrug resistance,^{17,18} ligands of the Src SH2 protein,^{19,20} antitumor agents,^{21,22} inhibitors of mammalian 15-LOX,²³ CB1 cannabinoid receptor antagonists²⁴ and inhibitors of B-Raf kinase.²⁵ These have generated interest from synthetic organic/medicinal chemists to develop synthetic methodologies for the construction of these heterocyclic scaffolds.

4.1.1.1 Methods of Synthesis

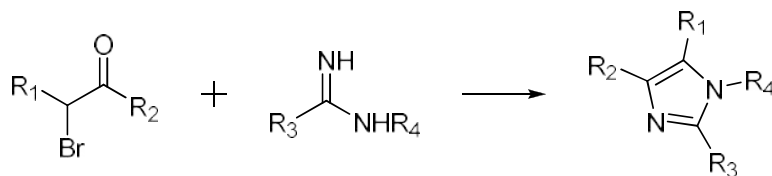
The wide-spread interest in tetra-substituted imidazole-containing structures has prompted extensive studies for their synthesis. The general method for the synthesis of 2,4,5 tri-substituted imidazole and 1,2,4,5 tetra-substituted imidazole involves a 3CR²⁶⁻²⁹ between 1,2-diketone, an aldehyde, and ammonium acetate and a 4CR³⁰⁻⁴⁹ between 1,2-diketone, an aldehyde, amine and ammonium acetate respectively (Scheme 4.1).

There are reports regarding synthesis of 1,2,4,5-tetra- substituted imidazoles involving the reaction of a 1,2-diketone, α -hydroxy/ acetoxy/ silyloxyketone or 1,2-ketomonoxime, an aldehyde, an amine and ammonium acetate carried out by (i) microwave irradiation in the presence of silica gel/zeolite HY or silica gel–NaHSO₄,⁵⁰⁻⁵² (ii) heating under reflux in suitable solvents or under neat condition at 140 °C in the presence of catalysts (Scheme 4.1).^{51,53-58}



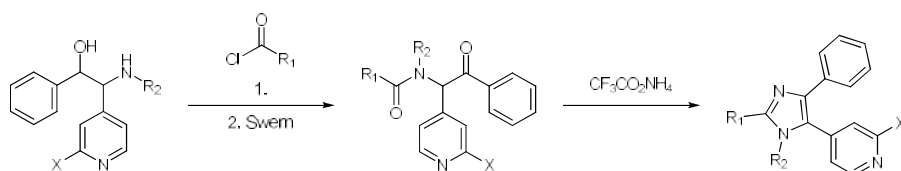
Scheme 4.1

The alternative approaches are the reaction of α -bromoketone with a substituted amidine for the synthesis of 2,4,5- tri-substituted and 1,2,4,5-tetra-substituted imidazoles (Scheme 4.2).^{23,24}



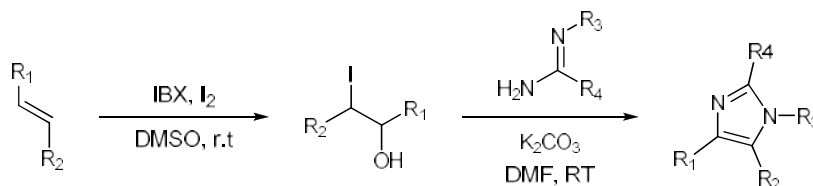
Scheme 4.2

Another method is the cyclocondensation of N-alkyl- α -acetamidoketone with ammonium acetate in acetic acid or with ammonium trifluoroacetate as solvent under reflux condition (Scheme 4.3).^{59,60}



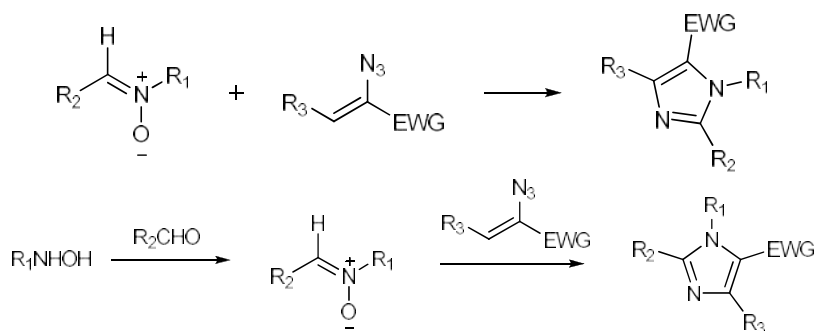
Scheme 4.3

Recently, the synthesis of 1,2,4,5-tetra-substituted imidazoles has been achieved from alkenes via a two step ketoiodination / cyclisation strategy (Scheme 4.4).⁶¹



Scheme 4.4

The reaction of nitrones, formed in situ by reaction of hydroxylamines and aldehydes, with 2-azido acrylates results in the formation of 1,2,4,5-tetra-substituted imidazoles via a one pot two component or a one pot three component method (Scheme 4.5).^{62,63}



Scheme 4.5

Other important synthetic methods include one pot thiazolium catalyzed addition of an aldehyde to an acyl imine followed by ring closure to the imidazole,⁶⁴ condensation of arylglyoxal, 1°-amine, carboxylic acids and isocyanates on Wang resin followed by cyclization in the presence of acetic acid,⁵⁹ by a hetero-Cope rearrangement,⁶⁵ the condensation of benzoin and benzoin acetate with aldehyde, 1°-amine, ammonia in the presence of copper acetate,⁶⁶ cyclization of sulphonamide with mesoionic 1,3-

oxazolinium-5-olates,⁶⁷ condensation of β -carbonyl-N-acyl-N-alkylamines with NH_4OAc in refluxing acetic acid,^{68,69} conversion of N-2-oxoamides with ammonium triflate,⁶⁰ besides others.^{48,53,70,71}

4.1.1.2 Comparison of Performance

In the last decade, use of various catalytic systems has been established for the synthesis of tetra-substituted imidazoles via a four-component condensation of aldehydes, 1,2-diketones, amines and ammonium acetate under microwave-irradiation, solvent free or classical conditions. The various catalytic systems such as silica gel or zeolite HY,⁵⁰ silica gel/ NaHSO_4 ,⁵² $\text{K}_5\text{CoW}_{12}\text{O}_4 \cdot 3\text{H}_2\text{O}$,⁷⁰ molecular iodine,⁷¹ $\text{HClO}_4\text{-SiO}_2$,⁵³ heteropolyacids,⁵⁶ $\text{InCl}_3 \cdot 3\text{H}_2\text{O}$,⁵⁸ $\text{FeCl}_3 \cdot 6\text{H}_2\text{O}$,⁵⁶ $\text{BF}_3\text{-SiO}_2$, AlCl_3 , MgCl_2 ,⁵⁴ alumina,⁷² 1,4-diazabicyclo [2,2,2]octane (DABCO),⁷³ $\text{Zr}(\text{acac})_4$,³¹ PPA-SiO_2 ,⁷⁵ nano- $\text{TiCl}_4\text{SiO}_2$,⁷⁶ nanocrystalline sulphated zirconia (SZ)³³ and silica-bonded propylpiperazine N-sulfamic acid (SBPPSA)⁷⁷ were used. LaCl_3 catalyzed synthesis used urea as a source of ammonia instead of ammonium acetate.⁷⁸ Synthesis of tetra-substituted imidazole using Bronsted acidic ionic liquid and N-methyl-2-pyrrolidinium hydrogen sulphate, as catalyst was reported by Shaterian *et al.*⁷⁹ These reports highlight the use of various catalysts. But the methods discussed are far away from the green chemistry approach.

4.1.2 Dendritic Complexes

Grafting catalytic sites on the periphery of dendrimers is the most straightforward and pioneering approach to construct dendritic catalysts which offer unprecedented opportunities for establishing active site multivalency and thus high loading capacity and ligand concentration.

The proximal interactions between catalytic groups and steric crowding at the periphery of dendritic catalysts may lead to cooperative effects and a certain selectivity profile respectively, which could further increase the catalytic effect.

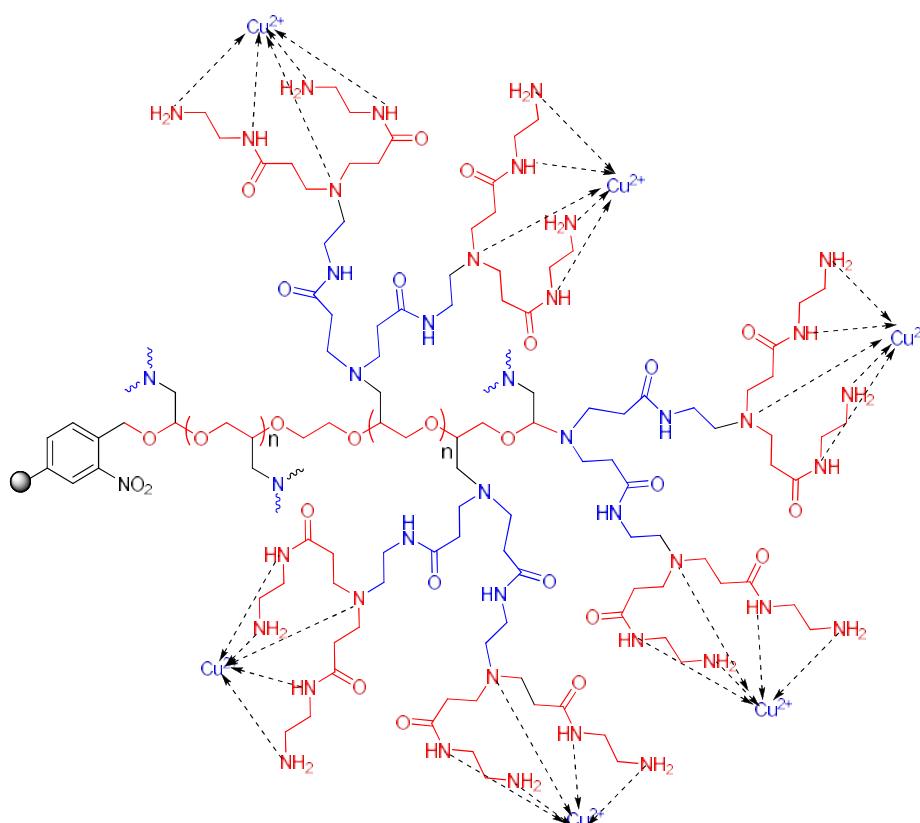


Fig 4.1 Merrifield resin supported dendrigraft EG-G2-Cu complex having ethylene glycol initiated PECH as core.

We have tried to develop copper complexes of dendrigraft polymer having ethylene glycol initiated polyepichlorohydrin as core, EG-Gn-Cu in order to increase the efficiency of the reaction by increasing the peripheral catalytic sites (Fig 4.1).

4.1.3 Origin and Objective of the Present Work

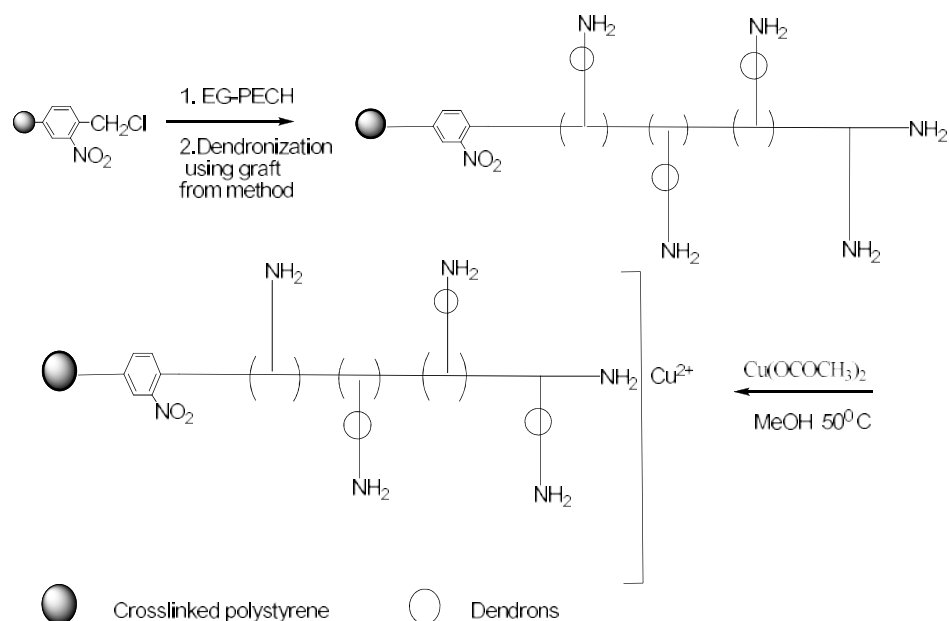
Recently, organic synthesis has utilized a green approach, due to certain advantages compared with conventional methods in terms of high selectivity, ease of manipulation, cleaner reaction profiles and relatively benign conditions. However, hazardous chemicals with often expensive acid catalysts, complex work up procedures and moderate yields have motivated researchers to develop user friendly catalysts. Therefore, the development of simple, efficient, clean, high-yielding and environmentally benign approaches using new catalysts for the synthesis of highly substituted imidazoles is an important task for organic chemists. Most of the reported catalysts were homogeneous and non-selective, eventhough, they apply green chemistry principles or the reported heterogeneous catalysts used high temperature and hazardous solvents. So we have tried to combine the benefits of both heterogeneous and dendritic behaviour to address the above mentioned issues.

The present chapter deals with the synthesis and characterization of copper complex of dendrigraft polymer having ethylene glycol initiated polyepichlorohydrin as core. The catalyst was employed for the synthesis of tetra- substituted imidazoles via the reaction between benzil, aldehyde, amine and ammonium acetate. The experimental parameters were optimized, scope of substrates, selectivity towards 3CR and 4CR were studied. Reusability of the catalyst was investigated. Dendritic EG-G2-Cu catalyst was experimented for the synthesis of tri-substituted imidazole also. The mechanism of the reaction was proposed. Catalytic behavior of dendritic palladium EG-G2-Pd catalyst towards the synthesis of tetra-substituted imidazole was also studied.

4.2 Results & Discussion

4.2.1 Synthesis of Copper Complex of Dendrigrraft Polymer having Ethylene Glycol Initiated PECH as Core

The synthesis of G_n dendrigrraft polymer having ethylene glycol initiated polyepichlorohydrin as core (EG- G_n) was reported in chapter.2. The amine capacity of G_0 , G_1 and G_2 dendrigrraft polymer was found to be 10.49, 18.06 and 24.96 mmols /g (Table 4.1) respectively. The copper complex of each of the EG- G_n polymer was synthesized by adopting the schematic procedure (Scheme 4.6).



Scheme 4.6 Synthesis of Merrifield resin supported dendrigrraft EG G_n -Cu complex having ethylene glycol initiated PECH as core.

For the complexation of dendrigrraft polymer with copper, the copper salt and solvent were optimized. It was found that, copper acetate in

methanol at a temperature of about 50 °C was the best condition for the complexation of copper with EG-Gn dendritic polymer. It is noteworthy that the catalyst is non-hygroscopic, stable and can be stored for a prolonged period of time without any change in its catalytic efficiency. The copper coordinated dendritic polymer was obtained as dark green powder.

4.2.2 Catalyst Characterization

4.2.2.1 ICP-AES Analysis

The copper loading for EG-G0-Cu, EG-G1-Cu and EG-G2-Cu based on ICP-AES analysis and confirmed by EDX analysis were found to be 15.54, 26.23 and 38.05 % of the polymer respectively. The results are given in Table 4.1. It is therefore assumed that an average of 2.03 ligands was bound to Cu ion in EG-G2 complex. The peak for ester was not present in the IR spectrum indicating that acetate ion was not included in the coordination sphere. The room temperature magnetic moments of the copper (II) complexes fall in range 1.9 - 2.2 B.M, which are very close to the spin only value for d^9 configuration. The Cu complexes were paramagnetic in nature, as was evident from the magnetic susceptibility measurements, which was consistent with the presence of Cu centers in their +2 oxidation state.

Table 4.1 Analytical data for EG-Gn and EG-Gn-Cu

Polymer	Amine capacity (mmols/g)	Copper loading (%) (ICP-AES)	Copper loading (mmols/g)	Copper loading (%) (EDX)
EG-G0-(Cu)	10.49	15.54	2.45	12.34
EG-G1-(Cu)	18.06	26.23	4.13	24.13
EG-G2-(Cu)	24.96	38.05	5.99	33.05

4.2.2.2 SEM & Energy Dispersive X-ray (EDX) Analysis

The SEM micrographs revealed that the smooth and flat surface of the starting Merrifield resin got disrupted and became crushed into irregular clusters. But after complexation with copper, the polymer showed metallic lustre (Fig 4.2 a & b). EDX spectra clearly showed Cu, C, N and O as the constituents of the catalysts. The results presented in Table 4.1 are the average of the data from the scanned regions. The data obtained on the composition of the compounds from the energy dispersive X-ray spectroscopy, were consistent with the elemental analysis values (Table 4.1).

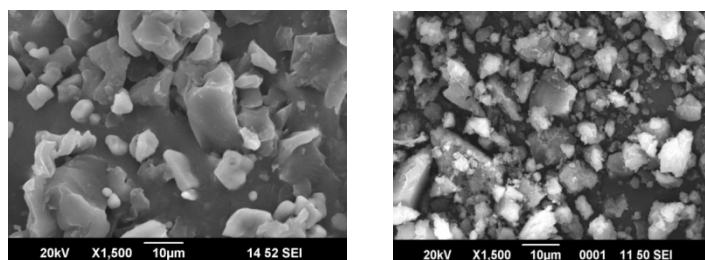


Fig 4.2 Scanning electron micrographs of (a) EG-G2 (b) EG-G2-Cu polymer

4.2.2.3 IR Spectral Studies

The IR spectra showed characteristic differences between the spectral pattern originating from the dendrigraft–copper complexes and the spectra of the dendrigraft polymer. The IR spectra are presented in Fig 4.3 and the significant features are summarized in Table 4.2.

The broadness of the band due to stretching of amine was observed to be reduced to a small extent in the spectrum of the copper complex suggesting coordination of Cu by the dendritic amine ligands. Apart from the typical absorptions at *ca.* 3474 (ν_{sym} (NH)), 2918 ($\nu_{\text{aliphatic}}$ (CH)), 1655 ($\nu_{\text{secondary amide}}$ (CO)), 1569 (ν_{bend} (NH)), or ($\nu_{\text{stretch asymm}}$ (N-O)),

1389 (ν_{bend} (C-O-H)) or $\nu_{\text{stretch symm}}$ (N-O), 997 ($\nu_{\text{CN stretch}}$ (C-NH)) and 720 cm^{-1} ($\nu_{\text{NH wag}}$ (CH-NH)), the spectra of EG-G2-Cu showed new band at *ca.* 940 cm^{-1} which was attributable to ν_{stretch} (Cu-N), giving clear indication of the binding of copper during complexation of copper ions to dendritic polymeric matrix.

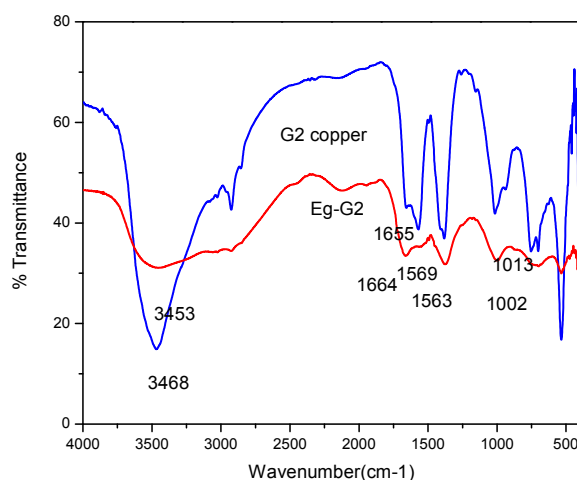


Fig 4.3 IR spectra of EG-G2 & EG-G2-Cu

Upon complexation of Cu ions with the dendritic EG-G2 resins, the spectra of EG-G2-Cu exhibited a distinct shift of ν_{stretch} (NH) to a lower frequency and that of ν_{bend} (NH) to a higher frequency (Table 4.2), compared to the uncomplexed polymer, along with some sharpening of bands.

Table 4.2. Infrared (IR) spectral data for EG-G2 and EG-G2-Cu

Polymer	ν_{stretch} (NH)	ν_{bend} (NH)	ν_{stretch} (NHCO)	ν_{bend} (C-OH)	ν_{stretch} (C-N)	ν_{stretch} (Cu-N)	ν_{wag} (NH)
EG-G2	3520	1563	1664	1395	1002	-	770
EG-G2-Cu	3474	1569	1655	1389	997	940	720

The position of the ν_{stretch} (NH) absorption in the polymeric complex was altered by 51 cm^{-1} to lower frequency region. The prominent absorption at

ca. 770 cm^{-1} has been narrowed and shifted towards lower frequency region at *ca.* 720 cm^{-1} assigned to $\nu_{\text{wag}}(\text{N-H})$ of primary or secondary amines of EG-G2-Cu.

4.2.2.4 Electronic Spectral Studies (UV-Vis DRS)

The diffuse reflectance UV-Visible spectra of EG-G2-Cu (Fig 4.4) displayed a broad peak in the region of 580-780 nm with maximum intensity at 667 nm which is characteristic of five coordinated copper complexes having square pyramidal geometry.

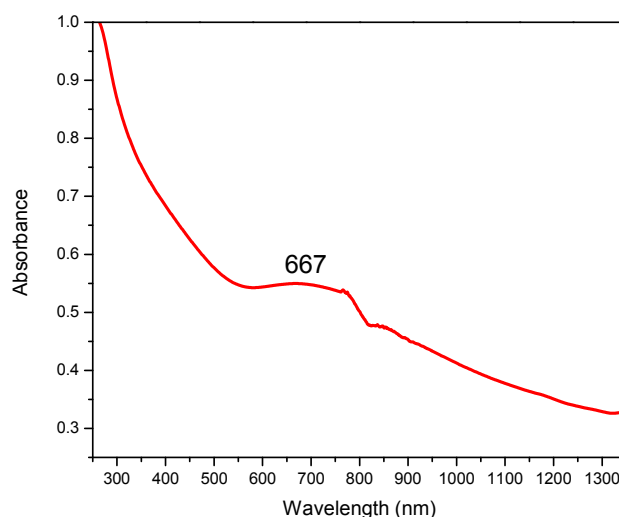


Fig 4.4 UV-Vis DRS spectrum of EG-G2-Cu

The absorption band may be ascribed to the absorption due to overlapping of allowed d-d transitions in copper after coordination with dendritic ligands.

4.2.2.5 EPR Spectral Studies

EPR Spectral studies of EG-G2-Cu show typical axial spectra with four hyperfine lines, which is characteristic of monomeric copper (II) complexes. The g and A values are obtained from the simulated

spectrum (Fig 4.5) given in Table 4.3. In the present case, g_{\parallel} is found to be greater than g_{\perp} . This predicts a square pyramidal geometry to five coordinated complex rather than a trigonal bipyramidal structure which would be expected to have g_{\perp} greater than g_{\parallel} .^{80,81} Thus EG-G2-Cu comprises of coordination of copper to two amine nitrogens, two amide nitrogens and one tertiary nitrogen of amidoamine unit.

Table 4.3 Splitting parameters g and A

Polymer	g_{\parallel}	g_{\perp}	g_{av}	A_{\parallel}	A_{\perp}	A_{av}
EG-G2-Cu	2.27	2.06	2.13	187.94	13.81	68.13

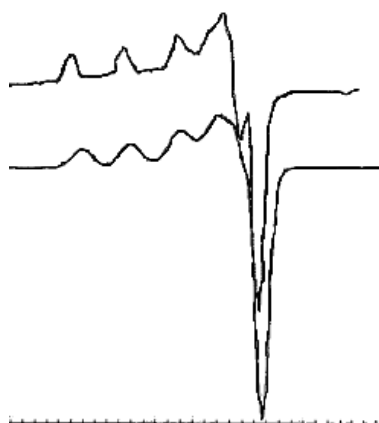


Fig 4.5 Experimental and simulated EPR spectra of EG-G2-Cu

4.2.2.6 X-ray Diffraction Studies

The room-temperature X-ray diffraction patterns of the dendrigraft polymer, EG-G2 with ethylene glycol initiated PECH as core and the copper complexed dendrigraft polymer EG-G2-Cu on Merrifield resin are overlaid in the figure (Fig 4.6). The EG-G2 sample displayed diffraction peaks at 2θ values of 20.0, 23.3, 31.1, 35.4, 40.1, 46.8, 62.8, 64.2, and 68.1°. These values are close to the ones observed for the

EG-G2-Cu, which were ascribed to the (200), (100), (110), (440), (111), (410), (303), (430) and (610) planes, respectively.

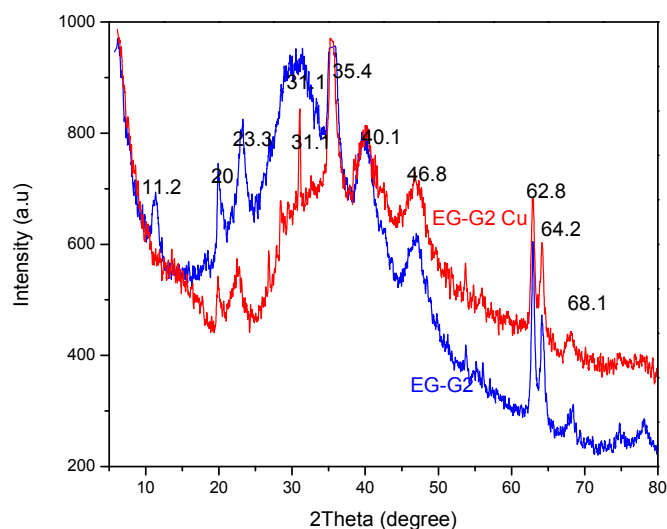


Fig 4.6 X-ray diffraction (XRD) pattern of EG-G2 and EG-G2-Cu polymer

After complexation with copper, the diffraction peak at 2θ value of 11.2° corresponding to (222) got disappeared and peak at 2θ value of 31.1° corresponding to (110) plane got narrowed indicating a mixed behaviour of crystalline and amorphous nature. This observation confirms that the copper ion has been anchored to the polymer matrix to yield the polymer supported dendritic copper catalyst EG-G2-Cu.

4.2.2.7 X-ray Photoelectron Spectroscopy

XPS is an effective technique for studying the electronic properties of the species formed on the surface. Fig 4.7 represents the Cu (2p) XPS spectra of the polymer anchored Cu complex. The catalyst displayed characteristic $\text{Cu}2p_{3/2}$ singlet peak located at 933 eV. Eventhough, the value of binding energy at 933 eV predicts copper to be

in the +1 oxidation state, the strong satellite peaks at 942.4, 940.7 and 961.6 confirms copper to be in the +2 oxidation state.

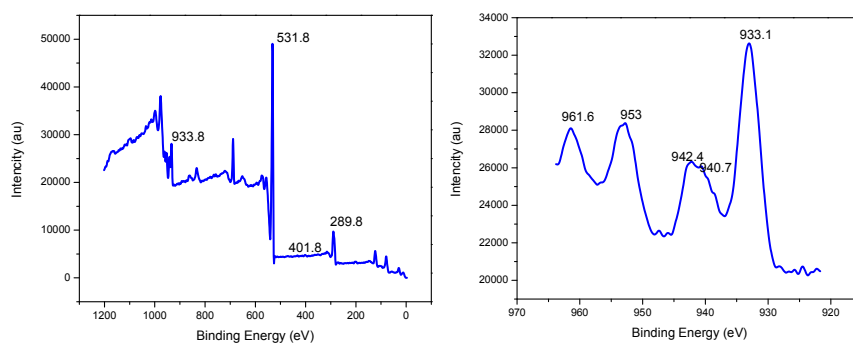


Fig 4.7 XPS spectra of Cu (2p_{3/2}) peak for EG-G2-Cu (a) wide (b) deconvoluted

The presence of Cu (II) in supported dendritic complex has thus been confirmed from the results of XPS analysis. The XPS results are also consistent with the paramagnetic nature of the catalysts, as evidenced by the magnetic susceptibility measurements.

4.2.2.8 TG-DTG Analysis

Evaluation of the thermogravimetric data of the EG-G2 functionalized resins and the corresponding Cu loaded dendrigraft polymer was performed. Considerable extent of decomposition was observed in the thermogram of both EG-G2 and EG-G2-Cu at the temperature 412.9 and 398.8°C owing to the degradation of the polymeric backbone (Fig 4.8). In EG-G2-Cu polymer, the first step of the decomposition is attributable to the loss of non-coordinated water, occurring at a temperature of about 74.7°C. Apart from this, a decomposition step with a weight loss of 30.5 % occurs in the temperature range of 150-300 °C. By analogy with the thermal decomposition characteristics of EG-G2 having decomposition with a weight loss of 17.3 % and 14.9 % occurring in the temperature

range of 160-220°C and 230-320°C respectively, it was revealed that copper ions are incorporated into the polymer.

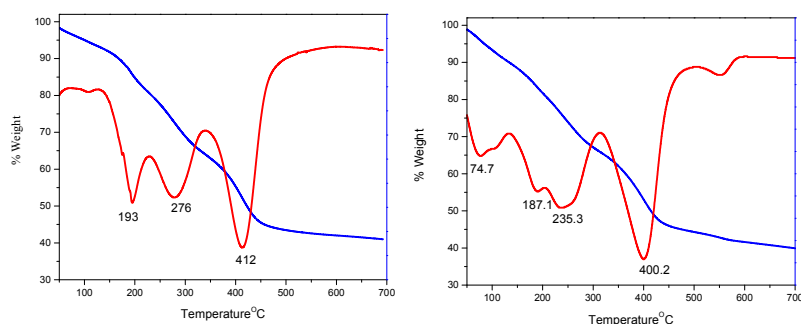


Fig 4.8 TG-DTG plot of (a) EG-G2 and (b) EG-G2-Cu polymer

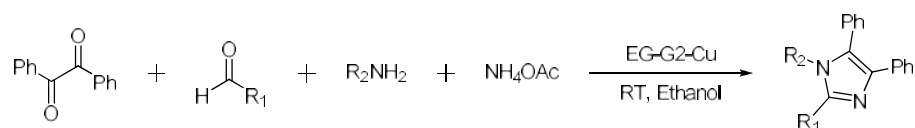
Similar decomposition pattern with difference in the amount of decomposition clearly predicts the bonding of copper to the dendron moiety. We have ascribed this decomposition to the release of amines as nitrogen, carbonyls as CO or CO₂ and the degradation of the polymeric backbone to be left with a residue containing copper oxide or hydroxide.

4.2.3 Catalytic Activity of Resin Supported Dendrigrraft EG-Gn-Cu Complex

4.2.3.1 Synthesis of Tetra- substituted Imidazole

In a survey of catalytic activity, dendrigrraft EG-Gn copper and palladium (chapter.5) complexes were employed in the synthesis of tetra-substituted imidazole. For a model study, benzaldehyde and aniline together with benzil and ammonium acetate were chosen as model compounds (Scheme 4.7). One pot reaction between these reactants was performed in the presence of different generations of EG-Gn copper catalyst. All the generations showed good catalytic behavior. In order to

optimize the reaction conditions, the effect of various reaction parameters, such as type of solvent, reaction temperature, substrate ratio, catalyst concentration, etc., were evaluated using benzil, benzaldehyde, aniline and ammonium acetate as model substrates and EG-G2-Cu as the catalyst. Our emphasis in the present work has been to conduct the reactions using environmentally safe solvents including water and to avoid the use of chlorinated solvents. Nevertheless, apart from water, methanol, ethanol, acetonitrile, THF, we have screened the reaction under neat reaction condition (solvent free condition) as well.



Scheme 4.7. Synthesis of tetra-substituted imidazole

The nature of solvent was observed to have a profound effect on the activity of the catalyst and the product selectivity of the reaction.

Table 4.4 Optimization of solvent

Solvent	Yield (%) ^a
No solvent	78
CH ₃ CN	30
Ethanol	92
Methanol	88
Water	62
THF	30

^aReaction Conditions: benzaldehyde (1 mmol), aniline (1 mmol), benzil (1 mmol), NH₄OAc (4 mmol). 2h, RT, Catalyst (30 mg), Yield after purification,

The reactions were performed at ambient temperature under magnetic stirring. From the results presented in Table 4.4, it is evident that the reaction conducted in the molar ratio of benzil: aldehyde: amine: ammonium acetate at 1: 1: 1: 4 in ethanol at room temperature proceeded smoothly to selectively yield tetra-substituted imidazole.

Table 4.5 Optimization of amount of catalyst

Amount of catalyst (mg)	Amount of catalyst (mol %)	Yield (%) ^a
5	3.0	80
10	6.0	85
15	9.0	88
20	12.0	92
30	18.0	92

^aReaction Conditions: benzaldehyde (1 mmol), aniline (1 mmol), benzil (1 mmol), NH₄OAc (4 mmol), 2h, Solvent (ethanol), Yield after purification, RT

Increasing the catalyst amount shows an increase in the percentage yield from 80 % (with 3.0 mol % catalyst) to 92 % (with 12.0 mol % catalyst). Eventhough, solvent free condition gave 78% yield and water gave 62% yield, ethanol was found to be the optimum solvent of choice. Thus, in order to attain high conversion, the substrate molar ratio, benzil: aldehyde: amine: ammonium acetate in the ratio 1:1:1:4 and catalyst 20 mg (12 mol %) in ethanol at room temperature was found to be the optimum condition.

Further, the effect of generation of the catalyst on tetra-substituted imidazole synthesis (Table 4.6) was evaluated. All generations of the catalyst showed good catalytic behaviour towards the synthesis of tetra-

substituted imidazole. In the case of benzaldehyde with aniline, G0, G1 and G2 dendrigraft copper catalyst showed 90 %, 92 % and 92 % conversion respectively with 100 % selectivity towards tetra-substituted imidazole. Therefore, all generations of EG-Gn-Cu are active catalysts with 100 % selectivity. The negative dendritic effect was not pronounced here and usual concept of slow reaction of supported catalysts was not observed.

Table 4.6 Generation effect on the synthesis of tetra-substituted imidazole^a

Generation	Yield (%)
EG-G0-Cu	90
EG-G1-Cu	92
EG-G2-Cu	92

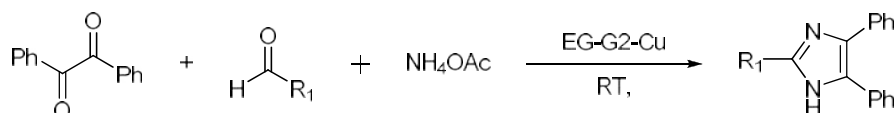
^a Reaction Conditions: benzaldehyde (1 mmol), aniline (1 mmol), benzil (1 mmol), NH₄OAc (4 mmol), 2h, Solvent (ethanol), Yield after purification, RT

After optimizing the reaction conditions, scope of different substrates was evaluated (Table 4.7). Most of the substrates showed completion of the reaction within 1-2 hours and gave good-to-excellent yields, with 100 % selectivity towards tetra-substituted imidazole. It can be observed that the process tolerates both electron donating and electron withdrawing substituents on the aldehyde.

Table 4.7 EG-G2-Cu catalyzed synthesis of tetra-substituted imidazoles^a

 (Time, Yield)		
 4a (2h, 92%)	 4b (2h, 90%)	 4c (1h, 94%)
 4d (2h, 92%)	 4e (2h, 94%)	 4f (1h, 95%)
 4g (1h, 92%)	 4h (1h, 94%)	 4i (2h, 88%)
 4j (2h, 92%)	 4k (3h, 78%)	 4l (3h, 90%)
 4m (4h, 75%)	 4n (1h, 94%)	 4o (3h, 85%)
 4p (2h, 90%)		
^a Reaction Conditions: benzaldehyde (1 mmol), aniline (1mmol), benzil (1 mmol), NH ₄ OAc (4 mmol), EG-G2-Cu (12 mol %), Solvent (ethanol), ^b Yield after purification, RT		

With the same optimum reaction conditions, (without using the amine), we have investigated the scope of dendritic copper-catalyst EG-G2-Cu towards the synthesis of tri- substituted imidazole derivatives also (Scheme 4.8).

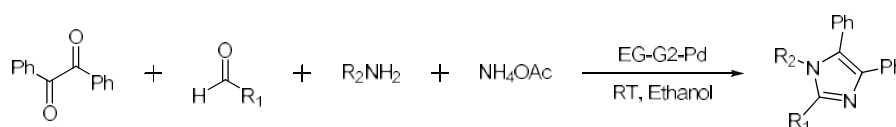


Scheme 4.8. Synthesis of tri-substituted imidazoles

Table 4.8 Dendritic copper-catalyzed synthesis of tri-substituted imidazoles

			(Time, Yield)
4a' (1h, 92%)	4b' (2h, 92%)	4c' (1h, 94%)	
4d' (2h, 92%)	4e' (1h, 92%)	4f' (2h, 90%)	
4g' (3h, 78%)	4h' (2h, 90%)	4i' (3h, 82%)	
4j' (3h, 84%)			
^a Reaction Conditions: benzaldehyde (1 mmol), benzil (1 mmol), NH ₄ OAc (4 mmol), Solvent (ethanol), RT, Catalyst (EG-G2-Cu 12 mol%), Yield after purification			

As shown in Table 4.8, the catalyst showed excellent reactivity towards the selected substrates. In order to compare the catalytic behaviour of dendritic copper with that of dendritic palladium catalyst and also to check whether palladium based catalyst can catalyse the synthesis of tetra-substituted imidazole derivatives, we have tried the 4CR reaction (Scheme 4.9).



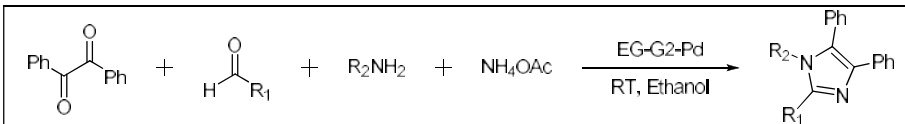
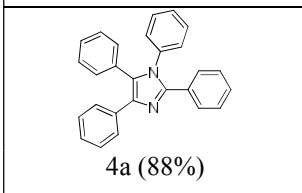
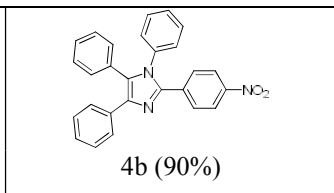
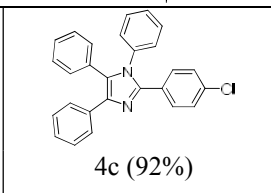
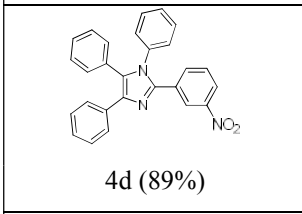
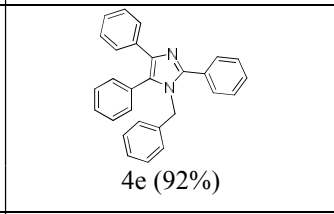
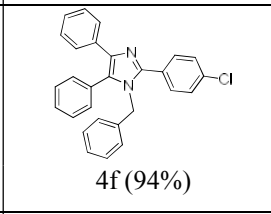
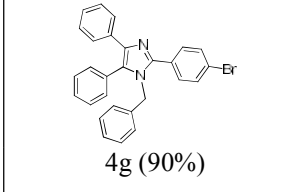
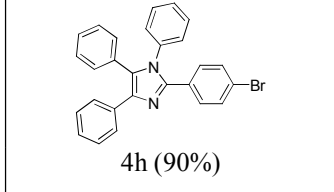
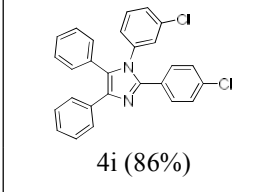
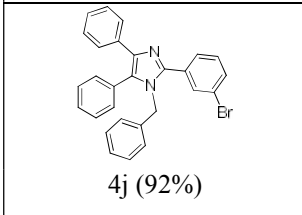
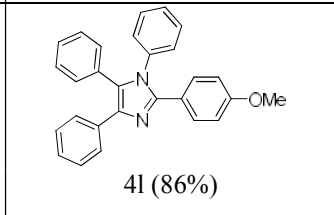
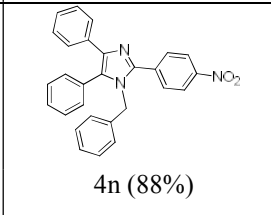
Scheme 4.9

Generally, palladium catalysts are selective towards certain carbon-carbon bond forming reactions like Suzuki, Heck, Sonogashira as well as hydrogenation reactions. We have tried the palladium catalyst EG-G2-Pd for the synthesis of tetra-substituted imidazoles. The results are tabulated in Table 4.9. We have tried with few substrates and dendritic palladium catalyst showed excellent reactivity as that of EG-G2-Cu towards the synthesis of tetra-substituted imidazoles. It was noticed that at higher catalyst concentration (ie. ≥ 10 mg), the reaction took only 5-8 h for the completion, while at lower catalyst concentration (ie. < 5 mg), the reaction took 24 h for the completion with 100 % selectivity for the selected substrates.

All the reactions were monitored by TLC. After the completion of the reaction, ethyl acetate was added to the reaction mixture and the catalyst was filtered. The filtrate was concentrated to afford the crude product which was purified either by recrystallisation from ethanol or by column chromatography using hexane:ethyl acetate (7:3 v/v) as eluent.

The products were characterized by spectral data and through comparison of the physical constants with those reported in the literature.

Table 4.9 Dendritic palladium catalyzed synthesis of tetra-substituted imidazole

		
		
4a (88%)	4b (90%)	4c (92%)
		
4d (89%)	4e (92%)	4f (94%)
		
4g (90%)	4h (90%)	4i (86%)
		
4j (92%)	4l (86%)	4n (88%)
^a Reaction Conditions: benzaldehyde (1 mmol), aniline (1 mmol), benzil (1 mmol), NH ₄ OAc (4 mmol). Solvent (Ethanol), 5-8 h, Catalyst (EG-G2-Pd:20 mg), Yield after purification, RT		

4.2.3.2 Recyclability of the Catalysts

After completion of the reaction, the solution was filtered, washed with ethanol, ethyl acetate (3 -10 mL), acetone and dried under vacuum

at 50⁰C for about 5h. The catalyst recovered was weighed and reused without loss of significant catalytic activity.

Table 4.10 Recycling of Dendritic Copper Catalyst, EG-G2-Cu ^a

No. of Cycles	Catalyst weight (mg)	Catalyst recovered (mg)	Recovery (%)	Product yield (%)
1	20	19.5	97.5	92.0
2	19.5	18	92.3	92.0
3	18	18	100	92.0
4	18	15	83.3	90.0
5	15	12	80.0	88.0

^aReaction Conditions: benzaldehyde (1 mmol), aniline (1 mmol), benzil (1 mmol), NH₄OAc (4 mmol). Solvent (Ethanol), 2h, Catalyst (EG-G2-Cu 20 mg), Yield after purification, RT

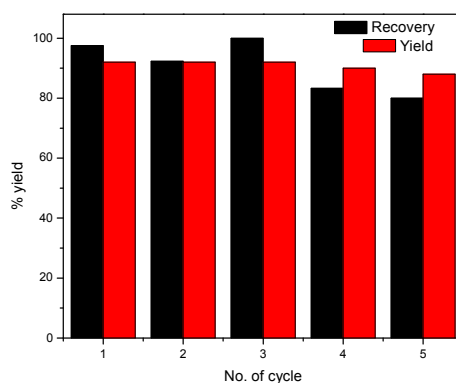
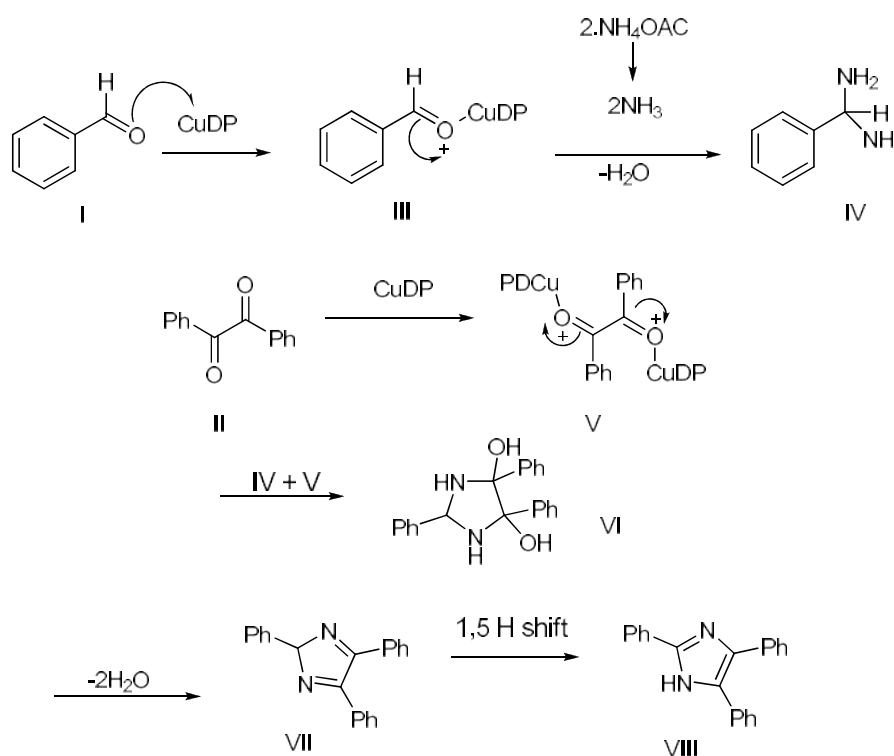


Fig 4.9 Bar diagram showing the recyclability of EG-G2-Cu catalyst

Details regarding catalyst recovery with percentage yield and the corresponding bar diagram are depicted in Table 4.10 and Fig 4.9. Successive runs were carried out in order to see the recyclability of the catalyst. After fifth cycle, 80 % of catalyst was recovered and reused with 88 % conversion.

4.2.3.3 The Proposed Mechanism

In order to explore the mechanism of the dendritic copper-catalyzed 4CR and 3CR, a control experiment was performed without the catalyst. Treatment of the reactants in the absence of the catalyst gave no product. The most probable mechanism for the synthesis of 2,4,5-tri-substituted imidazoles is shown in Scheme 4.10.

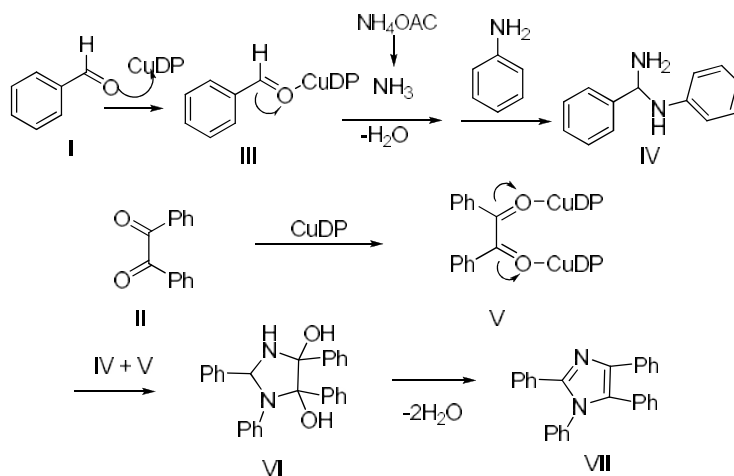


Scheme 4.10 Proposed mechanism of the formation of tri-substituted imidazole

Initially, the dendritic copper catalyst can simultaneously activate the carbonyl groups of aldehyde I and benzil II to decrease the energy of the transition state. The nucleophilic attack of the nitrogen of ammonia, obtained from NH₄OAc on the activated carbonyl group III, resulted in

the formation of diamine intermediate IV. This intermediate condenses with benzil V to form intermediate VII which in turn rearranges to the tri-substituted imidazoles by a [1,5]-H shift.

Similarly, a plausible mechanism for the synthesis of 1,2,4,5-tetra-substituted imidazoles is presented in Scheme 4.11. After the activation of the carbonyl group of the aryl aldehyde I, and the nucleophilic attack of the nitrogen of ammonia, obtained from NH_4OAc , and also the nucleophilic attack of aniline on III resulted in the intermediate IV. In the presence of dendritic copper catalyst, intermediate IV condenses with carbonyl group activated benzil V to form intermediate VI which in turn forms tetra-substituted imidazoles by dehydration.



Scheme 4.11 Proposed mechanism for the formation of 1,2,4,5-tetra-substituted imidazole

4.3 Conclusions

In conclusion, we have developed a highly efficient dendritic copper catalyzed procedure for the synthesis of 1,2,4,5 tetra-substituted

imidazole based on one pot four component condensation of 1,2 diketone, aldehyde, amine and ammonium acetate under benign conditions. The copper complexes of G0, G1 and G2 dendrigraft polymer having ethylene glycol initiated polyepichlorohydrin as core were characterized and they were found to be excellent catalysts for the 4CR reaction between 1,2 diketone, aldehyde, amine and ammonium acetate. The reaction occurred well even with low generation ie. EG-G0-Cu catalyst. After optimizing the reaction conditions, a detailed study of synthesis of tetra-substituted imidazole derivatives was done with EG-G2 copper catalyst. A brief investigation on the synthesis of tri-substituted imidazole derivative was also done. EG-G2-Cu catalyst was compared with EG-G2-Pd catalyst and found that EG-G2-Cu catalyst was superior to EG-G2-Pd with respect to the reaction time. The main features of the synthesis are: ethanol or water was used as the solvent, even small amount of catalyst was found to drive the reaction and the reaction was found to be feasible under solvent free condition also. All the reactions were performed at room temperature and outstanding tolerance of functional groups was noticed. The synthetic protocols are straightforward, safe, environmentally clean, and free from halogenated solvents or any other additives such as a co-catalyst or acid. Procedural simplicity, simple recovery and reusability of catalysts meet the requirements of benign chemistry. Further investigation on application of this catalyst for other organic reactions is in progress.

4.4 Experimental Section

4.4.1 Materials

Anhydrous copper acetate, benzil, aldehydes, amines and ammonium acetate are purchased from local vendors and used as received. All solvents were purified by standard procedures prior to use.

4.4.2 Synthesis of copper complex of dendrigraft EG-G2 polymer having ethylene glycol initiated polyepichlorohydrin as core

Same as 3.4.2.

4.4.3 General procedure for the synthesis of tetra-substituted imidazoles

The mixture of benzil (1.0 mmol), aldehyde (1.0 mmol), amine (1.0 mmol) and NH_4OAc (4.0 mmol) in ethanol as solvent was stirred at RT in the presence of EG-G2-Cu catalyst (12 mol %). After the completion of the reaction (solid mass formation), the reaction mixture was diluted with water, the solid mass precipitated was filtered off, extracted with ethyl acetate to remove the catalyst, concentrated under rotary vacuum evaporation to dryness and the crude product was recrystallized from ethanol to afford tetra-substituted imidazole or further purified by column chromatography using the eluent, petroleum ether : ethyl acetate / hexane : ethyl acetate in the ratio 7:3.

4.4.4 General procedure for the synthesis of tri-substituted imidazoles

The mixture of benzil (1.0 mmol), aldehyde (1.0 mmol) and NH_4OAc (4.0 mmol) in ethanol as solvent was stirred at RT in the presence of EG-G2-Cu catalyst (12 mol %). After the completion of the reaction

(solid mass formation), the reaction mixture was diluted with water, the solid mass precipitated was filtered off, extracted with ethyl acetate to remove the catalyst, concentrated under rotary vacuum evaporation to dryness and the crude product was recrystallized from ethanol to afford tri-substituted imidazole.

4.4.5 Test for Heterogeneity of the Reaction

The filtrate obtained by separating the solid catalyst after completion of the reaction was extracted with ethyl acetate. The aqueous layer was subsequently treated with a fresh batch of reactants in a reaction vessel and the reactions were allowed to continue. There was no formation of the product. This suggests that the reaction does not proceed after removal of the catalyst. Moreover, the presence of copper could not be detected when the filtrate, obtained after isolating the solid catalysts by filtration, was subjected to AAS analysis. The possibility of the copper species leaching out of the catalyst can thus be ruled out on the basis of the evidence gathered, which also proves the heterogeneous nature of the catalytic process.

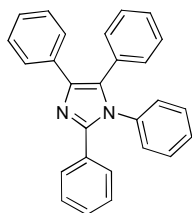
4.4.6 Regeneration of the Catalyst

The reusability of the catalyst for subsequent catalytic cycles was examined using benzil, benzaldehyde, aniline and ammonium acetate as substrates. After the completion of the reaction, the solid catalyst was separated from the reaction mixture by washing the product with ethyl acetate, ethanol and acetone. The catalyst was dried under vacuum at 50°C for about 5h. The dried solid catalyst was weighed and added to a fresh reaction mixture of benzil, benzaldehyde, aniline and ammonium acetate. The progress of the reaction was monitored by thin layer chromatography (TLC) and LCMS. The procedure was repeated for five reaction cycles.

4.5 Characterization of Products

A) 1,2,4,5-Tetra-substituted imidazole

1) 1,2,4,5-Tetraphenyl-1H-imidazole



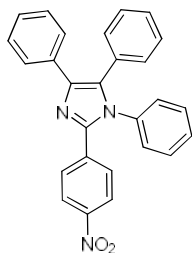
White needle solid; m.p. 216–218 °C.

^1H NMR (400 MHz, DMSO-*d*₆) δ : 7.16–7.49 (m, 20H, H-Ar) ppm.

^{13}C NMR (100 MHz, DMSO-*d*₆) δ : 128.63, 128.70, 130.05, 130.85, 131.02, 131.55, 132.53, 132.67, 132.92, 133.87, 134.26, 134.81, 135.41, 136.23, 137.11, 138.40, 139.54 ppm.

MS, *m/z* : 372.16.

2) 2-(4-Nitrophenyl)-1,4,5-triphenyl-1H-imidazole



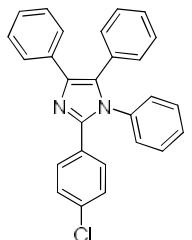
Yellow solid; m.p. 190–192 °C.

^1H NMR (400 MHz, DMSO-*d*₆) δ : 7.15–7.36 (m, 17H, H-Ar), 7.47 (d, *J* = 7.4 Hz, 2H, H-Ar) ppm.

^{13}C NMR (100 MHz, DMSO-*d*₆) δ : 127.30, 127.50, 127.70, 128.0, 128.20, 129.31, 129.70, 129.85, 130.10, 131.54, 132.69, 133.60, 133.68, 145.0, 149.72 ppm.

MS, *m/z* : 417.15.

3) 2-(4-Chlorophenyl)-1,4,5-triphenyl-1H-imidazole

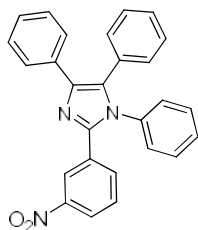


Off-white crystal; m.p. 160–163 °C;

^1H NMR (400 MHz, DMSO-*d*₆) δ : 7.15–7.36 (m, 17H, H-Ar), 7.47 (d, *J* = 7.4 Hz, 2H, H-Ar) ppm.

^{13}C NMR (100 MHz, DMSO-*d*₆) δ : 127.30, 127.50, 127.70, 128.0, 128.20, 129.31, 129.70, 129.85, 130.10, 131.54, 132.69, 133.60, 133.68, 145.0, 149.72 ppm.

MS, *m/z* : 406.12.

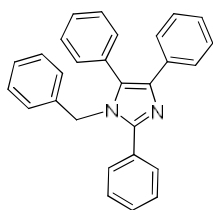
4) 2-(3-Nitrophenyl)-1,4,5-triphenyl-1H-imidazole

Yellow solid; m.p. 242–245 °C.

¹H NMR (400 MHz, DMSO-*d*₆) δ: 7.30– 7.53 (m, 10H), 7.78 (t, J = 8 Hz, 1H), 8.51 (d, J = 8 Hz, 1H), 8.95 (t, J = 1.8 Hz, 1H), 9.41 (d, J = 8 Hz, 1H), 13.10 (s, 1H) ppm.

¹³C NMR (100 MHz, DMSO-*d*₆) δ: 119.40, 122.61, 127.13, 128.44, 128.68, 130.44, 131.17, 131.82, 143.38, 148.37 ppm.

MS, m/z : 417.15.

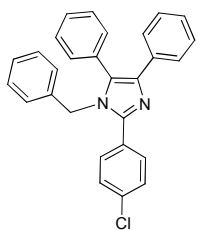
5) 1-Benzyl-2,4,5-triphenyl-1H-imidazole

White solid; m.p 162-165°.

¹H NMR (400 MHz, DMSO-*d*₆) δ: 5.13 (s, 2H), 6.82 (m, 2H), 7.2 (m, 4H), 7.35 (m, 4H), 7.4 (m, 4H), 7.6 (d, J = 8 Hz, 2H), 7.67 (m, 4H) ppm.

¹³C NMR (100 MHz, DMSO-*d*₆) δ: 48.41, 124.86, 125.41, 125.88, 126.53, 127.24, 127.25, 127.84, 127.78, 130.48, 130.79, 131.03, 131.79, 137.33 ppm.

MS, m/z : 386.18.

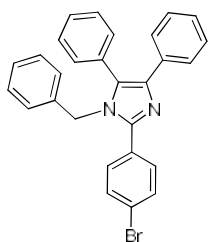
6) 1-Benzyl-2-(4-chlorophenyl)-4,5-diphenyl-1H-imidazole

White solid; m.p 162-163°.

¹H NMR (400 MHz, DMSO-*d*₆) δ: 5.1 (s, 2H), 6.8 (m, 2H), 7.25 (m, 7H), 7.4 (m, 6H), 7.6 (m, 4H) ppm.

¹³C NMR (100 MHz, DMSO-*d*₆) δ: 49.41, 125.86, 126.51, 126.78, 127.53, 128.14, 128.25, 128.74, 128.87, 130.48, 130.79, 131.03, 131.79, 137.33 ppm.

MS, m/z : 420.14.

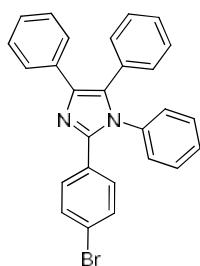
7) 1-Benzyl-2-(4-bromophenyl)-4,5-diphenyl-1H-imidazole

White solid; m.p. 169–170⁰ C.

¹H NMR (400 MHz, DMSO-*d*₆) δ : 4.86 (s, 2H), 6.61–7.46 (m, 19H) ppm.

¹³C NMR (100 MHz, DMSO-*d*₆) δ : 49.41, 126.86, 127.51, 127.88, 128.63, 129.14, 129.25, 129.74, 129.87, 131.48, 131.79, 132.03, 132.89, 138.43 ppm.

MS, m/z : 464.09.

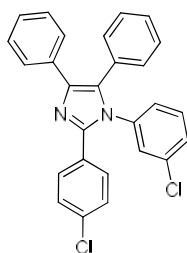
8) 2-(4-Bromophenyl)-1,4,5-triphenyl-1H-imidazole

White powder; m.p. 165–168⁰C.

¹H NMR (400 MHz, DMSO-*d*₆) δ : 7.40– 7.12 (m, 17H, Ar), 7.94 (d, 2H, Ar) ppm.

¹³C NMR (100 MHz, DMSO-*d*₆) δ : 123.0, 124.4, 125.2, 126.0, 127.4, 128.1, 128.3, 128.4, 128.5, 128.6, 128.9, 129.1, 129.2, 129.4, 129.6, 130.3, 131.0, 132.6, 133.2, 136.1, 136.3, 139.7, 144.6, 147.0 ppm.

MS, m/z : 450.07.

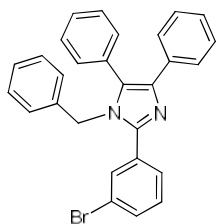
9) 1-(3-Chlorophenyl)-2-(4-chlorophenyl)-4,5-diphenyl-1H-imidazole

White crystals; m.p. 182–184⁰C.

¹H NMR (400 MHz, DMSO-*d*₆) δ : 7.30– 7.53 (m, 10H), 7.94 (d, 2H), 7.78 (d, J = 8 Hz, 2H), 8.51 (d, J = 8 Hz, 1H), 8.95 (t, J = 1.8 Hz, 1H), 9.41 (d, J = 8 Hz, 1H), 13.10 (s, 1H).

¹³C NMR (100 MHz, DMSO-*d*₆) δ : 127.30, 127.50, 127.70, 128.0, 128.20, 129.31, 129.70, 129.85, 130.10, 131.54, 132.69, 133.65, 133.74, 146.0, 149.82 ppm.

MS, m/z : 440.08.

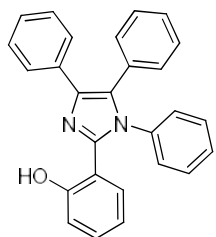
10) 1-Benzyl-2-(3-bromophenyl)-4,5-diphenyl-1H-imidazole

White solid; mp: 148 - 150°C.

^1H NMR (400 MHz, DMSO-*d*6) δ : 7.66 - 6.82 (m, 19H, Ar), 5.11 (s, 2H, CH₂) ppm.

^{13}C NMR (100 MHz, DMSO-*d*6) δ : 132.17, 131.86, 130.99, 130.00, 129.04, 128.86, 128.77, 128.69, 128.57, 128.11, 127.51, 127.22, 126.75, 126.51, 125.98, 125.90, 48.31 ppm.

MS, *m/z* : 464.09.

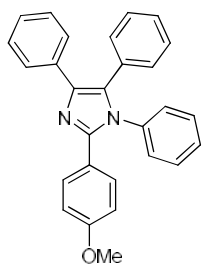
11) 2-(1,4,5-Triphenyl-1H-imidazol-2-yl) phenol

White powder; m.p. 252–254°C.

^1H NMR (400 MHz, DMSO-*d*6) δ : 6.54 (t, *J* = 8.0 1H, H-Ar), 6.65 (d, 1H, H-Ar), 6.93 (d, 1H, H-Ar), 7.16–7.43 (m, 16H, H-Ar), 12.57 (s, 1H, OH) ppm.

^{13}C NMR (100 MHz, DMSO-*d*6) δ : 115.30, 122.51, 124.61, 125.48, 126.92, 127.35, 128.90, 129.35, 130.47, 131.74, 135.65, 136.24, 137.61, 139.66, 145.82, 155.72 ppm.

MS, *m/z* : 388.16.

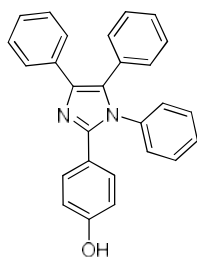
12) 2-(4-Methoxyphenyl)-1,4,5-triphenyl-1H-imidazole

Milky crystal; m.p. 177–180°C.

^1H NMR (400 MHz, DMSO-*d*6) δ : 3.24 (s, 3H, CH₃), 6.83 (d, *J* = 7.4 Hz, 2H, H-Ar), 7.23–7.41 (m, 15H, H-Ar), 7.47 (d, *J* = 7.4 Hz, 2H, H-Ar) ppm.

^{13}C NMR (100 MHz, DMSO-*d*6) δ : 55.57, 114.07, 123.30, 126.83, 128.60, 128.77, 128.89, 129.12, 129.16, 129.24, 130.12, 131.10, 131.29, 131.59, 135.0, 137.07, 137.27, 146.49, 160.0 ppm.

MS, *m/z* : 402.17.

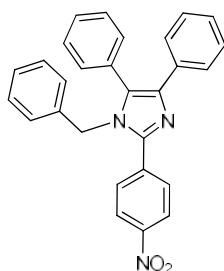
13) 4-(1,4,5-Triphenyl-1H-imidazol-2-yl) phenol

White powder; m.p. 282–285⁰C.

¹H NMR (400 MHz, DMSO-*d*₆) δ : 6.87–6.91 (d, *J* = 8Hz, 2H), 7.15–7.49 (m, 15H), 7.61–7.65 (d, *J* = 8.2Hz) ppm.

¹³C NMR (100 MHz, DMSO-*d*₆) δ : 115.3, 119.8, 125.3, 126.0, 126.7, 127.9, 128.2, 128.5, 128.6, 129.3, 131.6, 131.8, 135.3, 137.3, 146.6, 159.3 ppm.

MS, *m/z* : 388.16.

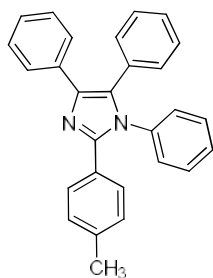
14) 1-Benzyl-2-(4-nitrophenyl)-4,5-diphenyl-1H-imidazole

Yellow solid; m.p 170 - 172⁰C.

¹H NMR (400 MHz, DMSO-*d*₆) δ : 5.1 (s, 2H), 6.8 (m, 2H), 7.25 (m, 7H), 7.4 (m, 6H), 7.6 (m, 4H), ppm.

¹³C NMR (100 MHz, DMSO-*d*₆) δ : 49.41, 125.86, 126.51, 126.78, 127.53, 128.14, 128.25, 128.74, 128.87, 130.48, 130.79, 131.03, 131.79, 137.33 ppm.

MS, *m/z* : 431.16.

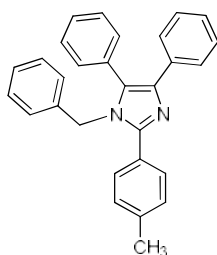
15) 1,4,5-Triphenyl-2-p-tolyl-1H-imidazole

Yellow needle solid; m.p. 186–188 °C.

¹H NMR (400 MHz, DMSO-*d*₆) δ : 2.25 (s, 3H, CH₃), 7.07 (d, *J* = 8Hz, 2H, H-Ar), 7.08–7.45 (m, 15H, HAr), 7.46 (d, *J* = 8Hz, 2H, H-Ar) ppm.

¹³C NMR (100 MHz, DMSO-*d*₆) δ : 21.20, 126.83, 126.84, 128.03, 128.61, 128.83, 128.90, 129.13, 129.59, 130.92, 131.54, 131.59, 134.92, 137.19, 138.29, 146.61 ppm.

MS, *m/z* : 386.18.

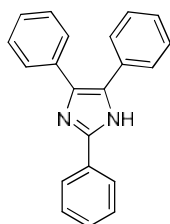
16) 1-Benzyl-4,5-diphenyl-2-p-tolyl-1H-imidazole

White solid; m.p. 164–166⁰C.

¹H NMR (400 MHz, DMSO-*d*6) δ : 2.08 (s, 3H), 4.91 (s, 2H), 6.61–7.40 (m, 19H) ppm.

¹³C NMR (100 MHz, DMSO-*d*6) δ : 22.52, 49.41, 127.15, 127.47, 127.94, 128.46, 129.22, 129.72, 129.92, 130.10, 130.45, 131.03, 132.23, 138.80, 140.01, 146.34 ppm.

MS, m/z : 400.19.

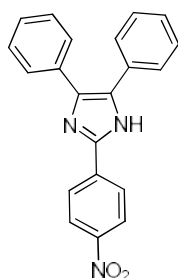
B) 2,4,5-Tri-substituted imidazole**1) 2,4,5-Triphenyl-1H-imidazole**

White solid; m.p. 271–272⁰C.

¹H NMR (400 MHz, DMSO-*d*6) δ : 12.7 (s, 1H, NH), 8.1 (d, J/4.8 Hz, 2H), 7.1–7.9 (m, 13H, Ar-H);

¹³C NMR (100 MHz, DMSO-*d*6) δ : d 146, 136, 135.4, 130.8, 130, 129, 128.75, 128.3, 127.5, 127, 125.6 ppm;

MS, m/z : 296.13.

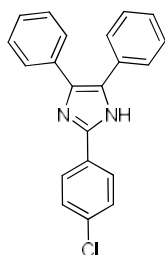
2) 2-(4-Nitrophenyl)-4,5-diphenyl-1H-imidazole

Orange solid; mp: 199–201 ⁰C.

¹H NMR (400 MHz, DMSO-*d*6) δ : 11.7 (s. br., NH), 7.00–8.52 (m., 14H, Ar-H).

¹³C NMR (100 MHz, DMSO-*d*6) δ : 148.069, 147.460, 145.633, 137.891, 134.737, 131.435, 131.103, 130.341, 129.631, 128.568, 126.862, 126.659, 124.165 ppm.

MS, m/z : 341.12.

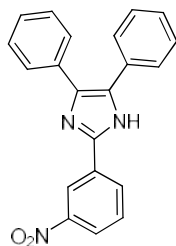
3) 2-(4-Chlorophenyl)-4,5-diphenyl-1H-imidazole

White solid, mp : 264-266⁰C.

¹H NMR (400 MHz, DMSO-*d*6) δ : 10.544 (br. S., 1H, NH), 8.11 (d, J8.4 Hz, 2H, Ar-H), 7.294-7.562 (m, 12H, Ar-H) ppm.

¹³C NMR (100 MHz, DMSO-*d*6) δ : 144.428, 137.296, 135.008, 132.748, 130.927, 129.201, 128.772, 128.667, 128.562, 128.429, 128.200, 127.857, 127.075, 126.837, 126.598 ppm.

MS, m/z : 330.09.

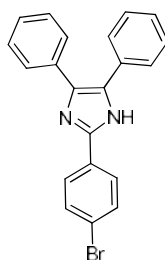
4) 2-(3-Nitrophenyl)-4,5-diphenyl-1H-imidazole

Yellow solid; m.p. 315–317⁰C.

¹H NMR (400 MHz, DMSO-*d*6) δ : 7.30–7.53 (m, 10H), 7.78 (t, J = 8 Hz, 1H), 8.51 (d, J = 8 Hz, 1H), 8.95 (t, J = 1.8 Hz, 1H), 9.41 (d, J = 8 Hz, 1H), 13.10 (s, 1H) ppm.

¹³CNMR (100 MHz, DMSO-*d*6) δ : 119.4, 122.6, 127.1, 128.4, 128.6, 130.4, 131.1, 131.8, 143.3, 148.3 ppm.

MS, m/z : 341.12.

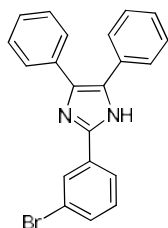
5) 2-(4-Bromophenyl)-4,5-diphenyl-1H-imidazole

White solid, mp : 249-251⁰C.

¹H NMR (400 MHz, DMSO-*d*6) δ : δ 12.02 (s, 1H), 7.40-7.44 (m, 4H), 7.37(d, 2H), 7.26-7.30 (m, 4H), 7.23-7.28 (m, 2H) 6.97-7.04 (d, 2H).

¹³C NMR (100 MHz, DMSO-*d*6) δ : 124.165, 126.659, 126.862, 128.568, 129.631, 130.341, 131.103, 131.435, 134.737, 137.891, 148.069, 145.633, 147.460 ppm.

MS, m/z : 374.04.

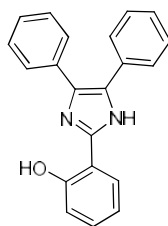
6) 2-(3-Bromophenyl)-4,5-diphenyl-1H-imidazole

White solid; m.p. 120–122^oC.

¹H NMR (400 MHz, DMSO-*d*₆) δ : 7.26–7.78 (m, 14H),
9.40 (s, 1H) ppm.

¹³C NMR (100 MHz, DMSO-*d*₆) δ : 121.8, 125.6, 126.0,
126.7, 127.4, 127.7, 127.7, 128.1, 131.0 ppm.

MS, m/z : 374.04.

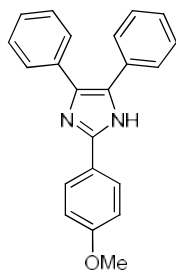
7) 2-(4,5-Diphenyl-1H-imidazol-2-yl) phenol

White solid; m.p. 209–211^oC.

¹H NMR (400 MHz, DMSO-*d*₆) δ : 12.74 (br. s. 1H, NH),
7.17-7.23 (m, 10H, Ar-H), 6.96-7.01 (d, J = 8.05Hz, 1H),
6.8 - 6.95 (d, j=7.4 Hz, 2H) ppm.

¹³C NMR (100 MHz, DMSO-*d*₆) δ : 146.0, 136.0, 130.08,
130.0, 129.0, 128.9, 128.4, 128.2, 127.6, 126.7, 125.6 ppm.

MS, m/z : 312.13.

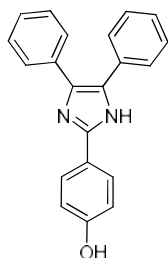
8) 2-(4-Methoxyphenyl)-4,5-diphenyl-1H-imidazole

White solid; mp : 230-233^oC.

¹H NMR (400 MHz, DMSO-*d*₆) δ : 12.52 (s, 1H, NH),
8.03 (d, J=8.80 Hz, 2.0 Hz, 2H), 7.70-7.10(m, 10H, Ar-H),
7.03 (dt, J=8.8 Hz, 2.0 Hz, 2H), 3.81 (s, 3H, CH₃).

¹³C NMR (100 MHz, DMSO-*d*₆) δ : 158.32, 145.09,
136.01, 134.62, 131.38, 12130, 127.4, 126.01, 123,07,
113.89, 54.62 ppm.

MS, m/z : 326.14.

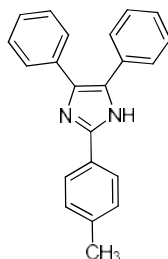
9) 4-(4,5-Diphenyl-1H-imidazol-2-yl) phenol

White solid, m.p : 267-269°C.

^1H NMR (400 MHz, DMSO-*d*6) δ : 12.20 (s, 1H, NH), 9.40 (s, 1H, OH), 7.90 (d, J8.4 Hz, 2H), 7.52–7.29 (m, 10H, Ar-H), 6.80 (d, J8.4 Hz, 2H).

^{13}C NMR (100 MHz, DMSO-*d*6) δ : 157.6, 146.65, 127.12, 125.7, 124.3, 121.9, 114.75, 112.85, 98.55, 95.46 ppm.

MS, m/z : 312.13.

10) 4,5-Diphenyl-2-p-tolyl-1H-imidazole

Colourless needle; m.p : 234-235°C.

^1H NMR (400 MHz, DMSO-*d*6) δ : 7.86 (d, 2H, J = 8.1 Hz), 7.50 (br. d, 4H, J \approx 7.8 Hz), 7.21–7.31 (m, 8H), 2.38 (s, 3H, CH₃) ppm.

^{13}C NMR (100 MHz, DMSO-*d*6) δ : 146.2, 138.9, 132.9, 129.6, 128.6, 127.8, 127.4, 127.1, 125.2, 21.3.

MS, m/z : 310.15.

4.6 References

- [1] D'Souza D. M., Mueller T. J. J., *Chemical Society Reviews*, **2007**, 36, 1095-1108.
- [2] Climent J. M., Corma A., Iborra S., *RSC Advances*, **2012**, 2, 16-58.
- [3] Yanlong G., *Green Chemistry*, **2012**, 14, 2091-2128.
- [4] Ren Y. M., Cai C., Yanga R. C., *RSC Advances*, **2013**, 3, 7182-7204.
- [5] Maurya M. R., *Current Organic Chemistry*, **2012**, 16, 73-88.
- [6] de Silva J. A. L., Frausto de Silva J. J. R., Pombeiro A. J. L., *Coordination Chemistry Reviews*, **2011**, 255, 2232-2248.

-
- [7] Wolkenberg S. E., Wisnoski D. D., Leister W. H., Wang Y., Zhao Z. J., Lindsley C. W., *Organic Letters*, **2004**, 6, 1453-1456.
- [8] Shilcrat S. C., Mokhallalati M. K., Fortunak J. M. D., Pridgen L. N., *Journal of Organic Chemistry*, **1997**, 62, 8449-8454.
- [9] Sisko J., *Journal of Organic Chemistry*, **1998**, 63, 4529-4531.
- [10] Gallagher T. F., Fierthompson S. M., Garigipati R. S., Sorenson M. E., Smietana J. M., Lee D., Adams J. L., *Bioorganic & Medicinal Chemistry Letters*, **1995**, 5, 1171-1176.
- [11] Gallagher T. F., Seibel G. L., Kassis S., Laydon J. T., Blumenthal M. J., Lee J. C., Adams J. L., *Bioorganic & Medicinal Chemistry*, **1997**, 5, 49-64.
- [12] Antolini M., Bozzoli A., Ghiron C., Kennedy G., Rossi T., Ursini A., *Bioorganic & Medicinal Chemistry Letters*, **1999**, 9, 1023-1028.
- [13] de Laszlo S. E., Hacker C., Li B., Kim D., MacCoss M., Mantlo N., Hagmann W. K., *Bioorganic & Medicinal Chemistry Letters*, **1999**, 9, 641-646.
- [14] Liverton N. J., Butcher J. W., Claiborne C. F., Claremon D. A., Libby B. E., Nguyen K. T., O'Keefe S. J., *Journal of Medicinal Chemistry*, **1999**, 42, 2180-2190.
- [15] Revesz L., Blum E., Di Padova F. E., Buhl T., Feifel R., Gram H., Rucklin G., *Bioorganic & Medicinal Chemistry Letters*, **2004**, 14, 3595-3599.
- [16] Mader M., de Dios A., Shih C., Bonjouklian R., Li T., White W., Anderson B. D., *Bioorganic & Medicinal Chemistry Letters*, **2008**, 18, 179-183.

- [17] Newman M. J., Rodarte J. C., Benbatoul K. D., Romano S. J., Zhang C. Z., Krane S., Mayer L. D., *Cancer Research*, **2000**, 60, 2964-2972.
- [18] Sarshar S., Zhang C. Z., Moran E. J., Krane S., Rodarte J. C., Benbatoul K. D., Mjalli A. M. M., *Bioorganic & Medicinal Chemistry Letters*, **2000**, 10, 2599-2601.
- [19] Zhang C. Z., Sarshar S., Moran E. J., Krane S., Rodarte J. C., Benbatoul K. D., Mjalli A. M. M., *Bioorganic & Medicinal Chemistry Letters*, **2000**, 10, 2603-2605.
- [20] Deprez P., Mandine E., Vermond A., Lesuisse D., *Bioorganic & Medicinal Chemistry Letters*, **2002**, 12, 1287-1289.
- [21] Wang L., Woods K. W., Li Q., Barr K. J., McCroskey R. W., Hannick S. M., Sham H. L., *Journal of Medicinal Chemistry*, **2002**, 45, 1697-1711.
- [22] Sharma V. M. G., Ramesh A., Singh A., Srikanth G., Jayaram V., Divya D., Malhotra S. V., *Medicinal Chemical Communications*, **2014**, 5, 1751-1760.
- [23] Weinstein D. S., Liu W., Ngu K., Langevine C., Combs D. W., Zhuang S., Robl J. A., *Bioorganic & Medicinal Chemistry Letters*, **2007**, 17, 5115-5120.
- [24] Lange J. H. M., van Stuijvenberg H. H., Coolen H., Adolfs T. J. P., McCreary A. C., Keizer H. G., Kruse C. G., *Journal of Medicinal Chemistry*, **2005**, 48, 1823-1838.
- [25] Takle A. K., Brown M. J. B., Davies S., Dean D. K., Francis G., Gaiba A., Wilson D. M., *Bioorganic & Medicinal Chemistry Letters*, **2006**, 16, 378-381.

- [26] Zang H., Su Q., Mo Y., Cheng B.-W. , Jun S., *Ultrasonics Sonochemistry*, **2010**, 17, 749-751.
- [27] Chauveau E., Marestin C., Schiets F. , Mercier R., *Green Chemistry*, **2010**, 12, 1018-1022.
- [28] Shelke K. F., Sapkal S. B., Kakade G. K., Shingate B. B. , Shingare M. S., *Green Chemistry Letters and Reviews*, **2010**, 3, 27-32.
- [29] Dake S. A., Khedkar M. B., Irmale G. S., Ukalgaonkar S. J., Thorat V. V., Shintre S. A. , Pawar R. P., *Synthetic Communications*, **2012**, 42, 1509-1520.
- [30] Safari J., Khalili S. D., Rezaei M., Banitaba S. H. , Meshkani F., *Monatshefte Fur Chemie*, **2010**, 141, 1339-1345.
- [31] Hasaninejad A., Zare A., Shekouhy M. , Rad J. A., *Journal of Combinatorial Chemistry*, **2010**, 12, 844-849.
- [32] Li S., Hong M., *Journal of the American Chemical Society*, **2011**, 133, 1534-1544.
- [33] Teimouri A., Chermahini A. N., *Journal of Molecular Catalysis A-Chemical*, **2011**, 346, 39-45.
- [34] Zarnegar Z. , Safari J., *RSC Advances*, **2014**, 4, 20932-20939.
- [35] Moghanian H., Mobinikhaledi A., Deinavizadeh M., *Research on Chemical Intermediates*, **2015**, 41, 4387-4394.
- [36] Kurumurthy C., Kumar G. S., Reddy G. M., Nagender P., Rao P. S. , Narsaiah B., *Research on Chemical Intermediates*, **2012**, 38, 359-365.
- [37] Mukhopadhyay C., Tapaswi P. K. , Drew M. G. B., *Tetrahedron Letters*, **2010**, 51, 3944-3950.
- [38] Kumar D., Kommi D. N., Bollineni N., Patel A. R. , Chakraborti A. K., *Green Chemistry*, **2012**, 14, 2038-2049.

- [39] Das P. J., Das J., Ghosh M., Sultana S., *Green & Sustainable Chemistry*, **2013**, 3, 6-13.
- [40] Safari J., Gandomi-Ravandi S., Akbari Z., *Journal of Advanced Research*, **2013**, 4, 509–514.
- [41] Zolfigol A. M., Bagheri S., Moosavi-Zare A. R., Vahdat S. M., *RSC Advances*, **2015**, 5, 32933-32940.
- [42] Moosavi-Zare A. R., Abdolkarim Z., Zolfigol A. M., Shekouhy M., *RSC Advances*, **2014**, 4, 60636-60639.
- [43] Samanta S., Roy D., Khamarui D., Maiti D. K., *Chemical Communications*, **2014**, 50, 2477-2479.
- [44] Zarnegar Z., Safari J., *New Journal of Chemistry*, **2014**, 38, 4555-4558.
- [45] Esmaeilpour M., Javidi J., Zandia M., *New Journal of Chemistry*, **2015**, 39, 3388-3391.
- [46] Kannan V., Sreekumar K., *Journal of Molecular Catalysis A-Chemical*, **2013**, 376, 34-39.
- [47] Kulsum K., Zeba N. S., *Industrial Engineering Chemistry Research*, **2015**, 54, 6611–6618.
- [48] Boominathan S. S. K., Chen C. Y., Huang P. J., Hou R. J., Wang J. J., *New Journal of Chemistry*, **2015**, 39, 6714-6717.
- [49] Zarnegar Z., Safari J., *New Journal of Chemistry*, **2014**, 38, 4555-4565.
- [50] Balalaie S., Arabanian A., *Green Chemistry*, **2000**, 2, 274-276.
- [51] Balalaie S., Hashemi M. M. , Akhbari M., *Tetrahedron Letters*, **2003**, 44, 1709-1711.

- [52] Karimi A. R., Alimohammadi Z., Azizian J., Mohammadi A. A., Mohammadizadeh M. R., *Catalysis Communications*, **2006**, 7, 728-732.
- [53] Kantevari S., Vuppalapati S. V. N., Biradar D. O., Nagarapu L., *Journal of Molecular Catalysis A-Chemical*, **2007**, 266, 109-113.
- [54] Sadeghi B., Mirjalili B. B. F., Hashemi M. M., *Tetrahedron Letters*, **2008**, 49, 2575-2577.
- [55] Sangshetti J. N., Kokare N. D., Kotharkar S. A., Shinde D. B., *Chinese Chemical Letters*, **2008**, 19, 762-766.
- [56] Heravi M. M., Derikvand F., Bamoharram F. F., *Journal of Molecular Catalysis A-Chemical*, **2007**, 263, 112-114.
- [57] Heravi M. M., Derikvand F., Haghghi M., *Monatshefte Fur Chemie*, **2008**, 139, 31-33.
- [58] Das Sharma S., Hazarika P., Konwar D., *Tetrahedron Letters*, **2008**, 49, 2216-2220.
- [59] Zhang C. Z., Moran E. J., Woiwode T. F., Short K. M., Mjalli A. M. M., *Tetrahedron Letters*, **1996**, 37, 751-754.
- [60] Claiborne C. F., Liverton N. J., Nguyen K. T., *Tetrahedron Letters*, **1998**, 39, 8939-8942.
- [61] Donohoe T. J., Kabeshov M. A., Rathi A. H., Smith I. E. D., *Organic & Biomolecular Chemistry*, **2012**, 10, 1093-1101.
- [62] Hu B., Wang Z., Ai N., Zheng J., Liu X.-H., Shan S., Wang Z., *Organic Letters*, **2011**, 13, 6362-6365.
- [63] Hu B., Ai N., Wang Z., Xu X., Lia X., *ARKIVOK*, **2012**, (VI), 222-228.

- [64] Frantz D. E., Morency L., Soheili A., Murry J. A., Grabowski E. J. J., Tillyer R. D., *Organic Letters*, **2004**, 6, 843-846.
- [65] Lantos I., Zhang W-Y., Shui X., Eggleston D. S., *The Journal of Organic Chemistry*, **1993**, 58, 7092-7095.
- [66] Lipshutz B. H., Morey M. C., *The Journal of Organic Chemistry*, **1983**, 48, 3745-3750
- [67] Consonni R., Croce P. D., Ferraccioli R., Rosa C. L., *Journal of Chemical Research (Synopses)*, **1991**, 7, 188-189.
- [68] Evans D. A., Lundy K. M., *Journal of the American Chemical Society*, **1992**, 114, 1495-1496.
- [69] Schneiders P., Heinze J., Baumgartel H., *Chemische Berichte*, **1973**, 106, 2415-2417.
- [70] Nagarapu L., Apuri S., Kantevari S., *Journal of Molecular Catalysis A-Chemical*, **2007**, 266, 104-108.
- [71] Kidwai M., Mothsra P., Bansal V., Somvanshi R. K., Ethayathulla A. S., Dey S., Singh T. P., *Journal of Molecular Catalysis A-Chemical*, **2007**, 265, 177-182.
- [72] Usyatinsky A. Y., Khmelnsky Y. L., *Tetrahedron Letters*, **2000**, 41, 5031-5034.
- [73] Kidwai M., Mothsra P., *Tetrahedron Letters*, **2006**, 47, 5029-5031.
- [74] Murthy S. N., Madhav B., Nageswar Y. V. D., *Tetrahedron Letters*, **2010**, 51, 5252-5257.
- [75] Montazeri N., Pourshamsian K., Khoddadi M., Kazem K., *Oriental Journal of Chemistry*, **2011**, 27, 1023-1026.

- [76] Mirjalili B. F., Bamoniri A. H., Zamani L., *Scientia Iranica*, **2012**, 19, 565-568.
- [77] Niknam K., Deris A., Naeimi F., Majleci F., *Tetrahedron Letters*, **2011**, 52, 4642-4645.
- [78] Manafi M. R., Manafi P., Kalaei M. R., *E-Journal of Chemistry*, **2012**, 9, 1773-1777.
- [79] Shaterian H. R., Ranjbar M., *Journal of Molecular Liquids*, **2011**, 160, 40-49.
- [80] Thakurta S., Roy P., Rosair G., Gomez-Garcia C. J., Garribba E., Mitra S., *Polyhedron*, **2009**, 28, 695-702.
- [81] Singh V. P., *Spectrochimica Acta Part A*, **2008**, 71, 17-22.

Chapter-5

COMPLEXATION OF DENDRIGRAFT POLYMER EG-G2 WITH PALLADIUM AND SYNTHESIS OF BENZOXAZOLE DERIVATIVES

Abstract

The palladium complex of dendrigraft polymer having ethylene glycol initiated polyepichlorohydrin as core was synthesized and characterized. Physicochemical characterization techniques like ICP-AES, SEM, EDX, UV-Vis-DRS, FT-IR, XRD, TG-DTG and XPS were used to characterize the palladium complex. Palladium complexes of G0, G1 and G2-EG-G2 were all found to be excellent catalysts for benzoxazole synthesis via the reaction between o-aminophenol and aldehydes. A detailed study of the synthesis of benzoxazole derivatives was done with EG-G2 palladium catalyst.

5.1 Introduction

5.1.1 Benzoxazole Synthesis

Benzoxazoles are important because of their occurrence in a number of natural products and their potential use in medicinal chemistry.^{1,2} Specifically, substituted benzoxazoles have drawn significant attention due to their biological activity and diverse medicinal uses such as gram-positive antibacterial agents,^{3,4} antibiotics,⁵ antiparasitic,⁶ anti-inflammatory,⁷ antimicrobial,⁸⁻¹⁰ anti-viral,¹¹ and anticancer agents.^{12,13} Benzoxazole

derivatives are well-known kind of heterocycles that have considerable importance in the field of materials chemistry, in particular, due to their fluorescence properties. The electronic states and related behaviour are mainly attributed to the planarity and rigidity of the delocalized electronic system. Taking advantage of this distinctive attribute, several groups have used these types of compounds in a number of different applications, such as electronic devices,¹⁴ sensors for metals,¹⁵ as well as their use as photoluminescent dyes,¹⁶ photochromatic agents¹⁷ and laser dyes.¹⁸ The benzoxazole ring system is a feature of several biological/ medicinal/ agrochemical active compounds (Fig 5.1).

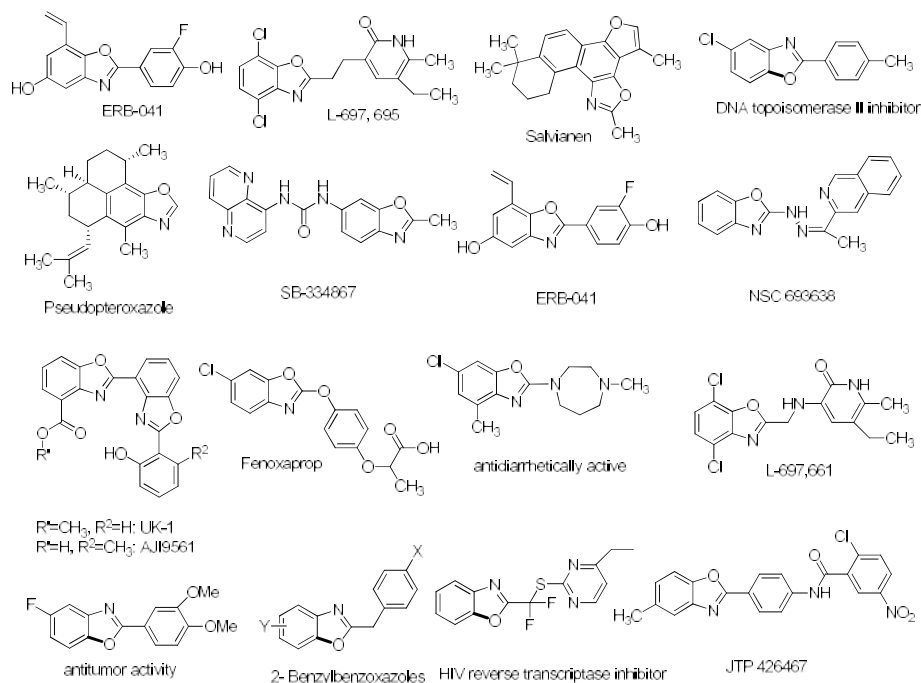
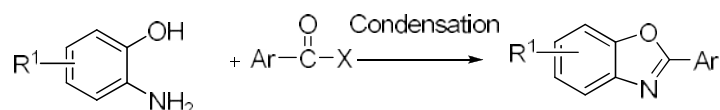


Fig 5.1 Bioactive compounds having benzoxazole scaffold¹⁻¹²

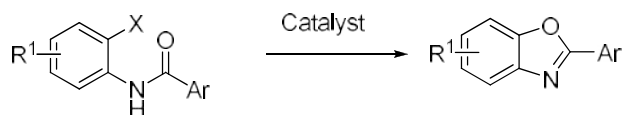
5.1.1.1 Methods of Synthesis

The classic methods to prepare benzoxazoles are mainly based on the condensation of 2-aminophenols with carbonyl-containing substrates in the presence of strong acids or oxidants (Scheme 5.1).¹⁹⁻²⁵



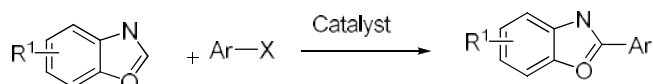
Scheme 5.1

The metal-catalyzed cyclization of o-haloanilides afforded an alternative procedure for the facile synthesis of aryl-substituted benzoxazoles.²⁶⁻³¹ Simple N-arylbenzamides were successfully employed for this kind of reaction via transition-metal-catalyzed tandem C–H functionalization/ C–O bond formation.^{28,32-36} They have also been synthesized via direct base mediated intramolecular C–O bond formation of o-haloanilides under transition metal free conditions (Scheme 5.2).^{37,38}



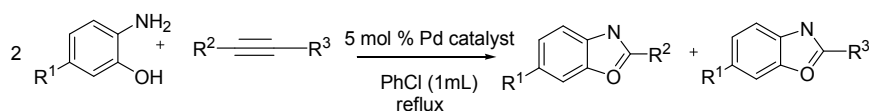
Scheme 5.2

The direct arylation of benzoxazole C–H bonds has stimulated considerable interest. Various 2-aryl-substituted benzoxazoles were synthesized from benzoxazoles and aryl halides³⁹⁻⁴⁴ as well as other coupling partners.⁴⁵⁻⁵² Under oxidative reaction conditions, simple arenes were able to couple with benzoxazoles via transition-metal catalyzed double C–H activation (Scheme 5.3).⁵³⁻⁵⁸



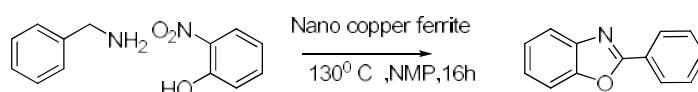
Scheme 5.3

The palladium catalyzed cleavage of C–C triple bonds in the presence of o-aminophenol is another approach for the synthesis of benzoxazoles (Scheme 5.4).⁵⁹



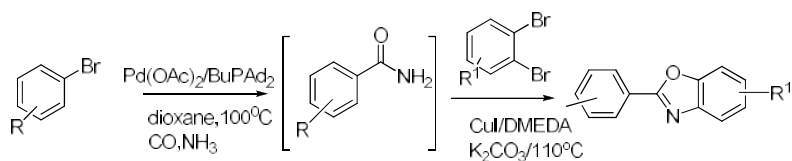
Scheme 5.4

A new, green and sustainable approach for the synthesis of 2-substituted benzoxazole using a one pot redox cascade condensation reaction of benzyl amine and 2-nitrophenol, catalysed by Cu Ferrite NPs was reported.⁶⁰ Cu Ferrite NPs are magnetically separable, air stable and can be recycled up to fifth cycle without a significant loss in catalytic activity (Scheme 5.5).



Scheme 5.5

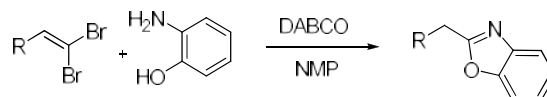
Starting from aryl bromides and 1,2-dibromobenzenes, palladium-catalyzed aminocarbonylation and subsequent copper catalyzed coupling reaction gave a variety of substituted benzoxazoles in moderate to good yields (Scheme 5.6).⁶¹



Scheme 5.6

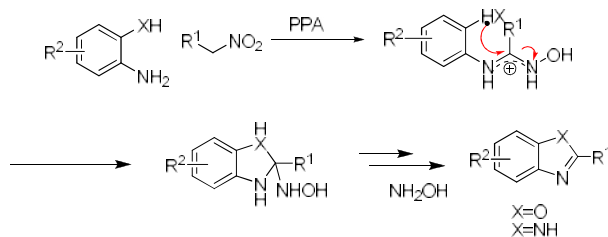
Direct coupling of 1,1-dibromoethenes with 2-aminophenols was achieved to form the corresponding benzoxazoles under mildly basic reaction conditions.⁶² Even though 1,1-dibromoethenes have to be

derived from aryl carboxaldehydes or glyoxalate for the reaction, this method still provides a new route to the preparation of benzoxazoles, complementing to existing synthetic strategies (Scheme 5.7).



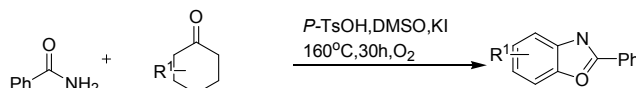
Scheme 5.7

PPA-induced umpolung triggers efficient nucleophilic addition of unactivated anilines to nitroalkanes to produce N-hydroxyimidamides. The latter undergo sequential acid-promoted cyclocondensation with ortho-OH moieties to afford benzoxazoles (Scheme 5.8).⁶³



Scheme 5.8

A transition-metal-free method for the synthesis of 2-arylbenzoxazoles from readily available cyclohexanones and benzamides was reported recently.⁶⁴ The combined use of KI, p-TsOH and DMSO significantly improved the reaction yields. Cyclohexanones were smoothly dehydrogenated and acted as the aryl source using oxygen as the oxidant (Scheme 5.9).



Scheme 5.9

Other metal complexes like Ruthenium (II),^{65,66} Pd(II)⁵⁹ complexes, gold nanoparticles supported on titanium dioxide,⁶⁷ titanium,⁶⁸ and cobalt⁶⁹

catalysts have also been employed in recent times to afford benzoxazoles. But these protocols suffer from drawbacks, such as homogeneous condition, higher temperatures, and longer reaction times. Therefore, there is a scope for the improvement in the synthetic strategy, particularly towards the reduction of the reaction time using reusable dendritic catalyst.

5.1.1.2 Comparison of Performance

In the last decade, use of various catalytic systems has been established for the synthesis of benzoxazole derivatives via the reaction between aldehydes and o-aminophenol. The various catalytic systems such as ZnO-NPs (10 mg, EtOH, RT, 2-8 min, 90-99%),⁷⁰ Pd(OAc)₂ (Cs₂CO₃, DMF, O₂, 70-88%),⁷¹ CeO₂ NP (10 mol%, H₂O, RT, 20-40 min, 58-97%),⁷² IBX (EtOAc, 80°C, 12 h, 73-98%),⁷³ Cu NP/SiO₂ (10 mol %; methanol, RT, 4-8 h, 72-86 %),⁷⁴ Cu NP (K₂CO₃, MeOH, 3-5 h, 80-100°C),⁷⁵ Pd₂(dba)₃/xantphos (Toluene; 110 °C/TFA, 8-13 h, 67-85%),⁷⁶ PTSA (10 mol %; water, 70°C, 1-5 h, 60-97%),⁷⁷ NaCN (10 mol %; DMF, air, RT, 8-12 h, 71%)⁷⁸ were used.

5.1.2 Dendritic Complexes

Metal complexes of dendritic chelating agents have attracted the attention of many research groups not only because of the potential applications they offer, but also due to the complex structure they possess. Although palladium can exist in a number of different oxidation states, useful organic methods are dominated by the use of Pd(0) and Pd(II),^{79,80} although the utility of Pd(IV)⁸¹ has been steadily emerging in its own right. The increased stability of the even-numbered oxidation states (e.g., 0, +2, +4) can be rationalized by the low tendency of palladium to undergo one-

electron or radical processes; conversely, it readily participates in two-electron oxidation or reduction.⁸⁰ The ability of palladium to undergo facile and reversible two-electron processes has contributed to its widespread use as a catalyst, since each oxidation state can yield different chemistry. In the present work, we have tried to develop palladium complexes of dendrigraft polymer having ethylene glycol initiated polyepichlorohydrin as core, EG-Gn-Pd in order to check the efficiency of the developed palladium catalyst for organic reactions. (Fig 5.2)

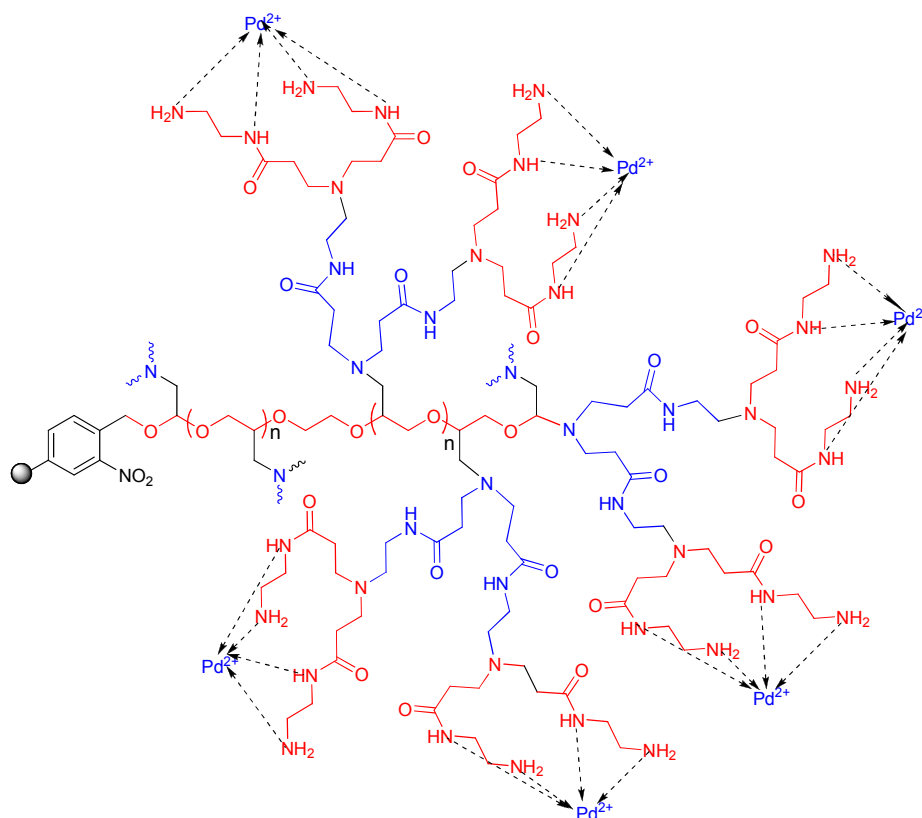


Fig 5.2 Merrifield resin supported dendrigraft EG-G2-Pd catalyst having ethylene glycol initiated PECH as core

5.1.3 Objective of the Present Work

The high yield of benzimidazole derivatives obtained using GLR-G2-Cu catalyst, prompted us to try the synthesis of its analogue, benzoxazoles. Most of the reported procedures for benzoxazole synthesis have used copper or other metal catalysts. Dendritic palladium catalysts are reported by Sreekumar⁸² and Portnoy⁸³ independently for coupling reactions like Heck, Suzuki etc. Reports on palladium catalysed benzoxazole synthesis are only few.^{59,71} They were non dendritic, and homogeneous, even though, they showed high efficiency. So we have tried to synthesize benzoxazole derivatives using dendritic palladium catalyst by adopting the combined benefits of both heterogeneous and dendritic behaviour.

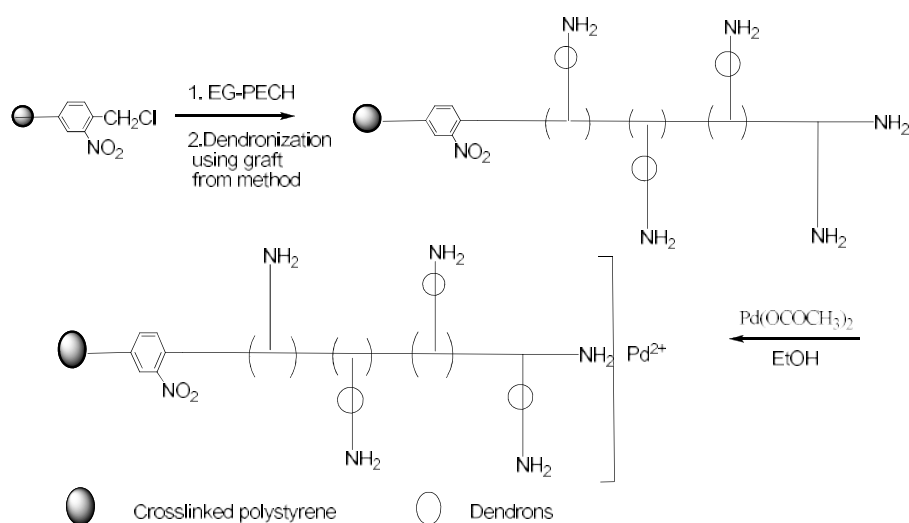
The present chapter deals with the synthesis and characterization of EG-G_n-Pd, palladium complexed dendrigraft polymer having ethylene glycol initiated polyepichlorohydrin as core. The catalyst was employed for the synthesis of benzoxazole derivatives via the reaction between *o*-aminophenol and aldehyde. The experimental parameters were optimized, scope of substrates and reusability of the catalyst were investigated. The mechanism of the reaction is also proposed in this chapter. Finally, we compare the other series of palladium dendrigraft polymers, GLR-G2-Pd and PEN-G2-Pd towards the synthesis of benzoxazole derivatives.

5.2 Results & Discussion

5.2.1 Synthesis of Palladium Complex of Dendrigraft Polymer having Ethylene Glycol initiated PECH as Core

The synthesis of G_n dendrigraft polymer having ethylene glycol initiated polyepichlorohydrin as core (EG-G_n) was reported in chapter 2.

The amino group loading of G_0 , G_1 and G_2 dendrigraft polymer was found to be 10.49, 18.06 and 24.96 mmols g^{-1} respectively (Table 5.1). The palladium complex of each of the EG- G_n polymer was synthesized by adopting the schematic procedure (Scheme 5.10).



Scheme 5.10. Merrifield resin supported dendrigraft EG- G_2 -Pd having ethylene glycol initiated PECH as core.

For the complexation of dendrigraft polymer with palladium, the palladium salt and solvent was optimized. It was found that palladium acetate in ethanol at room temperature was found to be the best condition for the complexation of palladium with EG- G_n dendritic polymer. In comparison with copper, 24 h and room temperature condition was enough for maximum complexation. The palladium coordinated dendritic polymer appeared as black powder.

5.2.2 Catalyst Characterization

The synthesized catalyst was characterized with different techniques which are discussed.

5.2.2.1 ICP-AES Analysis

The palladium loading for EG-G0-Pd, EG-G1-Pd and EG-G2-Pd, based on ICP-AES analysis and confirmed by EDX analysis, were found to be 35.41, 44.23 and 56.85 % of the polymer, respectively and the results are given in Table 5.1. It is therefore assumed that average of 2.34 ligands was bound to Pd moieties in EG-G2 complex. The peak for ester was not present in the IR spectrum indicating that acetate ion was not included in the co-ordination sphere.

Table 5.1 Analytical data for EG-Gn and EG-Gn-Pd

Polymer	Amine capacity (mmols/g)	Palladium loading (%) (ICP-AES)	Palladium loading (mmols/g)	Palladium loading (%) (EDX)
EG-G0-(Pd)	10.49	35.41	3.33	31.51
EG-G1-(Pd)	18.06	44.23	4.16	38.56
EG-G2-(Pd)	24.96	56.85	5.34	49.45

The room temperature magnetic moments of the palladium (II) complexes was approximately equal to zero, which is very close to the spin only value for Pd d^8 . The Pd complexes were diamagnetic in nature, as was evident from the magnetic susceptibility measurements, which was consistent with the presence of Pd centers in their +2 oxidation states. The geometry around the metal ion is suggested as square planar.

5.2.2.2 SEM & Energy Dispersive X-ray (EDX) Analysis

The Scanning Electron Micrograph of the Pd complex shows small clusters and appear to be in the minimum surface area compared with copper complexes. The micrographs also revealed that palladium complexes have less compactness and metallic lusture as compared with the copper complexes (Fig 5.3).

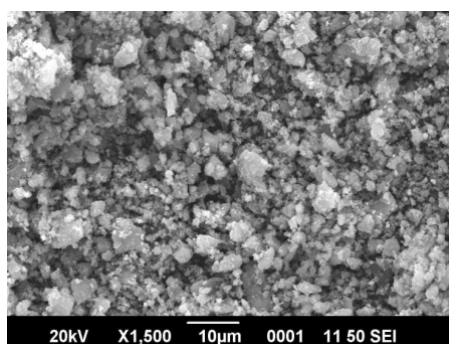


Fig 5.3 Scanning electron micrograph of EG-G2-Pd

EDX spectra clearly showed Pd, C, N and O as the constituents of the catalyst. The results presented in Table 1 are the average of the data from the scanned regions. The data obtained on the composition of the compounds from the energy dispersive X-ray spectroscopy, were consistent with the elemental analysis values (Table 5.1).

5.2.2.3 IR Spectral Studies

The IR spectra showed characteristic differences between the spectral pattern originating from the dendrigraft–palladium complexes and the spectra of the dendrigraft polymer. The IR spectra are presented in Fig 5.4. In the FTIR spectra of this complex, both the amide carbonyl band and primary amino group bands underwent a shift from their original values. The

stretching and bending bands due to primary amino groups underwent a negative shift from 3474 cm^{-1} to 3444 cm^{-1} and 1380 cm^{-1} to 1378 cm^{-1} . The carbonyl stretching band of the amide underwent a shift from 1666 cm^{-1} to 1624 cm^{-1} to lower frequency region. The vibration due to NH (bend) was shifted towards higher frequency region from 1551 to 1572 cm^{-1} .

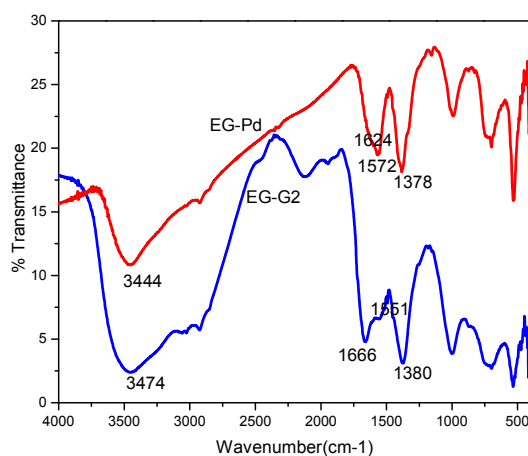


Fig 5.4 IR spectra of EG-G2 and EG-G2-Pd

This suggests that, primary amino groups and amide groups of the polymer play a role in the complex formation with palladium. The absence of ester peak in the IR spectra rules out the presence of acetate ion of palladium acetate after complexation.

5.2.2.4 Electronic Spectral Studies (UV-Vis DRS)

The diffuse reflectance UV-Vis spectra of EG-G2-Pd (Fig 5.5) displayed a broad peak in the region of 257 nm and 850 nm. The absorption corresponding to 257 nm is due to the charge transfer transition from N to vacant d orbital of Pd bands and the absorption at 850 nm is due to overlapping of allowed d-d transitions in palladium after coordination with dendritic ligands.

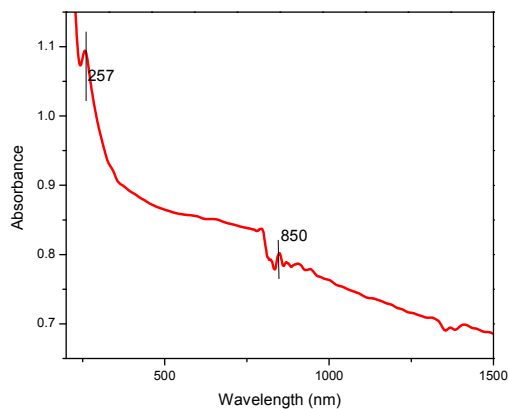


Fig 5.5 UV-Vis-DRS spectrum of EG-G2-Pd

5.2.2.5 X-ray Diffraction Studies

From the XRD spectrum, after complexation the peak at 2 theta value of 31 gets narrowed which shows the polymer became more crystalline and the peak at 11.3, 19.8, and 23.2 got disappeared and peaks at 2 theta value of 63 and 64 got reduced in intensity. The disappearance of peak and reduction in intensity revealed that orderness of the plane got reduced.

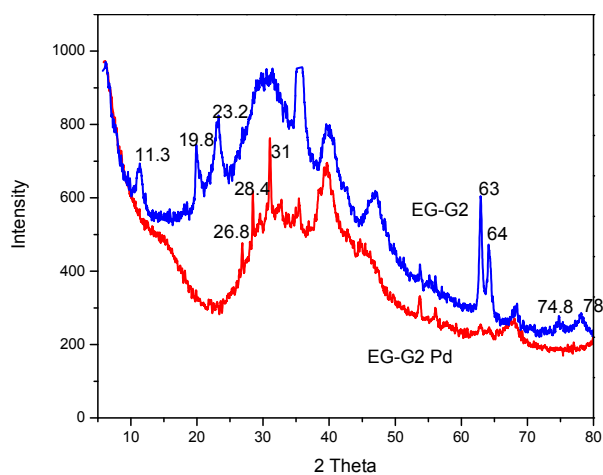


Fig 5.6 X-ray diffraction (XRD) pattern of EG-G2 and EG-G2-Pd

5.2.2.6 X-ray Photoelectron Spectroscopy

XPS wide spectrum shows binding energy corresponding to carbon, oxygen, nitrogen and palladium. The XPS deconvoluted spectrum shows binding energy value corresponding to palladium Pd(5/2) at 335.2. This value is lower than the expected binding energy (337) of Pd⁺² state. The lowering of binding energy value is due to the effect of neighbouring nitrogen ligand coordinated to palladium metal. Thus the incorporation of palladium in supported dendritic polymer has been confirmed from the results of XPS analysis.

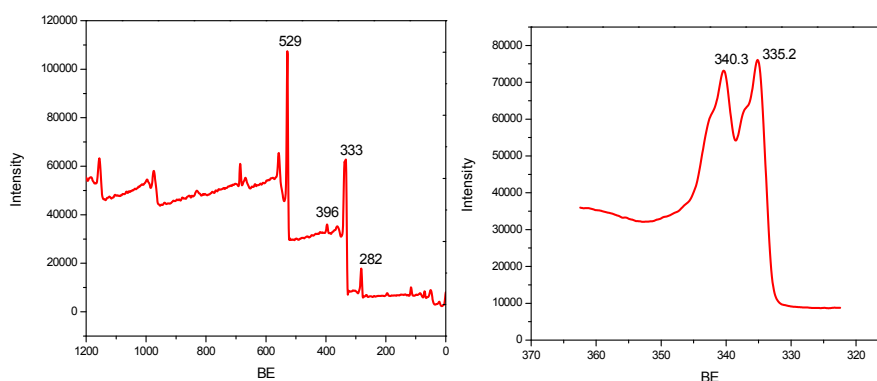


Fig 5.7 XPS spectra of EG-G2-Pd (a) wide (b) deconvoluted

5.2.2.7 TG-DTG Analysis

Evaluation of the thermogravimetric data of the EG-G2 functionalized resins and the corresponding Pd loaded dendrigraft polymer was performed. Considerable extent of decomposition was observed in the thermogram of both EG-G2 and EG-G2-Pd at the temperature 412.9 and 386.8 °C owing to the degradation of the polymeric backbone (Fig 5.8).

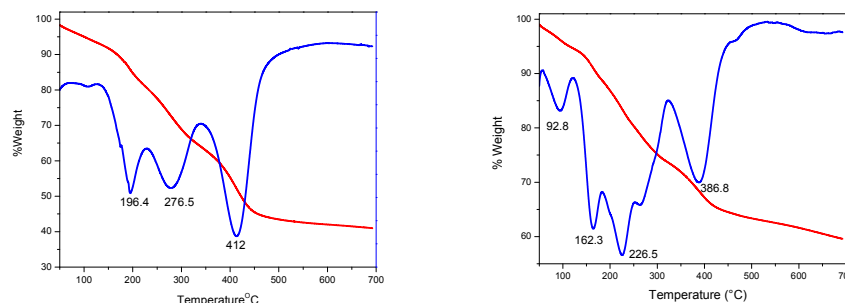


Fig 5.8 TG-DTG plot of (a) EG-G2 and (b) EG-G2-Pd

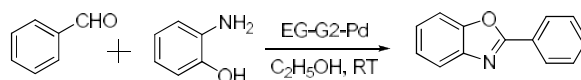
In EG-G2-Pd polymer, the first step of the decomposition is attributable to the loss of non-coordinated water, occurring at a temperature range of 92.8 °C. By analogy with the thermal decomposition characteristics of EG-G2 having decomposition with a weight loss of 17.3 % and 14.9 % occurring in the temperature of 160-220 °C and 230-320 °C respectively, EG-G2-Pd, shows decomposition step with a weight loss of 24% occurring at the temperature range of 120–320 °C.

5.2.3 Catalytic Activity of Resin Supported Dendrigrraft EG-Gn-Pd Complex

5.2.3.1 Synthesis of Benzoxazole Derivatives

In a survey of catalytic activity, dendrigrraft EG-Gn palladium complexes were employed in the synthesis of benzoxazole derivatives. A variety of benzoxazole derivatives has been synthesized in excellent yields from aromatic aldehyde (Scheme 5.11). In order to optimize the reaction conditions, the effect of various reaction parameters, such as type of solvent, reaction temperature, substrate ratio, catalyst concentration, etc., were evaluated by using benzaldehyde and o-aminophenol as model substrates and EG-G2-Pd as the catalyst. Different solvent systems such as

water, toluene, methanol, ethanol, acetonitrile and DMF were screened as solvents for the reaction.



Scheme 5.11 Synthesis of benzoxazole

The nature of solvent was observed to have a profound effect on the activity of the catalyst and the product selectivity of the reaction. The reactions were performed at ambient temperature under magnetic stirring. From the results presented in Table 5.2 & 5.3, it was evident that the reaction conducted in the molar ratio of *o*-aminophenol: benzaldehyde of 1:1 in ethanol at room temperature proceeded smoothly to selectively yield 2-phenylbenzo[d]oxazole as the exclusive product.

Table 5.2 Optimization of solvent

Solvent	Yield (%) ^a
DMF	54
CH ₃ CN	54
Ethanol	88
Methanol	84
Toluene	48
Water	42

^a Reaction Conditions: *o*-aminophenol (1 mmol), benzaldehyde (1 mmol). K₂CO₃ (2 mmol). RT, 8h, EG-G2-Pd:10 mg.

Most of the palladium catalysts are active at high temperature. So we have tried to find out the optimized temperature condition for benzoxazole synthesis. It was found that the reaction at temperature of about 50^oC took only 3h to obtain maximum yield.

Table 5.3 Optimization of temperature

Temperature (°C)	Time (h)	Yield (%)
30	8	87
50	3	88
80	3	88
^a Reaction Conditions: <i>o</i> -aminophenol (1 mmol), benzaldehyde (1 mmol), K ₂ CO ₃ (2 mmol). Ethanol, EG-G2-Pd: 10 mg.		

Increasing the temperature from 50 °C to 80 °C shows no noticeable increase in yield. But it was interesting that the reaction at room temperature also gave good yield even though it took 8 h time.

Increasing the catalyst amount increases the yield of the reaction from 60% (with 2.7 mol % catalyst) to 88% (with 5.4 mol% catalyst). Out of the different solvents tried, ethanol was found to be the solvent of choice. Thus, in order to attain high conversion, the substrate molar ratio of benzaldehyde and *o*-aminophenol was selected as 1:1 and 10 mg catalyst (5.4 mol%) in ethanol at 50°C in the presence of air have been found to be the optimum.

Table 5.4 Optimization of amount of catalyst

Amount of catalyst (mg)	Amount of catalyst (mol%)	Yield(%) ^a
5	2.7	60
10	5.4	88
15	8.0	88
20	10.7	88
^a Reaction Conditions: <i>o</i> -aminophenol (1 mmol), benzaldehyde (1 mmol). K ₂ CO ₃ (2 mmol), 50 °C, Ethanol, 3h.		

Further, we have studied the effect of generation of the catalyst on benzoxazole synthesis (Table 5.4). G0, G1 and G2 dendrigraft palladium catalyst showed 80, 85 and 88% yield respectively. Therefore, all generations of EG-Gn-Pd are active catalysts towards the synthesis of benzoxazole derivatives. The negative dendritic effect was not pronounced in the present case and usual concept of slow reaction of supported catalysts was also not observed.

Table 5.5 Effect of generation of the catalyst on the synthesis of benzoxazole derivatives^a

Polymer	%Yield
EG-G0-Pd	80
EG-G1-Pd	85
EG-G2-Pd	88

^a Reaction Conditions: o-aminophenol (1 mmol), benzaldehyde (1 mmol), K₂CO₃ (2 mmol), 50 °C, Ethanol, EG-Gn-Pd: 10 mg, 3h. The yield was determined by GC.

Comparison of EG-G2-Pd catalyst with other series such as GLR-G2-Pd and PEN-G2-Pd showed that EG-G2-Pd was more suitable in terms of time of the reaction while, PEN-G2-Pd was the best choice in terms of yield of the product (Table 5.6). This may be due to the simple orientation of EG-G2-Pd in comparison with GLR-G2-Pd and PEN-G2-Pd, which facilitate the palladium assisted cyclisation with the imine bond. After optimizing the reaction conditions, scope of different substrates was examined (Table 5.7). Most of the reactions of o-aminophenol with aromatic aldehydes resulted in good yields, irrespective of whether an electron-withdrawing or an electron-donating group was present. The vital role of the catalyst, leading to the formation of the desired product, was confirmed by conducting a blank experiment without the catalyst.

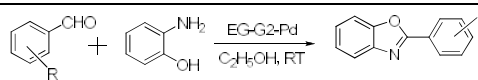
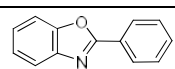
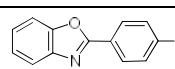
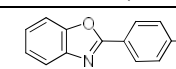
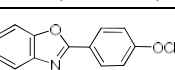
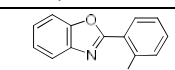
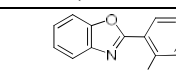
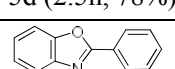
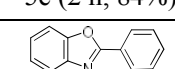
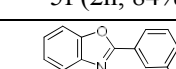
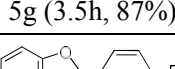
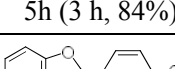
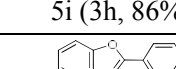
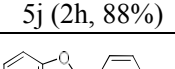
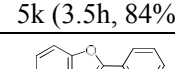
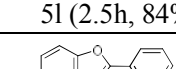
Table 5.6 Effect of different dendritic core

Polymer	Pd loading (%) (ICP-AES)	% Yield
EG-G2-Pd	56.85	88
GLR-G2-Pd	62.45	85
PEN-G2-Pd	58.72	84

^a Reaction Conditions: o-aminophenol (1 mmol), benzaldehyde (1 mmol), K₂CO₃ (2 mmol). 50 °C, Ethanol, Catalyst: 10 mg, 3h, Isolated yield.

In the absence of the catalyst, the reaction was sluggish and there was no evidence for product formation. Results show that dendritic effect enhances the catalytic behaviour to a large extent.

Table 5.7 Synthesis of benzoxazole derivatives^a

		
5a-5o (time, yield)		
 5a (3h, 88%)	 5b (3.5h, 86%)	 5c (3.5h, 84%)
 5d (2.5h, 78%)	 5e (2 h, 84%)	 5f (2h, 84%)
 5g (3.5h, 87%)	 5h (3 h, 84%)	 5i (3h, 86%)
 5j (2h, 88%)	 5k (3.5h, 84%)	 5l (2.5h, 84%)
 5m (2h, 80%)	 5n (3h, 74%)	 5o (3h, 81%)

^a Reaction Conditions: o-aminophenol (1mmol), aldehyde (1mmol), K₂CO₃ (2 mmol), 50 °C, Ethanol, EG-G2-Pd: 10mg, Isolated yield.

5.2.3.2 Recyclability of the Catalyst

After completion of the reaction, the solution was filtered, washed with ethyl acetate (3 -10 mL), acetone and dried at room temperature. The catalyst recovered was weighed and reused. Details regarding catalyst recovery with percentage yield and the corresponding bar diagram are depicted in Table 5.8 and Fig 5.9. Successive runs were carried out in order to see the recyclability of the catalyst. After fifth cycle, 42% of product yield was obtained with a catalyst recovery of 94.3 %.

Table 5.8 Recycling of EG-G2-Pd catalyst^a

No.of Cycles	Catalyst weight (mg)	Catalyst recovered (mg)	Recovery (%)	Product yield ^a (%)
1	10	9.8	98.0	88
2	9.8	9.5	96.9	75
3	9.5	9.3	97.8	62
4	9.3	8.9	95.6	55
5	8.9	8.4	94.3	42

^a Reaction Conditions: o-aminophenol (1 mmol), benzaldehyde (1 mmol). K₂CO₃ (2 mmol), 50 °C, Ethanol, EG-G2-Pd: 10 mg, 3h. The yield was determined by GC.

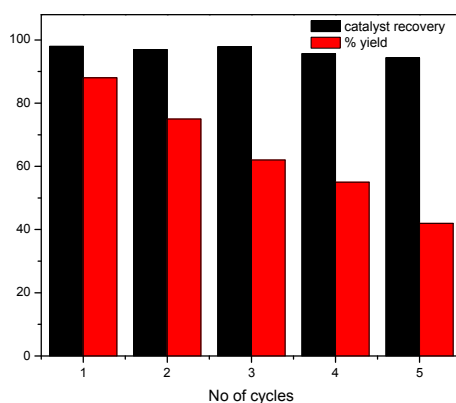
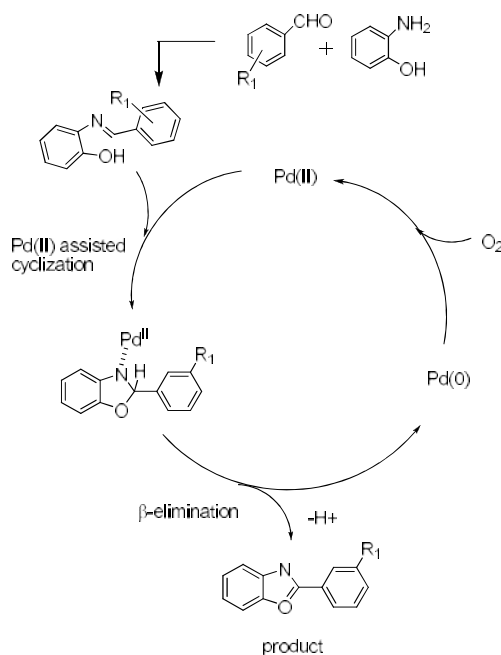


Fig 5.9 Bar diagram showing recycling of EG-G2-Pd catalyst^a

5.2.3.3 The Proposed Mechanism

Organopalladium intermediates are of primary importance in synthetic reactions. One of the fundamental properties of the palladium (II) is that, it interacts with the π -bonded electrons to form π -complexes that are subjected to nucleophilic attack. It is assumed that the palladium (II) can react with C=N bond to form π -complex (Scheme 5.12), which then undergoes nucleophilic attack and the subsequent β -elimination followed by aromatization to give benzoxazole.



Scheme 5.12. Possible mechanism for palladium-catalyzed reaction of o-aminophenol with aldehydes.

5.3 Conclusions

In conclusion, we have developed a dendritic palladium catalyst for the conjugation of o-aminophenol with aldehydes. The developed

palladium complexes of G0, G1 and G2 dendrigraft polymer having ethylene glycol initiated polyepichlorohydrin as core were characterized and were found to be good catalysts for the synthesis of benzoxazole derivatives *via* the reaction between o-aminophenol with aldehydes. The reaction occurred even with low generation *ie.*, EG-G0-Pd polymer. After optimizing the reaction conditions, a detailed study of the synthesis of benzoxazole derivatives was done with EG-G2 palladium catalyst. The palladium catalyst of different series such as EG-G2-Pd, GLR-G2-Pd and PEN-G2-Pd are active catalysts for the synthesis of benzoxazole. The main features of the synthesis include: air was used as the terminal oxidant, ethanol was used as the solvent, only small amount of catalyst was needed to drive the reaction and water was the only by-product in this reaction. Even though the reactions are feasible at room temperature, reactions were carried out at a slightly higher temperature, 50°C. The catalyst showed outstanding tolerance of functional groups on aldehyde. The synthetic protocols are straightforward, safe, environmentally clean, and free from halogenated solvents. Procedural simplicity and simple recovery of catalysts meet the requirements of benign chemistry. Further investigation on application of this catalyst for other organic reactions is in progress.

5.4 Experimental Section

5.4.1 Materials

Anhydrous palladium acetate, o-aminophenol and aldehydes were purchased from local vendors and were used as received. All solvents were purified by standard procedures prior to use.

5.4.2 Synthesis of palladium complex of dendrigraft EG-G2 polymer having ethylene glycol initiated polyepichlorohydrin as core

Merrifield resin supported EG-Gn polymer was allowed to swell in DMF for 2 h. A 50 mL round bottom flask was charged with 250 mg of Merrifield resin supported EG-Gn polymer having “x” mmols of amine capacity. Quantitative amount corresponding to “x” mmols of anhydrous palladium acetate in 10 mL ethanol was added to the reaction flask. The reaction mixture was stirred at room temperature for about 24 h. The polymer was filtered and washed with water. The filtrate and washings were collected together and concentrated. The concentrated solution was used for the estimation of metal ions by standard methods. The polymer-supported metal complex was washed with methanol (20 mL x 3), dioxane (20 mL x 3) and acetone (20 mL x 3) followed by drying at RT for 3 h.

5.4.3 General procedure for the synthesis of benzoxazole derivatives

A 25 mL RB flask having side inlet was charged with a magnetic stirrer and ethanol (5.0 mL). o-aminophenol (1.0 mmol), aldehyde (1.0 mmol) and catalyst EG-G2-Pd (5.4 mol%, 10 mg) were added to the flask. The mixture was stirred at 50 °C under aerated condition. The completion of the reaction was monitored by TLC. After completion of the reaction, reaction mixture was diluted with distilled water (2x10 ml) and the synthesized 2-arylbenzoxazole was extracted with ethylacetate (2x 15 ml). The organic layer was dried over anhydrous Na₂SO₄, solvent was removed by vacuum evaporation. The crude product, thus obtained

was subjected to purification by column chromatography on silica gel using hexane: ethyl acetate (5:2 v/v) as eluent to yield 2-arylbenzoxazole.

5.4.4 Test for Heterogeneity of the Reaction

With an aim to confirm that the cyclization reaction occurred *via* a heterogeneous catalytic process, and to examine whether there was any leaching of the metal complex from the polymer-bound dendrigraft catalyst, viz. EG-G2-Pd, into the reaction medium during the synthesis of benzoxazole, separate experiments were conducted under standard conditions. The filtrate obtained by separating the solid catalyst after completion of the reaction was extracted with ethyl acetate. The presence of palladium could not be detected when the filtrate, obtained after isolating the solid catalysts by filtration, was subjected to AAS analysis. The possibility of the palladium species leaching out of the catalyst can thus be ruled out on the basis of the evidence gathered, which also proves the heterogeneous nature of the catalytic process.

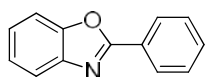
5.4.5 Regeneration and Recycling of the Catalyst

The reusability of the catalysts for subsequent catalytic cycles was examined using benzaldehyde and *o*-aminophenol as the substrate. In the oxidative cyclisation reaction, after the completion of the reaction, the solid catalyst was separated from the reaction mixture by filtration, washed with ethyl acetate, methanol and acetone. It was dried. The dried solid catalyst was weighed, oxidised and added to a fresh reaction mixture of benzaldehyde (1mmol), and *o*-aminophenol (1 mmol) and ethanol (5 mL). The progress of the reaction was monitored by thin layer

chromatography (TLC) and GCMS. The procedure for the above mentioned system was repeated for five reaction cycles.

5.5 Characterization of Products

2-Phenylbenzoxazole (5a)

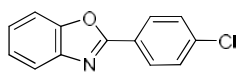


Colourless solid; m.p: 102-104°C.

$^1\text{H NMR}$ (400 MHz, CDCl_3): δ 8.27- 8.24 (m, 2H), 7.79-7.76 (m, 1H), 7.60-7.57 (m, 1H), 7.54-7.51 (m, 3H), 7.38-7.32 (m, 2H).

MS, m/z: 195.07.

2-(4-Chlorophenyl)benzoxazole (5b)

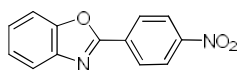


Colourless solid; mp: 143-145°C.

$^1\text{H NMR}$ (400 MHz, CDCl_3): δ 7.28-7.32 (m, 2H, Ar-H); 7.40-7.45 (m, 2H, Ar-H); 7.49-7.53 (m, 1H, Ar-H); 7.66-7.70 (m, 1H, Ar-H); 8.10-8.13 (m, 2H, Ar-H).

MS, m/z: 229.03.

2-(4-Nitrophenyl)benzoxazole (5c)

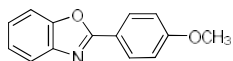


Yellow solid; mp: 262-264 °C

$^1\text{H NMR}$ (400 MHz, CDCl_3) δ : 7.75-8.11 (m, 4H, Ar-H); 8.22-8.5 (4H, m, Ar-H).

MS, m/z: 239.

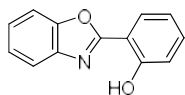
2-(4-Methoxyphenyl)benzoxazole (5d)



Off white solid; m.p: 97-99 °C.

$^1\text{H NMR}$ (400 MHz, CDCl_3): δ 8.20 (d, $J = 9.2$ Hz, 2H), 7.74-7.72 (m, 1H), 7.56-7.54 (m, 1H), 7.35-7.31 (m, 2H), 7.03 (d, $J = 9.2$ Hz, 2H), 3.89 (s, 3H).

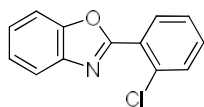
MS, m/z: 225.08.

2-(Benzoxazol-2-yl)phenol (5e)

Pink red solid; m.p: 122-124.

$^1\text{H NMR}$ (400 MHz, CDCl_3) δ 8.68 (s, 1H, OH), 7.41 (t, 2H, Ar, $J = 8.0$ Hz), 7.23–7.17 (m, 1H, Ar), 7.14 (dd, 1H, Ar, $J = 7.9, 1.4$ Hz), 7.04–6.96 (m, 4H, Ar).

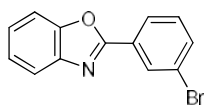
MS, m/z: 211.06.

2-(2-Chlorophenyl)benzoxazole (5f)

Light pink red solid; m.p: 70-73°C.

$^1\text{H NMR}$ (400 MHz, CDCl_3): δ 8.15 (dd, $J = 1.6, 5.6$ Hz, 1H), 7.87-7.83 (m, 1H), 7.64-7.61 (m, 1H), 7.59-7.56 (m, 1H), 7.48-7.37 (m, 4H).

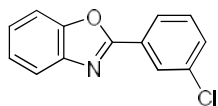
MS, m/z: 229.03.

2-(3-Bromophenyl)benzoxazole (5g)

Beige colour solid; m.p: 128-130 °C.

$^1\text{H NMR}$ (400 MHz, CDCl_3): δ 8.26 (s, 1H), 8.16-8.13 (m, 1H), 7.80-7.77 (m, 1H), 7.61-7.58 (m, 1H), 7.52-7.44 (m, 2H), 7.39- 7.37 (m, 2H).

MS, m/z: 273.

2-(3-Chlorophenyl)benzoxazole (5h)

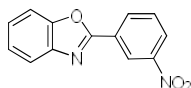
Light pink red solid; m.p: 131-133 °C.

$^1\text{H NMR}$ (400 MHz, CDCl_3): δ 8.26 (s, 1H), 8.16-8.13 (m, 1H), 7.80-7.77 (m, 1H), 7.61-7.58 (m, 1H), 7.52-7.44 (m, 2H), 7.39- 7.37 (m, 2H).

MS, m/z: 229.03

2-(3-Nitrophenyl)benzoxazole (5i)

Colorless solid; mp 184-186°C.

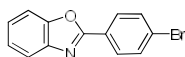


$^1\text{H NMR}$ (400 MHz, CDCl_3) δ : 7.38 (q, 1H, $J = 8.4$ Hz, Ar-H); 7.54 (d, 1H, $J = 9.1$ Hz, Ar-H); 7.72 (d, 1H, $J = 8.4$ Hz, Ar-H); 7.78 (s, 1H, Ar-H); 8.39 (d, 1H, $J = 8.8$ Hz, Ar-H); 8.55 (d, 1H, $J = 7.6$ Hz, Ar-H); 9.07 (s, 1H, Ar-H).

MS, m/z : 240.05

2-(4-Bromophenyl)benzoxazole (5j)

Pale yellow solid; mp: 142-144°C.

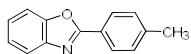


$^1\text{H NMR}$ (400 MHz, CDCl_3) δ : 7.30-7.37 (m, 2H, Ar-H); 7.50-7.55 (m, 1H, Ar-H); 7.60-7.65 (m, 2H, Ar-H); 7.70-7.75 (m, 1H, Ar-H); 8.05-8.10 (m, 2H, Ar-H).

MS, m/z : 273.

2-p-Tolylbenzoxazole (5k)

Colourless solid; m.p: 114-116°C.

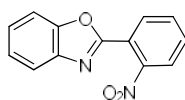


$^1\text{H NMR}$ (400 MHz, CDCl_3): δ 8.15 (d, $J = 8$ Hz, 2H), 7.77-7.75 (m, 1H), 7.58-7.56 (m, 1H), 7.35-7.32 (m, 4H), 2.44 (s, 3H).

MS, m/z : 209.08.

2-(2-Nitrophenyl)benzoxazole (5l)

Yellow solid; m.p: 101-103°C.

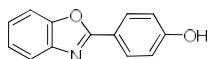


$^1\text{H NMR}$ (400MHz, CDCl_3): δ 8.15 (dd, $J = 1.6, 5.6$ Hz, 1H), 7.87-7.83 (m, 1H), 7.64-7.61 (m, 1H), 7.59-7.56 (m, 1H), 7.48-7.37 (m, 4H); MS, m/z : 229.03.

MS, m/z : 240.05

4-(Benzoxazol-2-yl)phenol (5m)

White solid; m.p: 180-182 °C.

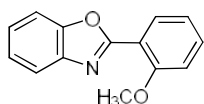


¹H NMR (400 MHz, CDCl₃) δ 8.53 (s, 1H, OH), 7.76 (d, 2H, Ar, J = 8.5 Hz), 7.69 (d, 1H, Ar, J = 8.5 Hz), 7.09 (t, 1H, Ar, J = 7.7 Hz), 6.94–6.89 (m, 3H, Ar), 6.83 (t, 1H, Ar, J = 8.3 Hz).

MS, m/z: 211.06 4.

2-(2-Methoxyphenyl)benzoxazole (5n)

Beige colour solid; m.p: 54-56 °C.

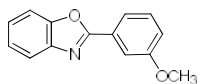


¹H NMR (400 MHz, CDCl₃): δ 8.13 (d, J = 8.8 Hz, 1H), 7.83-7.80 (m, 1H), 7.60-7.57 (m, 1H), 7.51-7.47 (m, 1H), 7.35-7.32 (m, 2H), 7.13-7.07 (m, 2H), 4.02 (s, 3H).

MS, m/z: 225.08.

2-(3-Methoxyphenyl)benzoxazole (5o)

Yellow solid; m.p: 70-73°C.



¹H NMR (400 MHz, CDCl₃) δ 8.26 (s, 1H), 8.16-8.13 (m, 1H), 7.80-7.77 (m, 1H), 7.61-7.58 (m, 1H), 7.52-7.44 (m, 2H), 7.39- 7.37 (m, 2H), 3.89(s, 3H).

MS, m/z: 225.08.

5.6 References

- [1] Das P. J., Sultana S., *Green and Sustainable Chemistry*, **2013**, 3, 6-13.
- [2] Boydston A. J., Vu P. D., Dykhno O. L., Chang V., Wyatt A. R., II, Stockett A. S., Bielawski C. W., *Journal of the American Chemical Society*, **2008**, 130, 3143-3156.
- [3] Kusumi T., Ooi T., Walchi M. R., Kakisawa H., *Journal of the American Chemical Society*, **1988**, 110, 2954–2958.

-
- [4] Suto M. J., Turner W. R., *Tetrahedron Letters*, **1995**, 36, 7213-7216.
- [5] Chaney M. O., Demarco P. V., Jones N. D., Occolowitz J. L., *Journal of the American Chemical Society*, **1974**, 96, 1932-1933.
- [6] David L., Dergomard A., *The Journal of Antibiotics*, **1982**, 35, 14-1411.
- [7] Srinivas A., Sagar J. V., Srangapani M., *Journal of Chemical and Pharmaceutical Research*, **2010**, 2, 319-322.
- [8] Alper-Hayta S., Arisoy M., Temiz-Arpaci O., Yildiz I., Aki E., Oezkan S., Kaynak F., *European Journal of Medicinal Chemistry*, **2008**, 43, 2568-2578.
- [9] Tekiner-Gulbas B., Temiz-Arpaci O., Yildiz I., Altanlar N., *European Journal of Medicinal Chemistry*, **2007**, 42, 1293-1299.
- [10] Yildiz-Oren I., Tekiner-Gulbas B., Yalcin I., Temiz-Arpaci O., Aki-Sener E., Altanlar N., *Archiv der Pharmazie*, **2004**, 337, 402-405.
- [11] Gong B. Q., Hong F., Kohm C., Bonham L., Klein P., *Bioorganic & Medicinal Chemistry Letters*, **2004**, 14, 1455-1459.
- [12] McKee M. L., Kerwin S. M., *Bioorganic & Medicinal Chemistry*, **2008**, 16, 1775-1783.
- [13] Oksuzoglu E., Temiz-Arpaci O., Tekiner-Gulbas B., Eroglu H., Sen G., Alper S., Yalcin I., *Medicinal Chemistry Research*, **2008**, 16, 1-5.
- [14] Ko C. W., Tao Y. T., Danel A., Krzeminska L., Tomasik P., *Chemistry of Materials*, **2001**, 13, 2441-2446.
- [15] Tian Y., Chen C.-Y., Yang C.-C., Young A. C., Jang S.-H., Chen W.-C., Jen A. K. Y., *Chemistry of Materials*, **2008**, 20, 1977-1987.

- [16] Kocher C., Smith P., Weder C., *Journal of Materials Chemistry*, **2002**, 12, 2620-2626.
- [17] Varga A., Aki-Sxener E., Yalcin I., Temiz-Arpaci O., Tekiner-Gulbasx B., Cherepnev G., Molnar J., *In Vivo*, **2005**, 19, 1087-1091.
- [18] Heathcock C. H., Trost B. M., Flemming I., *In Comprehensive Organic Synthesis, Eds.*, Pergamon Press, New York, **1991**, 2, 181-231.
- [19] Riadi Y., Mamouni R., Azzalou R., El Haddad M., Routier S., Guillaumet G., Lazar S., *Tetrahedron Letters*, **2011**, 52, 3492-3495.
- [20] Bose D. S., Idrees M., *Synthesis-Stuttgart*, **2010**, 398-402.
- [21] Wen X., El Bakali J., Deprez-Poulain R., Deprez B., *Tetrahedron Letters*, **2012**, 53, 2440-2443.
- [22] Zhao S., Chen Y., Song Y.-F., *Applied Catalysis A-General*, **2014**, 475, 140-146.
- [23] Endo Y., Backvall J. E., *Chemistry - A European Journal*, **2012**, 18, 13609-13613.
- [24] Yu Z., Ma L., Yu W., *Synlett*, **2012**, 1534-1540.
- [25] Kalkhambkar R. G., Laali K. K., *Tetrahedron Letters*, **2012**, 53, 4212-4215.
- [26] Itoh T., Mase T., *Organic Letters*, **2007**, 9, 3687-3689.
- [27] Zou B., Yuan Q., Ma D., *Angewandte Chemie-International Edition*, **2007**, 46, 2598-2601.
- [28] Bonnamour J., Bolm C., *Organic Letters*, **2008**, 10, 2665-2667.
- [29] Viirre R. D., Evindar G., Batey R. A., *Journal of Organic Chemistry*, **2008**, 73, 3452-3459.

- [30] Ma D., Xie S., Xue P., Zhang X., Dong J., Jiang Y., *Angewandte Chemie-International Edition*, **2009**, 48, 4222-4225.
- [31] Wang H., Wang L., Shang J., Li X., Wang H., Gui J., Lei A., *Chemical Communications*, **2012**, 48, 76-78.
- [32] Ueda S., Nagasawa H., *Angewandte Chemie-International Edition*, **2008**, 47, 6411-6413.
- [33] Ueda S., Nagasawa H., *Journal of Organic Chemistry*, **2009**, 74, 4272-4277.
- [34] Evindar G., Batey R. A., *Journal of Organic Chemistry*, **2006**, 71, 1802-1808.
- [35] Kantam M. L., Venkanna G. T., Kumar K. B. S., Balasubrahmanyam V., Bhargava S., *Synlett*, **2009**, 1753-1756.
- [36] Wu F., Zhang J., Wei Q., Liu P., Xie J., Jiang H., Dai B., *Organic & Biomolecular Chemistry*, **2014**, 12, 9696-9701.
- [37] Peng J., Zong C., Ye M., Chen T., Gao D., Wang Y., Chen C., *Organic & Biomolecular Chemistry*, **2011**, 9, 1225-1230.
- [38] Yuan Y., Thome I., Kim S. H., Chen D., Beyer A., Bonnamour J., Bolm C., *Advanced Synthesis & Catalysis*, **2010**, 352, 2892-2898.
- [39] Turner G. L., Morris J. A., Greaney M. F., *Angewandte Chemie-International Edition*, **2007**, 46, 7996-8000.
- [40] Do H.-Q., Daugulis O., *Journal of the American Chemical Society*, **2007**, 129, 12404-12405.
- [41] Sanchez R. S., Zhuravlev F. A., *Journal of the American Chemical Society*, **2007**, 129, 5824-5825.

- [42] Lewis J. C., Berman A. M., Bergman R. G., Ellman J. A., *Journal of the American Chemical Society*, **2008**, 130, 2493-2500.
- [43] Zhao D., Wang W., Yang F., Lan J., Yang L., Gao G., You J., *Angewandte Chemie-International Edition*, **2009**, 48, 3296-3300.
- [44] Huang J., Chan J., Chen Y., Borths C. J., Baucom K. D., Larsen R. D., Faul M. M., *Journal of the American Chemical Society*, **2010**, 132, 3674-3675.
- [45] Hachiya H., Hirano K., Satoh T., Miura M., *Angewandte Chemie-International Edition*, **2010**, 49, 2202-2205.
- [46] Zhang F., Greaney M. F., *Angewandte Chemie-International Edition*, **2010**, 49, 2768-2771.
- [47] Liu B., Qin X., Li K., Li X., Guo Q., Lan J., You J., *Chemistry-A European Journal*, **2010**, 16, 11836-11839.
- [48] Ranjit S., Liu X., *Chemistry-A European Journal*, **2011**, 17, 1105-1108.
- [49] Kirchberg S., Tani S., Ueda K., Yamaguchi J., Studer A., Itami K., *Angewandte Chemie-International Edition*, **2011**, 50, 2387-2391.
- [50] Liu B., Guo Q., Cheng Y., Lan J., You J., *Chemistry-A European Journal*, **2011**, 17, 13415-13419.
- [51] So C. M., Lau C. P., Kwong F. Y., *Chemistry-A European Journal*, **2011**, 17, 761-765.
- [52] Muto K., Yamaguchi J., Itami K., *Journal of the American Chemical Society*, **2012**, 134, 169-172.
- [53] Xi P., Yang F., Qin S., Zhao D., Lan J., Gao G., You J., *Journal of the American Chemical Society*, **2010**, 132, 1822-1824.

- [54] Han W., Mayer P., Ofial A. R., *Angewandte Chemie-International Edition*, **2011**, 50, 2178-2182.
- [55] Malakar C. C., Schmidt D., Conrad J., Beifuss U., *Organic Letters*, **2011**, 13, 1378-1381.
- [56] Wang Z., Li K., Zhao D., Lan J., You J., *Angewandte Chemie-International Edition*, **2011**, 50, 5365-5369.
- [57] Gong X., Song G., Zhang H., Li X., *Organic Letters*, **2011**, 13, 1766-1769.
- [58] Wu G., Zhou J., Zhang M., Hu P., Su W., *Chemical Communications*, **2012**, 48, 8964-8966.
- [59] Xie H. Z., Gao Q., Liang Y., Wang H. S., Pan Y. M., *Green Chemistry*, **2014**, 16, 2132-2135.
- [60] Sarode S. A., Bhojane J. M., Nagarkar J. M., *Tetrahedron Letters*, **2015**, 56, 206-210.
- [61] Wu X.-F., Neumann H., Neumann S., Beller M., *Tetrahedron Letters*, **2013**, 54, 3040-3042.
- [62] Tao K., Zheng J., Liu Z., Shen W., Zhang J., *Tetrahedron Letters*, **2010**, 51, 3246-3249.
- [63] Aksenov A. V., Smirnov A. N., Aksenov N. A., Bijieva A. S., Aksenova I. V., Rubin M., *Organic & Biomolecular Chemistry*, **2015**, 13, 4289-4295.
- [64] Cao X., Cheng X., Bai Y., Liu S., Deng G.-J., *Green Chemistry*, **2014**, 16, 4644-4648.
- [65] Khalafi-Nezhad A., Panahi F., *ACS Catalysis*, **2014**, 4, 1686-1692.

- [66] Liu J., Liu Q., Yi H., Qin C., Bai R., Qi X., Lei A., *Angewandte Chemie-International Edition*, **2014**, 53, 502-506.
- [67] Tang L., Guo X., Yang Y., Zha Z., Wang Z., *Chemical Communications*, **2014**, 50, 6145-6148.
- [68] Lee J. J., Kim J., Jun Y. M., Lee B. M., Kim B. H., *Tetrahedron*, **2009**, 65, 8821-8831.
- [69] Saha P., Ali M. A., Ghosh P., Punniyamurthy T., *Organic & Biomolecular Chemistry*, **2010**, 8, 5692-5699.
- [70] Banerjee S., Payra S., Saha A., Sereda G., *Tetrahedron Letters*, **2014**, 55, 5515-5520.
- [71] Chen W.-H., Pang Y., *Tetrahedron Letters*, **2009**, 50, 6680-6683.
- [72] Shelkar R., Sarode S., Nagarkar J., *Tetrahedron Letters*, **2013**, 54, 6986-6990.
- [73] Chen F., Shen C., Yang D., *Tetrahedron Letters*, **2011**, 52, 2128-2131.
- [74] Inamdar S. M., More V. K., Mandal S. K., *Tetrahedron Letters*, **2013**, 54, 579-583.
- [75] Kidwai M., Bansal V., Saxena A., Aerry S., Mozumdar S., *Tetrahedron Letters*, **2006**, 47, 8049-8053.
- [76] Mase T., Itoh T., *Pure and Applied Chemistry*, **2008**, 80, 707-715.
- [77] Azizi N., Amiri A. K., Baghi R., Bolourtchian M., Hashemi M. H., *Monatshefte fur Chemie*, **2009**, 140, 1471-1473.
- [78] Cho Y.-H., Lee C.-Y., Cheon C.-H., *Tetrahedron*, **2013**, 69, 6565-6573.

- [79] Beccalli E. M., Brogini G., Martinelli M., Sottocornola S., *Chemical Reviews*, **2007**, 107, 5318-5365.
- [80] Negishi E., *Handbook of Organopalladium Chemistry for Organic Synthesis*, Ed., Wiley-Interscience, New York **2002**.
- [81] Desai L. V., Sanford M. S., *Angewandte Chemie-International Edition*, **2007**, 46, 5737-5740.
- [82] Krishnan G. R., Sreekumar K., *Soft Materials*, **2010**, 8, 114-129.
- [83] Dahan A., Portnoy M., *Journal of the American Chemical Society*, **2007**, 129, 5860-5869.

Chapter-6

COPPER COMPLEXES OF CHIRAL MODIFIED DENDRIGRAFT PEN-G2 AND AZA DIELS-ALDER REACTION

Abstract

The chiral modification of PEN-G2 dendrigraft polymer having pentaerythritol initiated polyepichlorohydrin as core has been done. The copper complex of chiral modified PEN-G2 dendrigraft polymer was synthesized and characterized. The copper complex of PEN-G2 dendrigraft polymer was found to be an excellent catalyst for the synthesis of isoquinuclidines via Aza Diels-Alder reaction between cyclohexenone and imines. The catalyst exhibited superior enantioselectivity. Reusability of the catalyst was studied for five cycles.

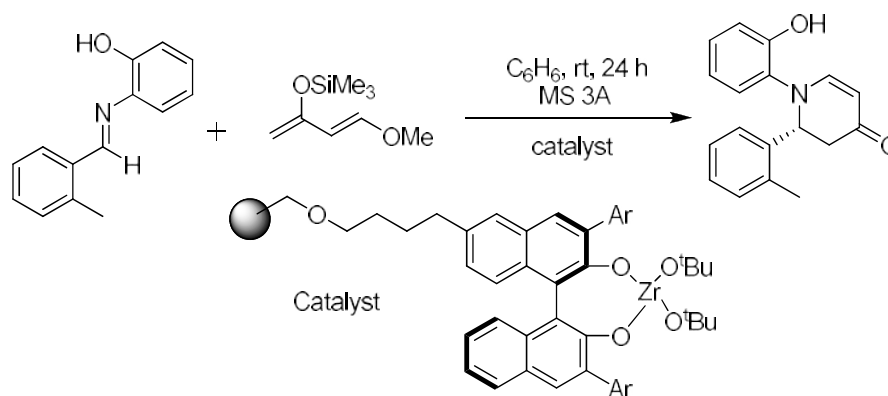
6.1 Introduction

6.1.1 Aza Diels-Alder Reaction

Asymmetric reactions using chiral catalysts provide the most promising method for construction of chiral molecules.¹⁻⁵ Catalytic aza Diels-Alder reaction is one of the useful methods for the synthesis of chiral nitrogen containing heterocycles.⁶⁻⁹ Using aza Diels-Alder reaction, we can synthesize isoquinuclidines (azabicyclo [2.2.2] octanes) having N-bicyclic structures. They are the structural elements of numerous naturally occurring alkaloids with interesting biological properties.¹⁰⁻¹¹ A number of chiral Lewis acids and chiral Brønsted acids, as organocatalysts were

reported for the activation of imine functional groups.¹²⁻³⁷ In particular, chiral phosphoric acid based organocatalyst was used for the activation of imine functional group which resulted in a number of asymmetric additions of various nucleophiles to imines.³⁸⁻⁵²

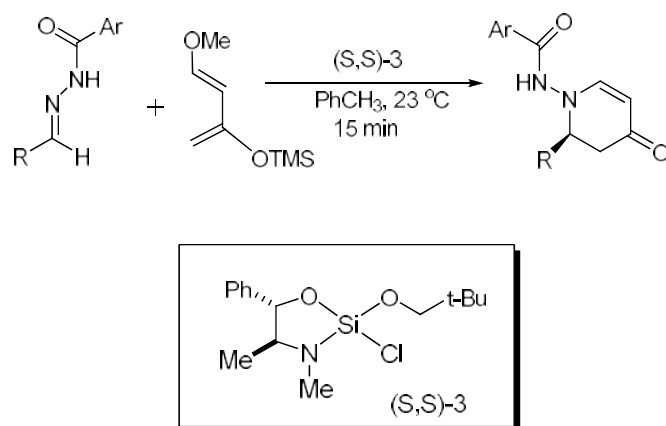
In 1996, Kobayashi *et al.* reported the first examples of catalytic asymmetric aza Diels-Alder reaction using a chiral ytterbium catalyst.⁵³ They reported asymmetric reactions using azadienes or iminodienes. Later, they reported chiral zirconium-binaphthol complexes for the asymmetric reactions of azadienophiles or imino dienophiles with Danishefsky's diene.^{15,17,54-55} They had done the structure optimization of the chiral BINOL zirconium catalyst and found that, in the presence of 1-5 mol % of Merrifield resin supported chiral BINOL zirconium catalyst, aza Diels-Alder reaction proceeded smoothly to afford the corresponding piperidine derivatives in high yields with high enantioselectivities (Scheme 6.1).¹⁶



Scheme 6.1

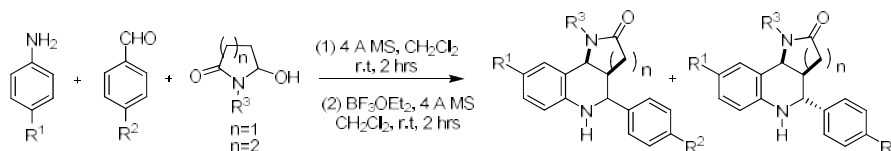
Silane Lewis acid is effective for the enantioselective promotion of (formal) aza Diels-Alder (ADA) reaction of acylhydrazones with Danishefsky's diene, adding to the versatility of this practical family of

silicon Lewis acids. The reactions are extraordinarily simple to perform, and generally provide good yields and enantioselectivities (Scheme 6.2).⁵⁶



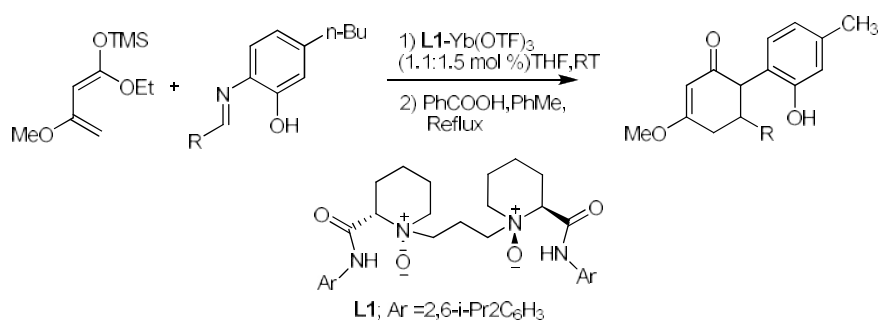
Scheme 6.2

An efficient synthesis of hexahydropyrrolo[3,2-*c*]quinolin-2-ones and hexahydropyridino[3,2-*c*]quinolin-2-ones has been developed in moderate to high yields by one-pot two-step aza Diels-Alder reaction. Here, *N*-arylimines formed in situ from anilines and benzaldehydes were reacted with cyclic enamides formed in situ from 5-hydroxypyrrolidin-2-ones and 6-hydroxypiperidin-2-ones by $\text{BF}_3 \cdot \text{OEt}_2$ -promoted dehydration in dichloromethane at room temperature. The hexahydropyrrolo[3,2-*c*]quinolin-2-ones were formed as a single *exo*-stereoisomer in most cases and hexahydropyridino[3,2-*c*]quinolin-2-ones were formed as a mixture of *exo*- and *endo*-isomers favoring the *endo*-diastereomer (Scheme 6.3).⁵⁷



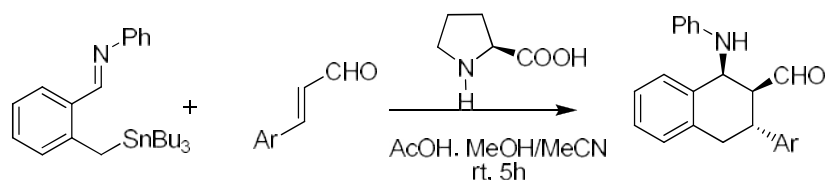
Scheme 6.3

The chiral N,N' -dioxide-Yb(OTf)₃ complex-catalyzed enantioselective aza Diels-Alder reaction of Brassard's diene with aldimines has been developed, giving the corresponding α, β -unsaturated δ -lactam derivatives in moderate yields with good enantioselectivities under mild conditions. Isolation of the reaction intermediate indicates that this asymmetric aza Diels-Alder reaction proceeds through a stepwise Mannich-type pathway (Scheme 6.4).⁵⁸



Scheme 6.4

Catalytic asymmetric Diels-Alder reaction of α -amino-*o*-quinodimethane with α, β -unsaturated aldehydes was achieved with high diastereo- and enantioselectivities in the presence of L-proline, which acts as a promoter to generate the quinodimethane from the corresponding precursor as well as a chiral catalyst for the enantioselective Diels-Alder reaction (Scheme 6.5).⁵⁹

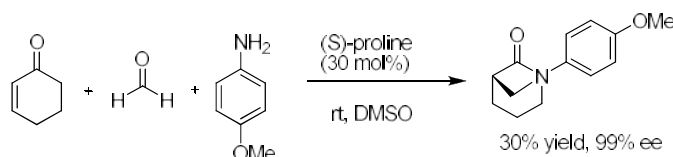


Scheme 6.5

6.1.1.1 Comparison of Performance

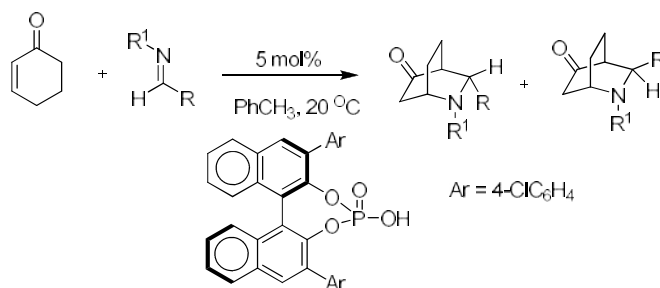
To date, there have been only a few reports regarding direct aza hetero-Diels-Alder reaction of cyclohexenone with aromatic aldimines which are discussed below.

The amino acid catalyzed asymmetric aza Diels-Alder reaction between aqueous formaldehyde, unsaturated cyclic ketones, and aromatic amines furnished the desired azabicyclic ketones (24-48h) with >99% ee (Scheme 6.6)⁶⁰



Scheme 6.6

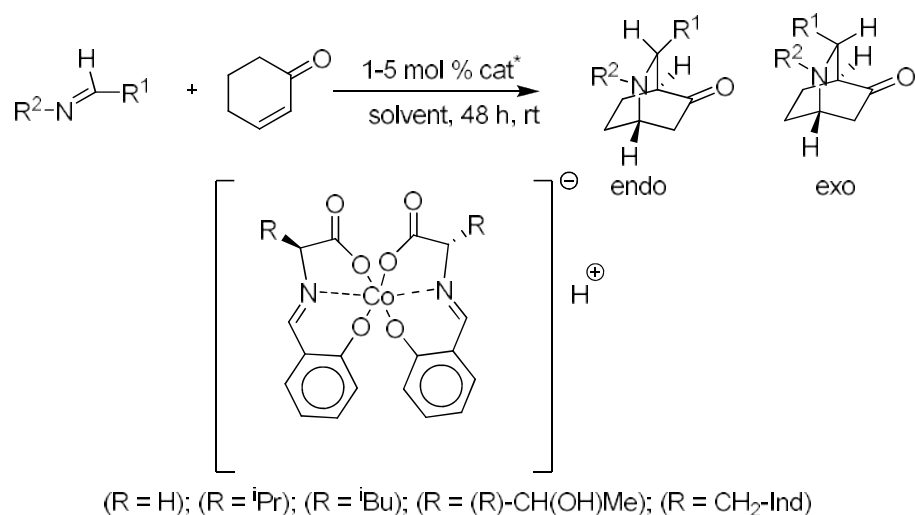
A chiral phosphoric acid, derived from 3,3-di(4-chlorophenyl)-H₈-binol, exhibited superior enantioselectivity, affording fairly good yields for the reaction of a range of aromatic aldimines with cyclohexenone within 6 days (Scheme 6.7).⁶¹



Scheme 6.7

Co(III) anionic complexes of Schiff bases obtained from salicylaldehydes and enantiomerically pure amino acids act as a novel

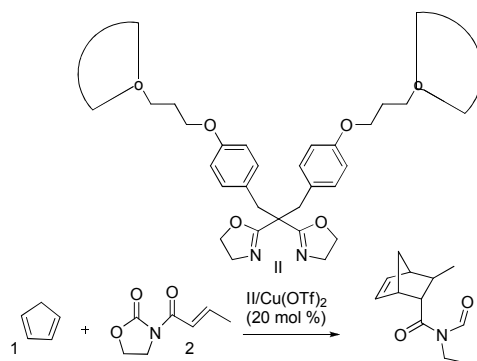
chiral Bronsted acid to catalyse aza Diels-Alder reaction in CCl_4 (Scheme 6.8).⁶²



Scheme 6.8

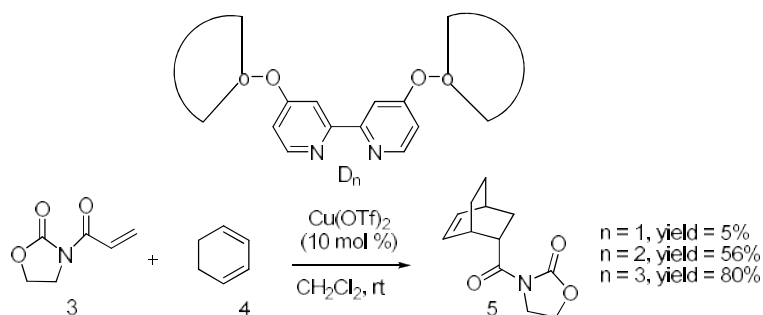
6.1.2 Dendritic Catalysts

A comparison between homogeneous, heterogeneous and dendritic heterogeneous catalyst systems is discussed. Polymer-supported Lewis acids are known to catalyze cycloadditions and polymer-loaded or dendrimer-loaded copper catalysts have been reported to be promoters of Diels-Alder reactions.⁶³ Menger *et al.* described the synthesis of polystyrene-based metallo-polymers containing copper and their use as catalysts in Diels Alder reaction.⁶⁴ Results suggest that metallo-polymers give better yields than the $\text{Cu}(\text{OAc})_2$ catalyzed reaction. Chow *et al.* reported the synthesis of dendritic bis(oxazoline)/Cu(II) complexes and their use as catalysts in the Diels-Alder reaction of 1 with 2 (Scheme 6.9).⁶⁵⁻⁶⁶



Scheme 6.9

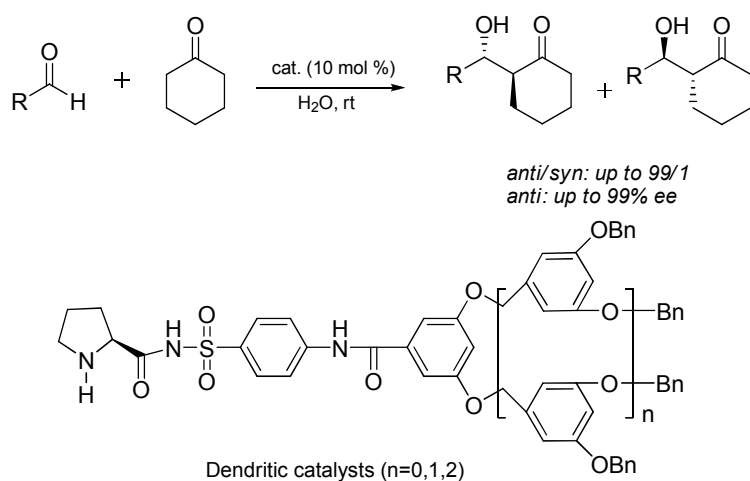
In this reaction, the size of the dendrimers had a strong influence on the kinetics of the reaction with a possible folding-back of the dendritic sectors towards the metallic site for higher-order dendrimers. Fujita *et al.* reported the use of dendritic bipyridines D_n as ligands for $\text{Cu}(\text{OTf})_2$ in the Diels-Alder reaction of various dienes and dienophiles.⁶⁷



(Scheme 6.10)

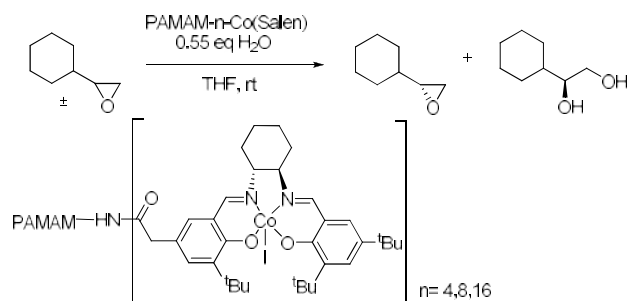
For example, the Diels-Alder reaction of 3 and 4 proceeded with excellent *endo* selectivity (no *exo* stereoisomer was detected), and a positive dendritic effect was observed as the yield of 5 increased with the size of the dendrimers. Indeed, the first-order dendrimer D_1 led to a poor yield of 5 (5 %), but D_2 furnished 5 in 56 % yield, and the third-order dendrimer D_3 gave an optimum yield of 80% (Scheme 6.10).

The direct aldol reactions catalyzed by chiral dendritic catalysts derived from N-prolylsulfonamide gave the corresponding products in high isolated yields (up to 99%) with excellent anti diastereoselectivities (up to ~99:1) and enantioselectivities (up to ~99% ee) in water.⁶⁸ In addition, the catalyst could be recovered by precipitation and filtration and reused for at least five times without loss of catalytic activity (Scheme 6.11).



(Scheme 6.11)

PAMAM dendrimer-bound Co(salen) complexes were used for hydrolytic kinetic resolution (HKR) of (*rac*)-1,2-epoxyhexane (Scheme 6.12) and (*rac*)-vinylcyclohexane epoxide as substrates.⁶⁹ In this reaction, highly enantio-enriched (>98% ee) epoxide at 50 % conversion was achieved. The best results were obtained with the first generation (4-branch) metallo-dendrimer and the efficiency of catalyst on a per-metal basis was in the following order: 4-Co (salen)- PAMAM > 8-Co (salen)- PAMAM > 16-Co (salen)-PAMAM. This “dendrimer effect” was thought to arise from restricted conformation imposed by the dendrimer structure, which enhanced the cooperative interactions between Co-salen units.



(Scheme 6.12)

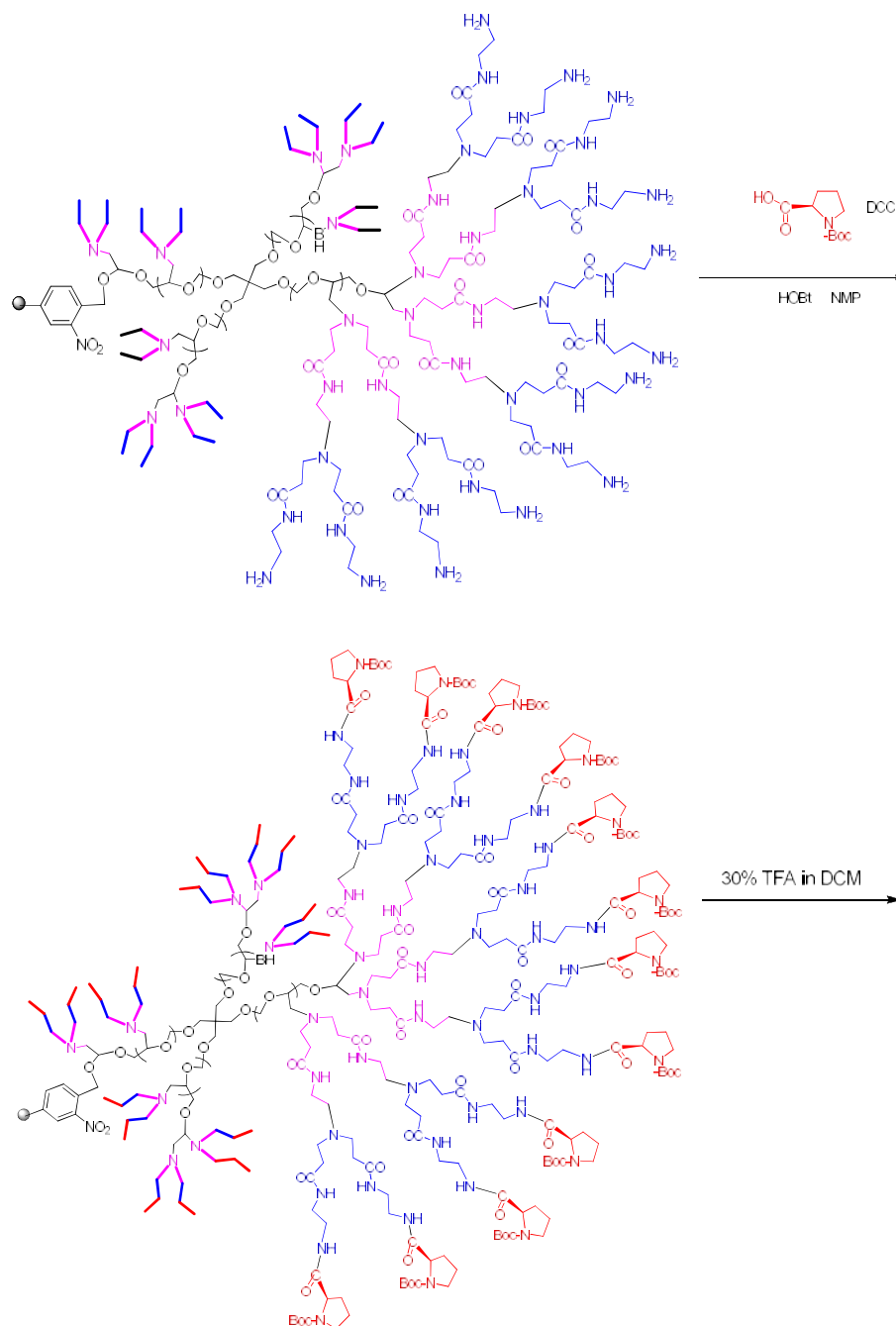
6.1.3 Objective of the Present Work

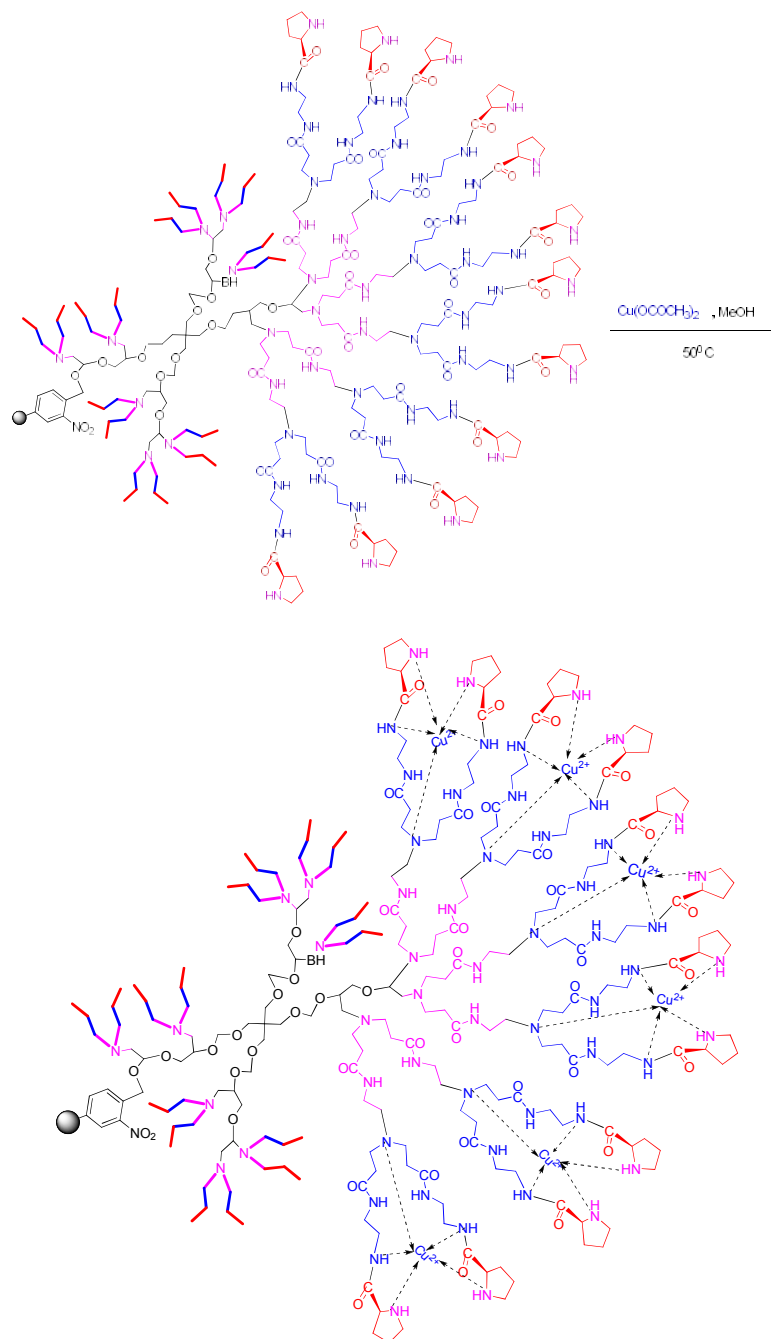
While, rather fruitful results have been reported in catalytic asymmetric Diels-Alder reactions,^{1-9,62,70-71} successful results are limited in asymmetric aza Diels-Alder reactions using dendritic systems. Amino acid derivatives have been utilized as catalysts for enantioselective cycloadditions such as the Diels-Alder reaction.^{36,72-78} These results⁷⁹⁻⁸⁵ have led us to investigate whether an amino acid-metal complex of dendritic system could be able to mediate the classical aza Diels-Alder reaction through a catalytic enamine mechanism. Herein, we report the direct catalytic aza Diels-Alder reaction of cyclohexene oxide with aldimines, achieved with good diastereo- and enantioselectivities in the presence of a copper complex of proline modified dendrigraft polymer supported on Merrifield resin with pentaerythritol initiated polyepichlorohydrin as core.

6.2 Results & Discussion

6.2.1 Synthesis of Copper Complex of Chiral Modified PEN-Gn Dendrigraft Polymer

The synthesis of the resin supported chiral modified dendrigraft PEN-Gn copper complex was achieved by adopting a three-step methodology, as shown in Scheme 6.13.





Scheme.6.13

The synthesis of Gn dendrigraft polymer having pentaerythritol initiated polyepichlorohydrin as core (PEN-G_n) was reported in Chapter.2. The amino group loading of G1 and G2 dendrigraft polymer was found to be 16.02 and 25.12 mmols/g respectively. Chiral modification of PEN-G2 polymer was done using Boc-L-proline followed by deprotection using trifluoroacetic acid. After chiral modification, amount of proline was found to be 12.54 and 20.63 mmol g⁻¹ for G1 and G2 respectively. Chiral modified dendrigraft PEN-G2 polymer was complexed with copper using copper acetate in methanol at a temperature of about 50 °C. Chiral PEN-Gn-Cu was found to be non-hygroscopic, stable and can be stored for a prolonged period of time without any change in its catalytic efficiency. The copper coordinated dendritic polymer appeared as light green powder.

6.2.2 Catalyst Characterization

6.2.2.1 ICP-AES Analysis

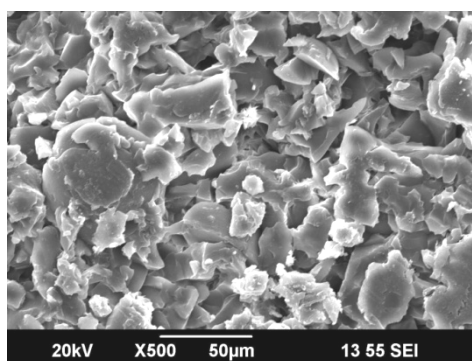
The copper capacity of PEN-G1-Cu and PEN-G2-Cu, based on ICP-AES analysis and confirmed by EDX analysis, were found to be 20.40, 32.36 % of the polymer, respectively (Table 6.1). It is therefore assumed that an average of 2.03 ligands was bound to Cu²⁺ ions in chiral PEN-G2 complex. Acetate ions were completely replaced by the dendritic ligands. The room temperature magnetic moment of the copper (II) PEN-G2 complex was found to be 2.1B.M. The Cu compounds were paramagnetic in nature, as was evident from the magnetic susceptibility measurement, which was consistent with the presence of Cu centers in their +2 oxidation state.

Table. 6.1 Analytical data for chiral PEN-Gn and chiral PEN-Gn-Cu

Polymer	Proline NH capacity (mmol/g)	Copper (%) ICP-AES	Copper (mmol/g) ICP-AES	Copper (%) EDX
Chiral PEN-G1-(Cu)	12.54	20.40	3.21	19.23
Chiral PEN-G2-(Cu)	20.63	32.36	5.09	30.27

6.2.2.2 SEM and Energy Dispersive X-ray (EDX) Analysis

The SEM micrographs of chiral PEN-G2-Cu polymer shows disordered aggregates and aggregated particles look flattened and show metallic lustre (Fig.6.1). EDX spectrum confirmed the presence of Cu, C, N and O as the constituents of the polymer. The results presented in Table 6.1 are the average of the data from scanned regions. The data obtained on the composition of the compounds from the energy dispersive X-ray spectroscopy, were consistent with the elemental analysis values (Table 6.1).

**Fig.6.1** Scanning electron micrograph of Chiral PEN-G2-Cu

6.2.2.3 IR Spectral Studies

The IR spectra showed characteristic differences between the spectral pattern originating from the dendrigraft PEN-G2 polymer,

proline modified dendrigraft PEN-G2 polymer and the corresponding copper complex. The IR spectra are presented in Fig 6.2. Dendrigraft PEN G2 polymer on Boc-proline modification showed bands at 1740 cm^{-1} due to ester carbonyl stretching of Boc carbonyl group. On deprotection, the peak at 1740 cm^{-1} got disappeared and showed only the peak due to amide at 1692 cm^{-1} .

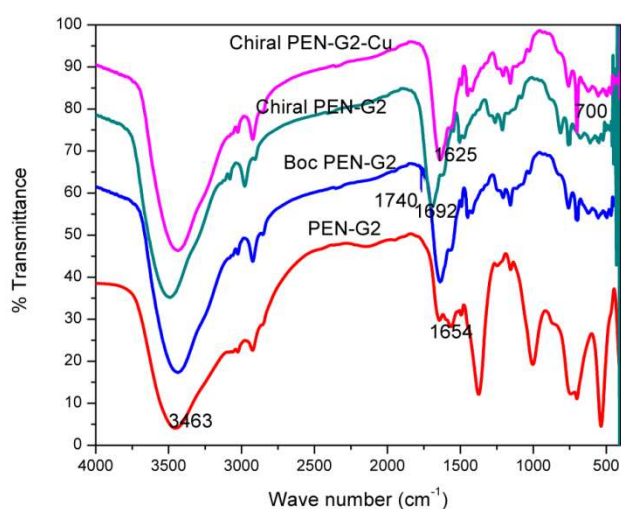


Fig.6.2 IR Spectra of chiral PEN G2-Cu

Proline modified polymer on complexation with copper showed a distinct shift towards lower frequency region. Stretching due to proline NH was lowered around 64 cm^{-1} and that of amide carbonyl stretching was lowered from 1692 cm^{-1} to 1625 cm^{-1} . The peak at 1508 cm^{-1} is due to stretching vibrations of secondary amine. Bending vibrations due to primary amine at 1610 cm^{-1} in the PEN-G2 polymer got modified by the secondary NH vibrations in chiral PEN-G2 polymer. The peak at 1200 cm^{-1} is due to the CH_2 wagging of cyclopentane ring. After chiral modification, the peak at 1007 cm^{-1} in PEN-G2 due to the ethereal C-O

stretching got merged with nearby peaks and shifted towards higher frequency region. The narrow peak at 700 cm^{-1} can be assigned to Cu-N stretching.

6.2.2.4 Electronic Spectral Studies (UV-Vis DRS)

UV-Vis DRS spectrum of Cu complex of proline modified PEN-G2 shows two peaks with maximum intensity at 671 nm and 839 nm (Fig 6.3). The peak at 839 nm relates to a distorted octahedral geometry and the peak at 671 nm to a square pyramidal geometry characteristic of five coordinated species.⁸⁶ But on compilation of other characteristic data, the square pyramidal geometry may be assigned to chiral PEN-G2-Cu complex. The peak at 671 nm and 839 nm may be ascribed to the absorption due to overlapping of allowed d-d transitions in copper after coordination with dendritic ligands.

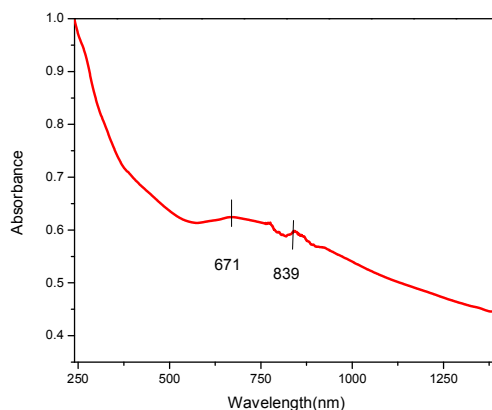


Fig.6.3. UV-Vis-DRS spectrum of Cu complex of proline modified PEN-G2

6.2.2.5 EPR Spectral Studies

EPR Spectral studies of Cu complex of proline modified PEN-G2 show typical axial spectra with four hyperfine lines, which is

characteristic of monomeric copper (II) complexes. The g and A values are obtained from the simulated spectrum (Fig 6.4) given in Table 6.2. In all the cases g_{\parallel} was found to be greater than g_{\perp} . This predicts a square pyramidal geometry to five coordinated complex rather than a trigonal bipyramidal structure which would be expected to have g_{\perp} greater than g_{\parallel} .⁸⁷⁻⁸⁸ Thus the chiral PEN-G2-Cu comprises of coordination of copper to two proline nitrogens, two amide nitrogens and one tertiary nitrogen of amidoamine unit.

Table 6.2 Splitting parameters g and A

Polymer	g_{\parallel}	g_{\perp}	g_{av}	A_{\parallel}	A_{\perp}	A_{av}
PEN-G2-Cu	2.28	2.07	2.14	195	12.8	69.83

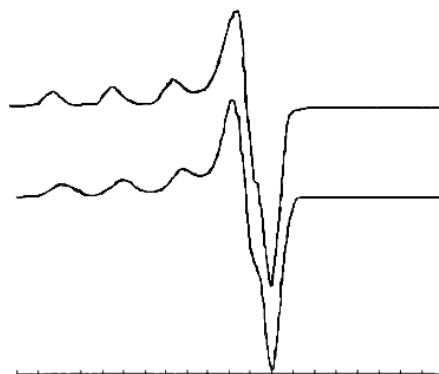


Fig 6.4 Experimental and simulated spectra of Cu complex of proline modified PEN-G2

6.2.2.6 X-ray Diffraction Studies

The room-temperature X-ray diffraction patterns of the pentaerythritol initiated dendrigraft polymer, PEN-G2 and the Copper complex of the chiral dendrigraft polymer PEN-G2-Cu on Merrifield resins are overlaid in the figure (Fig 6.5). After chiral modification and

complexation, the peaks corresponding to various 2θ values in PEN-G2 have disappeared indicating the loss of crystalline nature of the polymer complex. This observation confirms that the copper has been anchored to the polymer matrix to yield the polymer supported dendritic copper catalyst PEN-G2-Cu.

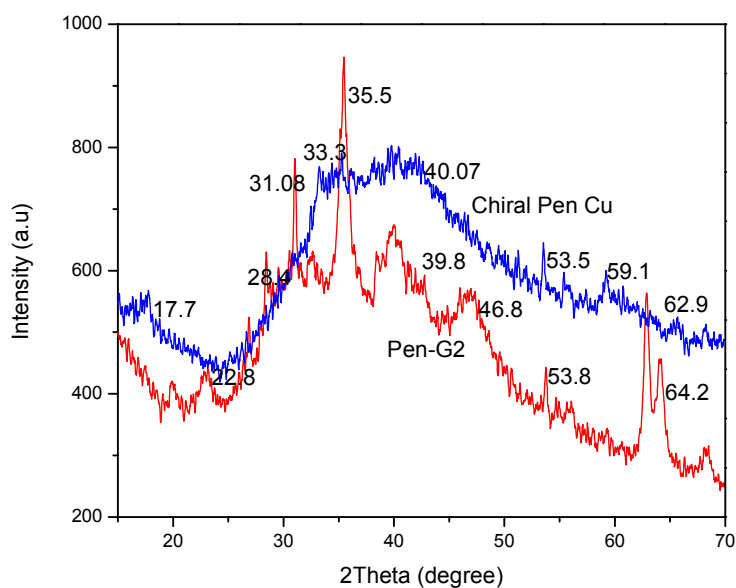


Figure.6.5. X-ray diffraction (XRD) pattern of PEN-G2 and PEN-G2-Cu

6.2.2.7 X-ray Photoelectron Spectroscopy

Fig 6.6 presents the Cu (2p) XPS spectra of the PEN-G2 Cu catalyst. The catalyst displayed characteristic Cu $2p_{3/2}$ singlet with peak located at 934.6 eV. Strong satellite peaks were observed at 942.7, 954.7 and 962.6 eV. The noted binding energy values are in good agreement with the available literature data for Cu ions in the 2+ oxidation state.⁸⁹ The presence of Cu (II) in supported dendritic polymer has thus been confirmed from the results of XPS analysis.

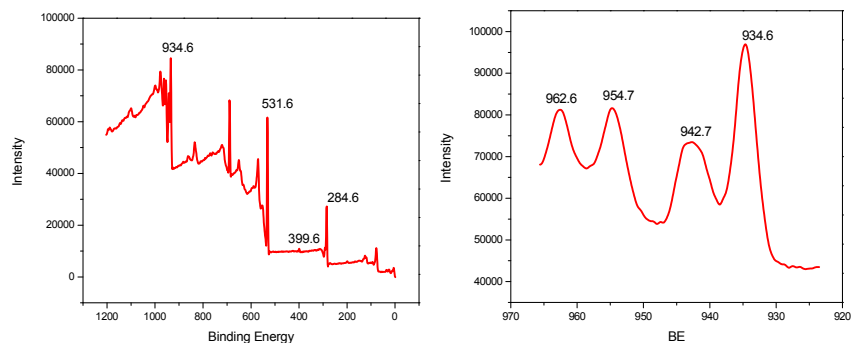


Fig 6.6. XPS spectra of Cu ($2p_{3/2}$) peak for PEN-G2-Cu (a) wide (b) deconvoluted

6.2.2.8 TG-DTG Analysis

A comparative evaluation of the thermogravimetric data of the PEN-G2 functionalized resins and the corresponding Cu loaded PEN-G2 dendrigraft polymer is shown in the figure (Fig 6.7). An intense decomposition is observed in the thermogram of both PEN-G2 and PEN-G2-Cu at temperatures above 400°C owing to the degradation of the polymeric backbone.⁹⁰

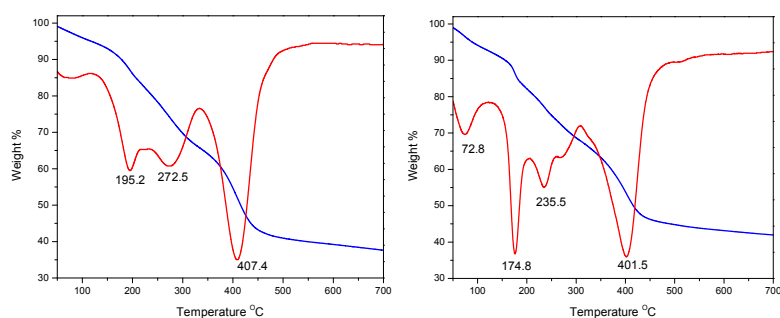


Fig 6.7. TG-DTG plot of (a) PEN-G2 and (b) PEN-G2-Cu

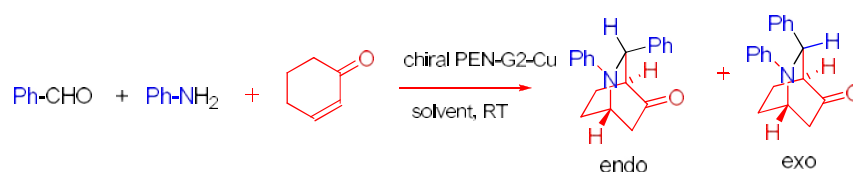
Apart from this, in the case of PEN-G2-Cu, a decomposition step with a weight loss of 25% occurs in the temperature range of $150\text{--}250^{\circ}\text{C}$. The thermal decomposition of PEN-G2 shows a weight loss of 30% which

occurs in the temperature range of 120-320 °C. From the reports regarding polyepichlorohydrin and Merrifield resin,⁹¹ this decomposition is ascribed to the release of amines as nitrogen, carbonyls as CO or CO₂ and the degradation of the polymeric backbone to be left with a residue containing copper oxide or hydroxide. The first step of decomposition in chiral PEN-G2-Cu is attributable to the loss of non-coordinated water, occurring in the temperature range of 65-105 °C. The TG-DTG analysis data for the dendrigraft polymers are thus in agreement with the percentage composition.

6.2.3 Catalytic Activity of Resin Supported Dendrigraft PEN-Gn-Cu Complex

6.2.3.1 Synthesis of Isoquinuclidines

In a survey of catalytic activity, chiral dendrigraft PEN-G1 and G2 copper complexes were employed in the synthesis of Isoquinuclidines (Scheme 6.14).



Scheme 6.14 Aza Diels-Alder reaction of cyclohexenone with aldimines

It was found that chiral PEN-G2-Cu catalyst was more efficient than chiral PEN-G1-Cu catalyst. A variety of aldehydes as substrates has been tried. The effects of various reaction parameters, such as type of solvent, reaction temperature, catalyst concentration, etc., were evaluated using benzaldehyde, aniline and cyclohexenone as model substrates and chiral PEN-G2-Cu as the catalyst. Optimization studies of solvent and catalyst concentration are shown in Table 6.3 and 6.4.

The reaction of cyclohexenone with imine was carried out in several solvents at an ambient temperature of 30 °C for 5h. The results are summarized in Table. 6.3. As shown in the table, selected solvents provide the product in reasonable yield with enantiomeric excess greater than 70 %. CCl₄ was chosen as the preferred solvent for further studies, because the best endo/exo ratio of the product was observed in this solvent. The efficiency of the catalyst was tested by varying the catalyst concentration.

Table 6.3 Optimization of solvent^a

Entry	Solvent	Yield (%) ^b	(endo/exo) ^c	ee (%) ^d
1	DMSO	60	82/18	80
2	CCl ₄	82	92/08	90
3	Ethanol	78	76/24	74
4	Hexane	72	50/50	64
5	Toluene	82	60/40	75
6	THF	78	55/45	78
7	CH ₃ CN	82	75/25	74

^a Reaction Conditions: Cyclohexenone (1 mmol), benzaldehyde (1 mmol), aniline (1 mmol). RT, PEN-G2-Cu: 20 mg, ^b Isolated yield of endo and exo, ^c Determined by ¹H NMR, ^d Enantiomeric excess of the major product was determined by chiral HPLC analysis (Chiralpak IB-3 chiral stationary phase, iPrOH/hexane (1:9), 254 nm).

As shown in Table 6.4, there was no appreciable change in the enantiomeric excess of the major product while decreasing the catalyst loading from 10 to 5 mol %. However, the best yield and % ee were achieved at 5.1 mol % of the catalyst. We have also checked the influence of the amount of solvent of the reaction mixture on the catalyst efficiency. A dilution led to a decrease of the yield but the best % ee of the product was achieved with 3 ml of carbon tetrachloride.

Table 6.4 Optimization of Amount of Catalyst^a

Entry	Catalyst Amount (mg)	Catalyst Amount (mol %)	Yield (%) ^b	(endo/exo) ^c	ee (%) ^d
1	2.0	1.02	53	60/40	72
2	7.0	3.57	65	75/25	74
3	10.0	5.10	82	92/08	90
4	15.0	7.64	82	88/12	78
5	20.0	10.19	82	90/10	90

^a Reaction Conditions: Cyclohexenone (1mmol), benzaldehyde (1mmol), aniline (1mmol). CCl₄-3ml, RT, ^b Isolated yield of endo and exo, ^c Determined by ¹H NMR, ^d Enantiomeric excess of the major product was determined by chiral HPLC analysis (Chiralpak IB-3 chiral stationary phase, iPrOH/hexane (1:9), 254 nm).

Having established the optimum reaction conditions, effect of generation of the dendrigraft PEN-G_n-Cu was studied (Table 6.5). A positive dendritic effect was observed as the % ee increased with generation of the polymer. Indeed, first generation resulted in endo/exo ratio of 75/25, the second generation furnished endo/exo product ratio with 92/08 with 90% ee.

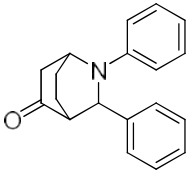
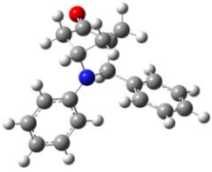
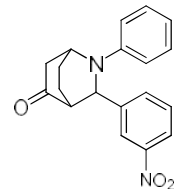
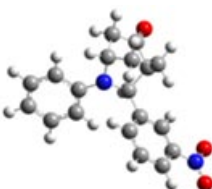
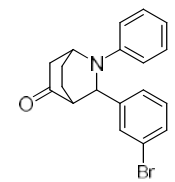
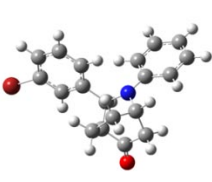
Table 6.5 Effect of Generation of the Dendrigraft PEN-G₂-Cu^a

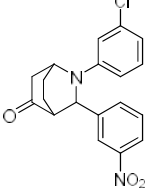

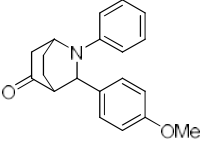
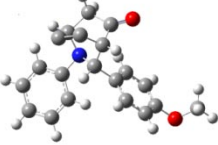
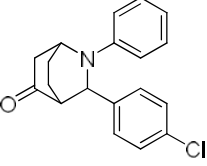
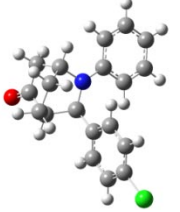
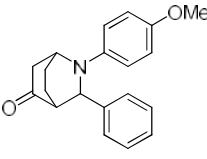
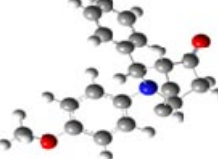
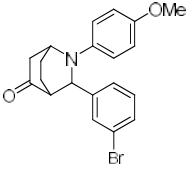
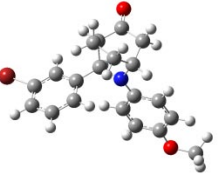
Polymer	Yield (%) ^b	(endo/exo) ^c	ee (%) ^d
PEN-G1-Cu	80	75/25	85
PEN-G2-Cu	82	92/08	90

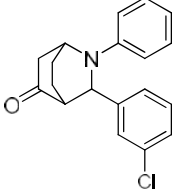

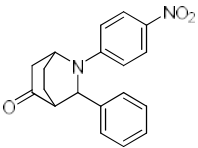
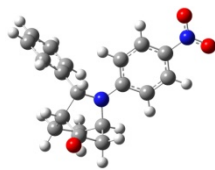
^a Reaction Conditions: Cyclohexenone (1mmol), benzaldehyde (1mmol), aniline (1mmol). CCl₄-3ml, RT, Catalyst amount: 5.1mol% ^b Isolated yield of endo and exo, ^c Determined by ¹H NMR, ^d Enantiomeric excess of the major product was determined by chiral HPLC analysis (Chiralpak IB-3 chiral stationary phase, iPrOH/hexane (1:9), 254 nm).

After optimizing the reaction conditions, scope of different substrates was evaluated (Table 6.6). All the substrates selected were studied for 3 h. Most of the reactions of cyclohexenone with imines resulted in good diastereo and enantioselectivity irrespective of the functional group on the aromatic ring. ^1H NMR and GC-MS spectra of few diastereomers are shown in Fig 6.8-6.12. The distereomeric ratio can be found out from proton NMR spectrum as well as from the GCMS. In GCMS, splitting pattern corresponding to endo and exo will be different which helps to predict diastereomeric ratio.

Table 6.6 Asymmetric Aza Diels-Alder Reaction of Cyclohexenone with Aldimines^a

Aza Diels-Alder product	Optimized structure	Yield(%) ^b	endo/exo ^c	ee (%) ^d
 6a	 -864.53	82	92/08	90
 6b	 -1068.95	82	88/12	84
 6c	 -3435.51	84	87/13	86

 6d	 -1528.53	62	84/16	78
 6e	 -979.69	82	88/12	88
 6f	 -1324.78	84	80/20	88
 6g	 -979.69	85	88/12	90
 6h	 -3550.67	76	90/10	86

 <p>6i</p>	 <p>-1324.79</p>	89	90/10	90
 <p>6j</p>	 <p>-1069.64</p>	68	60/40	88
<p>^a Reaction Conditions: Cyclohexenone (1mmol), aldehyde (1mmol), amine (1mmol). CCl₄-3ml, RT, Catalyst amount: 5.1mol%, 3h, ^b Isolated yield of endo and exo, ^c Determined by ¹H NMR, ^d Enantiomeric excess of the major product was determined by chiral HPLC analysis (Chiralpak IB-3 chiral stationary phase, iPrOH/hexane (1:9), 254 nm).</p>				

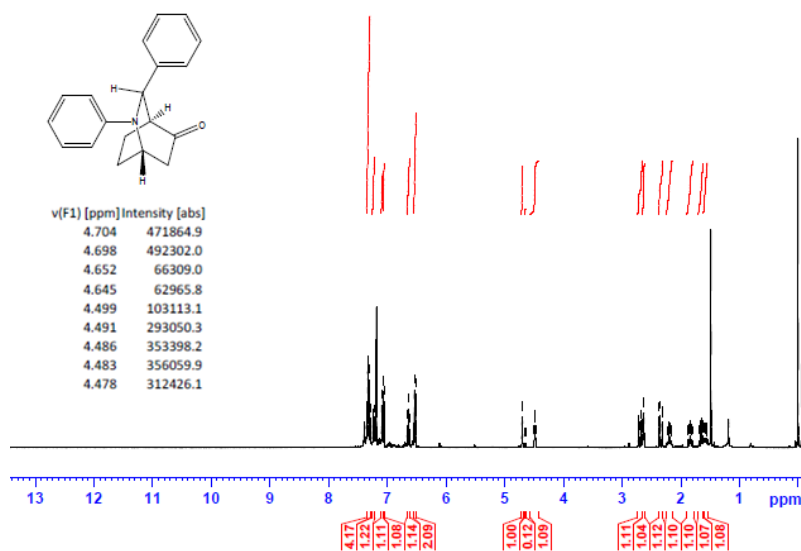


Fig 6.8 ¹H NMR spectrum of 2,3-Diphenyl-2-azabicyclo[2.2.2]octan-5-one (6a)

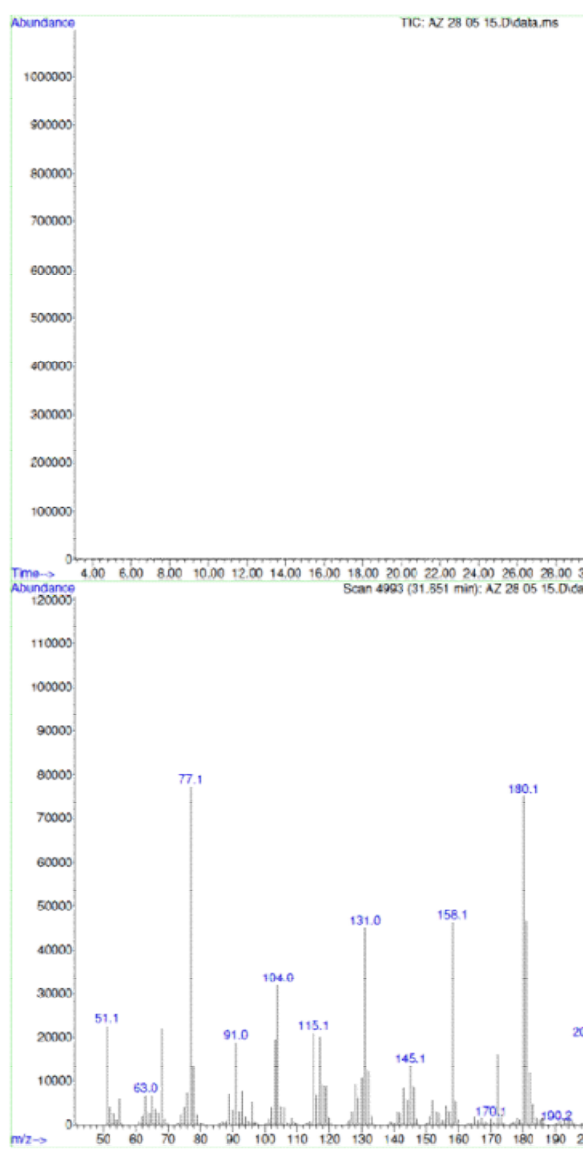


Fig 6.9 GC-MS spectrum of 2,3-Diphenyl-2-azabicyclo[2.2.2]octan-5-one (6a)

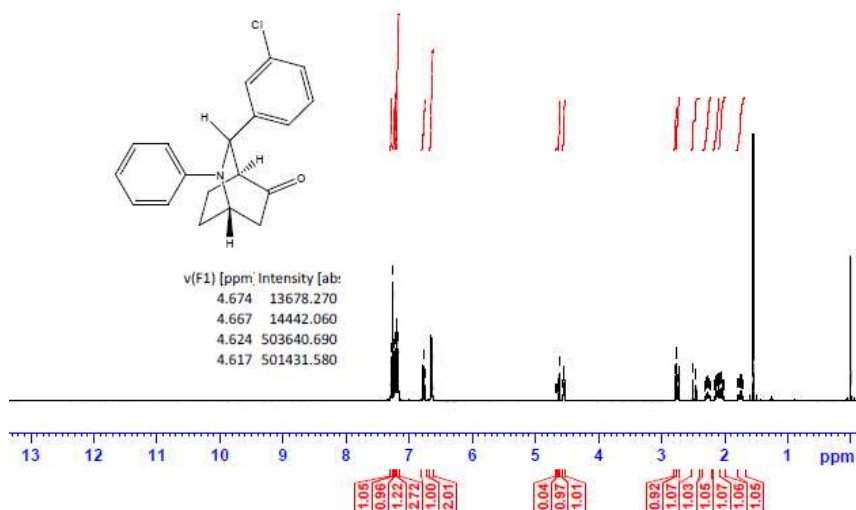


Fig 6.10 ^1H NMR spectrum of 3-(3-Chlorophenyl)-2-phenyl-2-azabicyclo [2.2.2]octan-5-one (6i)

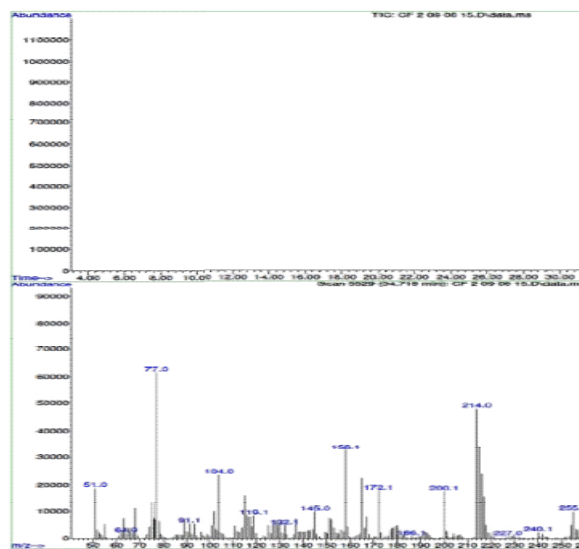


Fig 6.11 GC-MS spectrum of 3-(3-Chlorophenyl)-2-phenyl-2-azabicyclo [2.2.2] octan-5-one (6i-endo)

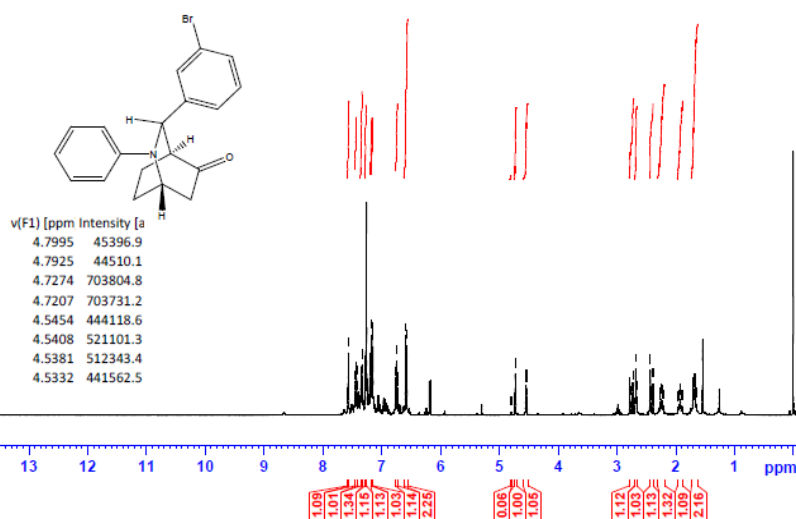


Fig 6.12 ^1H NMR spectrum of 3-(3-Bromophenyl)-2-phenyl-2-azabicyclo[2.2.2]octan-5-one (6c)

In order to find whether the yield of the Aza Diels Alder product depends on its ground state energy, structure of the products were optimized using B3LYP exchange correlation functional and 6-31G basis set.^{92,93} The optimized energy i.e. lowest energy of the compound to be in the stable state, is depicted in the table (Table 6.6). As per the energy values, the compound 6a has maximum energy; so we expect it to have low yield (endo product) compared with others. But experimental results show endo/exo ratio of 92:08. In some other cases, the experimental values are agreeable with the theoretical value. For example, compound 6h have least energy value (-3550.67) which shows yield of about 90:10. These results show that formation of Aza Diels-Alder product cannot be predicted by ground state energy values alone, but other factors (kinetic and thermodynamic factors) have to be considered in order to predict the formation of the product theoretically.

6.2.3.2 Recyclability of the Catalysts

After completion of the reaction, the solution was filtered, washed with ethyl acetate (3-10 mL), acetone and vacuum dried at 50⁰C for about 5h. The catalyst recovered was weighed and reused without loss of significant catalytic activity. Details regarding catalyst recovery with percentage yield are depicted in Table 6.7. Successive runs were carried out in order to examine the recyclability of the catalyst. After fifth cycle, 87.8 % of catalyst was recovered and reused with 74% ee.

Table 6.7. Recycling of chiral PEN-G2-Cu catalyst^a

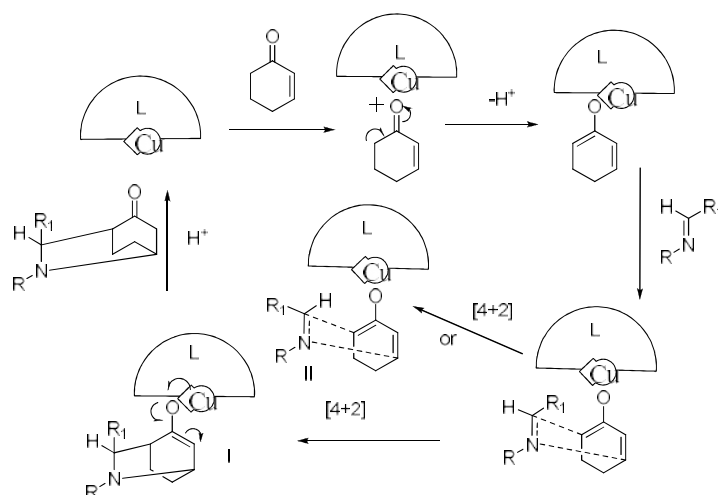
No.of Cycles	Catalyst weight (mg)	Catalyst recovered (mg)	Recovery (%)	Product yield (%) ^b	Endo/exo ^c	ee (%) ^d
1	10	9.2	92.0	82	92/08	90
2	9.2	8.4	91.3	78	82/18	82
3	8.4	7.8	92.9	74	78/22	78
4	7.8	7.4	94.9	65	75/25	74
5	7.4	6.5	87.8	65	74/26	74

^a Reaction Conditions: Cyclohexenone (1mmol), benzaldehyde (1mmol), aniline (1mmol). CCl₄-3ml, RT, 3h, ^b Isolated yield of endo and exo, ^c Determined by ¹H NMR, ^d Enantiomeric excess of the major product was determined by chiral HPLC analysis (Chiralpak IB-3 chiral stationary phase, iPrOH/hexane (1:9), 254 nm).

6.2.3.3 The Proposed Mechanism

It is well known that a carbonyl compound possessing α -hydrogens will enolize under acidic conditions and the formed enolate will attack imines formed from aldehydes and amines. (4+2) diene-dienophile

cycloaddition of enolate with aldimine generates intermediate I and II. Finally catalyst leaves the system to form the product, endo and exo.



Scheme 6.15 Possible mechanism for Aza Diels Alder reaction of cyclohexenone with aldimines

6.3 Conclusions

In conclusion, we have developed a highly efficient chiral dendritic copper catalyzed method for the cycloaddition of cyclohexenone with aldimines. The developed copper complexes of chiral G1 and G2 dendrigraft polymer having pentaerythritol initiated polyepichlorohydrin as core were characterized. Aza Diels-Alder reaction between systems like imines and cyclohexenone are rare and reported works are base catalyzed or catalyzed by other metals. So we found that copper complexes can catalyze Aza Diels-Alder reaction like Diels-Alder reaction. The reaction occurs more efficiently with high generation dendrigraft polymer in comparison with low generation G1 dendrigraft polymer. After optimizing the reaction conditions, a detailed study of aza Diels-Alder reaction was done with chiral PEN-G2

copper catalyst. The main features of the synthesis are: only small amount of catalyst was needed to drive the reaction and all the reactions were performed at room temperature. The catalyst performs well with good diastereoselectivity and good enantiomeric excess. Procedural simplicity, simple recovery and reusability of catalysts meet the requirements of benign chemistry. So the present catalyst will be of wide practical application in similar reactions. Further investigation on the application of this catalyst for other organic reactions is in progress.

6.4 Experimental Section

6.4.1 Materials

Anhydrous copper acetate, cyclohexenone, aldehydes, amines, Boc-L-Proline, DCC, NMP, HOBT and TFA were all purchased from local vendors and used as received. All solvents were purified by standard procedures prior to use.

6.4.2 Modification of Dendrigraft PEN-G2 Polymer with Boc Proline

Active ester of amino acid was prepared by adding 2.5 meq of HOBT (1.69 g) and 2.5 meq of DCC (2.58 g) to a solution of Boc-L-Proline (2.69 g) in NMP. This was stirred for 5 min. and the HOBT ester of amino acid was added to the amino resin, PEN-G2 (0.5 g). The mixture was shaken for 48 h until the disappearance of blue colour with ninhydrin. DMSO was added to the mixture and shaken for 15 min. At the end of 15 min. DIEA was added. The unreacted reagents and byproducts were filtered off. The resin was washed with DCM: MeOH (66:33 v/v), DCM, NMP and dried under vacuum at 50°C.

Amount of Boc-proline: 0.021 mol g⁻¹; Yield: 0.58 g.

IR (cm⁻¹): 3460, 2934, 1740, 1652, 1539, 1366, 1103, 725.

Solid state ¹³C NMR (100 MHz): 172, 168.2, 167.8, 167.2, 152, 144.3, 122.2, 79.5, 76, 73, 61, 60.3, 47, 43, 38.8, 34, 29, 27, 23, 20.9 ppm.

6.4.3 Deprotection of Boc from Dendrigrraft PEN-G2 Polymer

The resin (0.5 g) was treated with 30 % TFA in DCM for 5h. The reaction was monitored using ninhydrin test and IR spectrum. The TFA solution was filtered and the resin was washed with DCM. This was treated with 5 % DIEA in DCM (5min) & 5 % DIEA in NMP: DCM mixture (1:1 v/v) to get the desired product. Finally, proline modified PEN-G2 polymer was dried at 50 °C.

Proline NH capacity: 0.021 mol/g; Yield: 0.46 g;

IR (cm⁻¹): 3460, 2982, 1692, 1525, 1454, 1250, 1117, 750.

Solid state ¹³C NMR (100 MHz): 168, 167.5, 167, 142.3, 122.4, 79.9, 73, 64, 62.3, 49, 42, 37, 35, 30, 25, 20.2 ppm.

6.4.4 Synthesis of Copper Complex of Proline Modified Dendrigrraft EG-G2 Polymer

A 50 mL round bottom flask was charged with 250 mg of Merrifield resin supported proline modified PEN-G2 polymer having 20.63 mmols/g of amine capacity. It was allowed to swell in DMF for 2 h. Quantitative amount of anhydrous copper acetate (0.021 mol, 0.94 g) in 10 mL methanol was added to the reaction flask. The reaction mixture was stirred at 50 °C for about two days (48h). The polymer was filtered and washed with water. The filtrate and washings were collected together

and concentrated. This concentrated solution was used for the estimation of metal ions by standard methods. The polymer-supported metal complex was washed with methanol (20 mL x 3), dioxane (20 mL x 3) and acetone (20 mL x 3) followed by drying at 50 °C for 3 h.

Dark green powder; Copper loading: 0.005 molg⁻¹; Yield: 0.32 g.

6.4.5 General Procedure for Aza Diels Alder Reaction

A 25 mL RB flask was charged with a magnetic stirrer and CCl₄ (3.0 mL). Cyclohexenone (1.0 mmol), and the catalyst PEN-G2-Cu (5.1 mol%, 10 mg) were added to the flask. To the resulting solution after 2 min of stirring, the Schiff base of aniline and benzaldehyde (1mmol) was added. The reaction mixture was stirred at room temperature for 3h. After the completion of the reaction (TLC and GC determination), the resulting solution was filtered, washed with ethyl acetate, methanol and acetone, and concentrated by a rotary vacuum evaporator. The product was separated by passing through a silica column using the eluent, hexane : ethyl acetate (9:1). The chemical yield and diastereomer ratio were determined from ¹H NMR spectrum. Product purification and diastereomer separation were made by column chromatography on SiO₂ (hexane/EtOAc/Et₃N 40:10:1). The enantiomeric purity was determined by chiral HPLC analysis (Chiralpak IB-3 chiral stationary phase, iPrOH/hexane (1:9), 254 nm).

6.4.6 Test for Heterogeneity of the Reaction

To examine whether there was any leaching of the metal complex from the polymer-bound dendrigraft catalyst, viz. chiral-PEN-G2-Cu, into the reaction medium during the aza Diels-Alder reaction, separate experiments were conducted under standard conditions. The filtrate

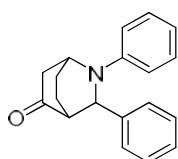
obtained by separating the solid catalyst after completion of the reaction was extracted with ethyl acetate. The aqueous layer was subsequently treated with a fresh batch of reactants in a reaction vessel and the reactions were allowed to continue. There was no formation of the product. This suggests that the reaction does not proceed after removal of the catalyst. Moreover, the presence of copper could not be detected when the filtrate, obtained after isolating the solid catalysts by filtration, was subjected to AAS analysis. The possibility of the copper species leaching out of the catalyst can thus be ruled out on the basis of the evidence gathered, which also proves the heterogeneous nature of the catalytic process.

6.4.7 Regeneration of the Catalyst

The reusability of the catalyst for subsequent catalytic cycles was examined using cyclohexenone, benzaldehyde and aniline as the substrates. After the completion of the reaction, the solid catalyst was separated from the reaction mixture by filtration, washed with CCl_4 , ethyl acetate, methanol and acetone. It was dried in vacuum at $50\text{ }^\circ\text{C}$ for about 5h. The dried solid catalyst was weighed and added to a fresh reaction mixture of cyclohexenone (1 mmol), benzaldehyde (1 mmol) and aniline (1 mmol) and CCl_4 (3 mL). The progress of the reaction was monitored by thin layer chromatography (TLC) and GCMS. The procedure for the above mentioned system was repeated for five reaction cycles.

6.5 Characterization of Products

1) 2,3-Diphenyl-2-azabicyclo[2.2.2]octan-5-one (6a)

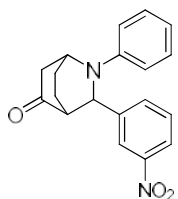


Brown solid.

$^1\text{H NMR}$ (400 MHz, CDCl_3): 7.368(t, $J=8,1\text{H}$); 6.774(d, $J=9,2\text{H}$); 6.598(d, $J=9,2\text{H}$); 4.535(d, $J=2.5, 1\text{H}$); 4.415(m, 1H); 3.726(s, 3H); 2.758(m, 1H); 2.706(m, 1H); 2.472(m, 1H); 2.246(m, 1H); 2.119(m, 1H); 2.027(m, 1H); 1.735(m, 1H).

MS (m/z): 277.15; $t\text{R}$ (min) (HPLC) = 3.06 and 5.59.

2) 3-(3-Nitrophenyl)-2-phenyl-2-azabicyclo[2.2.2]octan-5-one (6b)

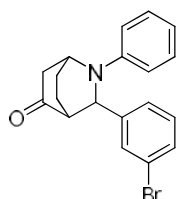


Brown solid.

$^1\text{H NMR}$ (400 MHz, CDCl_3): 1.65–1.85 (m, 1H), 1.95–2.35 (m, 3H), 2.48 (dd, 1H , $J = 19.0, 2.3$), 2.65–2.85 (m, 2H), 4.55 (br m, 1H), 4.63 (br m, 1H), 6.64 (d, 2H , $J = 8.2$), 6.77 (t, 1H , $J = 7.2$), 7.13–7.33 (m, 6H).

MS (m/z): 322.13; $t\text{R}$ (min) (HPLC) = 3.38 and 4.34.

3) 3-(3-Bromophenyl)-2-phenyl-2-azabicyclo[2.2.2]octan-5-one (6c)

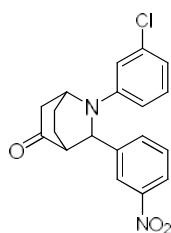


Brown solid.

$^1\text{H NMR}$ (400 MHz, CDCl_3): 7.565(s, 1H); 7.435(d, $J=8,1\text{H}$); 7.343(d, $J=8,1\text{H}$); 7.260(d, $J=8,1\text{H}$); 7.176(d, $J=7.5,1\text{H}$); 7.154(d, $J=7.5,1\text{H}$); 6.746(t, $J=8,1\text{H}$); 6.570(d, $J=8,2\text{H}$); 4.724(d, $J=2.5,1\text{H}$); 4.540(m, 1H); 2.728(dt, $J=10,3, 1\text{H}$); 2.646(q, $J=3,1\text{H}$); 2.410(dd, $J=10,3,1\text{H}$); 2.244(m, 1H); 1.942(m, 1H); 1.678(m, 2H).

MS (m/z): 355.06; $t\text{R}$ (min) (HPLC) = 5.38 and 6.24.

4) 2-(3-Chlorophenyl)-3-(3-nitrophenyl)-2-azabicyclo[2.2.2]octan-5-one (6d)

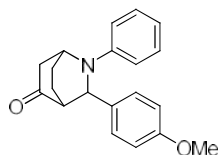


Brown solid.

^1H NMR (400 MHz, CDCl_3): 7.439(s, 1H); 7.352(d, $J=8,1\text{H}$); 7.225(d, $J=8,1\text{H}$); 7.168(t, $J=8,1\text{H}$); 6.774(s, $J=9,1\text{H}$); 6.598(d, $J=9,2\text{H}$); 6.438(d, $J=9,1\text{H}$); 4.537(d, $J=2.5,1\text{H}$); 4.418(m, 1H); 2.755(m, 1H); 2.706(q, 1H); 2.472(m, 1H); 2.246(m, 1H); 2.119(m, 1H); 2.027(m, 1H); 1.735(m, 1H).

MS m/z : 356.09; tR (min) (HPLC) = 4.85 and 6.63.

5) 3-(4-Methoxyphenyl)-2-phenyl-2-azabicyclo[2.2.2]octan-5-one (6e)

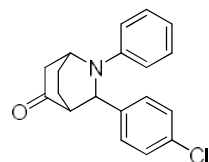


Brown solid.

^1H NMR (400 MHz, CDCl_3): 7.439(s, 1H); 7.352(d, $J=8,1\text{H}$); 7.225(d, $J=8,1\text{H}$); 7.168(t, $J=8,1\text{H}$); 6.774(d, $J=9,2\text{H}$); 6.598(d, $J=9,1\text{H}$); 4.535(d, $J=2.5,1\text{H}$); 4.415(m, 1H); 3.726(s, 3H); 2.758(m, 1H); 2.706(m, 1H); 2.472(m, 1H); 2.246(m, 1H); 2.119(m, 1H); 2.027(m, 1H); 1.735(m, 1H).

MS (m/z): 307.16; tR (min) (HPLC) = 5.71 and 6.14.

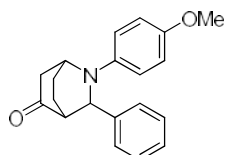
6) 3-(4-Chlorophenyl)-2-phenyl-2-azabicyclo[2.2.2]octan-5-one (6f)



Brown solid.

^1H NMR (400 MHz, CDCl_3): 1.65-1.85 (m, 1H), 1.95-2.35 (m, 3H), 2.40-2.55 (m, 1H), 2.65-2.85 (m, 2H), 4.55 (br m, 1H), 4.64 (br m, 1H), 6.65 (d, 2H, $J=8.3$), 6.76 (t, 1H, $J=7.5$), 7.00 (dd, 2H, $J=8.6$), 7.19 (dd, 2H, $J=7.5, 8.3$), 7.23-7.33 (m, 2H).

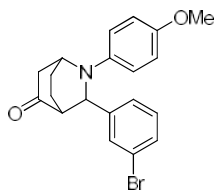
MS (m/z): 311.11; tR (min) (HPLC) = 4.84 and 5.60.

7) 2-(4-Methoxy-phenyl)-3-phenyl-2-aza-bicyclo[2,2,2]octan-5-one (6g)

Brown solid.

^1H NMR (400 MHz, CDCl_3): 1.73(m, 1H), 2.03(m, 1H), 2.15(m, 1H), 2.27(m, 1H), 2.47(dd, $J = 2.48\text{Hz}$ 1H), 2.74(m, 1H), 2.76(dd, $J = 2.48\text{Hz}$ 1H), 3.72(s, 3H), 4.44(s, 1H), 4.58(d, $J = 2.51\text{Hz}$ 1H), 6.61-6.65(m, 2H), 6.75-6.79(m, 2H), 7.21-7.31ppm(m, 5H).

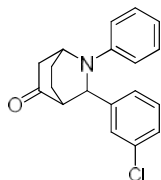
MS (m/z): 307.16; tR (min) (HPLC) = 4.80 and 5.10.

8) 3-(3-Bromo-phenyl)-2-(4-methoxy-phenyl)-2-aza-bicyclo [2.2.2] octan-5-one (6h)

Brown solid.

^1H NMR (400 MHz, CDCl_3): 7.439(s, 1H); 7.352(d, $J=8,1\text{H}$); 7.225(d, $J=8,1\text{H}$); 7.168(t, $J=8,1\text{H}$); 6.774(d, $J=9,2\text{H}$); 6.598(d, $J=9,2\text{H}$); 4.537(d, $J=2.5,1\text{H}$); 4.418(m,1H); 3.724(s, 3H); 2.755(m,1H); 2.706(q,1H); 2.472(m,1H); 2.246(m,1H); 2.119(m,1H); 2.027(m,1H); 1.735(m,1H).

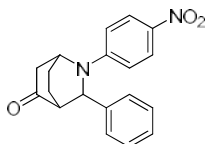
MS (m/z): 385.07; tR (min) (HPLC) = 4.85 and 6.63.

9) 3-(3-Chlorophenyl)-2-phenyl-2-azabicyclo[2.2.2]octan-5-one (6i)

Brown solid.

^1H NMR (400 MHz, CDCl_3): 7.287(s, 1H); 7.236(d, $J=8,1\text{H}$); 7.214(d, $J=8,1\text{H}$); 7.201-7.161(m,3H); 6.768(t, $J=8,1\text{H}$); 6.642(d, $J=9,2\text{H}$); 4.620(d, $J=3,1\text{H}$); 4.547(m,1H); 2.777(q,1H); 2.746(dt, $J=8,2, 1\text{H}$); 2.482(dd, $J=8,2,1\text{H}$); 2.276(m,1H); 2.125(m,1H); 2.045(m,1H).

MS (m/z): 311.11; tR (min) (HPLC) = 4.38 and 5.24.

10) 2-(4-Nitrophenyl)-3-phenyl-2-azabicyclo[2.2.2]octan-5-one (6j)

Brown solid.

¹H NMR (400 MHz, CDCl₃): 7.299(d, J=8,2H); 7.165(d, J=8,2H); 7.145(d, J=8,2H); 6.735(t, J=7,1H); 6.574(d, J=8,2H); 4.721(d, J=2.5,1H); 4.528(m,1H); 2.739(dt, J=10,3, 1H); 2.672(q, J=3,1H); 2.395(dd, J=10,3,1H); 2.235(m, 1H); 1.906(m, 1H); 1.662(m, 2H).

MS (m/z): 322.13; tR (min) (HPLC) = 4.53 and 4.93.

6.6 References

- [1] Ojima I., *Catalytic Asymmetric Synthesis*, VCH, New York, **1993**.
- [2] Noyori R., *Asymmetric Catalysis in Organic Synthesis*, John Wiley & Sons, New York **1994**.
- [3] Rueping M., Nachtsheim B. J., Ieawsuwan W., Atodiresei I., *Angewandte Chemie-International Edition*, **2011**, 50, 6706-6720.
- [4] Eschenbrenner-Lux V., Kumar K., Waldmann H., *Angewandte Chemie-International Edition*, **2014**, 53, 11146-11157.
- [5] Cao Z.-Y., Brittain W. D. G., Fossey J. S., Zhou F., *Catal. Sci. Technol.*, **2015**, 5, 3441-3451.
- [6] Memeo M. G., Quadrelli P., *Chemistry-A European Journal*, **2012**, 18, 12554-12582.
- [7] Kobayashi S., Ishitani H., *Chemical Reviews*, **1999**, 99, 1069-1094.
- [8] Kagan H. B., Riant O., *Chemical Reviews*, **1992**, 92, 1007-1019.
- [9] Jorgensen K. A., *Angewandte Chemie-International Edition*, **2000**, 39, 3558-3588.

- [10] Schluter A. D., in *Functional Molecular Nanostructures*, Schluter A. D (ed), **2005**, 245, 151-191.
- [11] Ishizu K., Tsubaki K., Mori A., Uchida S., *Progress in Polymer Science*, **2003**, 28, 27-54.
- [12] Akiyama T., Itoh J., Fuchibe K., *Advanced Synthesis & Catalysis*, **2006**, 348, 999-1010.
- [13] Itoh J., Fuchibe K., Akiyama T., *Angewandte Chemie-International Edition*, **2006**, 45, 4796-4798.
- [14] Tambar U. K., Lee S. K., Leighton J. L., *Journal of the American Chemical Society*, **2010**, 132, 10248-10250.
- [15] Kobayashi S., Komiyama S., Ishitani H., *Angewandte Chemie-International Edition*, **1998**, 37, 979-981.
- [16] Kobayashi S., Kusakabe K., Ishitani H., *Organic Letters*, **2000**, 2, 1225-1227.
- [17] Kobayashi S., Kusakabe K., Komiyama S., Ishitani H., *Journal of Organic Chemistry*, **1999**, 64, 4220-4221.
- [18] Yamashita Y., Mizuki Y., Kobayashi S., *Tetrahedron Letters*, **2005**, 46, 1803-1806.
- [19] Josephsohn N. S., Snapper M. L., Hoveyda A. H., *Journal of the American Chemical Society*, **2003**, 125, 4018-4019.
- [20] Mancheno O. G., Arrayas R. G., Carretero J. C., *Journal of the American Chemical Society*, **2004**, 126, 456-457.
- [21] Yao S. L., Saaby S., Hazell R. G., Jorgensen K. A., *Chemistry-A European Journal*, **2000**, 6, 2435-2448.

-
- [22] Taylor M. S., Jacobsen E. N., *Angewandte Chemie-International Edition*, **2006**, 45, 1520-1543.
- [23] Connon S. J., *Angewandte Chemie-International Edition*, **2006**, 45, 3909-3912.
- [24] Takemoto Y., *Organic & Biomolecular Chemistry*, **2005**, 3, 4299-4306.
- [25] Bolm C., Rantanen T., Schiffrers I., Zani L., *Angewandte Chemie-International Edition*, **2005**, 44, 1758-1763.
- [26] Schreiner P. R., *Chemical Society Reviews*, **2003**, 32, 289-296.
- [27] Sigman M. S., Jacobsen E. N., *Journal of the American Chemical Society*, **1998**, 120, 5315-5316.
- [28] Wenzel A. G., Jacobsen E. N., *Journal of the American Chemical Society*, **2002**, 124, 12964-12965.
- [29] McDougal N. T., Schaus S. E., *Journal of the American Chemical Society*, **2003**, 125, 12094-12095.
- [30] Okino T., Hoashi Y., Takemoto Y., *Journal of the American Chemical Society*, **2003**, 125, 12672-12673.
- [31] Nugent B. M., Yoder R. A., Johnston J. N., *Journal of the American Chemical Society*, **2004**, 126, 3418-3419.
- [32] Huang Y., Unni A. K., Thadani A. N., Rawal V. H., *Nature*, **2003**, 424, 146-146.
- [33] Thadani A. N., Stankovic A. R., Rawal V. H., *Proceedings of the National Academy of Sciences of the United States of America*, **2004**, 101, 5846-5850.

- [34] Okino T., Hoashi Y., Furukawa T., Xu X. N., Takemoto Y., *Journal of the American Chemical Society*, **2005**, 127, 119-125.
- [35] Momiyama N., Yamamoto H., *Journal of the American Chemical Society*, **2005**, 127, 1080-1081.
- [36] Unni A. K., Takenaka N., Yamamoto H., Rawal V. H., *Journal of the American Chemical Society*, **2005**, 127, 1336-1337.
- [37] Fuerst D. E., Jacobsen E. N., *Journal of the American Chemical Society*, **2005**, 127, 8964-8965.
- [38] Uraguchi D., Sorimachi K., Terada M., *Journal of the American Chemical Society*, **2004**, 126, 11804-11805.
- [39] Uraguchi D., Terada M., *Journal of the American Chemical Society*, **2004**, 126, 5356-5357.
- [40] Akiyama T., Itoh J., Yokota K., Fuchibe K., *Angewandte Chemie-International Edition*, **2004**, 43, 1566-1568.
- [41] Akiyama T., Morita H., Itoh J., Fuchibe K., *Organic Letters*, **2005**, 7, 2583-2585.
- [42] Rowland G. B., Zhang H. L., Rowland E. B., Chennamadhavuni S., Wang Y., Antilla J. C., *Journal of the American Chemical Society*, **2005**, 127, 15696-15697.
- [43] Rueping M., Sugiono E., Azap C., Theissmann T., Bolte M., *Organic Letters*, **2005**, 7, 3781-3783.
- [44] Hoffmann S., Seayad A. M., List B., *Angewandte Chemie-International Edition*, **2005**, 44, 7424-7427.
- [45] Storer R. I., Carrera D. E., Ni Y., MacMillan D. W. C., *Journal of the American Chemical Society*, **2006**, 128, 84-86.

- [46] Seayad J., Seayad A. M., List B., *Journal of the American Chemical Society*, **2006**, 128, 1086-1087.
- [47] Uraguchi D., Sorimachi K., Terada M., *Journal of the American Chemical Society*, **2005**, 127, 9360-9361.
- [48] Terada M., Machioka K., Sorimachi K., *Angewandte Chemie-International Edition*, **2006**, 45, 2254-2257.
- [49] Rueping M., Antonchick A. R., Theissmann T., *Angewandte Chemie-International Edition*, **2006**, 45, 3683-3686.
- [50] Rueping M., Sugiono E., Azap C., *Angewandte Chemie-International Edition*, **2006**, 45, 2617-2619.
- [51] Mayer S., List B., *Angewandte Chemie-International Edition*, **2006**, 45, 4193-4195.
- [52] Chen X.-H., Xu X.-Y., Liu H., Cun L.-F., Gong L.-Z., *Journal of the American Chemical Society*, **2006**, 128, 14802-14803.
- [53] Ishitani H., Kobayashi S., *Tetrahedron Letters*, **1996**, 37, 7357-7360.
- [54] Ishitani H., Ueno M., Kobayashi S., *Journal of the American Chemical Society*, **1997**, 119, 7153-7154.
- [55] Hattori K., Yamamoto H., *Tetrahedron*, **1993**, 49, 1749-1760.
- [56] Lee S. K., Tambar U. K., Perl N. R., Leighton J. L., *Tetrahedron*, **2010**, 66, 4769-4774.
- [57] Zhang W., Dai Y., Wang X., Zhang W., *Tetrahedron Letters*, **2011**, 52, 6122-6126.
- [58] Chen Z., Lin L., Chen D., Li J., Liu X., Feng X., *Tetrahedron Letters*, **2010**, 51, 3088-3091.
- [59] Shirakawa H., Sano H., *Tetrahedron Letters*, **2014**, 55, 4095-4097.

- [60] Sunden H., Ibrahim I., Eriksson L., Cordova A., *Angewandte Chemie-International Edition*, **2005**, 44, 4877-4880.
- [61] Liu H., Cun L.-F., Mi A.-Q., Jiang Y.-Z., Gong L.-Z., *Organic Letters*, **2006**, 8, 6023-6026.
- [62] Maleev V. I., Skrupskaya T. y. V., Yashkina L. V., Mkrtychyan A. F., Saghyan A. S., Il'in M. M., Chusov D. A., *Tetrahedron-Asymmetry*, **2013**, 24, 178-183.
- [63] Yamamoto H., *Lewis Acids in Organic Synthesis*, Wiley-VCH, Weinheim, **2000**.
- [64] Menger F. M., Tsuno T., *Journal of the American Chemical Society*, **1989**, 111, 4903-4907.
- [65] Mak C. C., Chow H. F., *Macromolecules*, **1997**, 30, 1228-1230.
- [66] Chow H. F., Mak C. C., *Journal of Organic Chemistry*, **1997**, 62, 5116-5127.
- [67] Fujita K.I., Muraki T., Hattori H., Sakakura T., *Tetrahedron Letters*, **2006**, 47, 4831-4834.
- [68] Wu Y., Zhang Y., Yu M., Zhao G., Wang S., *Organic Letters*, **2006**, 8, 4417-4420.
- [69] Breinbauer R., Jacobsen E. N., *Angewandte Chemie-International Edition*, **2000**, 39, 3604-3607.
- [70] He L., Laurent G., Retailleau P., Folleas B., Brayer J.-L., Masson G., *Angewandte Chemie-International Edition*, **2013**, 52, 11088-11091.
- [71] Reymond S., Cossy J., *Chemical Reviews*, **2008**, 108, 5359-5406.
- [72] Juhl K., Jorgensen K. A., *Angewandte Chemie-International Edition*, **2003**, 42, 1498-1501.

- [73] Yamamoto Y., Momiyama N., Yamamoto H., *Journal of the American Chemical Society*, **2004**, 126, 5962-5963.
- [74] Hayashi Y., Yamaguchi J., Hibino K., Sumiya T., Urushima T., Shoji M., Hashizume D., Koshino H., *Advanced Synthesis & Catalysis*, **2004**, 346, 1435-1439.
- [75] Northrup A. B., MacMillan D. W. C., *Journal of the American Chemical Society*, **2002**, 124, 2458-2460.
- [76] Ramachary D. B., Chowdari N. S., Barbas C. F., *Angewandte Chemie-International Edition*, **2003**, 42, 4233-4237.
- [77] Ahrendt K. A., Borths C. J., MacMillan D. W. C., *Journal of the American Chemical Society*, **2000**, 122, 4243-4244.
- [78] Sunden H., Dahlin N., Ibrahim I., Adolfsson H., Cordova A., *Tetrahedron Letters*, **2005**, 46, 3385-3389.
- [79] Casas J., Engqvist M., Ibrahim I., Kaynak B., Cordova A., *Angewandte Chemie-International Edition*, **2005**, 44, 1343-1345.
- [80] Cordova A., Sunden H., Engqvist M., Ibrahim I., Casas J., *Journal of the American Chemical Society*, **2004**, 126, 8914-8915.
- [81] Sunden H., Engqvist M., Casas J., Ibrahim I., Cordova A., *Angewandte Chemie-International Edition*, **2004**, 43, 6532-6535.
- [82] Cordova A., *Accounts of Chemical Research*, **2004**, 37, 102-112.
- [83] Borgevig A., Sunden H., Cordova A., *Angewandte Chemie-International Edition*, **2004**, 43, 1109-1112.
- [84] Cordova A., *Chemistry-A European Journal*, **2004**, 10, 1987-1997.
- [85] Cordova A., Sunden H., Borgevig A., Johansson M., Himo F., *Chemistry-A European Journal*, **2004**, 10, 3673-3684.

- [86] Zhou L., Russell D. H., Zhao M. Q., Crooks R. M., *Macromolecules*, **2001**, 34, 3567-3573.
- [87] Thakurta S., Roy P., Rosair G., Gomez-Garcia C. J., Garribba E., Mitra S., *Polyhedron*, **2009**, 28, 695-702.
- [88] Singh V. P., *Spectrochimica Acta Part A*, **2008**, 71, 17-19.
- [89] Biesinger M. C., Lau L. W. M., Gerson A. R., Smart R. S. C., *Applied Surface Science*, **2010**, 257, 887-898.
- [90] Sahu S. K., Panda S. P., Sadafule D. S., Kumbhar C. G., Kulkarni S. G., Thakur J. V., *Polymer Degradation and Stability*, **1998**, 62, 495-500.
- [91] Pisharath S., Ang H. G., *Polymer Degradation and Stability*, **2007**, 92, 1365-1377.
- [92] Becke A. D., *Journal of Chemical Physics*, **1993**, 98, 5648-5652.
- [93] Stephens P. J., Devlin F. J., Chabalowski C. F., Frisch M. J., *Journal of Physical Chemistry*, **1994**, 98, 11623-11627.

7.1 Summary of the Work

Most of the works discussed in the field of dendritic catalysis were using dendrimers or hyperbranched polymers. Focus of present thesis was on the new trend in dendritic architecture, *i.e.*, dendronized or dendrigraft polymer. During the last few years, dendronized as well as dendrigraft polymers were well documented for their application in the field of material science due to their structural perfection. Nobody, within our knowledge, have tried these systems for catalytic applications, particularly, the synthesis of these systems on a polymer support. The present thesis has attempted to undertake the challenge to synthesize the dendrigraft architecture on polystyrene support. The intention was to create the dendrigraft architecture having large amount of peripheral functionality even at the low generation level. The present approach was centred on the synthesis of dendrigraft systems on the polystyrene support and functionalization of the periphery of the low generation polymer.

In the present thesis, we have developed a novel family of dendrigraft amidoamine polymers having pentaerythritol, glycerol and ethylene glycol initiated polyepichlorohydrin as core. The graft from or divergent method along with solid phase strategy was adopted for the synthesis. The different generations G0, G1 and G2 were synthesized and characterized. Characterization of dendrigraft amidoamine polymer

having pentaerythritol initiated polyepichlorohydrin as core has been done after photolytic cleavage of the same from the support. Amount of amino group in the G0, G1 and G2 series was found to be comparable for dendrigraft polymer having ethylene glycol and pentaerythritol initiated polyepichlorohydrin as core while the same was found to be higher for dendrigraft polymer having glycerol initiated polyepichlorohydrin as core. This may be due to the monodispersity and high molecular weight of glycerol initiated polyepichlorohydrin compared to other polycore polyepichlorohydrin.

In chapter 3 of thesis, an attempt was made to develop a highly efficient dendritic copper catalyzed method for the conjugation of aromatic 1, 2-diamine with aldehydes and ketones. The copper complexes of G0, G1 and G2 dendrigraft polymer having glycerol initiated polyepichlorohydrin as core were synthesized and characterized, were found to be excellent catalysts for the synthesis of benzimidazole derivatives *via* the reaction between 1, 2-phenylenediamine with carbonyl compounds. The reaction occurred even with low generation *ie.*, GLR-G0-Cu polymer. After optimizing the reaction conditions, a detailed study of the synthesis of benzimidazole derivatives was done with GLR-G2 copper catalyst. Comparison of GLR-G2-Cu catalyst with nondendritic copper acetate was also done. The main features of the synthesis include: air was used as the terminal oxidant, ethanol was used as the solvent, only small amount of catalyst was needed to drive the reaction and water was the only by-product in this reaction. All the reactions were performed at room temperature and it showed outstanding tolerance of both aldehydes and ketones. The synthetic protocols are

straightforward, safe, environmentally clean, and free from halogenated solvents or any other additives such as a co-catalyst or acid. Procedural simplicity, simple recovery and reusability of catalysts meet the requirements of benign chemistry.

The chapter 4 of thesis has discussed the development of a highly efficient dendritic copper catalyzed procedure for the synthesis of 1,2,4,5 tetra-substituted imidazoles based on one pot four component condensation of 1,2 diketone, aldehyde, amine and ammonium acetate under benign conditions. The copper complexes of G0, G1 and G2 dendrigraft polymer having ethylene glycol initiated polyepichlorohydrin as core were synthesized and characterized and they were found to be excellent catalysts for the 4CR reaction between 1,2 diketone, aldehyde, amine and ammonium acetate. The reaction occurred well even with low generation ie. EG-G0-Cu catalyst. After optimizing the reaction conditions, a detailed study of synthesis of tetra-substituted imidazole derivatives was done with EG-G2 copper catalyst. A brief investigation on the synthesis of tri-substituted imidazole derivative was also done. EG-G2-Cu catalyst was compared with EG-G2-Pd catalyst and found that EG-G2-Cu catalyst was superior to EG-G2-Pd with respect to the reaction time. The main features of the synthesis are: ethanol or water was used as the solvent, even small amount of catalyst was found to drive the reaction and the reaction was found to be feasible under solvent free condition also. All the reactions were performed at room temperature and outstanding tolerance of functional groups was noticed. The synthetic protocols are straightforward, safe, environmentally clean, and free from halogenated solvents or any other additives such as a co-catalyst or acid.

In chapter 5 of the thesis, the development of a dendritic palladium catalyst for the conjugation of o-aminophenol with aldehydes was discussed. The developed palladium complexes of G0, G1 and G2 dendrigraft polymer having ethylene glycol initiated polyepichlorohydrin as core were characterized and were found to be good catalysts for the synthesis of benzoxazole derivatives *via* the reaction between o-aminophenol with aldehydes. The reaction occurred even with low generation *ie.*, EG-G0-Pd catalyst. After optimizing the reaction conditions, a detailed study of the synthesis of benzoxazole derivatives was done with EG-G2 palladium catalyst. The palladium catalyst of different series such as EG-G2-Pd, GLR-G2-Pd and PEN-G2-Pd were found as active catalysts for the synthesis of benzoxazole. The main features of the synthesis were; air was used as the terminal oxidant, ethanol was used as the solvent, only small amount of catalyst was needed to drive the reaction and water was the only by-product in this reaction. Even though the reactions are feasible at room temperature, reactions were carried out at moderate temperature, 50⁰C. The catalyst showed outstanding tolerance of functional groups on aldehyde. The synthetic protocols are straight forward, safe, environmentally clean, and free from halogenated solvents.

Chapter 6 of the thesis has elaborated on the development of a highly efficient chiral dendritic copper catalyzed method for the cycloaddition of cyclohexenone with aldimines. The copper complexes of chiral G1 and G2 dendrigraft polymer having pentaerythritol initiated polyepichlorohydrin as core were characterized. Aza Diels-Alder reaction between systems like imines and cyclohexenone are rare and reported

works are base catalyzed or catalyzed by other metals under homogeneous conditions. It was found that copper complexes could catalyze aza Diels-Alder reaction like Diels-Alder reaction. The reaction occurred more efficiently with high generation dendrigraft polymer in comparison with low generation G1 dendrigraft polymer. After optimizing the reaction conditions, a detailed study of aza Diels-Alder reaction was done with chiral PEN-G2 copper catalyst. The main features of the synthesis are: only small amount of catalyst was needed to drive the reaction and all the reactions were performed at room temperature. The catalyst performed well with good diastereoselectivity and good enantiomeric excess. All the catalysts reported in this thesis could be recycled.

Procedural simplicity, simple recovery and reusability of catalysts meet the requirements of benign chemistry. So the synthesized catalysts will be of wide practical application in similar reactions. Further investigation on the application of these catalysts for other organic reactions is in progress.

7.2 Major Achievements

- Even though there are large number of reports on dendronized polymer having linear polymeric core, amidoamine dendrigraft polymer having polyepichlorohydrin as core is a new one.
- Within our knowledge, there are only two reports on dendrigraft polymers having branched polymeric core. We have developed dendrigraft polymers having branched polymeric core like glycerol and pentaerythritol initiated polyepichlorohydrin as core.

- So far, no reports have appeared on the synthesis of dendrigraft polymers on a solid resin support. The present thesis has demonstrated the success of the approach to certain extent in developing the dendrigraft polymer on a resin support.
- As expected, the amount of amine functionality increased from G0 to G2 dendrigraft polymer.
- The present attempt to cleave the dendrigraft polymer from the support was successful. Molecular mass obtained in the case of G0 dendrigraft polymer was agreeable with the theoretical value. But G1 and G2 dendrigraft polymers showed defective structure.
- Metal complexes of dendrigraft polymers for catalytic applications were not yet reported. We have succeeded in developing metal complexes of dendrigraft polymers and used them as catalysts.
- Even though benign catalysts were reported for the synthesis of benzimidazole and tetra-substituted imidazole derivatives, the catalysts discussed in the thesis are more beneficial in terms of their heterogeneous nature.
- Generally, palladium catalysts are reported for C-C coupling reactions; the developed palladium catalyst was successfully used for synthesis of benzoxazole and tetra-substituted imidazole derivatives.
- We have succeeded in carrying out the aza Diels Alder reaction with excellent enantiomeric excess using chiral modified dendrigraft polymer catalyst.

7.3 Future Outlook

Catalysis reactions of metal complexes of dendrigraft polymers were studied in the thesis. No attempt was made to study the catalytic efficiency of the metal free polyamines. Hence it could be desirable to study the performance of dendrigraft polyamine as a base catalyst. Periphery modification can be done with more acidic functionality like p-toluene sulphonyl fluoride in order to further increase catalyst efficiency. Comparison of solid phase strategy for the synthesis of dendrigraft polymers can be compared with solution phase strategy. Other easy cleavage strategies have to be developed to cleave the dendrigraft polymer from the support. The nature of the dendrigraft polymers having glycerol and ethylene glycol initiated polyepichlorohydrin as core could be studied in detail after photolytic cleavage from the resin. We have to develop methods to synthesize dendronized polymers with perfect structures on a solid support. Palladium nano particles embedded in dendrigraft polyamine could be used as catalysts for several organic reactions. Application of present catalysts could be explored for the synthesis of various heterocyclic compounds using MCR strategy.

Honours and Awards

- Best Paper Award, Chemical Sciences, 27th Kerala Science Congress, 27-29 January 2015, Alappuzha, Kerala.
- Certificate of Appreciation from Chancellor and Governor of Kerala during Prathiba Sangamam of Cochin University of Science and Technology for Securing the Best Paper Award at the Kerala Science Congress held at Alappuzha during 27-29 January 2015.
- Certificate of Appreciation from Vice Chancellor of Cochin University of Science and Technology during the National seminar “National Perspectives in Organic Chemistry” organized by Department of Applied Chemistry, Cochin University of Science and Technology.
- Certificate of Appreciation from Prof. V.N Rajasekaran Pillai, Former Vice Chairman of UGC and Executive Vice President of KSCSTE for the BEST PAPER AWARD in National seminar “Present and Future Scope of Nanoscience and Nanotechnology (BAM NANST - 2014)” organized by Post Graduate Department of Chemistry, Bishop Abraham Memorial College, Thiruthicad during 3-5 September 2014.

Publication

- **Smitha George** and K. Sreekumar, “Polyamidoamine Dendrigraft Polymer for the Conjugation of o-phenylenediamine with Carbonyl Compounds”, ISBN: 978-81-928129-2-2.

Conference Proceedings

- **Smitha George** and K. Sreekumar, “Chiral Dendrigrraft Polymer: A Novel Catalyst for the Asymmetric Synthesis of Isoquinuclidines”, 27th Kerala Science Congress, held at Alappuzha organized by Government of Kerala, KSCSTE, NATPAC and DST during 27-29 January 2015.
- **Smitha George** and K. Sreekumar, “Synthesis of Merrifield Resin Supported Polyamine Encapsulated Pd Nanoparticles”, National Seminar On “Present and Future Scope of Nanoscience and Nanotechnology (BAM NANST - 2014)” organized by Post Graduate Department of Chemistry, Bishop Abraham Memorial College, Thiruthicad during 3-5 September 2014.
- **Smitha George** and K. Sreekumar, “Polyamidoamine Dendrigrraft Polymer for the Conjugation of o-phenylenediamine with Carbonyl Compounds”, 24th Swedeshi Science Congress, organized by Swadeshi Science Movement and Thunchath Ezhuthachan Malayalam University, Tirur during 6-8 November 2014. ISBN: 978-81-928129-2-2.
- **Smitha George** and K. Sreekumar, “Development of Amidoamine Dendronized Copper Polymer as a Catalyst for the Synthesis of Monomers for Solar Cell Applications”, International Conference on Photonics and Solar Water Splitting, organized by Department of Physics, St.Terasas College, Ernakulam during 12-13 March 2015.
- **Smitha George** and K. Sreekumar, “Synthesis of Reusable PAMAM Dendrigrraft Polymer”, ISAS Conference, organized by

Indian Society of Analytical Science held at Kochi during 18-21 September 2014.

- **Smitha George** and K. Sreekumar, “Polyamine Cu Polymer as a Green Catalyst for Imidazole Synthesis”, National Seminar on Recent Advances in Chemistry, organized by Department of Chemistry, MES College, Ponnani during 2-3 September 2014.
- **Smitha George** and K. Sreekumar, “Design and Synthesis of Polymer Supported Dendrimer from Glycidyl Azide Polymer”, International Conference on Materials for the Millennium (MatCon), organized by Department of Applied Chemistry, Cochin University of Science and Technology during 11-13 January 2010.
- **Smitha George** and K. Sreekumar, “Fast and Convenient Synthesis of Low Generation, High Molecular Weight PAMAM Dendrimer”, National Seminar on Current Trends in Chemistry (CTriC), organized by Department of Applied Chemistry, Cochin University of Science and Technology during 17-18 January 2014.

Papers to be Communicated

- Synthesis of Merrifield Resin Supported Dendrigrft Polymer having Ethylene Glycol, Glycerol and Pentaerythritol Initiated Polyepichlorohydrin as Core.
- Synthesis of Benzimidazole Derivatives using Copper Complex of Dendrigrft Polymer having Glycerol Initiated Polyepichlorohydrin as Core.

- Synthesis of Benzoxazole Derivatives using Palladium Complex of Dendrigrft Polymer having Ethylene Glycol Initiated Polyepichlorohydrin as Core.
- Synthesis of Tetra-substituted Imidazole Derivatives using Copper and Palladium Complexes of Dendrigrft Polymer having Ethylene Glycol Initiated Polyepichlorohydrin as Core.
- Aza Diels-Alder Reaction of Cyclohexenone with Aldimines Catalysed by Dendrigrft Polymer having Chiral Periphery.